PEACH BOTTOM ATOMIC POWER STATION

UNITS 2 AND 3

MARK I LONG TERM PROGRAM PLANT UNIQUE ANALYSIS

DOCKET NUMBERS: 50-277 AND 50-278

PREPARED FOR

PHILADELPHIA ELECTRIC COMPANY

BECHTEL POWER CORPORATION
SAN FRANCISCO, CALIFORNIA

REVISION 0
APRIL 1982

ABSTRACT

A plant unique analysis has been performed on the Peach Bottom Atomic Power Station Units 2 and 3 primary containment suppression chambers and their internals, including all the modifications made to mitigate the loads and/or to strengthen the structural members. The loss of coolant accident (LOCA) loads defined in the Mark I Load Definition Report, the safety relief valve (SRV) discharge loads based on in-plant tests, and the normal loads specified in the Final Safety Analysis Report (FSAR) were used. The structural analysis techniques and the structural acceptance criteria were as specified in the Mark I Plant Unique Analysis Application Guide. The results of the evaluation show that the Peach Bottom Units 2 and 3 primary containment suppression chambers with their installed modifications meet all the code requirements and thus meet the original intended margin of safety.

ACRONYMS

ADS	Automatic Depressurization System
AISC	American Institute of Steel Construction
ASME	American Society of Mechanical Engineers
BWR	Boiling Water Reactor
CH	Chugging
CO	Condensation Oscillation
DBA	Design Basis Accident
ECCS	Emergency Core Cooling System
FSAR	Final Safety Analysis Report
FSTF	Full Scale Test Facility
HPCI	High Pressure Coolant Injection
IBA	Intermediate Break Accident
LDR	Load Definition Report
LOCA	Loss of Coolant Accident
LPCI	Low Pressure Coolant Injection
LTP	Long Term Program
MSIV	Main Steam Isolation Valve
NRC	Nuclear Regulatory Commission
OBE	Operating Basis Earthquake
PBAPS	Peach Bottom Atomic Power Station
PUA	Plant Unique Analysis
PUAAG	Plant Unique Analysis Application Guide
PULD	Plant Unique Load Definition
QSTF	Quarter Scale Test Facility
RCIC	Reactor Core Isolation Cooling
RHR	Residual Heat Removal
RPV	Reactor Pressure Vessel
SBA	Small Break Accident
SRV	Safety Relief Valve
SSE	Safe Shutdown Earthquake
STP	Short Term Program

CONTENTS

CONTENTS

ILLUSTRATIONS

TABLES

Section 1

INTRODUCTION

The Mark I primary containment, of which Peach Bottom is typical, consists of a drywell, a suppression chamber in the shape of a torus located below and encircling the drywell, and an interconnecting vent system. The torus is maintained approximately one-half full of water.

Basically, the design function of the torus is to provide a heat sink that is sufficient to condense and contain the steam that is released into the primary containment during a loss of coolant accident, known as a LOCA. In a design basis LOCA, steam discharged from both ends of a ruptured recirculation line pressurizes the drywell and is forced through the vent system into the suppression chamber where it is condensed in the suppression pool.

A second function of the torus is to condense the steam resulting from the discharge of a main steam safety relief valve (SRV). There are 11 relief valves in the drywell that bypass main steam through discharge piping down to the suppression pool and serve to prevent over-pressurization of the reactor pressure vessel.

In the early 1970s during testing of a future type containment, General Electric (GE) became aware of previously unknown suppression pool motion that occurs during the initial stages of a LOCA. Because this testing was conducted using the latest instrumentation and high-speed photography, previously undetected pool motion and dynamic loads became apparent.

In April 1972, at the German Wurgassen Nuclear Plant, a relief valve was opened during startup testing and failed to close. The reactor remained at full pressure and steam was discharged to the suppression pool until local pool temperatures were in excess of 170°F. The pool could not condense the steam and the dynamic loads that resulted from the pulsating steam jet acted on the torus, eventually causing leakage from the bottom liner plate.

As a result of LOCA testing and the stuck open relief valve experience, General Electric, in early 1975, informed Philadelphia Electric Company and the 15 other Mark I owners that potentially significant containment loading conditions had been identified and should be considered in the design of their facilities. In February, the NRC requested all concerned utilities to define their program to answer questions relating to these new loads. By April 1975, the generic Mark I Short Term Program (STP) was underway.

In the initial phase of the STP, the effort concentrated on an evaluation of the vent system and other internals of the torus primarily for pool swell loads. The LOCA related hydrodynamic loads were defined by the General Electric Company. The Mark I plants, grouped according to their physical and structural characteristics, were evaluated to identify representative plants. These were then evaluated by structural analyses and/or testing to define safety margins. Peach Bottom Atomic Power Station (PBAPS) Unit 2 was one of the generic plants chosen for the evaluation. The safety margin estimates for other plants were extrapolated from the results of the generic plant evaluation. The results of these generic evaluations are reported in References 1 through 8.

Subsequently, plant unique analyses were carried out for all Mark I operating plants. In recognition of the identified need for strengthening the torus support system, saddles were installed in both the units in 1976. The torus support system and the pipes externally attached to the torus were evaluated for the pool swell downward and upward loads. The results of the evaluation f Peach Bottom Units 2 and 3 are given in Reference 9. Based on these results, all Mark I plants including PBAPS requested and received exemptions from the Nuclear Regulatory Commission (NRC) for continued operation.

The Mark I Long Term Program (LTP) was initiated in 1976. The objectives of the LTP were twofold:

(a) The generic program was to define the design loads caused by a LOCA and SRV discharge, to formulate a structural acceptance criteria based

on the ASME Code, and to develop a Plant Unique Analysis Application Guide (PUAAG). The generic program also investigated ways to mitigate the loads.

(b) The plant unique program was to identify areas that needed load mitigation and/or structural modifications, to design and install the necessary hardware, and to demonstrate by plant unique analysis (PUA) that the modified structure met the specified acceptance criteria and the intended original margin of safety had been restored.

The generic program was a major effort to define the loads. Various subscale and in-plant tests were performed, scores of reports were generated, and a full-scale test facility was constructed which consisted of one complete torus bay, the equivalent of 1/16th of the Peach Bottom torus. All this was done in an effort to formulate methods of defining the magnitude of the dynamic pool loads that occur during LOCA and SRV events. In addition, parallel analytical efforts were undertaken.

The generic program was substantially completed in 1980 and the plant unique loads were defined. Analyses of the PBAPS torus revealed the need for mitigation of the loads and modification of the structural elements. T-Quenchers and vent header deflectors were designed for load mitigation. All the necessary hardware installation and modifications to the Unit 3 torus were completed in the fall of 1981 and to the Unit 2 torus in the spring of 1982. Modifications to torus attached pipes and supports in both units are in progress. Major modifications were:

(a) Installation of quenchers and 8-inch vacuum breakers on the SRV lines

(b) Tie down of the torus

(c) Installation of torus shell stiffeners

(d) Installation of torus nozzle stiffeners

(e) Installation of deflectors below the vent header in the non-vent bay

(f) Reinforcing of vent header-downcomer intersections

(g) Addition of new supports and modification of existing supports to the torus attached pipes

(h) Strengthening of torus internal structures and their supports.

Plant unique analyses were performed in accordance with NUREG-0661 guidelines (Reference 10) for the specified loads. The LOCA loads are defined in the Mark I Load Definition Report (LDR) (Reference 11). An extensive in-plant SRV discharge test program was conducted to define the SRV discharge loads. The results of the plant unique analyses were evaluated and compared with structural acceptance criteria.

This report contains the results of the evaluation for Peach Bottom Units 2 and 3. Section 2 describes the physical and structural characteristics of all the structures and piping considered. Section 3 describes the phenomena of LOCA and SRV discharge. Structural acceptance criteria are summarized in Section 4. Applied loads and load combinations given in the structural acceptance criteria are discussed in Section 5. The structural evaluation of the torus is given in Section 6. Sections 7 and 8 contain the results of the evaluation of the vent system and torus internals respectively. The last chapter summarizes the analyses. Modifications to torus attached piping supports in both units are underway. The results of the plant unique analysis for the torus attached piping will be submitted later as an addendum to this PUA report.

Section 2
GENERAL DESCRIPTION OF STRUCTURES

Section 2

GENERAL DESCRIPTION OF STRUCTURES

Each of the primary containments at Peach Bottom Units 2 and 3 is a pressure suppression system consisting of a drywell, a wetwell (torus) that stores a large volume of water, a connecting vent system between the drywell and torus, a vacuum relief system, containment cooling systems, and other service equipment. The drywell is a steel pressure vessel in the shape of an inverted light bulb and the wetwell is a torus-shaped steel pressure vessel located below and encircling the drywell. The general configuration of the drywell and torus is shown in Figure 2-1. The containment structural characteristics are given in Table 2-1.

The functions of the primary containment system are:

(a) To withstand the pressures resulting from a LOCA and/or SRV discharge and to provide a hold-up for the decay of any radioactive material released

(b) To store sufficient water to condense steam released as a result of a LOCA and/or SRV discharge and to supply water to the emergency core cooling systems.

2.1 DRYWELL

The drywell shown in Figure 2-1 is a steel pressure vessel with a spherical lower portion, a cylindrical upper portion, and an ellipsoidal top head. The overall height of the drywell is approximately 118 feet. The drywell is supported on a concrete foundation.

2.2 WETWELL

The wetwell (torus) shown in Figure 2-1 is a steel torus-shaped pressure vessel located below and encircling the drywell, having a major radius of

about 56 feet and a cross-sectional inside diameter of 31 feet. Figures 2-2 and 2-3 show the plan and the cross section of the torus respectively. The torus contains the suppression pool and an air space above the pool. The torus is constructed of 16 similar bays, eight of which have penetrations for the main vents.

2.3 VENT SYSTEM

Eight main vents connect the drywell vessel to a common equalizing vent header near the center of the torus as shown in Figure 2-4. The vent header serves as a sec nd plenum chamber in series with the drywell. From the bottom of the vent header, 96 downcomers extend down with about 4 feet of the lower ends submerged in water. Each pair of downcomers is braced near the bottom. The vent system is supported at the drywell and at 16 locations inside the torus. Bellows are provided outside the torus at the penetration of the main vent into the torus to seal the penetration and allow relative movement between the main vent and torus.

2.4 TORUS INTERNAL STRUCTURES AND PIPING

Other than the vent system and its supports, the structures and piping in the torus that have been evaluated for hydrodynamic loads are briefly described.

2.4.1 Submerged in the Pool

Emergency Core Cooling System (ECCS) Suction Nozzles. These are typically pipe nozzles with attached strainers that project into the torus to supply water obtained from the suppression pool to the ECCS piping system. These nozzles are subjected to submerged drag forces.

Strainers. Strainers are attached to the top of the suction nozzles to prevent the intake of particles larger than the minimum size allowed in the ECCS.

Return Line Supports. These supports are typically below the torus pool surface. They are constructed of rolled and fabricated structural steel members and struts. The supports provide restraints at the free end of the vertical return lines.

Quenchers and Supports. Quenchers are constructed of stainless steel pipes and their supports are constructed of carbon steel pipes spanning the area between the torus ring girders.

2.4.2 Partially Submerged in the Pool

SRV Discharge Lines. Inside the torus, SRV discharge lines penetrate the main vents above the pool surface and discharge through the newly installed quenchers at the bottom of the torus. Of the 11 lines, three are located in each of three main vents and two are in one main vent. Inside the torus, they are routed in three different configurations.

Return Lines. These lines range in size from 1 to 24 inches. All of them penetrate the torus above the pool level and discharge at various levels in the pool. They are supported at the torus penetrations and just below the pool surface. Figures 2-5 and 2-6 show the penetration locations for Units 2 and 3 respectively. Figure 2-7 is a set of cross sections showing the line routings inside the torus.

2.4.3 Above the Pool Surface

Vacuum Breakers and Nozzles. These are attached to the main vent-vent header intersections. They cantilever horizontally from the intersections.

Catwalk Platform. The catwalk platform provides access for inspection and maintenance. It serves no safety function and is supported from above at regular intervals around the torus. The floor of the platform consists of grating.

Spray Header. The spray header is a 4-inch diameter header with spray nozzles that is mounted at the top of the torus. The primary function of the header system is to condense steam that could bypass the suppression pool or to cool the torus atmosphere.

Monorail. This is used for handling equipment within the torus. It encircles the torus and is attached to it at selected points. It does not serve any safety function.

2.5 SRV DISCHARGE LINES IN THE DRYWELL

The 11 SRV discharge lines originate from the safety relief valves off the main steam lines and the routing external to the torus ends at the vent penetrations. Each of the 11 lines in a unit is routed differently and supported differently, but the routings in one unit are nearly identical to those in the second unit.

2.6 TORUS ATTACHED PIPING

Various pipes, ranging in diameter from 1 to 24 inches, penetrate the torus from the outside. Table 2-2 lists each penetration and system. These piping systems are classified as described in the following paragraphs.

The ECCS piping systems are:

- Residual heat removal (RHR) pump suction piping
- Core spray pump suction piping
- High pressure coolant injection (HPCI) pump suction piping
- HPCI turbine exhaust piping
- HPCI turbine vacuum pump discharge
- HPCI turbine drain piping.

Other piping systems required to maintain core cooling or to keep the torus's functional integrity following a LOCA are:

RHR test line bypass

RHR heat exchanger relief valve piping

RHR test line to torus

Torus and drywell purge piping

Containment atmosphere dilution piping

Reactor core isolation cooling (RCIC) pump suction piping

RCIC turbine exhaust piping

Core spray test lines

Hydrogen-recombiner piping

Torus drain and purification piping systems.

The remaining piping systems attached to the torus are not required to maintain core cooling following a LOCA. They consist of instrument piping and small diameter piping.

2.7 ACTIVE COMPONENTS

Active components consist of pumps and valves for the ECCS and isolation valves on piping connected to the torus.

2.8 TORUS PENETRATIONS

All nozzles on the torus to which the external piping is connected are considered to be torus penetrations. All torus penetrations greater than 6 inches in diameter have been reinforced.

Table 2-1

PLANT PHYSICAL CHARACTERISTICS

TORUS

Inner diameter	31'-0"
Number of sections	16
Shell plate thickness:	
(a) Main vent penetration	1.75"
(b) Top half excluding (a)	0.604"
(c) Bottom half	0.675"
Shell stiffeners (4 per bay)	WT6x25

SUPPORT SYSTEM

	Quantity	Size
Outer column	16	Built-up section
Inner column	16	
Saddle support	16 saddle supports not anchored. Each column is anchored with four 2-inch diameter rock bolts.	

RING GIRDER

Quantity	16
Type	T-beam

EARTHQUAKE RESTRAINT SYSTEM

Quantity	4
Type	Ties

VENT SYSTEM

	Quantity	Size
Vent pipe	8	81"
Vacuum breakers (internal)	12	21" OD
Vent header support columns	16 pairs	8" Sch 80
Downcomers	96	24" ID
Minimum submergence	4'-0"	
Maximum submergence	4'-5"	
Total water weight at max submergence	7850 kips	

Table 2-2

EXTERNAL PIPING ATTACHED TO TORUS

Penetration No.	Line Size (In.)	System Identification
N203	1"	Oxygen analyzer
N205 A and B	20"	Vacuum relief from building vent purge outlet
N206 A and B	2"	Level and pressure instrumentation
N209 A to D	1"	Air and water temperature
N210 A and B	18"	RHR torus cooling and pump test line
N211 A and B	6"	Containment cooling to spray header (RHR)
N212	12"	RCIC turbine exhaust
N214	24"	HPCI turbine exhaust
N216	4"	HPCI pump recirculation
N217 A and B	2"	RCIC turbine exhaust
N218 A to C	1"	Instrument air and oxygen analyzer
N219	18"	Purge exhaust
N221	2"	RCIC vacuum pump discharge
N223	2"	Condensate from HPCI turbine drain pot
N224	10"	Core spray test and flush*
N225	6"	RCIC pump suction
N226 A to D	24"	RHR pump suction
N227	16"	HPCI pump suction
N228 A to D	16"	Core spray pump suction
N229	6"	Core spray minimum flow*

Table 2-2 (Cont'd)

Penetration No.	Line Size (In.)	System Identification
N230	4"	RCIC pump recirculation
N231 A and B	3"	Electrical (1-3" canister EA Unit 2 (2-1" canister EA Unit 3
N233 A and B	10"	HPCI and RCIC test and flush*
N234	10"	Core spray test and flush
N235	4"	HPCI and RCIC test and flush**
N236 A and B	4"	Core spray minimum flow**

* Unit 2 only

** Unit 3 only

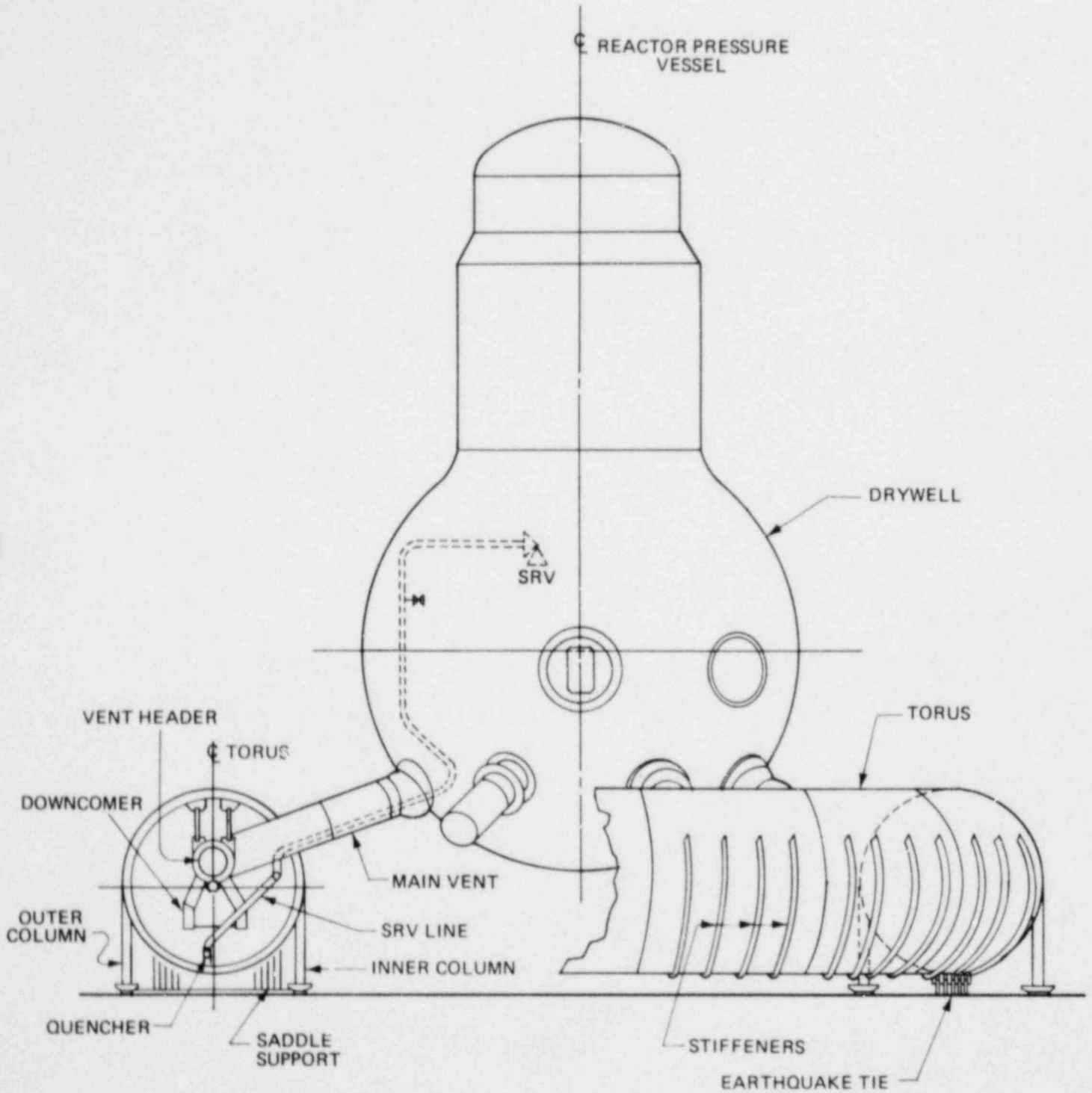

FIGURE 2-1 PEACH BOTTOM CONTAINMENT CONFIGURATION

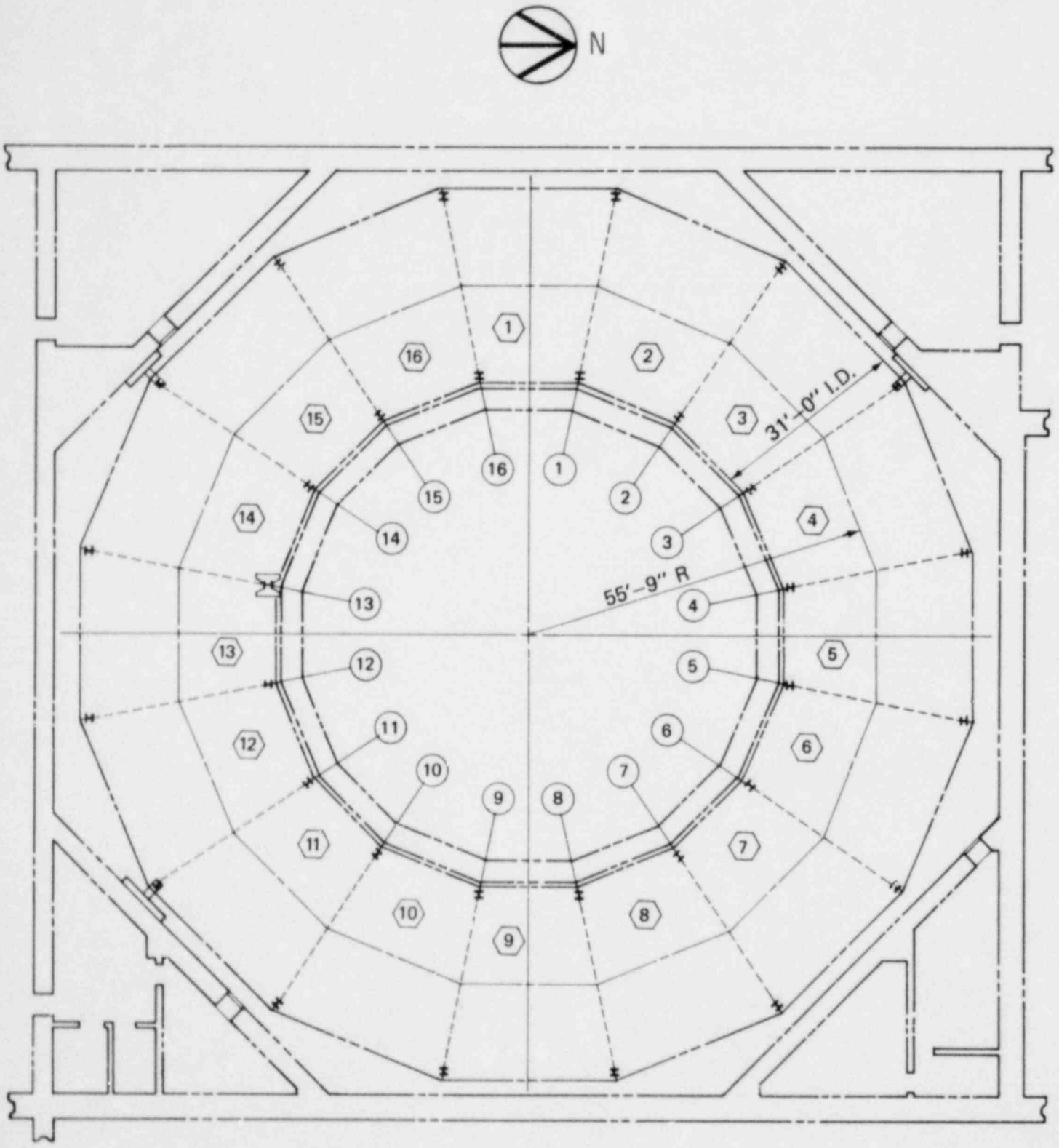

FIGURE 2-2 PLAN OF TORUS

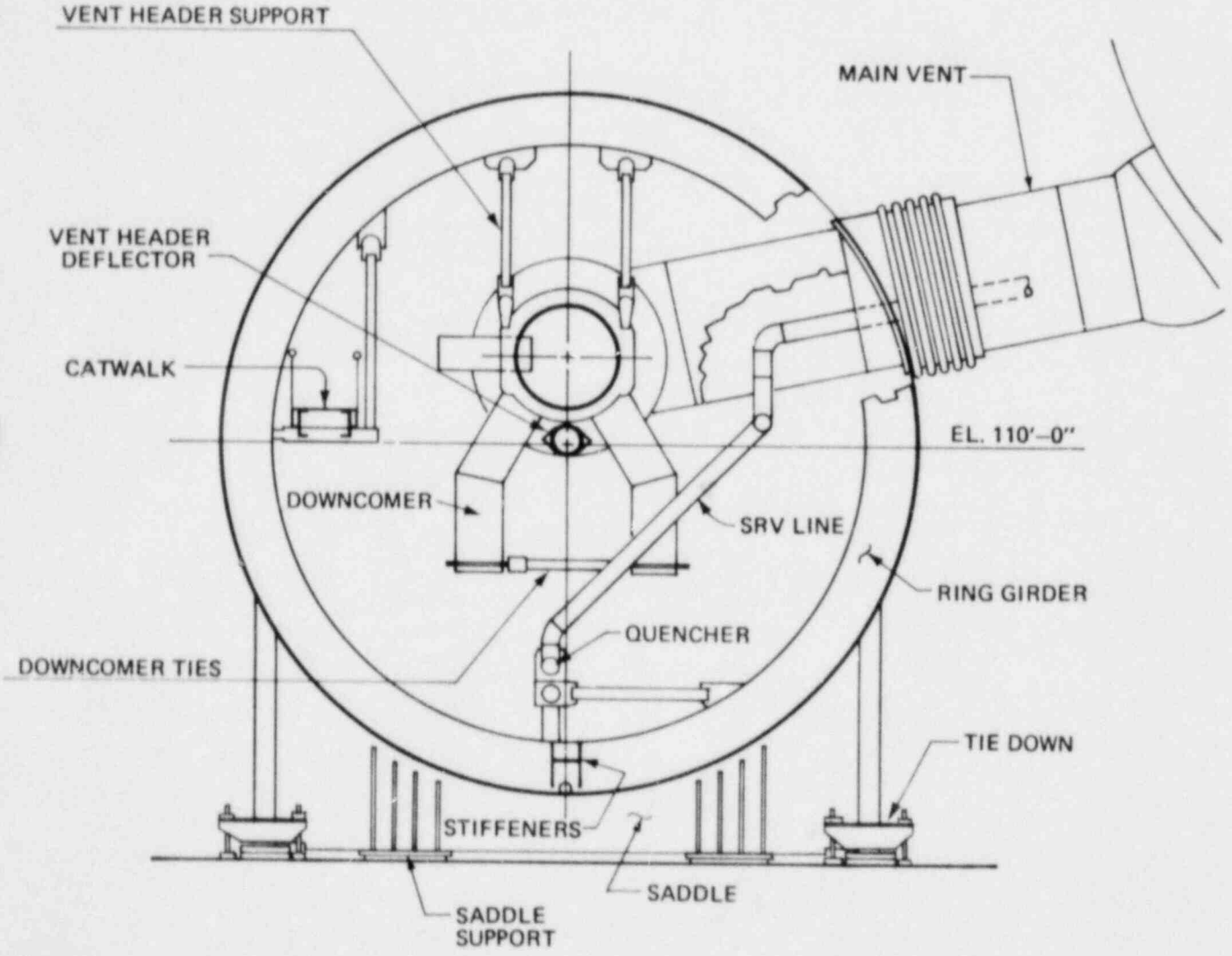

FIGURE 2-3 CROSS SECTION OF THE TORUS

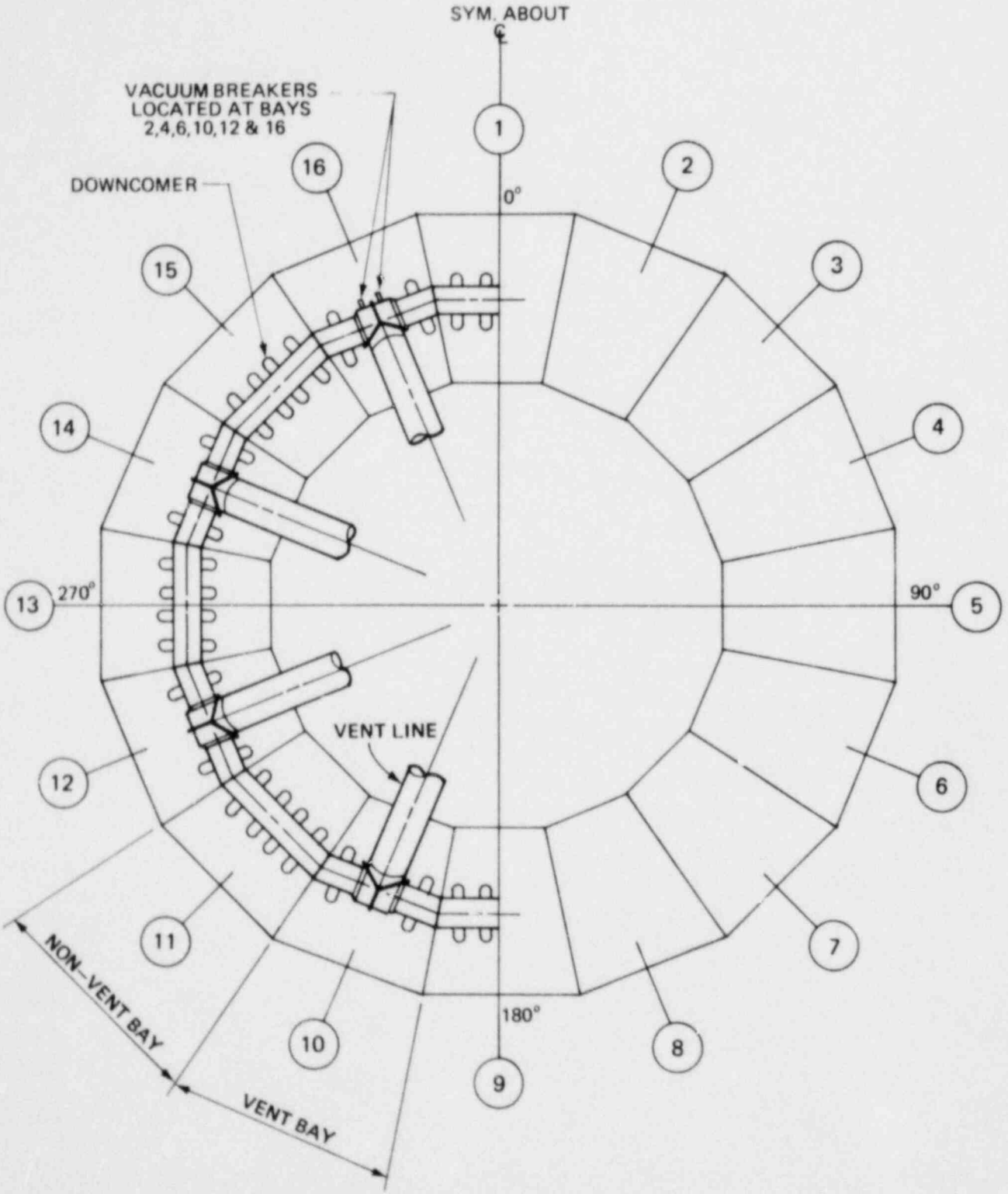

FIGURE 2-4 PLAN OF VENT SYSTEM

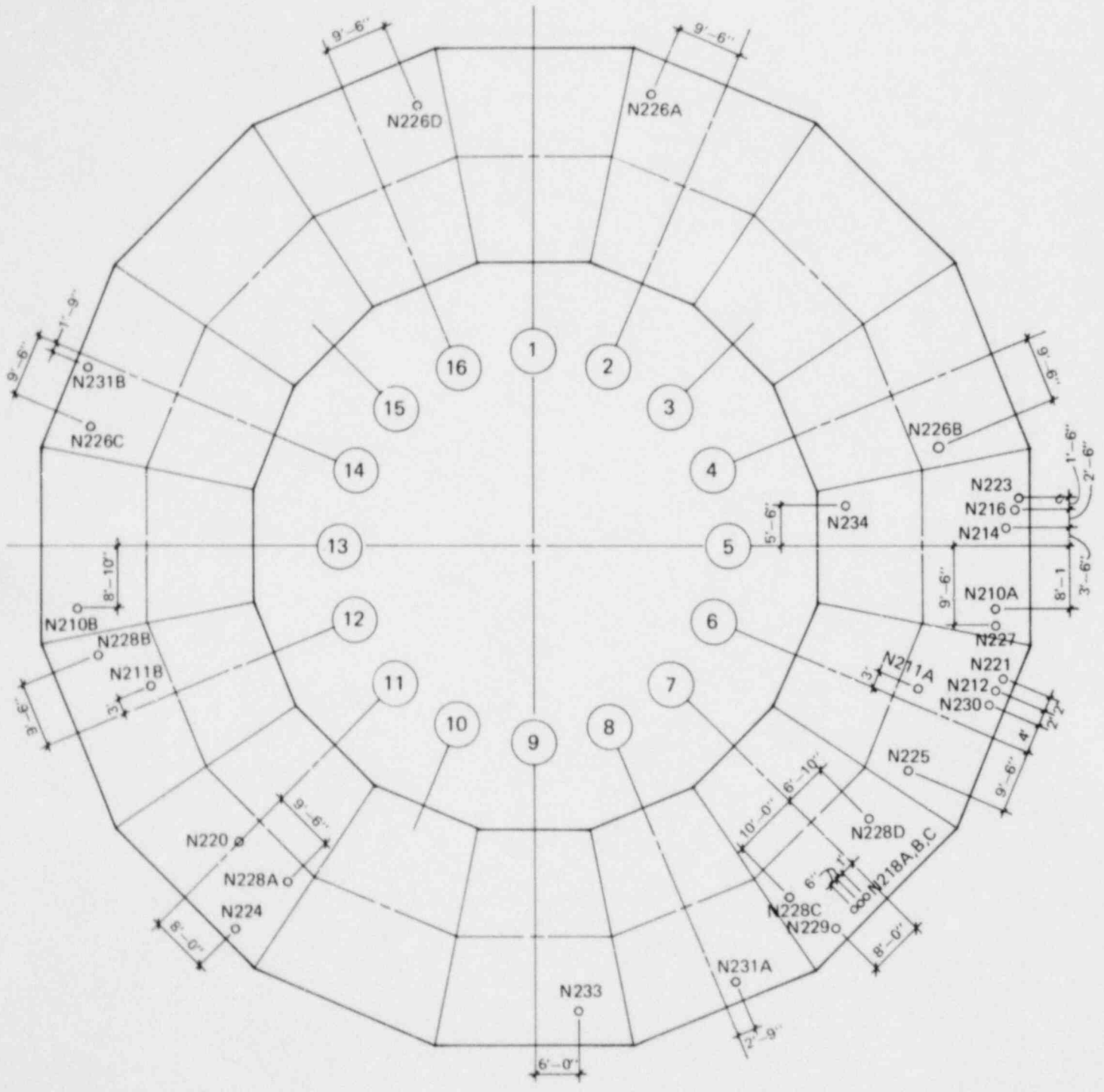

FIGURE 2-5 PLAN OF UNIT 2 TORUS PENETRATIONS

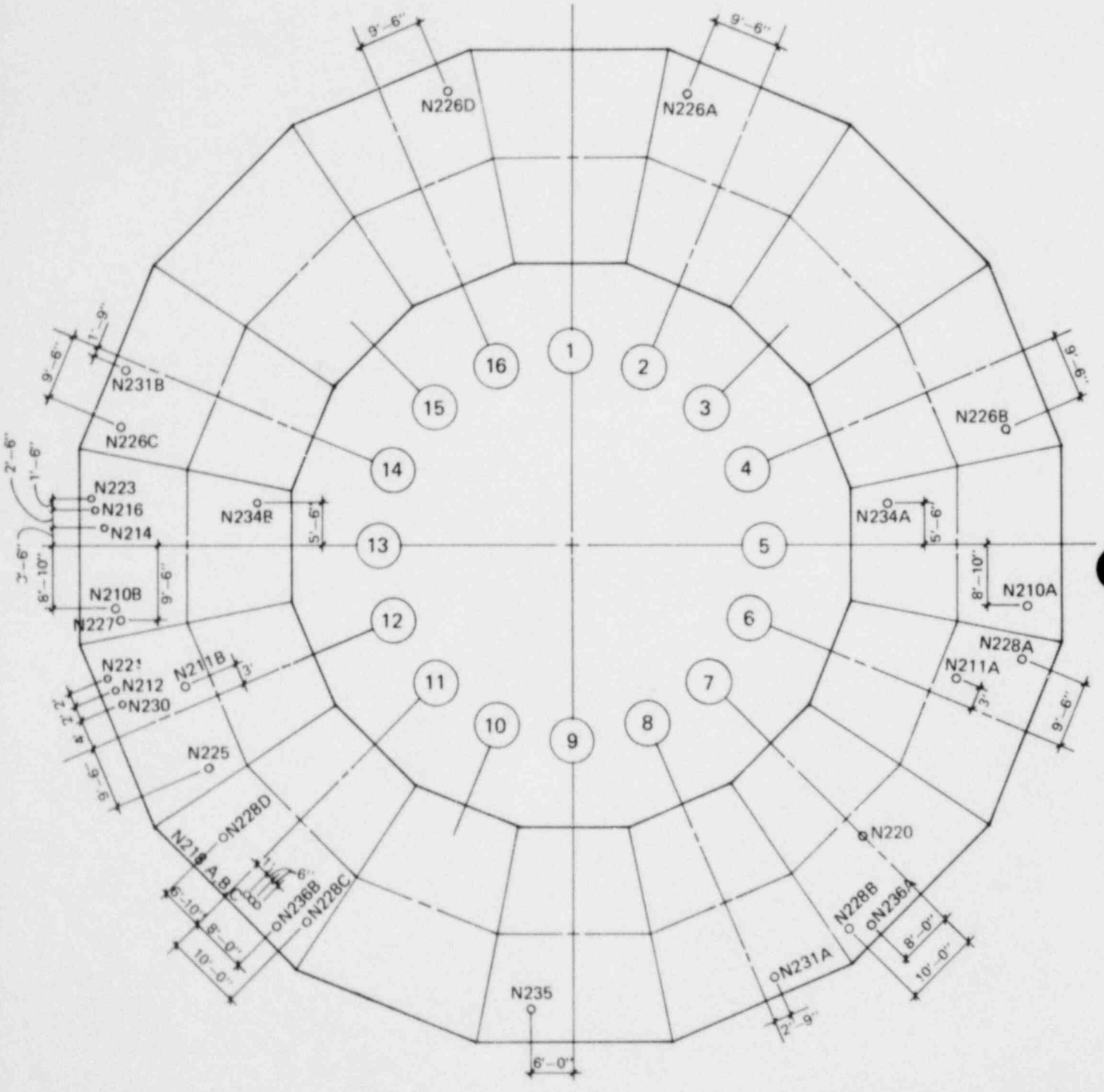

FIGURE 2-6 PLAN OF UNIT 3 TORUS PENETRATIONS

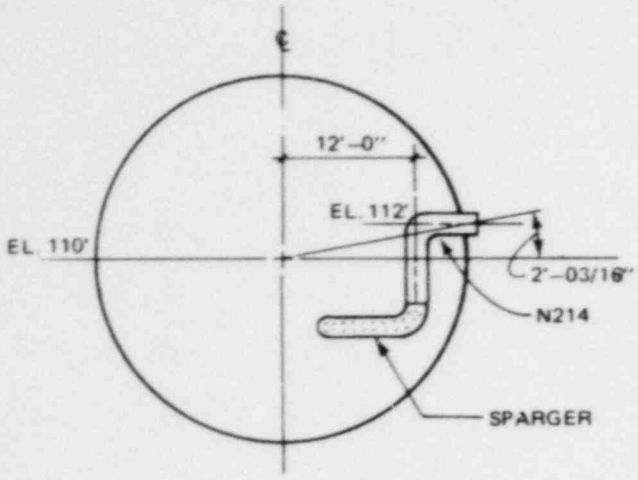

SECTION A

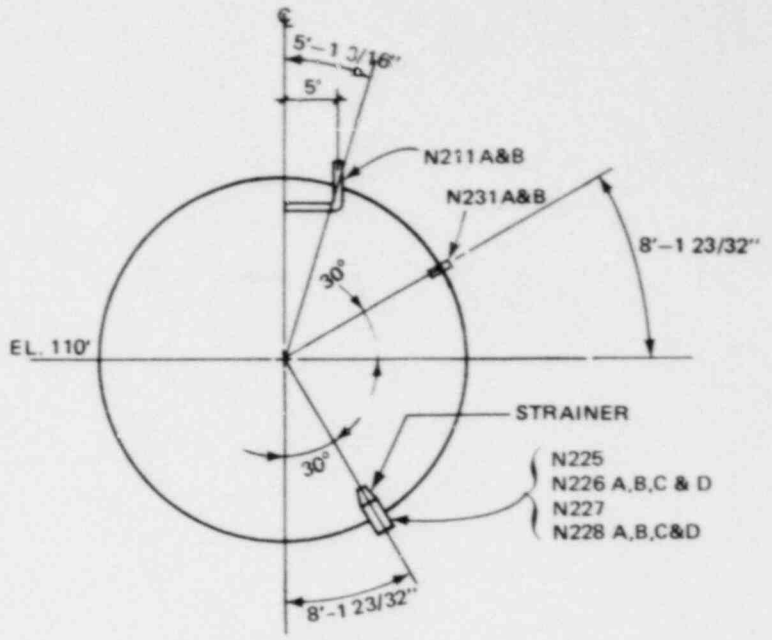

SECTION B

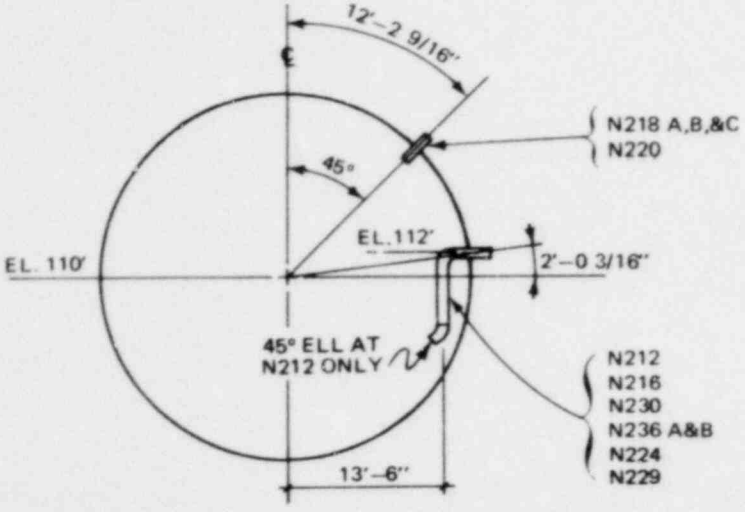

SECTION C

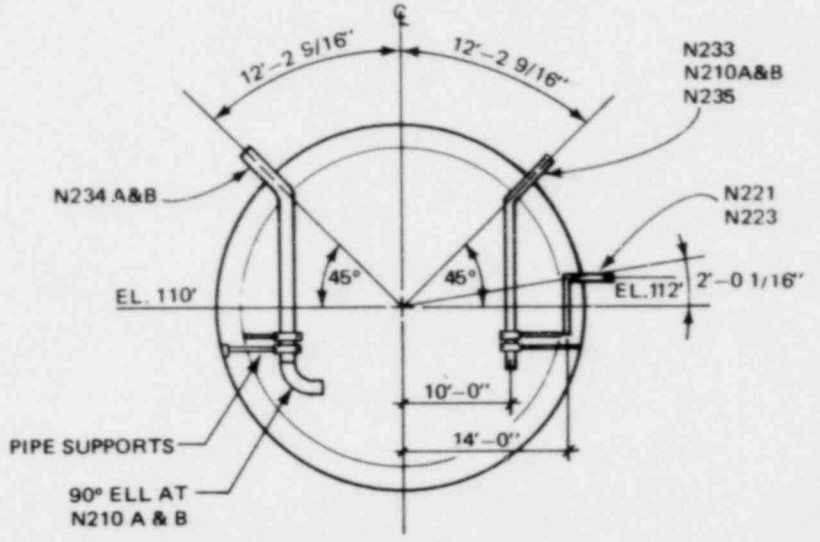

SECTION D

FIGURE 2-7 RETURN LINE ROUTINGS INSIDE TORUS

Section 3
REVIEW OF THE PHENOMENA

Section 3

REVIEW OF THE PHENOMENA

Reference 11 describes the LOCA and SRV discharge phenomena. This section summarizes the sequence of events for postulated LOCA and SRV actuation conditions and provides a basis for understanding the loading conditions which result from these hydrodynamic events.

For a postulated pipe break inside the drywell, three LOCA categories are considered. Based on postulated break size, they are referred to as design basis accident (DBA), intermediate break accident (IBA), and small break accident (SBA).

SRV actuation can occur as a result of a number of system conditions. Although the load magnitudes depend on the initial system conditions prior to SRV discharge, the sequence of the loads is the same for all conditions.

3.1 DESIGN BASIS ACCIDENT

The DBA for plants like Peach Bottom that employ jet pumps within the BWR is the instantaneous double-ended guillotine break of the BWR recirculation pump suction line at the reactor vessel nozzle safe-end welded to the pipe. This postulated break condition results in the maximum flow rate of primary system fluid and energy into the drywell, through the vent system, and into the wetwell. The DBA results in the maximum pressurization rate and peak pressure in the drywell, producing the most limiting pool swell and vent system thrust loads. The DBA event is evaluated up to the time the low pressure emergency core cooling system (ECCS) starts to flood the reactor vessel, which occurs at approximately 30 seconds after the pipe break. The use of this break to determine DBA loading has been verified by comparing the pressure response of a recirculation line break to that of a main steam line break.

The sequence of events within the wetwell that follow the postulated break is divided into two phases:

(a) Pool Swell - This phase covers the dynamic effects of drywell and vent system air being forced through the vent system into the suppression pool to the wetwell air space

(b) Steam Condensation - This phase covers the dynamic events during the period following initial air clearing when the flow into the suppression pool is a steam-air mixture. The steam is condensed at the downcomer exit while the air rises through the pool to the wetwell air space.

The reactor will automatically trip because of the high drywell pressure. Main steam line isolation will occur because of the low reactor water level. No mechanistic SRV actuation will occur because of the rapid reactor vessel depressurization and large rate of reactor fluid and energy inventory loss through the break. However, it is assumed that spurious actuation of a single SRV can occur at any time during the DBA.

With the postulated instantaneous rupture of a recirculation line, a pressure wave traveling at sonic velocity expands from the break location into the drywell atmosphere and through the vent system. The wave amplitude attenuates rapidly as it expands into the larger drywell volume. The wavefront enters the vent system with nearly uniform amplitude, but is greatly attenuated from its initial value at the break location.

The rapid bulk pressurization of the drywell immediately following a postulated DBA and prior to vent clearing theoretically generates a weak compressive wave in the downcomer water legs. This wave propagates through the suppression pool and induces a much attenuated loading on the torus shell. Loads caused by this phenomenon are negligible.

Immediately following the postulated DBA pipe rupture, the pressure and temperature of the drywell atmosphere and vent system increase rapidly. These combined pressure and temperature transients induce mechanical and thermal loadings on the main vents, vent header, and downcomers. With the drywell pressure increase, the water initially standing in the downcomers accelerates into the pool until the downcomers clear. As a result of this

water clearing process, the suppression pool water is accelerated, causing drag loads on structures within the suppression pool. Following downcomer water clearing, the downcomer air, which is at essentially drywell pressure, is exposed to the relatively low pressure of the wetwell, producing a downward reaction force on the torus. The consequent bubble expansion causes the pool water to swell in the torus, compressing the air space above the pool. During the early stages of this process, the pool swells in the bulk mode (i.e., a water ligament is accelerated upward by the rising air bubble motion) and structures close to the pool surface experience impact and drag loads as the water impacts and flows past them. Following the initial air bubble expansion and pool surface rise, the bubble pressure decreases as the bubble overexpands and the pool liquid mass decelerates. The net effect of the pool deceleration is an upward lifting force on the torus. Eventually, the bubbles break through to the torus air space and an air-water froth mixture continues upward because of the momentum previously imparted to the water. The upward motion of this froth mixture causes impingement loads on the torus and internal structures.

Gravity causes phase separation, pool upward movement stops, and the liquid falls back. Structures within the path of the fluid motion experience a downward loading; the submerged portion of the torus experiences a small pressure increase. Following pool fallback, waves on the suppression pool surface induce low magnitude loads on the downcomers, torus, and other structures close to the water surface.

The transient associated with drywell air venting to the pool typically lasts for 3 to 5 seconds. Because the air originally contained within the drywell and vent system is transferred to the wetwell air space, the wetwell experiences a rise in static pressure.

Following air carry-over, there is a period of high steam flow through the vent system. The discharge of steam into the pool and its subsequent condensation causes pool pressure oscillations that are transmitted to submerged structures and the torus shell. This phenomenon is referred to as condensation oscillation (CO). As the reactor vessel depressurizes, the

steam flow rate to the vent system decreases. The reduced steam flow rate leads to a reduction in the drywell/wetwell pressure differential. Steam condensation during this period of reduced steam flow is characterized by movement of the water/steam interface up and down within the downcomer as the steam volumes are condensed and replaced by surrounding pool water. This phenomenon is referred to as chugging. During the steam condensation period, the downcomers experience lateral loading caused by the asymmetric collapse of steam bubbles at the downcomer exit. Also, the submerged structures and containment walls experience pressure oscillations due to steam bubble formation and collapse.

Shortly after the postulated pipe rupture, the ECCS automatically begins to pump water from the plant condensate storage tank and/or the suppression pool into the reactor pressure vessel (RPV) to flood the reactor core. Eventually water cascades into the drywell from the break, causing steam condensation and drywell depressurization. As the drywell pressure falls below the pressure in the wetwell air space, the drywell vacuum relief system is actuated and air from the wetwell enters the drywell, equalizing the drywell and wetwell pressures slightly above their initial values.

Following vessel flooding and drywell/wetwell air space pressure equalization, suppression pool water is continually recirculated from the pool to the reactor vessel by the ECCS pumps. The core decay power results in a slow heat-up of the suppression pool. The suppression pool cooling mode of the residual heat removal (RHR) system is activated to remove energy from the suppression pool and return the containment to normal temperature conditions.

3.2 INTERMEDIATE BREAK ACCIDENT

An IBA is defined as a liquid line break of 0.1 square foot. The IBA for each Peach Bottom unit is a postulated pipe rupture small enough that rapid reactor depressurization will not occur but large enough that the high pressure coolant injection (HPCI) system cannot maintain reactor vessel water level.

The high drywell pressure resulting from the postulated accident conditions trips the reactor. The sequence of events following this trip can lead to closure of the main steam line isolation valves (MSIVs) because of low reactor water level. The closure of the MSIVs results in an increase in reactor pressure vessel pressure that is relieved by opening the SRVs.

Following the postulated break, steam fills the drywell causing the drywell pressure to increase slowly and displace the water initially in the submerged portion of the vent system into the suppression pool. The drywell pressure transient is sufficiently slow that the dynamic effect of water clearing in the vents is negligible. The subsequent clearing of air from the vent system occurs more slowly than for the DBA and thus imparts lower loads on the wetwell components. As the flow of air, steam, and water continues from the drywell to the wetwell, the pressure increases in the wetwell air space. Following the initial purge of air from the drywell, steam begins to flow through the vent system and condenses within the suppression pool. As with the DBA event, the condensation oscillation and chugging phenomena occur during the steam condensation process.

The automatic depressurization system (ADS) actuates at approximately 300 seconds after the accident because of the high drywell pressure and the low reactor water level caused by an IBA for a plant with turbine driven feedwater pumps (Reference 12), which is the case for Peach Bottom. The reactor is depressurized approximately 200 seconds after the ADS is initiated. Thus, the IBA is evaluated to 500 seconds. During operation of the ADS, steam from the RPV is vented directly to the suppression pool via the SRV discharge lines. As the reactor depressurizes, the core spray systems and the low pressure coolant injection (LPCI) mode of the RHR system are activated to flood the RPV and cool the core. Eventually, water cascades into the drywell causing steam condensation and drywell depressurization. As the drywell depressurizes below the pressure within the wetwell air space, the wetwell to drywell vacuum breakers open, equalizing the containment pressures and terminating the event. Because the reactor depressurization transient is slower for the IBA than for the DBA, more

decay heat is discharged into the suppression pool, which results in the suppression pool temperature being higher for the IBA than for the DBA at the time of complete reactor depressurization.

3.3 SMALL BREAK ACCIDENT

An SBA is defined as a 0.01 square foot steam break. The SBA for each Peach Bottom unit is a postulated pipe rupture in which the fluid loss rate from the reactor system is insufficient to depressurize the reactor and small enough that HPCI operation is sufficient to maintain reactor water level. Following the break, the drywell pressure slowly increases until the high drywell pressure trip setpoint is reached. Following the reactor trip, MSIV closure may occur due to the water level transient in the reactor. If the main steam lines isolate the reactor system, pressure increases and the SRV opens intermittently to control system pressure.

The drywell pressure increases gradually, depressing the water level in the vents until the water is expelled and air and steam enter the suppression pool. The rate of air flow is such that the air bubbles through the pool without causing pool swell. The steam is condensed and drywell air passes into the wetwell air space. A gradual pressurization of the wetwell results. Eventually, the steam-air flow through the vents results in essentially all the drywell air being transferred into the wetwell.

Condensation oscillation is not present because of the low mass flux but chugging may occur. It is assumed that there will be no operator action for 10 minutes following the pipe break. After 10 minutes, it is assumed that the operator will depressurize the reactor using the ADS. Therefore, the evaluation for chugging load was made only for a period of 600 seconds.

3.4 SAFETY RELIEF VALVE (SRV) DISCHARGE

Each of the 11 SRV discharge lines in Peach Bottom Units 2 and 3 is equipped with a General Electric quencher. The quencher is a perforated sparger consisting of two arms made of 12-inch schedule 80 pipe. Prior to the initial actuation of a safety relief valve caused by a normal

operational transient, the SRV discharge lines contain air at atmospheric pressure and suppression pool water in the submerged portion of the piping and the quenchers. Following an SRV actuation, steam enters the SRV discharge line, compressing the air within the line and expelling the water into the suppression pool. As the water is cleared, the SRV discharge piping undergoes a transient pressure loading. The submerged portion of the line and the quencher also experiences water clearing thrust loads caused by directional changes of momentum within the line and the quencher. The water jets entering the pool from the quencher cause drag loads on submerged structures.

Once the water has cleared from the discharge device, the compressed air enters the pool in the form of high pressure bubbles. These bubbles expand resulting in an outward acceleration of the surrounding pool water. The momentum of the accelerated water results in an overexpansion of the bubbles, causing the bubble pressure to become negative relative to the ambient pressure of the surrounding pool. This negative pressure slows and reverses the motion of the water, leading to a compression of the bubbles and a positive pressure relative to that of the pool. The bubbles continue to oscillate in this manner until they rise to the pool surface. As the bubbles oscillate, the associated local pool motion causes drag loads on nearby submerged structures. The positive and negative pressures developed within the bubbles attenuate with distance and result in a dynamic pressure loading on the submerged portion of the torus shell.

Following water and air clearing from the line, steam is discharged through the line to the suppression pool and condensed therein.

Following the closure of an SRV, pool water reenters the SRV discharge line. A rapid depressurization of the line occurs as the steam remaining in the line is condensed by the in-flowing water. This depressurization causes the water to reflood into the SRV discharge line above its initial level, creating a negative pressure in the pipe. The vacuum breaker valve on the SRV discharge line opens, allowing drywell gas to enter the line to equalize the pressure. The actual reflood water level is limited by the size of the SRV discharge line vacuum breaker.

Section 4
STRUCTURAL ACCEPTANCE CRITERIA

Section 4

STRUCTURAL ACCEPTANCE CRITERIA

The purpose of the Mark I Long Term Program (LTP) was to restore the original intended design safety margins of the structure. This was accomplished by installing necessary hardware modifications and then conducting a plant unique analysis using loads and structural acceptance criteria appropriate for the life of the plant.

The original torus design was based on normal static and seismic loads as documented in the Final Safety Analysis Report (FSAR) (Reference 12). Subsequently, suppression pool hydrodynamic loads, which are described in the Load Definition Report (LDR) (Reference 11), were identified.

The structural acceptance criteria used to evaluate the acceptability of the existing Mark I containment systems and to provide the basis for any modifications required to withstand presently defined loads are generally based on ASME Code, Section III, Division I, through Summer 1977 Addenda (or any later version) (Reference 13). Some alternatives to those criteria are provided in the Plant Unique Analysis Application Guide (Reference 14).

The complete reassessment of the Peach Bottom tori including modifications was based on structural acceptance criteria given in the PUAAG.

The main features of the structural acceptance criteria are explained in this chapter.

4.1 CLASSIFICATION OF STRUCTURAL COMPONENTS

A detailed classification of the structural components of the torus, vent system, and associated piping systems to be analyzed is given in the PUAAG. In summary, the classifications are as follows.

4.1.1 Torus

The torus shell including the ring girders and stiffeners, penetration elements, and attachment welds are Class MC components and are subject to subsection NE of the ASME Code (Reference 13).

4.1.2 Vent System

The main vent, vent header, downcomers, vent to torus bellows, and vent penetration attachment welds are Class MC components and are subject to subsection NE of the ASME Code (Reference 13).

4.1.3 Torus and Vent System Supports

The torus and vent system supports, e.g., columns, saddle plate, and seismic tie including welds and mechanical attachments to the building, are Class MC supports and are subject to rules given in subsection NF of the ASME Code (Reference 13).

4.1.4 Internal Structures

Nonpressure retaining structures such as deflectors are classified as internal structures and were designed in accordance with the rules given in subsection NF of the ASME Code (Reference 13). The catwalk platform grating was designed by rules given by the American Institute of Steel Construction (AISC) (Reference 15).

4.1.5 Piping Systems

External Piping and Supports. Piping external to and penetrating the torus or the external vents including the attachment weld to the torus or vent nozzle is either Class 2 or Class 3. Correspondingly, subsection NF supports for such external piping are either Class 2 or Class 3 component supports.

Internal Piping and Supports. Piping contained within the vents or torus and main steam safety relief valve piping contained within the torus, drywell, or external vents are Class 2 or Class 3. If the piping penetrates the torus or a vent, the attachment weld to the nozzle is a piping weld. Supports for such piping are Class 2 or Class 3 component supports.

Essential and Nonessential Piping Systems. A piping system or a portion of a piping system is essential if during or following the event combination being considered the system is necessary to ensure:

(a) The integrity of the reactor coolant pressure boundary

(b) The capability to shut down the reactor and maintain it in a safe shutdown condition

(c) The capability to prevent or mitigate the consequences of accidents that could result in potential offsite exposure.

Other piping systems are nonessential.

Conservatively, all the piping systems were considered essential in the plant unique analysis.

4.2 SERVICE LEVELS

A description and the consequences of different service levels are given in subsection NCA of the ASME Code and the PUAAG. A brief description of different service levels follows.

4.2.1 Service Level A

This level provides for a complete evaluation of all possible failure modes including fatigue and applies factors of safety consistent with the expectation that the event to which this level is assigned will actually occur; that is, they represent the performance of normal service functions.

Since the occurrence of such events has been anticipated and fully evaluated in the design, no operator action is required should the event occur.

4.2.2 Service Level B

The component or support must withstand these loadings without damage requiring repair. For Class MC vessels and component supports, Level B service limits are the same as Level A service limits. For other components, Level B service limits are the same as those applied to Level A except that the primary stress allowable is increased to account for possible pressure accumulation when relief valves are actuated.

4.2.3 Service Level C

Level C limits permit large deformations in areas of structural discontinuity. The occurrence of stress to Level C limits may necessitate the removal of the component from service for inspection or repair of damage to the component or support.

4.2.4 Service Level D

This level permits gross general deformations with some consequent loss of dimensional stability and damage requiring repair that may require removal of the component from service. This service level is applicable to nonsafety related structural elements.

4.2.5 Service Level E

This level is a special noncode limit applicable to nonsafety related structural elements where element failure may be acceptable if such failure does not result in significant damage to safety related items.

4.3 GENERAL ANALYSIS TECHNIQUES

Structural analyses for hydrodynamic loads were performed in accordance with the methods defined in the Load Definition Report (Reference 11). For those loads considered in the original design (seismic, dead loads), either the results of the original analyses were used or new analyses performed using the methods employed in the original plant design. Details of all analyses are given in the respective chapters that deal with the particular component.

4.4 STRESS COMBINATIONS

For loads resulting from two or more dynamic phenomena, the structural responses were combined in the following manner:

(a) Absolute Sum Method - The absolute sum of the peak stress components computed for the individual loading transients was generally used

(b) CDF Method - If the absolute sum method did not satisfy the structural acceptance criteria, the combined stress intensity value corresponding to 84% probability of nonexceedance from the cumulative distribution function (CDF) was used. The CDF method has been validated for use in the generic reports (Reference 16).

4.5 DAMPING VALUES

In the dynamic analyses it was permissible to use either the damping coefficients given in NRC Regulatory Guide 1.61 (Reference 17) or higher values determined by in-plant tests. For the Peach Bottom plant unique analysis, the conservative values given in the NRC Regulatory Guide were used.

Section 5
LOADS AND LOAD COMBINATIONS

Section 5

LOADS AND LOAD COMBINATIONS

The torus original design load and structural analysis techniques described in the Final Safety Analysis Report (FSAR) remain unchanged. Hydrodynamic loads associated with a LOCA are given in the Plant Unique Load Definition (PULD) Report (Reference 18) and the Load Definition Report (LDR) (Reference 11). SRV discharge loads are based on in-plant test data.

5.1 ORIGINAL DESIGN LOADS

The torus was originally designed based on normal static loads, seismic loads, and the quasi-static pressure loads caused by a LOCA. These loads are defined in Appendix M of the FSAR (Reference 12).

5.2 LOCA LOADS

LOCA loads are caused by a postulated pipe break inside the drywell. The three LOCA categories considered, selected on the basis of postulated break size, were the design basis accident (DBA), intermediate break accident (IBA), and small break accident (SBA). Although the load magnitudes depend on initial system conditions, the sequence of the loading phenomena is the same for all conditions.

5.3 SAFETY RELIEF VALVE ACTUATION

SRV discharge loads are caused by the oscillating air bubble released in the pool. Various system operating conditions (Reference 11) produce loads of varying magnitude and characteristics. Loads for Peach Bottom were defined from in-plant test data.

5.4 DESCRIPTION OF LOAD COMBINATIONS

Load combinations with service levels for a typical Mark I plant are given in Reference 14. Twenty-seven event combinations are identified. These 27 result in a large number of load combinations because different phenomena during LOCA and SRV discharge must be considered individually and separately. This number of design load combinations was reduced to governing sets of load combinations; these sets were assigned service levels applicable to Peach Bottom Units 2 and 3 as given in Tables 5-1 through 5-7. These governing load combinations for the following different structures are:

(a) Torus, bellows, drywell (at vent), attachment welds, torus support, and seismic supports

(b) Vent system including main vent, downcomer, and vent header but excluding vent header penetrations

(c) Vent header penetrations (main vent, downcomers)

(d) Internal supports

(e) Internal structure excluding vent header deflector

(f) Vent header deflector

(g) Internal piping system.

The rationale for the reduced number of design load combinations is:

(a) Chugging loads are the same during SBA, IBA, and DBA. The maximum internal pressure and thermal loads occur during an IBA for the torus. Chugging loads combined with SBA/DBA internal pressure and thermal loads are, therefore, not governing.

Section 5

LOADS AND LOAD COMBINATIONS

The torus original design load and structural analysis techniques described in the Final Safety Analysis Report (FSAR) remain unchanged. Hydrodynamic loads associated with a LOCA are given in the Plant Unique Load Definition (PULD) Report (Reference 18) and the Load Definition Report (LDR) (Reference 11). SRV discharge loads are based on in-plant test data.

5.1 ORIGINAL DESIGN LOADS

The torus was originally designed based on normal static loads, seismic loads, and the quasi-static pressure loads caused by a LOCA. These loads are defined in Appendix M of the FSAR (Reference 12).

5.2 LOCA LOADS

LOCA loads are caused by a postulated pipe break inside the drywell. The three LOCA categories considered, selected on the basis of postulated break size, were the design basis accident (DBA), intermediate break accident (IBA), and small break accident (SBA). Although the load magnitudes depend on initial system conditions, the sequence of the loading phenomena is the same for all conditions.

5.3 SAFETY RELIEF VALVE ACTUATION

SRV discharge loads are caused by the oscillating air bubble released in the pool. Various system operating conditions (Reference 11) produce loads of varying magnitude and characteristics. Loads for Peach Bottom were defined from in-plant test data.

5.4 DESCRIPTION OF LOAD COMBINATIONS

Load combinations with service levels for a typical Mark I plant are given in Reference 14. Twenty-seven event combinations are identified. These 27 result in a large number of load combinations because different phenomena during LOCA and SRV discharge must be considered individually and separately. This number of design load combinations was reduced to governing sets of load combinations; these sets were assigned service levels applicable to Peach Bottom Units 2 and 3 as given in Tables 5-1 through 5-7. These governing load combinations for the following different structures are:

(a) Torus, bellows, drywell (at vent), attachment welds, torus support, and seismic supports

(b) Vent system including main vent, downcomer, and vent header but excluding vent header penetrations

(c) Vent header penetrations (main vent, downcomers)

(d) Internal supports

(e) Internal structure excluding vent header deflector

(f) Vent header deflector

(g) Internal piping system.

The rationale for the reduced number of design load combinations is:

(a) Chugging loads are the same during SBA, IBA, and DBA. The maximum internal pressure and thermal loads occur during an IBA for the torus. Chugging loads combined with SBA/DBA internal pressure and thermal loads are, therefore, not governing.

(b) Pool swell loads are combined with DBA thermal loads and internal pressure according to the load definition; however, pool swell loads occur for only 0.75 second from the start of DBA and thermal loads for this period are negligible. Therefore, thermal loads are not combined with pool swell loads.

(c) Allowable stress intensities for service Levels A and B are the same. If the load combinations with service Level B bound those with service Level A, only load combinations with service Level B need be considered.

(d) Only two different SRV analyses are considered: single-valve and multiple-valve. The single-valve case analysis is performed with a bounding load for cases A1.1, A1.2, and A1.3. Similarly, the multiple-valve case analysis is performed for a bounding load of A3.1, A3.2, C3.1, C3.2, C3.3, and ADS A2.2. No significant SRV actuation occurs during CO and chugging due to a DBA.

These four observations are based on information contained in References 11, 13, 14, and 18.

5.5 LOAD TERMINOLOGY

The following defines the various terms used in Tables 5-1 through 5-7.

Symbol	Definition
N	Normal loads
LOCA	Loss of coolant accident
	LOCA events are indicated by:
	SBA - Small break accident
	IBA - Intermediate break accident
	DBA - Design break accident

T_A	Thermal effects caused by a LOCA
R_A	Pipe reaction caused by a LOCA
P_A	Internal pressure caused by a LOCA
OBE	Operating basis earthquake loads
SSE	Safe shutdown earthquake loads
SRV_m	Safety relief valve discharge loads - multiple-valve
SRV_s	Safety relief valve discharge loads - single-valve
PS	Pool swell loads
CO	Condensation oscillation loads
CH	Chugging loads

Table 5-1

GOVERNING LOAD COMBINATIONS FOR TORUS AND SUPPORT SYSTEM

Combination No.	Service Level	Load Combinations	Column No. in Table 5-1, Ref 14
1	A	$N+SRV_m+IBA(P_A+R_A+T_A)+CH+OBE$	14
2*	A	$N+OBE+DBA(R_A)+PS$	18
3	A	$N+DBA(P_A+T_A+R_A)+CO+OBE$	20
4	C	$N+SRV_m+IBA(P_A+R_A+T_A)+CH+SSE$	15
5	C	$N+SRV_s+DBA(R_A)+PS+SSE$	25
6	C	$N+DBA(P_A+R_A+T_A)+CO+SSE$	27

*(a) Evaluation for fatigue and primary plus secondary stress range is not required.

(b) For a torus shell, the S_m value may be replaced by 1.0 S_m times the plant unique dynamic load factor (DLF).

Table 5-2

GOVERNING LOAD COMBINATIONS FOR VENT SYSTEM

Combination No.	Service Level	Load Combinations	Column No. in Table 5-1, Ref 14
1	A	$N+SRV_m+IBA/SBA(P_A+R_A+T_A)+CH+OBE$	14
2*	A	$N+OBE+DBA(R_A)+PS$	18
3	A	$N+DBA(P_A+R_A+T_A)+CO+OBE$	20
4	C	$N+SRV_m+IBA/SBA(P_A+R_A+T_A)+CH+SSE$	15
5	C	$N+SRV_s+DBA(R_A)+PS+SSE$	25
6	C	$N+DBA(P_A+R_A+T_A)+CO+SSE$	27

*(a) Evaluation for fatigue and primary plus secondary stress range is not required.

(b) For the pool swell impingement region of the vent system, allowable stresses may be increased to service Level C.

Table 5-3

GOVERNING LOAD COMBINATIONS FOR VENT HEADER PENETRATION

Combination No.	Service Level	Load Combinations	Column No. in Table 5-1, Ref 14
1	A	$N+SRV_m+IBA/SBA(P_A+T_A+R_A)+OBE$	12
+ 2	A	$N+SRV_m+IBA/SBA(P_A+T_A+R_A)+CH+OBE$	14
+ 3*	A	$N+DBA(R_A)+PS+OBE$	18
+ 4	A	$N+DBA(P_A+R_A+T_A)+CO+OBE$	20
5	C	$N+SRV_m+IBA/SBA(P_A+T_A+R_A)+CH+SSE$	15
6	C	$N+SRV_s+DBA(R_A)+PS+SSE$	25
7	C	$N+DBA(P_A+R_A+T_A)+CO+SSE$	27

*(a) Evaluation for fatigue and primary plus secondary stress range is not required.

(b) For the pool swell impingement region of the vent system, allowable stresses may be increased to service Level C.

(c) For local membrane stress intensity and primary membrane plus bending stress intensity, the S_m values may be increased to 1.3 S_m.

Table 5-4

GOVERNING LOAD COMBINATIONS FOR INTERNAL SUPPORTS

Combination No.	Service Level	Load Combinations	Column No. in Table 5-1, Ref 14
1	A	$N+SRV_m+IBA(P_A+T_A+R_A)+CH+OBE$	14
2	A	$N+DBA(R_A)+PS+OBE$	18
3	A	$N+DBA(P_A+T_A+R_A)+CO+OBE$	20
4	C	$N+SRV_m+IBA(P_A+T_A+R_A)+CH+SSE$	15
5	C	$N+SRV_s+DBA(R_A)+PS+SSE$	25
6	C	$N+DBA(P_A+T_A+R_A)+CO+SSE$	27

Table 5-5

GOVERNING LOAD COMBINATIONS FOR
INTERNAL STRUCTURES (EXCEPT VENT HEADER DEFLECTOR)

Combination No.	Service Level	Load Combinations	Column No. in Table 5-1, Ref 14
1	A	$N+SRV_m+OBE$	2
2	A	$N+IBA(P_A+T_A+R_A)+CH$	5
3	C	$N+SRV_m+SSE$	3
4	C	$N+IBA(P_A+T_A+R_A)+OBE+CH$	8
5	C	$N+IBA(P_A+T_A+R_A)+SRV_m+CH$	11
6	D	$N+IBA(P_A+T_A+R_A)+CH+SSE$	9
7	D	$N+IBA(P_A+T_A+R_A)+CH+OBE+SRV_m$	14
8	E	$N+IBA(P_A+T_A+R_A)+CH+SSE+SRV_m$	15
9	E	$N+DBA(R_A)+PS+SRV_s+SSE$	25
10	E	$N+DBA(P_A+R_A+T_A)+CO+SSE$	27

Table 5-6

GOVERNING LOAD COMBINATIONS FOR VENT HEADER DEFLECTOR

Combination No.	Service Level	Load Combinations	Column No. in Table 5-1, Ref 14
1	A	$N+SRV_m+OBE$	2
2	A	$N+IBA(P_A+R_A+T_A)+CH$	5
3	C	$N+SRV_m+SSE$	3
4	C	$N+IBA(P_A+R_A+T_A)+CH+OBE$	8
5	C	$N+IBA(P_A+R_A+T_A)+SRV_m+CH$	11
6	D	$N+IBA(P_A+R_A+T_A)+CH+SRV_m+SSE$	15
7	D	$N+DBA(R_A)+PS+SRV_s+SSE$	25
8	D	$N+DBA(P_A+R_A+T_A)+CO+SSE$	27

Table 5-7

GOVERNING LOAD COMBINATIONS FOR INTERNAL PIPING SYSTEMS

Combination No.	Service Level*	Load Combinations	Column No. in Table 5-2, Ref 14
1	B	$N+SRV_m$	1
2	$B_{(3)}$	$N+SRV_m+SSE$	3
3	$B_{(3)}$	$N+SBA(P_A+T_A)+CH+SRV_m$	11
4	$B_{(4)}$	$N+SBA(P_A+T_A)+CH+SRV_m+SSE$	15
5	$B_{(4)}$	$N+IBA(P_A+T_A)+CH+SRV_m+SSE$	15
6	$B_{(4)}$	$N+DBA(P_A)+PS+SRV_s+SSE$	25
7	$B_{(4)}$	$N+DBA(P_A+T_A)+CO+SSE$	27
8	$B_{(4)}$	$N+DBA(P_A+T_A)+CH+SSE$	27

* (a) Service Levels $B_{(3)}$ and $B_{(4)}$ are the same as given in Reference 14.

Section 6
STRUCTURAL EVALUATION OF THE TORUS

Section 6

STRUCTURAL EVALUATION OF THE TORUS

The torus was originally designed for normal loads and pressures caused by a postulated LOCA. Since then, several modifications have resulted in mitigated loads and increased load carrying capacity of the torus. The modified torus was analyzed for the recently defined hydrodynamic loads and was evaluated against the structural acceptance criteria. The details of structural modifications, methods of load calculation, methods of structural analysis, and results of the structural evaluation follow.

6.1 DESCRIPTION OF STRUCTURES AND MODIFICATIONS

The torus is a steel toroidal pressure vessel with a major radius of about 56 feet and a cross-sectional diameter of 31 feet (Figure 2-1). It is about half full of water to quench the steam released during a LOCA and/or an SRV discharge.

The torus is constructed of 16 similar mitered bays. It is supported by ring girders welded at evenly spaced intervals to the inner surface of the shell at 16 locations, 32 columns (two each per ring girder), and 16 saddle supports. The saddles were added subsequent to the initial phase of the Short Term Program to provide additional structural capability over the original design. The columns and saddles rest on lubrite plates and carry the dead weight of the structure and the suppression pool water. Recently, each column was anchored to the foundation to resist uplift. To allow radial expansion of the torus caused by a temperature change, the saddles and columns are permitted to slide in the direction radial to the reactor pressure vessel. Seismic and other net horizontal loads are resisted by four equally spaced seismic ties located at the bottom of the torus and connected to the basemat.

The top half of the shell is 0.604 inch thick and the bottom half is 0.675 inch thick. Details of the columns and saddles are given in Table 2-1.

Four major modifications were made to the torus. They are the installation of the (a) quencher to reduce SRV discharge loads, (b) torus tie downs to resist uplift and a saddle, (c) shell stiffeners to increase the allowable compressive stresses and thus reduce the potential for local shell buckling, and (d) torus nozzle stiffeners to increase the load carrying capacity of the nozzles that connect the externally attached pipes to the torus.

Photographs of the items are shown in Figures 6-1 through 6-4. Figure 6-5 is a composite of the major modifications made to the torus and vent system. A brief summary of each of the above items is given below.

6.1.1 SRV Quencher and Supports

In the event of an SRV discharge, the steam-air mixture is conducted through the discharge piping into the suppression pool. The ramshead discharge device was replaced by a quencher discharge device. The quencher is a perforated sparger consisting of two arms made of 12-inch schedule 80 pipe. The quencher mitigates the hydrodynamic loads on the torus shell and eliminates unstable steam condensation.

A quencher was installed on each of the 11 discharge lines inside the torus. Each quencher is supported at a ring girder near the vertical centerline of the torus. Each of the two arms of a quencher is supported by a system of guides and support beams connected to the ring girder. Figures 6-6 through 6-8 show the quencher locations and their support details.

The following modifications were performed in conjunction with the installation of the quencher.

(a) Addition of a new 8-inch vacuum breaker in the SRV discharge piping in the drywell

(b) Attachment of elbows to the two RHR discharge lines to facilitate circulation of water inside the torus

(c) Installation of thermowells at 13 locations to monitor the temperature distribution during an extended SRV blowdown.

6.1.2 Torus Tie Downs

Figure 6-9 shows a typical torus tie down. The column base was anchored to prevent the torus from moving upward because of the combined effects of an earthquake, LOCA, and SRV discharge loads. The modification to each of the 32 supports typically consisted of attaching gusset plates and stiffener plates near the bottom of the columns. The columns were then anchored with four 2-inch diameter rock bolts to the existing concrete basemat.

6.1.3 Torus Shell Stiffeners

T-shaped shell stiffeners were added to increase the allowable compressive stresses and thus reduce the potential for local buckling of the shell due to hydrodynamic loads. The stiffeners consist of rolled steel tee-sections (WT6x25) attached circumferentially around the outside of the torus shell. These stiffeners extend to 30° above the horizontal centerline on the outer side of the torus and to 15° on the inner (reactor) side. Figure 6-10 shows the stiffeners.

6.1.4 Torus Penetration Stiffeners

Under hydrodynamic loads, the vibration of the torus shell and the externally attached piping systems imposes forces and moments at the torus-pipe interfaces. At these junctions on the outside of the shell, reinforcements consisting of 3/4-inch plates were added radially and around the pipes. These reinforcements, shown in Figure 6-11, substantially increase the load carrying capacity of the nozzles.

6.2 LOADS USED IN THE TORUS ANALYSIS

Normal and seismic loads are specified in the FSAR (Reference 12). Hydrodynamic loads caused by a LOCA are completely specified in the LDR (Reference 11) and the Peach Bottom PULD (Reference 18). The methods of

calculating plant unique SRV loads are also described in the LDR. The specific loads applicable to the Peach Bottom torus and used in the plant unique analysis are summarized below.

6.2.1 Normal Loads

Normal loads include the dead load, live load, and seismic load. The specific magnitudes of these loads are:

Dead Load. The dead load includes the weight of the structure, the weight of the water, and the support reaction.

Live Load. The live load includes 75 pounds per square foot (psf) loads on walkways.

Seismic Load. Horizontal seismic loads are:

Operating basis earthquake (OBE) = 0.05g
Safe shutdown earthquake (SSE) = 0.12g

Vertical seismic loads are 2/3 of horizontal seismic loads.

The OBE horizontal ground response spectra are shown in Figure 6-12.

Other Loads. The maximum external pressure under normal operating conditions is 2 psig.

The original design, in addition to the above, considered the pressure and other loads associated with a LOCA on a quasi-static basis.

6.2.2 LOCA Loads

Three distinct phases of a postulated LOCA can be identified. They were discussed in detail in Section 3. The three phases are pool swell during the air clearing phase, condensation oscillation during periods of high steam mass flow rate, and chugging during periods of low steam mass

flow rate. Each of the three phases imparts distinctly characteristic dynamic pressures on the shell. The origin and methods of calculating plant unique loads are discussed in detail in the LDR. The plant unique loads are summarized here.

6.2.2.1 Pool Swell Loads

During a postulated LOCA, the torus shell is subjected to two types of pressure transients: (1) submerged pressure transients caused by the downward pressure of water on the wetted area of the torus shell and (2) torus air space pressure transients caused by compression of the air space above the pool surface.

The definition of these two types of torus shell pressure transients was based on test data obtained from the Quarter Scale Test Facility (QSTF) and the 1/12 Scale Test Facility. The methodology used for applying the test data to this analysis is described in Reference 11. Plant unique test data and test results for specific loading conditions are contained in Reference 18. The test results were based on a two-dimensional model. Additional margins were incorporated to account for three-dimensional effects. These adjustments to the test results were based on empirical scale factors. Different scale factors were applied to the download phase and the upload phase of the transient.

6.2.2.2 Submerged Pressure Transients

The basis for the definition of submerged torus shell loads is the "average submerged pressure." The average submerged pressure is the "base" pressure used in determining the pressure history at any submerged point in the torus shell. This is plant unique and is based on QSTF and 1/12-scale test results. Figure 6-13 shows the plant unique average submerged pressure transient for Peach Bottom Units 2 and 3. These QSTF average pressures are adjusted by margins based on empirical relations defined in Reference 11. This additional margin works out to be 21.2% of the net download for the download phase of the transient.

6.2.2.3 Air Space Pressure Transients

The torus air space pressure transients are also based on QSTF tests. The plant unique pressure transient for this portion of the torus shell is shown in Figure 6-14. The magnitude of the QSTF pressure transient for the upload phase was increased by an additional margin of 21.5% of the net upload. The upload additional margin was applied only to that portion of the transient representing the upload phase, starting from the beginning of the upload phase to the end of the transient.

Figure 6-15 shows the adjusted pressure transients in the wetted surface and air space.

6.2.2.4 CO and Chugging Loads

CO and chugging loads are cyclic in nature whereas the pool swell load is a transient. Plant unique CO and chugging loads are defined in the LDR.

6.2.3 SRV Discharge Loads

SRV discharge loads on the torus are transient pressures on the submerged portion of the shell. The SRV discharge phenomenon is briefly described in Section 3. The method of defining the SRV discharge load is given in the LDR. It provides two alternative methods of calculating torus shell loads. They are:

(a) Calculation of shell pressures using the General Electric program QBUBS

(b) Calculation of shell pressures using in-plant SRV test data.

For Peach Bottom, the latter method was used. A detailed test program was conducted in Peach Bottom Unit 2 after the quenchers were installed. Shell pressures and structural responses were measured. The General Electric fluid model QBUBS which calculates the torus shell pressures was calibrated to calculate interface shell pressures. The calibrated program was then

used to calculate design case pressures. A 22.5° segment of the torus structural model was created and verified against the measured structural response. This model was then used to calculate the response under design case SRV discharge loads for the plant unique analysis.

6.2.3.1 In-Plant SRV Discharge Tests

Sixteen tests were conducted, out of which 13 were single-valve actuations and three were two-valve actuations. The test plan is given in Table 6-1. The tests consisted of actuating four different SRVs. The tests represent 12 first (cold) and four subsequent (hot) actuations. Subsequent actuations refer to the hot pipe only with a normal water level.

The objective of these tests was to obtain baseline plant specific information on interface pressures and the torus response due to an SRV discharge for use in the plant unique evaluation. The instrumentation chosen to acquire this data included pressure transducers, strain gages, displacement transducers, accelerometers, and a thermocouple.

Because the SRV discharge line routing is similar in three of the four quadrants of the torus (Figure 6-6), only one quadrant was instrumented with bay 15 designated as the test bay. One of the shortest lines, G, the longest line, K, and line H all discharge into this area. The majority of the instrumentation was located there. Two pressure transducers were located in the adjacent bay 14. The torus support between bays 14 and 15 was instrumented to determine support responses. The 24-inch nozzle for the RHR pump suction C adjacent to quencher G in bay 16 was also instrumented.

To ensure repeatability of the data base, a special air bleed valve was installed on the discharge lines that were planned to be tested more than once. This system ensured that the water leg in the discharge line was at the normal level prior to each test.

The transducers were wired to signal conditioning equipment in the vicinity of the containment. All outputs were simultaneously recorded on the Sangamo pulse code modulated data acquisition system (primary) and on the Data General computer system (secondary). All data were reduced and converted to engineering units using the Data General computer.

Pressure Gages. Eleven Sensotec pressure transducers were used in the test. Two were mounted in bay 14 and none were mounted in the test bay. The transducers were mounted as shown in Figure 6-16.

In addition, differential pressure transducers were installed on SRV discharge pipes G, H, and K. The pressure taps were placed 12 inches above the nominal water level and 3 feet below the water level. These transducers were used to ensure that the water in the individual SRV lines returned to its normal level following valve actuation so that the subsequent actuation could be conducted with a known water level.

Strain Gages. A total of 76 single weldable strain gages was installed for the test. Sixty-six of the gages were mounted to form 22 (3-gage) strain rosettes. The remaining 10 were used as single axis gages. Eleven of the strain rosettes were mounted on the outside surface of the torus shell in bay 15 between SRV lines H and K. The remaining 11 strain rosettes were installed on the inside surface of the torus shell at corresponding locations. The strain rosettes were located in a plan similar to that of the pressure transducers. Figure 6-17 shows the locations of the strain gages.

Four uniaxial strain gages were mounted outside of the torus on the 24-inch RHR pump suction nozzle C. These gages were located to determine bending and thrust loads in the piping attached to the torus. Six uniaxial strain gages were mounted on the torus support under SRV discharge line K. Locations were selected to determine the column load and the load distribution between the column and saddle support.

In addition to pressure and strain gages, displacement gages and accelerometers were used at selected locations to measure deflections and accelerations respectively.

Data Recording and Digitizing Systems. All the transducer signals were recorded in digital form during the test using a pulse code modulated data acquisition system. Selected channels were also plotted in analog form on a 6-inch oscillograph.

Sensor Calibration. All the sensors were installed when the torus was drained. The sensors used for this test were calibrated prior to refilling the torus. Zero levels were established prior to each test run. Thus, only dynamic oscillations about the zero level were measured.

Test Plan and Procedure. The test procedure consisted of actuation of the SRVs in a preselected sequence, with data being recorded by the instrumentation system described here. All valve actuations were effected manually by the plant operators. The tests were performed with the reactor near nominal operating pressure (975 psi) between 39.5% and 50% power. No drywell to wetwell differential pressure existed during the tests.

6.2.3.2 Summary of Test Results

(a) The maximum measured pressures were +10.2 psi and -6.3 psi for the two-valve cases. The maximum pressure for the single-valve actuation was found to be +9.3 psi and -5.9 psi for the subsequent actuation.

(b) The measured peak pressure values for the two-valve cases were only slightly higher than those for the single-valve cases. The addition of pressures by the absolute sum method was very conservative. Summing by the square root of the sum of the squares (SRSS) method is somewhat less conservative. The SRSS sum multiplied by 1.2 bounds all test data.

(c) The pressure magnitude and distribution were repeatable.

(d) The pressure distribution was symmetric about the centerline of the quencher.

(e) The pressures in the test bay caused by valve actuation 90° away were negligible.

(f) The maximum pressure with the T-Quencher was approximately three times lower than the value measured with a ramshead (Reference 19).

(g) The dominant frequencies of measured shell pressures for the cold pipe were found to be 6.1 Hz and 7.0 Hz for lines K and H respectively. The corresponding frequencies for the hot pipe were found to be 10.2 Hz and 10.5 Hz for lines K and H respectively.

(h) The frequency of the dynamic pressure increased as the line length decreased. The frequency values were 6.1 Hz and 7.0 Hz for line K (154 feet long) and line H (113 feet long) respectively.

(i) The frequency of the dynamic pressure increased as the temperature of the SRV line increased from cold to hot.

(j) The maximum measured hoop stress was 4.2 ksi for the two-valve case. The maximum measured hoop stress for the single-valve case was 3.0 ksi.

(k) The maximum measured axial stress was 3.7 ksi for the two-valve case and 3.3 ksi for the single-valve case. These values were measured near the ring girder and at the bottom of the shell.

(l) The maximum measured stress in the ramshead test in Peach Bottom Unit 2 (Reference 19) was as high as 13 ksi. Thus, the installation of quenchers near the centerline of the torus reduced the stress approximately by a factor of 3.

(m) The maximum stresses in the outside column were measured to be +6660 psi and -960 psi on the two opposite flanges. The maximum stress on the two flanges of the inside column were measured to be 2055 psi and 1080 psi. In the outer column, the bending and axial stresses were 3810 psi and 2870 psi respectively. The corresponding bending and direct stresses in the inner column flanges were 488 psi and 1568 psi, indicating a much lower bending on the inside column.

(n) The maximum axial load and bending moment on the outside column were 118 kips and 646 kip-inches respectively. The corresponding values for the inside column were 64 kips and 84 kip-inches.

(o) The maximum measured shell displacement was 0.11 inch at the bottom of the torus at midbay.

Pressure and Strain Data. Before the test data were plotted on the Calcomp plotter for visual inspection, the digitized data were baseline corrected. All the digitized raw data except the measured displacements were filtered using the Fourier transform technique to eliminate the 60 Hz supply line noise. All pressure test data were plotted on the Calcomp plotter. Stresses were calculated from the measured strains. Power spectral density analyses were carried out for pressure and other response parameters of the shell to determine the dominant frequencies.

Typical plots of pressure and strain time-histories are shown in Figures 6-18 through 6-21. Figure 6-18 is a plot of the pressure time-history of a cold pipe test and Figure 6-19 a similar plot of a hot pipe test. Figure 6-20 is a plot of hoop strain at the bottom of the shell. Figure 6-21 is the time-history plot of strain on the outside column. All strains are measured in micro inches per inch. Figures 6-22 and 6-23 are power spectral density curves for the corresponding pressure time-histories given in Figures 6-18 and 6-19.

The digitized data were scanned to obtain the extreme values, which were plotted along three cross sections and three logitudinal sections to obtain

the spatial peak pressure distribution and its attenuation away from the quencher. A typical spatial pressure distribution at a cross section is shown in Figure 6-24.

6.2.3.3 Calibration of Shell Pressure Model (QBUBS)

Using GE code RVFOR, the maximum pressure at the air/water interface (at the time the water is expelled from the discharge device) and the water clearing time are determined. These two values serve as input to QBUBS.

The pressure time-histories at a location of maximum test pressure were calculated by QBUBS. The code-calculated torus shell pressure time-histories were compared with in-plant test data at corresponding sensor locations. From this comparison, calibration factors were computed to match the largest measured positive peak pressure. The calibration factors for two cold pipe and two hot pipe tests, shown in Table 6-2, vary from a minimum of 1.33 to a maximum of 2.11. Conservatively, the maximum value of 2.11 was used for calculating the design case pressures.

6.2.3.4 Design Pressure Calculation

Due to the nature of an SRV discharge, various loading cases were defined. These cases included single-valve or multiple-valve first or subsequent actuation under normal or accident conditions.

For each of these loading cases, the GE code RVFOR was used to determine the maximum pressure at the air/water interface and the water clearing time for the discharge lines under consideration. These two values were then used in the QBUBS program to obtain torus shell pressures.

The above analyses were performed for the two discharge lines, K (the longest line) and H (one of the shortest lines). The longest line yields the maximum pressure amplitude and lowest frequency and the shortest line yields the highest frequency. From these results, the bounding pressure loads and frequencies were determined for each loading case. The bounding frequencies were adjusted according to the Mark I criteria (Reference 11):

(a) First Actuation - The frequency range was 0.75 times the minimum predicted frequency to 1.25 times the maximum predicted frequency.

(b) Subsequent Actuation - The frequency range was 0.6 times the minimum predicted frequency to 1.40 times the maximum predicted frequency.

The LDR (Reference 11) suggested the use of 65 cubic feet air volume if the line air volume exceeds 65 cubic feet. The air volume of line K exceeded 65 cubic feet; therefore, two QBUBS runs were executed, one run with an air volume of 65 cubic feet and the other with the actual volume. Results from the run with the actual air volume were used because they were more conservative.

The attenuation factors from quencher K to the 16 ring girder locations were calculated by the QBUBS code. Using these attenuation factors, the multiple-valve pressure was calculated. The all-valve case bounds the ADS case; therefore, the all-valve case was used for the analysis. The multiple-valve design case pressure was calculated as 1.2 times the SRSS of pressures due to six adjacent valves. The calculated pressure amplitude for each load case and the frequency band are shown in Table 6-3. For single-valve cases, the bounding amplitudes and frequency values of cases A1.1, A1.2, and A1.3 were used. For multiple-valve cases, the bounding pressure amplitudes and frequency values of cases A3.1, A3.2, C3.1, and C3.2 were used. These pressure amplitudes and frequencies, along with the normalized test time-histories and spatial distributions, were used in the plant unique analysis. This approach is conservative because it assumes that, during multiple-valve actuation, all the air bubbles have maximum pressure.

6.3 ALLOWABLE STRESSES

The allowable stresses for the plant unique evaluation are summarized below. The acceptance criteria were consistent with those specified in the PUAAG (Reference 14).

A component is considered adequate if the stresses meet ASME Code, Section III (Reference 13) limits. Code criteria for the torus and the support system are given in the following sections.

6.3.1 Torus Shell and Ring Girders

Acceptability was established for the torus shell and ring girders in accordance with the criteria for Class MC vessels given in subsection NE of the ASME Code. Specific stress intensity limits that must be satisifed included:

$$P_m < 1.0\ S_m$$

$$P_L < 1.5\ S_m$$

$$P_L + P_b < 1.5\ S_m$$

$$P_L + P_b + Q < 3.0\ S_m\ .$$

Stress on (the throat of) the fillet weld between the ring girders and torus shell may not exceed (0.55) S_m. The welds attaching the torus supports to the torus are considered part of the Class MC pressure boundary and are also subject to the (0.55) S_m limit.

The ASME Code requires that allowable compressive stresses should be based on critical buckling stresses. Critical buckling stresses were calculated based on ASME Code Case N284 (Reference 20) and are as follows:

(a)	Axial compression	10.64 ksi
(b)	Hoop compression (with end pressure)	8.72 ksi
(c)	Shear	15.64 ksi

In addition, the interaction between different compressive stresses was also checked as described in Reference 20.

6.3.2 Torus Support System

Acceptability of the torus support system was established in accordance with criteria for Class MC component supports given in subsection NF of the ASME Code. In the original design, the torus was supported on fabricated W-shaped columns. The design has since been modified by the addition of a full saddle between the original columns.

The original columns are considered as linear component supports. The criteria for linear component supports are given in Appendix XVII of the ASME Code and are similar to those in the AISC Manual (Reference 15), the original code of construction. The capacity of the columns is governed by limits for compressive stresses given in Appendix XVII of the ASME Code.

The added saddle was considered as a plate and shell type of component support. Code provisions that must be satisifed include:

$$\sigma_1 \leq S$$

$$\sigma_1 + \sigma_2 \leq 1.5\ S$$

where σ_1 is membrane stress, σ_2 is bending stress across the plate thickness, and S is the code allowable stress. The capacity of the saddle is governed by the membrane stress limit. Welds between the added saddle and the original columns are governed by subsection NF of the ASME code.

6.3.3 Anchor Bolts

As part of the torus support modifications, rock bolt tie downs were added at each column. The ASME Code allows the manufacturer's recommended design load for the anchor bolts. For the Williams rock bolts, the allowable is two-thirds of the elastic limit estimated by pull-out tests (Reference 21).

6.4 METHODS OF ANALYSIS

The torus is a thin shelled structure partially filled with water. The evaluation of the torus and its components and supports was carried out by different methods of analyses depending on the load definition. The mass of water is about seven times the mass of the torus structure. Therefore, the treatment of the water in the dynamic analysis is critical to obtaining reasonable results. Whether the mass of the fluid is included or not depends on the nature of the load definition. The following summarizes the theory of fluid-structure interaction and the types of analyses used for the LOCA and SRV discharge loads.

6.4.1 Fluid-Structure Interaction

The three methods of fluid-structure interaction (FSI) analyses are shown in Figure 6-25 and discussed below. The finite element technique can be used to obtain the response of a structure with contained fluid. The general formulation, Equation (6.2), considers an elastic structure and an acoustic fluid in which pressure p satisfies the wave equation:

$$\frac{1}{c^2}\left(\frac{\partial^2 p}{\partial t^2}\right) - \left(\frac{\partial^2}{\partial x^2} + \frac{\partial^2}{\partial y^2} + \frac{\partial^2}{\partial z^2}\right) p = 0 \ . \qquad (6.1)$$

The speed of sound in the fluid is represented by c. If both structure and fluid are modeled with finite elements, the matrix equations for the coupled fluid-structure system take the form:

$$\begin{bmatrix} M & O \\ +\rho A^T & Q \end{bmatrix} \begin{bmatrix} \ddot{u} \\ \ddot{P}_T \end{bmatrix} + \begin{bmatrix} K & -A \\ O & H \end{bmatrix} \begin{bmatrix} u \\ P_T \end{bmatrix} = \begin{bmatrix} O \\ F \end{bmatrix} \qquad (6.2)$$

where M and K are the usual structural mass and stiffness matrices, Q is the inertia matrix for the fluid, A is the area matrix converting pressure to force at the fluid-structure interface nodes, and ρ is the fluid's mass density. The matrix H is a pseudo-stiffness matrix and can be developed

based on the standard elastic element formulations by assigning appropriate values for shear modulus and Young's modulus. P_T is the total pressure field. F is the source applied in the fluid. This method corresponds to the source analysis, item (a) in Figure 6-25.

By solving the second of the two equations in (6.2) for a rigid containment, rigid wall pressures P_R can be calculated. By applying the rigid wall pressures P_R, the response of the fluid structure system can be obtained from the following set of equations:

$$\begin{bmatrix} M & O \\ +\rho A^T & Q \end{bmatrix} \begin{bmatrix} \ddot{u} \\ \ddot{P} \end{bmatrix} + \begin{bmatrix} K & -A \\ O & H \end{bmatrix} \begin{bmatrix} u \\ P \end{bmatrix} = \begin{bmatrix} AP_R \\ O \end{bmatrix} \tag{6.3}$$

This corresponds to the rigid wall pressure analysis shown in item (c) in Figure 6-25. Sonin (Reference 22) has proved that the two methods, source and rigid wall pressure analyses, are theoretically equivalent and give exactly the same results.

If compressibility effects are neglected, the matrix equations for the coupled fluid/structure system, Equation (6.3), reduce to (Reference 23):

$$(M + \rho A H^{-1} A^T)\ \ddot{u} + Ku = AP_R . \tag{6.4}$$

Thus, for the case of an incompressible fluid, the effect of the fluid can be represented in terms of added mass. The added mass matrix is given by:

$$M_a = \rho A H^{-1} A^T .$$

However, the product of the added mass matrix and the vector of shell accelerations at the fluid-structure interface is the vector of pressures caused by the fluid/structure interaction. Noting that the algebraic sum of the vector P_R and FSI pressures is the measured wall pressure, the dynamic matrix Equation (6.4) takes the form:

$$\ddot{M}u + ku = \{AP_R - M_a\ddot{u}\} \quad (6.5)$$

This matrix equation represents the analysis of the torus without fluid with measured wall pressures input at the wetted surface of the torus. In other words, this is the dry structure analysis, or item (d) in Figure 6-25. Implementation of the above theory in the NASTRAN computer program is detailed in Reference 23. LOCA loads; namely, pool swell loads, CO loads, and chugging loads defined in the LDR and the PULD, have rigid wall pressures. Therefore, the rigid wall pressure analysis represented by Equation (6.4) was used for LOCA loads. SRV discharge loads for Peach Bottom are based on in-plant test data that include the fluid-structure interaction effects. Therefore, the dry structure analysis represented by Equation (6.5) was used.

6.4.2 Models

Three separate models were used in the plant unique analysis. They are a 22.5° coupled fluid-structure model, a 22.5° dry structure model, and a 90° coarse coupled fluid-structure model. The 90° model was used for seismic analysis. The 22.5° coupled model was used to analyze LOCA loads. The 22.5° dry structure model was used to analyze SRV discharge loads. Figures 6-26 through 6-28 show the computer plots of the models.

6.4.2.1 Coupled Fluid-Structure Model

The coupled model was used for calculating stresses caused by LOCA loads. Because of cyclic symmetry, a 22.5° segment of the torus was considered (Figure 6-26). The model was developed using the NASTRAN computer program (Reference 24). The model has 1090 structural nodes and 1670 fluid nodes. The structure is represented by 1000 quadrilateral and two triangular shell elements. The fluid is represented by 984 hexagonal solid elements. The model includes one ring girder, support columns, one saddle support, and four stiffeners. The shell, webs of support columns, web of ring girder, and saddle support plate between columns were modeled using thin shell elements, QUAD4, available in NASTRAN. All flanges and stiffeners were

modeled using beam elements. The columns and saddle supports can slide in any direction. In the model, only the axial degree of freedom was restrained.

In the circumferential direction, the shell and the web of the ring girder were subdivided into 72 shell elements at 5° spacing. The smaller elements in the vicinity of the ring girder and miter joint permit the accurate determination of local stresses. Symmetric boundary conditions were imposed on the nodes at the radial planes of cyclic symmetry.

The torus contains water to a level about one foot below the horizontal centerline of the torus. The fluid was modeled using 20-node hexagonal solid elements. A total of 984 elements was used to model the fluid. A typical cross section of the fluid model is shown in Figure 6-27. The consistent mass matrix of the water was calculated (Reference 23) and added to the structural nodes.

6.4.2.2 Dry Structure Model

The dry structure model does not include the water. The model is exactly the same as the structural portion of the coupled model. This model was used to calculate the stresses caused by SRV discharge loads.

6.4.2.3 90° Model

Asymmetric loads such as horizontal seismic loads cannot be analyzed using a 22.5° model. Therefore, the coarse 90° model shown in Figure 6-28 was created. It consists of about 1150 nodes and 1200 quadrilateral elements. The fluid mass was lumped at the wetted surface nodes. Two sets of boundary conditions, symmetric-antisymmetric and antisymmetric-symmetric, were used for the seismic loads in two directions.

6.4.2.4 Dynamic Degrees of Freedom

Dynamic degrees of freedom are the same for both the coupled and the dry structural models. The consistent mass for the water and the structural

mass constitute the total mass at any node. The reduced dynamic models were obtained by assigning 325 dynamic degrees of freedom to the 22.5° models. Figures 6-29 and 6-30 show the distribution of the dynamic degrees of freedom. Each of the 14 rings of the analytical model was assigned 16 dynamic degrees of freedom in a radial direction. Eight of the rings (1, 3, 5, 7, 8, 10, 12, 14) were assigned eight dynamic degrees of freedom each in the tangential direction. Six of the above eight rings (except 1 and 14) had four dynamic degrees of freedom, each in the longitudinal direction. An additional 12 dynamic degrees of freedom were assigned to the columns. The remaining 64 dynamic degrees of freedom were assigned to the nozzle attachment points.

6.4.3 Static Analysis

The finite element model was checked by performing static analyses for point loads and uniform pressure. The wave front solution technique was used for the static analyses.

6.4.4 Modal Analysis

The modal analysis was performed to calculate the frequencies and mode shapes of the torus and to understand the dynamic characteristics of the model. A Guyan reduction was used to reduce the large number of static degrees of freedom to 401 dynamic degrees of freedom. A modified Given's method was used to extract the frequencies.

6.4.5 Analysis for LOCA Loads

Pool swell load is transient; CO and chugging loads are cyclic. Accordingly, a transient analysis was performed for the pool swell loads and frequency response analyses were carried out for the CO and chugging loads. Because all the LOCA loads are defined as rigid wall pressures, the coupled model was used for all the analyses.

6.4.5.1 Transient Analysis

A transient analysis was performed for pool swell loads by the direct integration method. A time step of 0.002 second was used. The stresses at critical elements, nodal deflections at important locations and torus penetrations, and reaction forces at all support locations as functions of time were calculated.

6.4.5.2 Frequency Response Analysis

Frequency response analyses were performed for periodic (CO and chugging) loads, which are specified as functions of frequencies from 1 Hz to 50 Hz in 1 Hz increments. If a structural frequency fell within an increment, the analyses were performed at that natural frequency of the structure. The stresses and other response quantities along with their phase differences were calculated. The contributions of all the frequencies were added together to obtain the response due to the specified loads. The load definitions for CO and chugging are similar but the amplitudes are different. Therefore, the results from one set of frequency analyses were ratioed in two different ways to obtain the separate results of the CO and chugging loads.

6.4.6 Analysis for SRV Discharge Loads

SRV discharge load definition requires applying the load at the frequency of highest structural response within the frequency band. The frequency band considered for Peach Bottom was from 4.09 Hz to 13.49 Hz, which conforms to the requirements of the LDR.

6.4.6.1 Frequency Response Analysis

To obtain the frequency of highest response within the band, a frequency response analysis was performed. The measured, normalized SRV discharge pressure shown in Figure 6-24 was applied on the dry structure. Frequency response analyses were carried out for frequencies betwen 1 Hz and 20 Hz at an interval of 1 Hz and at all natural frequencies between 4 Hz and 14 Hz.

Response quantities were calculated at critical locations and plotted as a function of frequency. Three such plots are shown in Figures 6-31 through 6-33. The frequency giving the maximum response was chosen by studying all the calculated response quantities.

6.4.6.2 Transient Analysis

From the analysis described in Section 6.4.6.1, the frequency of highest response within the frequency band was found to be 14 Hz. A transient analysis at this frequency was then carried out. In addition, analyses at the frequencies of 6 Hz and 10 Hz were performed for use in the torus-attached piping analysis. The maximum amplitudes of pressure, as calculated in Section 6.3, for single and multiple valves were used. For single-valve, the peak pressure was 13.67 psi; for multiple-valve, it was 21.34 psi. In both cases, the normalized spatial distributions remain the same. For 6 Hz and 10 Hz, normalized test time-histories were used. For 14 Hz, the test time-history corresponding to 7 Hz was adjusted to 14 Hz and used in the analysis. Transient analyses by direct integration were carried out in all three cases. Stresses at critical locations and column reactions were calculated. Nodal displacements at piping attachments and at a few critical shell nodes were obtained.

6.4.7 Stress Analyses

Results of the static and dynamic analyses were combined in accordance with the applicable load combinations and stress analyses were performed. A special-purpose FORTRAN program was used to calculate the ASME Code membrane and membrane plus bending stress intensities for the selected elements.

The following formulas were used for calculating the principal stresses:

$$\sigma_1 = 1/2\ (\sigma_x + \sigma_y) + \sqrt{1/4(\sigma_x - \sigma_y)^2 + \tau_{xy}^2}$$

$$\sigma_2 = 1/2\ (\sigma_x + \sigma_y) - \sqrt{1/4(\sigma_x - \sigma_y)^2 + \tau_{xy}^2}$$

$$\sigma_3 = \text{Negligible}$$

where

σ_x = normal stress in x direction

σ_y = normal stress in y direction

τ_{xy} = shear stress in x-y plane

$\sigma_1, \sigma_2, \sigma_3$ = principal stresses.

The principal stresses thus calculated were used to compute the stress intensities:

$$S_{12} = \sigma_1 - \sigma_2$$

$$S_{23} = \sigma_2 - \sigma_3$$

$$S_{31} = \sigma_3 - \sigma_1 .$$

The maximum stress intensity used for code stress evaluation was the absolute maximum of S_{12}, S_{23}, and S_{31}. Calculated stress intensities were compared with the code allowable values.

6.5 RESULTS OF ANALYSES

This section presents the results of the static and dynamic analyses. The structural behavior and a comparison of the calculated stresses with allowable stresses are given below.

6.5.1 Static Analyses

Static analyses for the dead weight and unit loads checked the accuracy of the model and the stiffness characteristics of the finite element model. The column reactions for the dead load case were compared with the estimated total weight of the structure. These results compared well and thus verified model accuracy.

6.5.2 Modal Analyses

Modal analyses of the coupled and dry torus shell models were performed to calculate the lowest few frequencies and mode shapes. A comparison of the frequencies is given in Table 6-4. The lowest three frequencies for the coupled model were 14.3, 15.1, and 15.8 Hz. The corresponding frequencies for the dry structure were 17.4, 17.9, and 22.4 Hz. The mode shapes are shown in Figures 6-34 through 6-39. The lowest frequency for the stiffened structure is about twice that of the unstiffened torus. Even the lowest frequency is higher than the highest frequency in the SRV frequency band. Thus, a relatively low response due to SRV loads can be expected.

6.5.3 Structural Evaluation

Figures 6-40 through 6-49 show the following selected response time-histories:

Figure	
6-40	Radial Displacement at Midbay Bottom Center Due to Pool Swell
6-41	Longitudinal Membrane Stress at Midbay Bottom Center Due to Pool Swell
6-42	Hoop Membrane Stress at Midbay Bottom Center Due to Pool Swell
6-43	Inside Column Reactions Due to Pool Swell
6-44	Outside Column Reactions Due to Pool Swell

6-45 Radial Displacement at Midbay Bottom Center Due to SRV Discharge

6-46 Longitudinal Membrane Stress at Midbay Bottom Center Due to SRV Discharge

6-47 Hoop Membrane Stress at Midbay Bottom Center Due to SRV Discharge

6-48 Inside Column Reaction Due to SRV Discharge

6-49 Outside Column Reaction Due to SRV Discharge.

These figures indicate that the responses in general follow the loads. The responses are relatively small.

The results of transient and frequency response analyses were combined in accordance with the governing load combinations and the resulting stress/stress intensity quantities were compared with the acceptance criteria allowable values. Shell stresses, ring girder stresses, stiffener stresses, and column loads were calculated for the torus and its support system.

Stress intensities as functions of time were calculated from the shell stresses. The peak values were compared with the ASME Code intensity allowable values. Longitudinal and hoop compressive stresses were compared with the code compressive allowable values. The stress intensity comparisons are given in Table 6-5. Compressive stress comparisons are given in Table 6-6. Tables 6-7 and 6-8 show stress intensity comparisons for the stiffeners and ring girders respectively.

A comparison of column and saddle plate stresses is shown in Table 6-9, and Table 6-10 gives a comparison of stresses in the earthquake tie. Note that in all these tables a comparison has been made for two service levels, A and C. This is because, out of all applicable load combinations, certain load combinations require meeting service Level A allowables and the others require meeting service Level C allowable values.

The tables show that all the calculated quantities including the compressive stresses meet the ASME Code allowable values.

6.6 FATIGUE EVALUATION

The torus shell experiences cyclic loads during SRV discharge, LOCA, and earthquake loads. A fatigue evaluation was performed for these cyclic loads. Since the stresses are higher at discontinuities, fatigue evaluation was considered at the junction of the shell and the ring girder, the saddle plate, and the miter joint. A fatigue evaluation was performed in accordance with the requirements of the ASME Code (Reference 13).

A fatigue evaluation was performed for the stresses caused by SRV loads as a normal operating condition and for combined stresses caused by SRV, LOCA, and earthquake (accidental) loads in accordance with load combinations defined in Section 5. Appropriate stress intensification factors were used to obtain the fatigue usage factor. The fatigue usage factor for normal operating conditions was combined with the usage factor for accident conditions. The combined (maximum) fatigue usage factor was calculated to be 0.89.

6.7 EXPANSION BELLOWS

Expansion bellows are flexible connections between the drywell vessel and the torus. These bellows are Class MC components subject to the rules given in subsection NE of the ASME Code (Reference 13).

Bellows expansion joint requirements are given in subsection NE of Reference 13. An elastic stress analysis was performed by the empirical approach given in Standards of the Expansion Joint Manufacturers Association, Inc (Reference 25).

A summary of the stress evaluation of the bellows is given in Table 6-11.

The fatigue usage factor is negligible. The ratio of the internal pressure at which the bellows become unstable to the maximum operating internal pressure should be more than 10 (Reference 13); the calculated ratio is 31.

Table 6-1

RELIEF VALVE DISCHARGE
TEST PLAN

Test No.	Condition	Description
1	SRVc-G	Bay away from test bay - cold
2	SRVh-G	Bay away from test bay - hot
3	SRVc-K	Test bay - longest line - cold
4	SRVh-K	Test bay - longest line - hot
5	SRVc-H	Test bay - shorter line - cold
6	SRVh-H	Test bay - shorter line - hot
7	SRVc-C	4 bays away from test bay - cold
8	SRVc-G	Bay away from test bay - cold
9	SRVc-K	Test bay - longest line - cold
10	SRVh-K	Test bay - longest line - hot
11	SRVc-H	Test bay - shorter line - cold
12	SRVc-K	Test bay - longest line - cold
13	SRVc-HG	Two valves - adjacent bay - cold
14	SRVc-KH	Two valves - test bay - cold
15	SRVc-K	Test bay - longest line - cold
16	SRVc-KH	Two valves - test bay - cold

Test identification

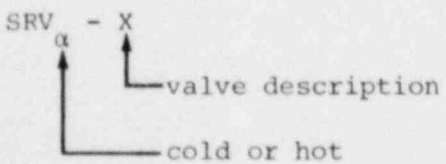

Table 6-2

QBUBS CALIBRATION FACTORS

Sensor Location	Test 3 (long line, cold test)	Test 4 (long line, hot test)	Test 5 (short line, cold test)	Test 6 (short line, hot test)
P2	1.33	2.03	-	-
P6	1.33	2.03	-	-
P12	-	-	2.11	1.74

Table 6-3

DESIGN CASE TORUS PRESSURES AND FREQUENCY RANGES

Load Case	Peak Pressure (psid)	Frequency Range (Hz)
A1.1	6.67	4.09 to 8.49
A3.1	6.67	4.09 to 8.49
A1.3	6.51	4.11 to 8.18
A1.2/A2.2/A3.2	7.53	6.25 to 11.63
C3.1	6.67	3.80 to 10.18
C3.2	7.53	5.31 to 13.49

Table 6-4

TORUS FREQUENCIES

	Frequency (Hz)	
No.	Dry Structure	Coupled Structure
1	17.35	14.28
2	17.90	15.03
3	22.41	15.75
4	22.53	16.27
5	23.15	17.58
6	23.48	17.93
7	27.02	18.19
8	27.56	20.35
9	28.68	20.78
10	29.70	21.32

Table 6-5

TORUS SHELL

SUMMARY OF STRESS INTENSITIES (SI)

Type of Stress Intensity	Service Level A			Service Level C		
	Allowable SI (ksi)	Calculated SI (ksi)	Ratio	Allowable SI (ksi)	Calculated SI (ksi)	Ratio
General Membrane (P_m)	19.30	12.66	0.66	38.00	13.60	0.36
Local Membrane (P_L)	28.95	20.80	0.72	57.00	22.12	0.39
Membrane Plus Bending ($P_L + P_b$)	28.95	14.91	0.52	57.00	17.08	0.30
Primary Plus Secondary ($P_L + P_b + Q$)	57.90	49.26	0.85	NOT APPLICABLE		

Table 6-6

SUMMARY OF STRESS EVALUATION
FOR COMPRESSIVE STRESSES

Type of Stress	Allowable Stress (ksi)	Calculated Stress	
		Due to Positive Pressure (ksi)	Due to Negative Pressure (ksi)
Hoop Compression	8.72	0.00	7.01
Meridional Compression	10.64	3.53	3.40
Shear	15.66	5.33	1.51
Interaction (Ratio)	1.00	0.45	0.84

Table 6-7

TORUS STIFFENERS

SUMMARY OF STRESS INTENSITIES (SI)

Type of Stress Intensity	Service Level A			Service Level C		
	Allowable SI (ksi)	Calculated SI (ksi)	Ratio	Allowable SI (ksi)	Calculated SI (ksi)	Ratio
Local Membrane (P_L)	20.85	13.50	0.65	54.00	13.81	0.26
Primary Plus Secondary ($P_L + P_b + Q$)	41.70	37.69	0.90	NOT APPLICABLE		

Table 6-8

TORUS RING GIRDER

SUMMARY OF STRESS INTENSITIES (SI)

Type of Stress Intensity	Service Level A			Service Level C		
	Allowable SI (ksi)	Calculated SI (ksi)	Ratio	Allowable SI (ksi)	Calculated SI (ksi)	Ratio
General Membrane (P_m)	19.30	13.46	0.70	38.00	15.41	0.41
Local Membrane (P_L)	28.95	14.68	0.51	57.00	18.12	0.32
Membrane Plus Bending ($P_L + P_b$)	28.95	14.05	0.49	57.00	16.29	0.29
Primary Plus Secondary ($P_L + P_b + Q$)	57.90	25.04	0.43	NOT APPLICABLE		

Table 6-9

SADDLE PLATE AND COLUMN
(PLATE TYPE SUPPORT)

SUMMARY OF STRESSES

Type of Stress	Service Level A			Service Level C		
	Allowable Stress (ksi)	Calculated Stress (ksi)	Ratio	Allowable Stress (ksi)	Calculated Stress (ksi)	Ratio
Membrane (σ_1)	19.30	17.30	0.90	23.16	19.11	0.83
Membrane Plus Bending Stress ($\sigma_1 + \sigma_2$)	28.95	18.51	0.64	34.74	20.66	0.59

Table 6-10

SEISMIC (EARTHQUAKE) TIE

(PLATE TYPE SUPPORT)

SUMMARY OF MAXIMUM STRESSES

Type of Stress	Service Level A			Service Level C		
	Allowable Stress (ksi)	Calculated Stress (ksi)	Ratio	Allowable Stress (ksi)	Calculated Stress (ksi)	Ratio
Membrane Stress (σ_1)	19.30	7.36	0.39	23.16	13.08	0.56
Membrane Plus Bending Stress ($\sigma_1 + \sigma_2$)	28.95	7.36	0.25	34.74	13.08	0.38

Table 6-11

EXPANSION BELLOWS

SUMMARY OF STRESS INTENSITIES (SI)

Type of Stress Intensity	Allowable SI (ksi)	Calculated SI (ksi)	Ratio
General Membrane (P_m)	16.40	5.90	0.36
Membrane Plus Bending ($P_L + P_b$)	24.60	8.70	0.35
Primary Plus Secondary ($P_L + P_b + Q$)	49.20	47.90	0.97

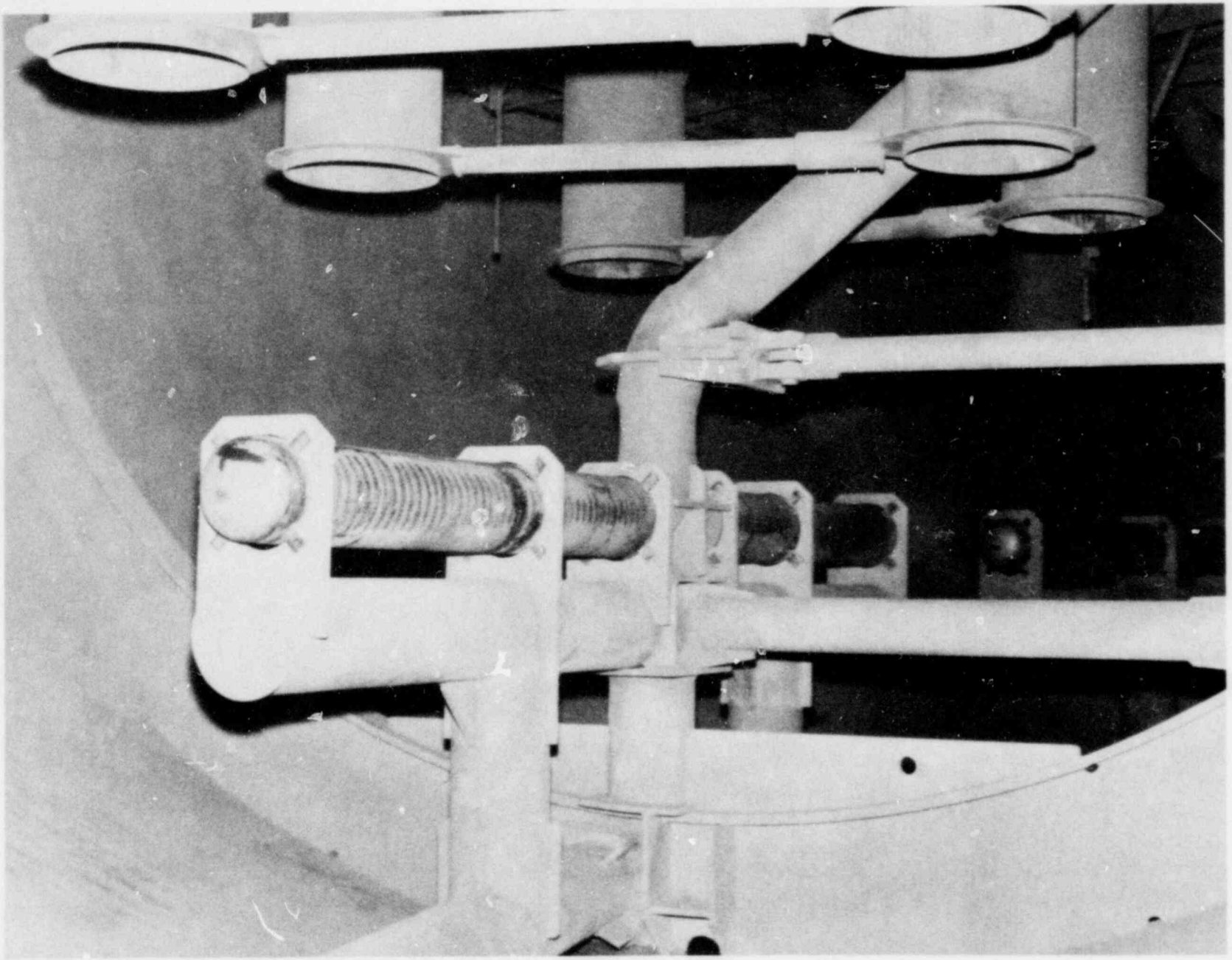

FIGURE 6-1 PICTORIAL VIEW OF T-QUENCHER AND SUPPORTS

FIGURE 6-2 PICTORIAL VIEW OF THE COLUMN TIE DOWN

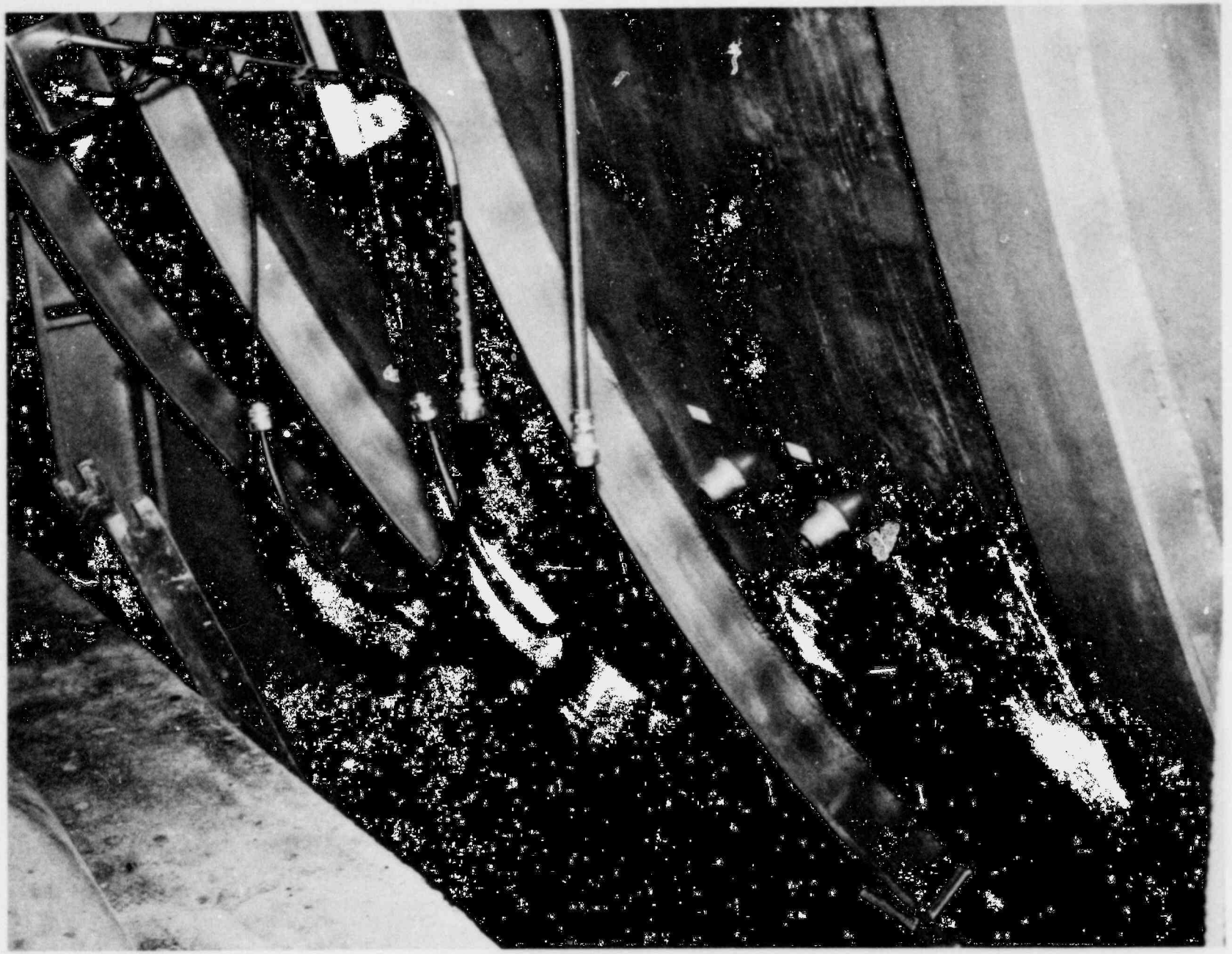

FIGURE 6-3 PICTORIAL VIEW OF THE TORUS SHOWING STIFFENERS AND THERMOWELLS

FIGURE 6-4 PICTORIAL VIEW OF THE TORUS NOZZLE REINFORCEMENT

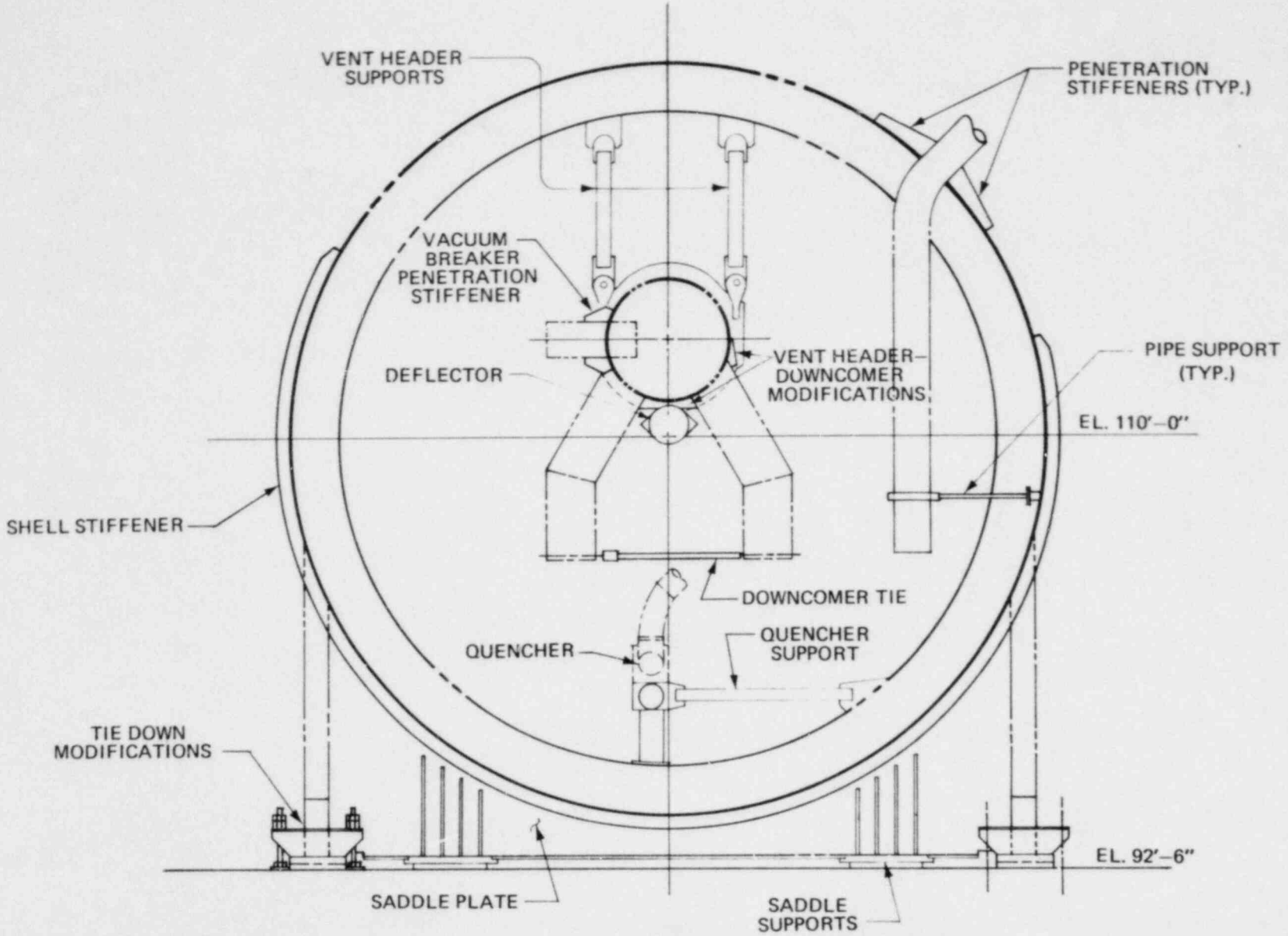

FIGURE 6-5 CROSS SECTION SHOWING MAJOR MODIFICATIONS

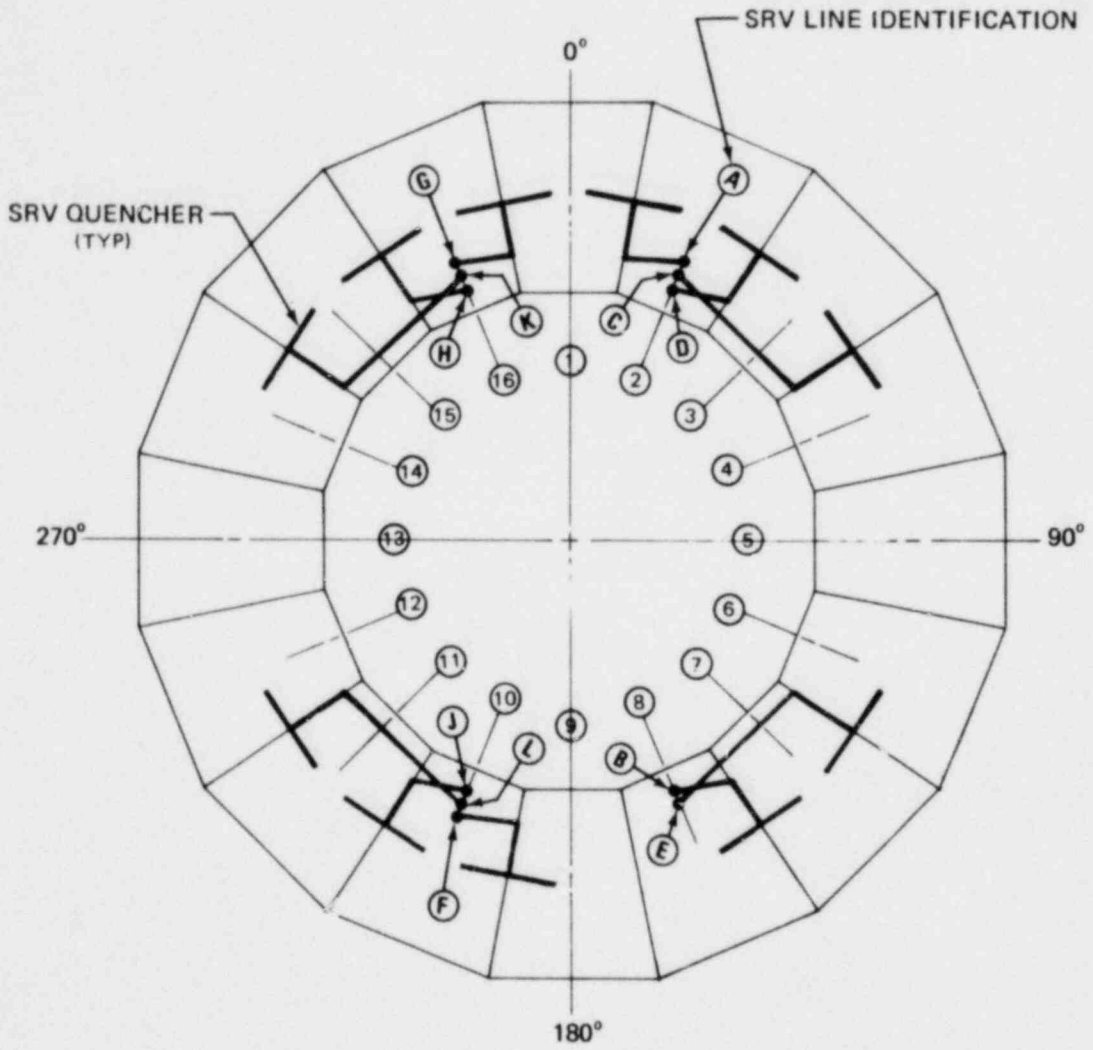

FIGURE 6-6 PLAN OF TORUS SHOWING THE LOCATION OF SRV QUENCHERS

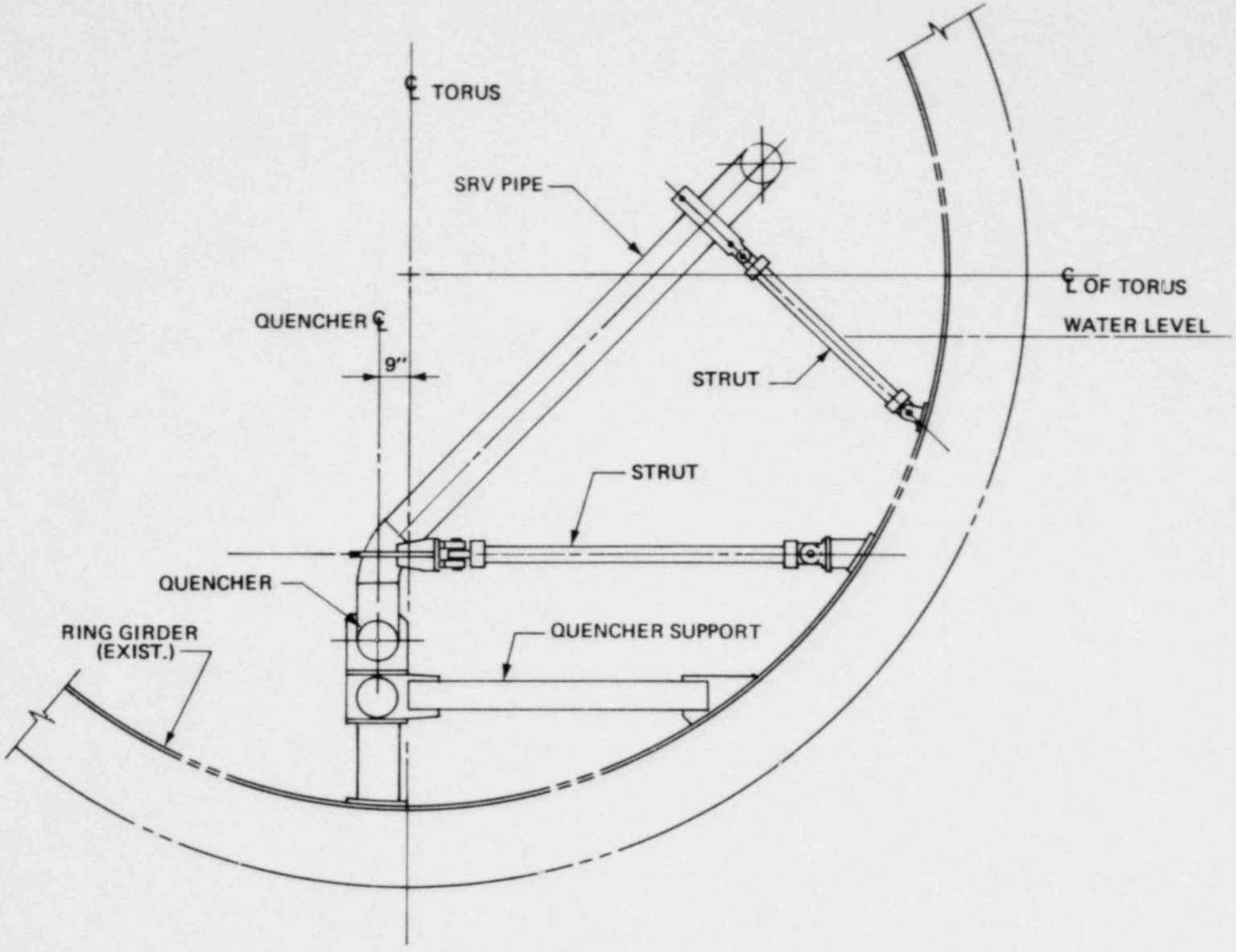

FIGURE 6-7 SRV DISCHARGE LINES AND SUPPORTS INSIDE TORUS

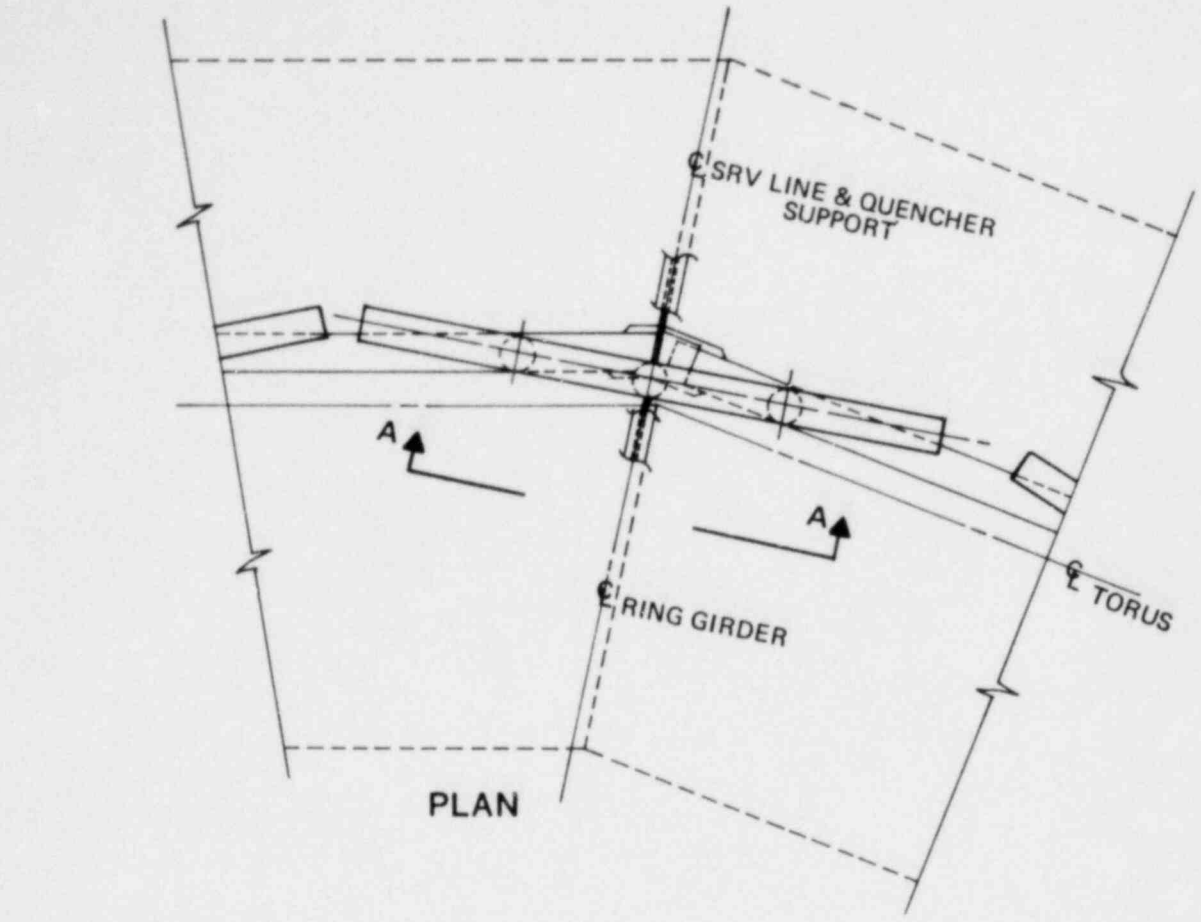

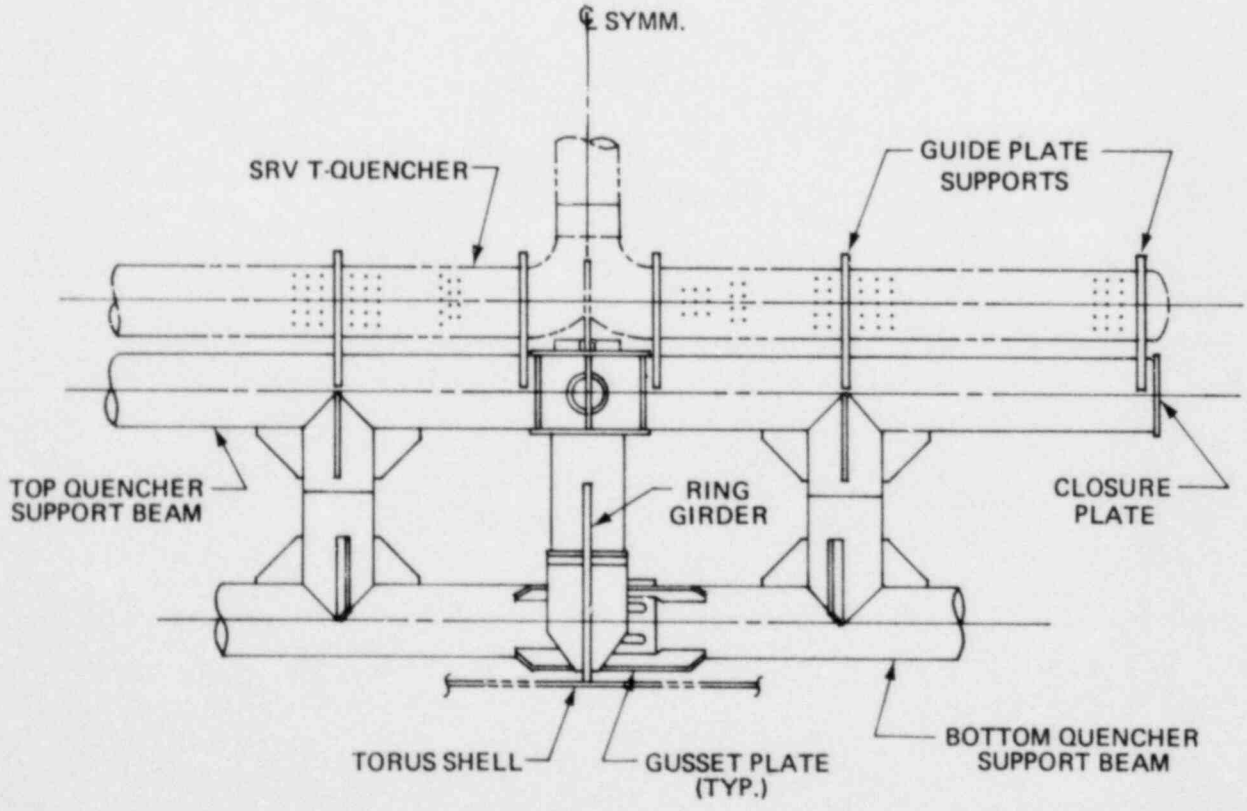

FIGURE 6-8 T-QUENCHER SUPPORT SYSTEM

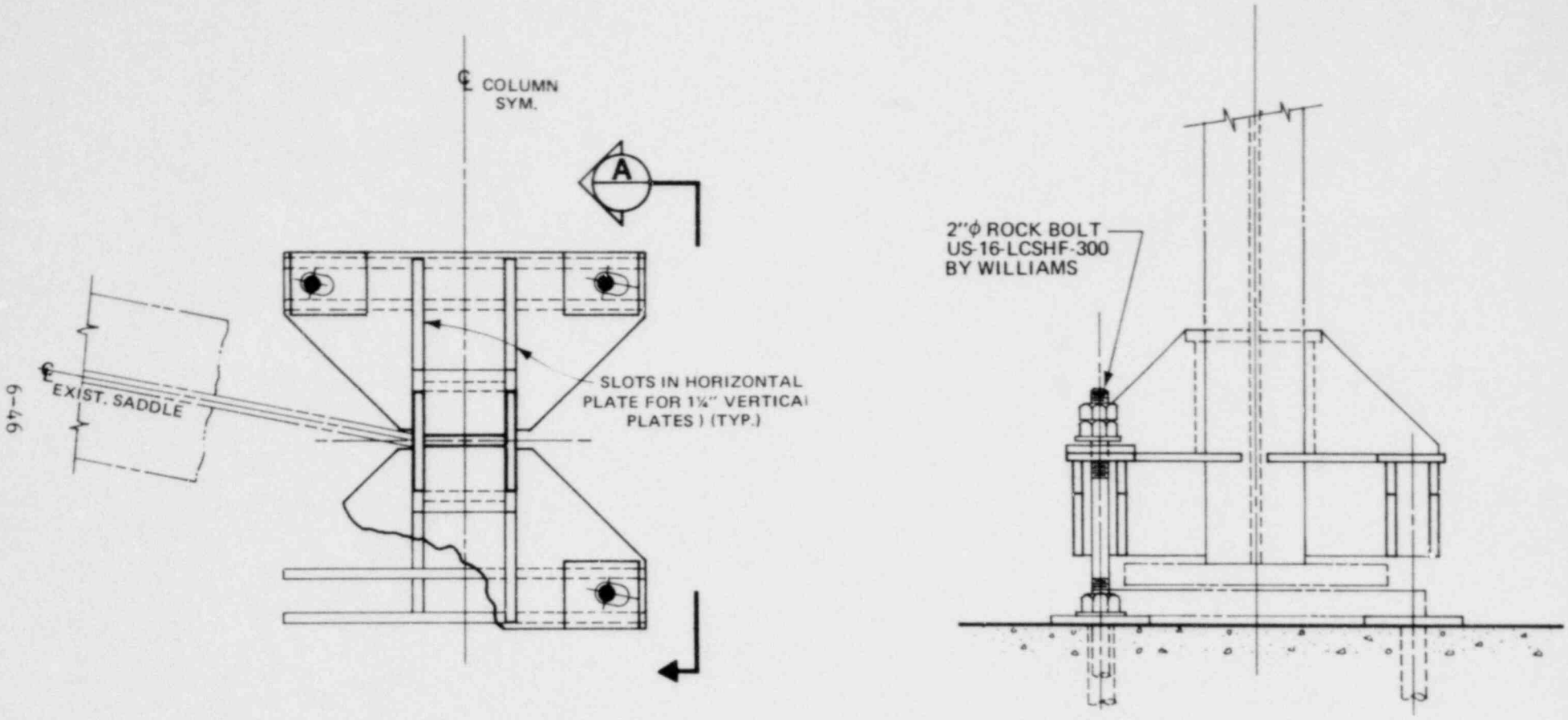

FIGURE 6-9 TYPICAL TORUS TIE DOWN

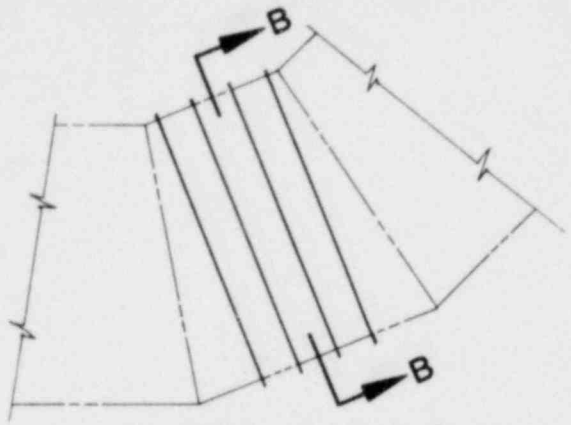

PARTIAL TORUS PLAN

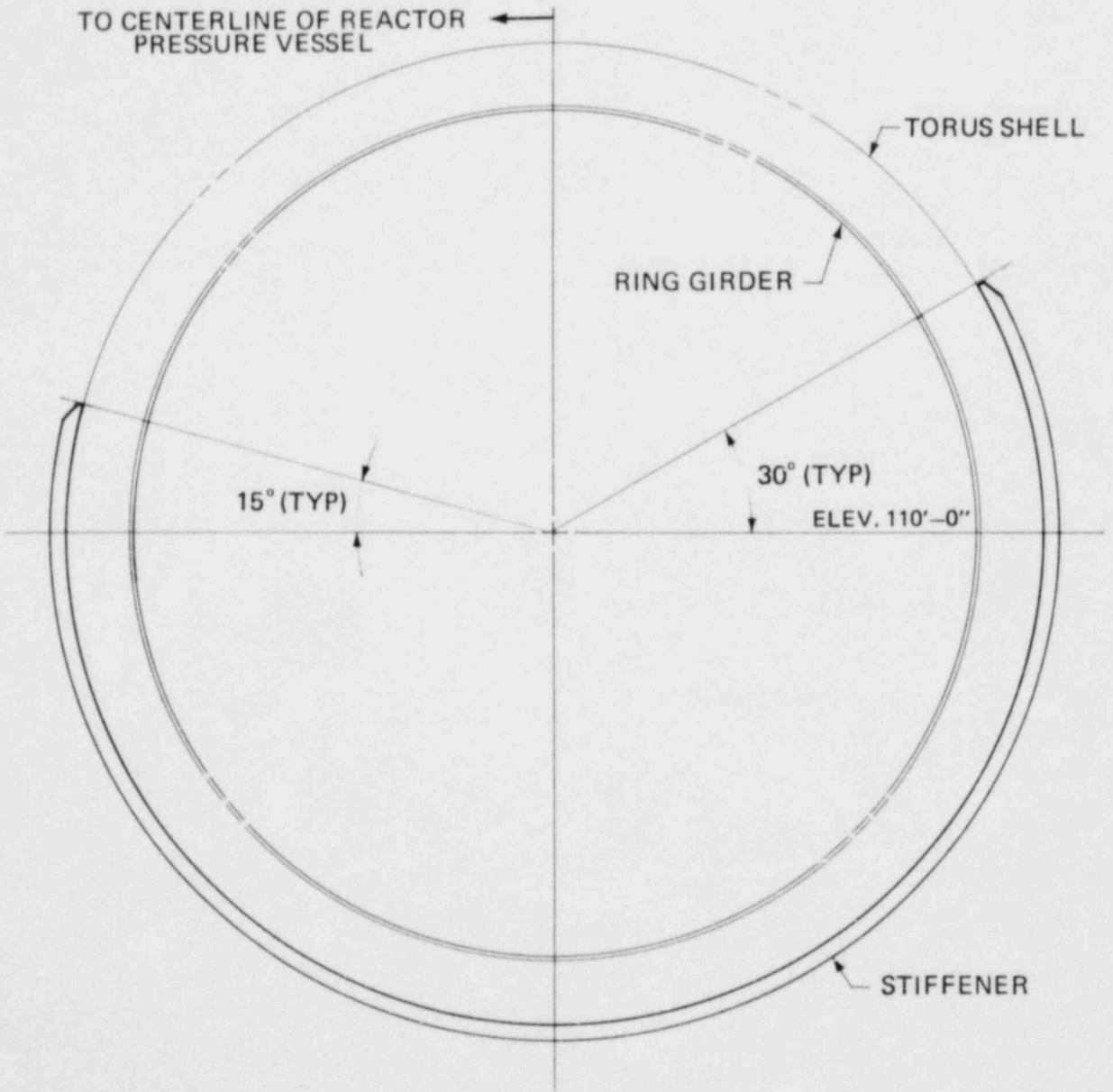

SECTION B–B

FIGURE 6-10 SHELL STIFFENERS

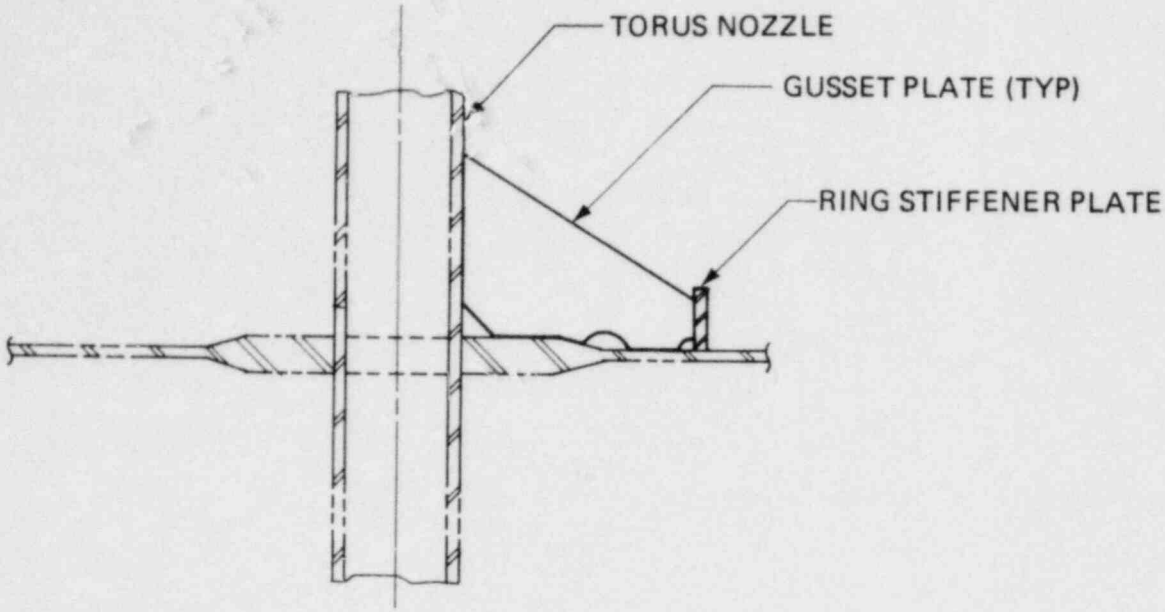

SECTION A–A

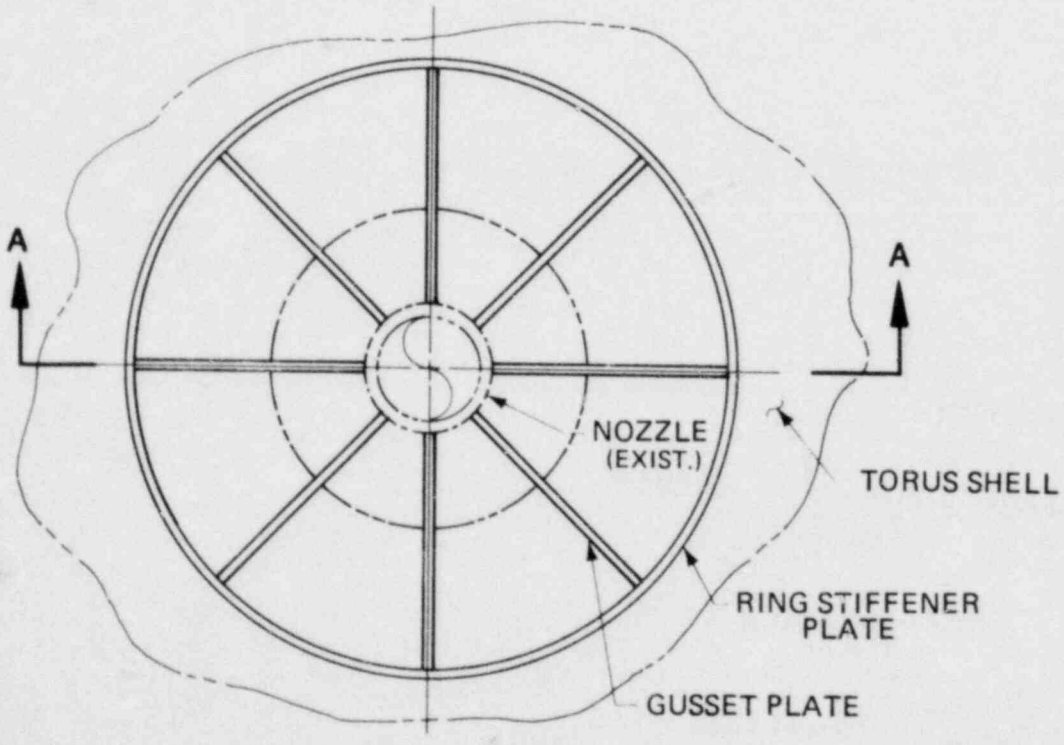

TYP. PLAN

FIGURE 6-11 TYPICAL NOZZLE REINFORCEMENT

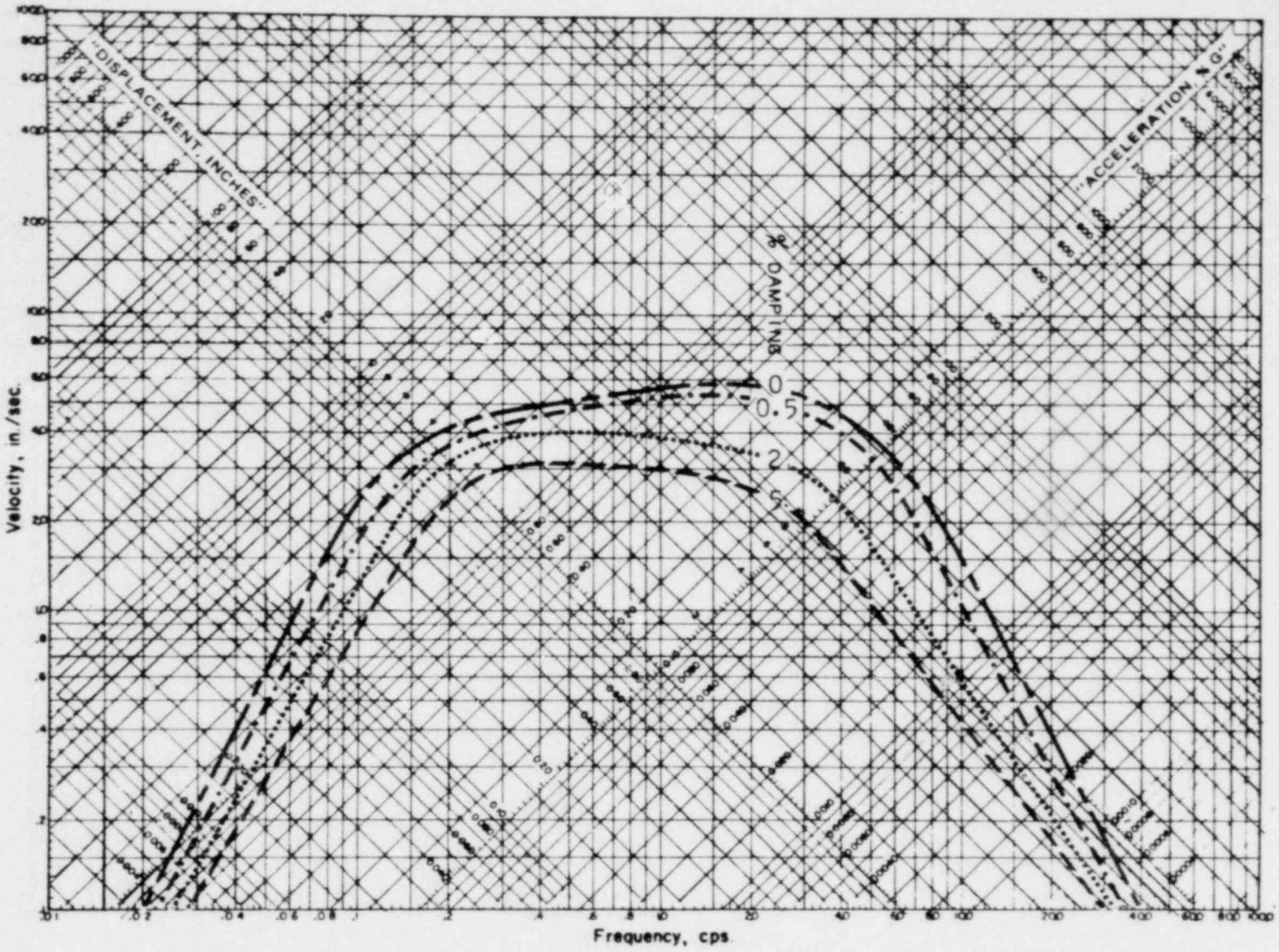

FIGURE 6-12 HORIZONTAL SEISMIC RESPONSE SPECTRUM
(OPERATING BASIS EARTHQUAKE)

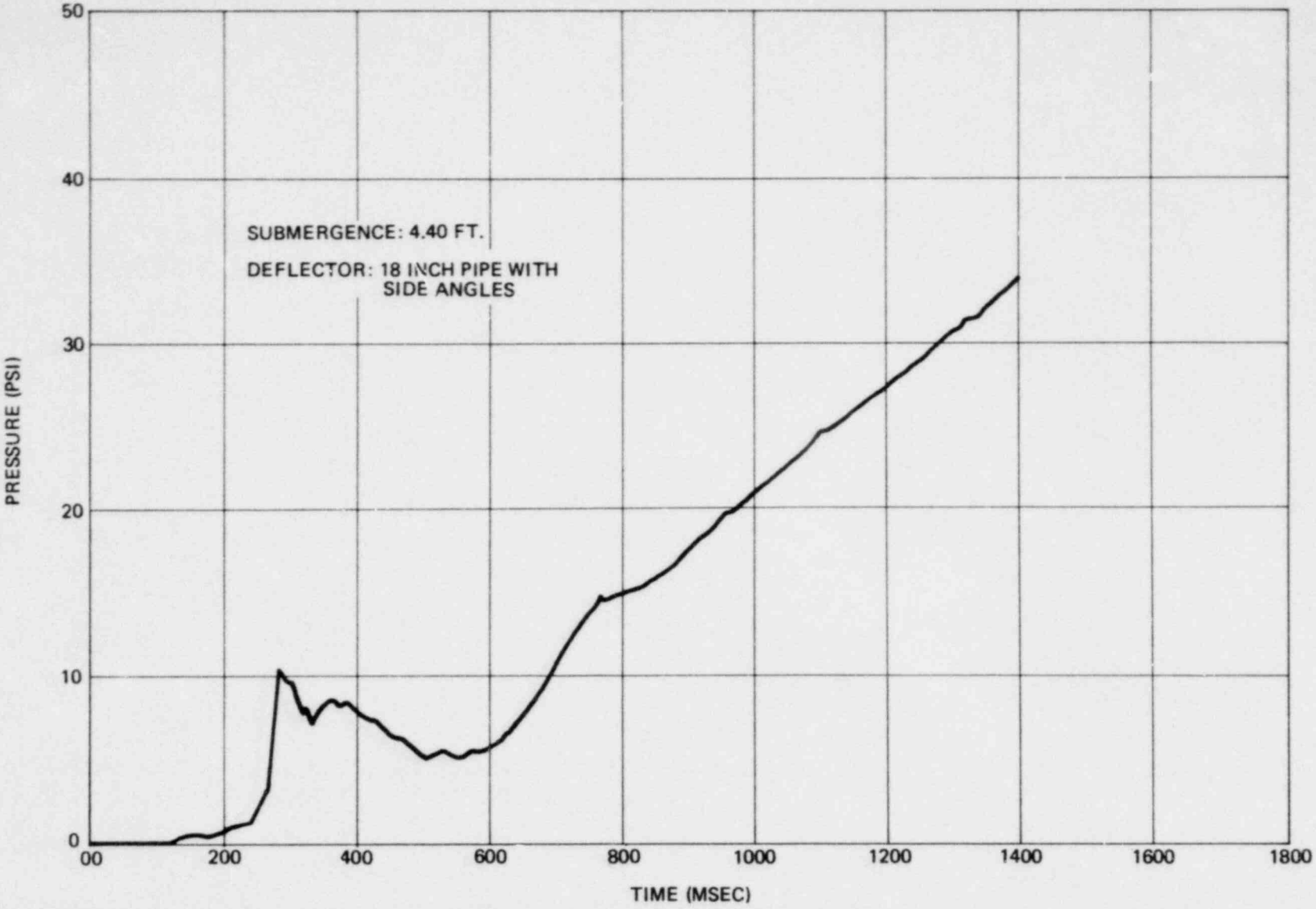

FIGURE 6-13 AVERAGE SUBMERGED PRESSURE

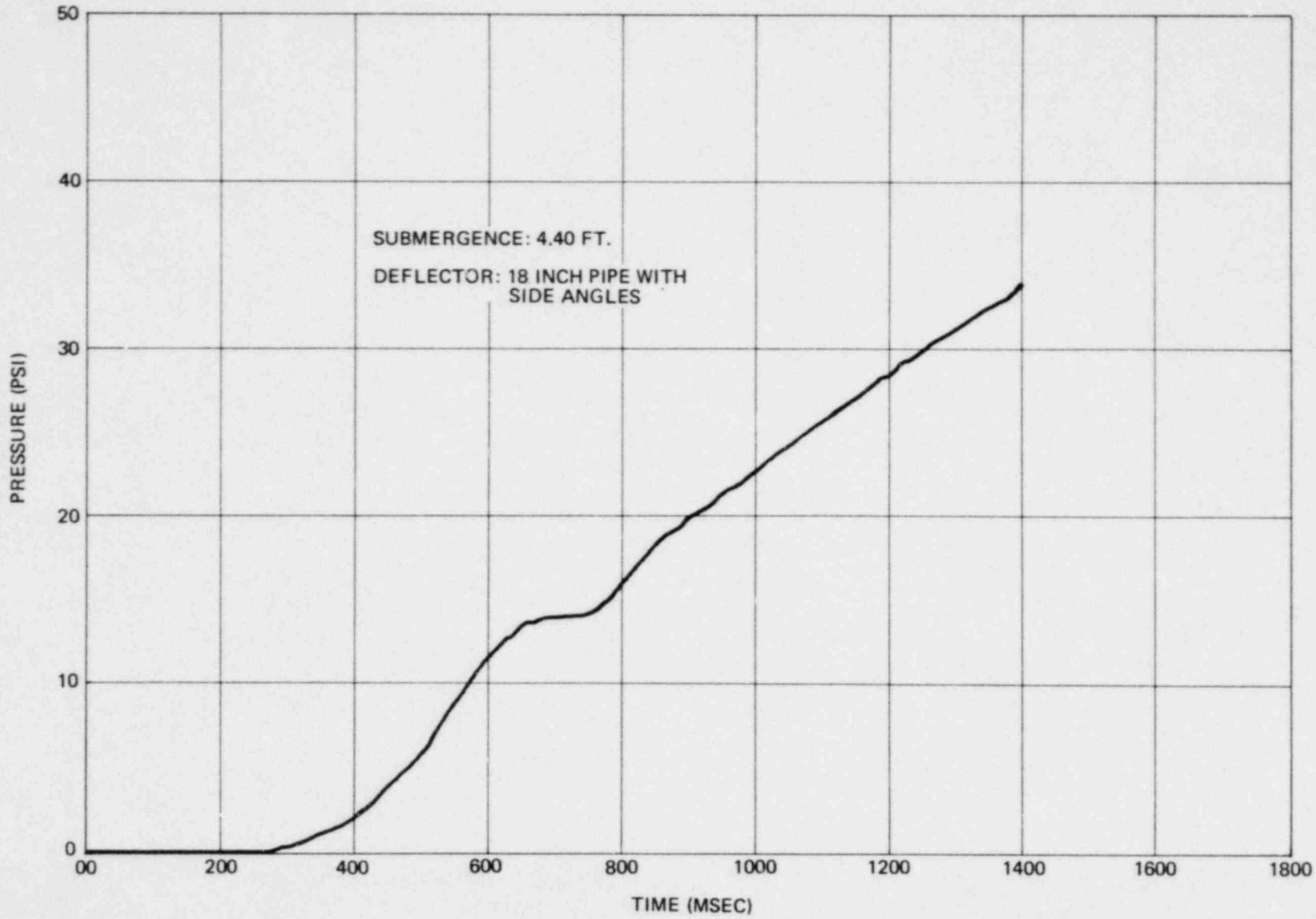

FIGURE 6-14 TORUS AIR PRESSURE

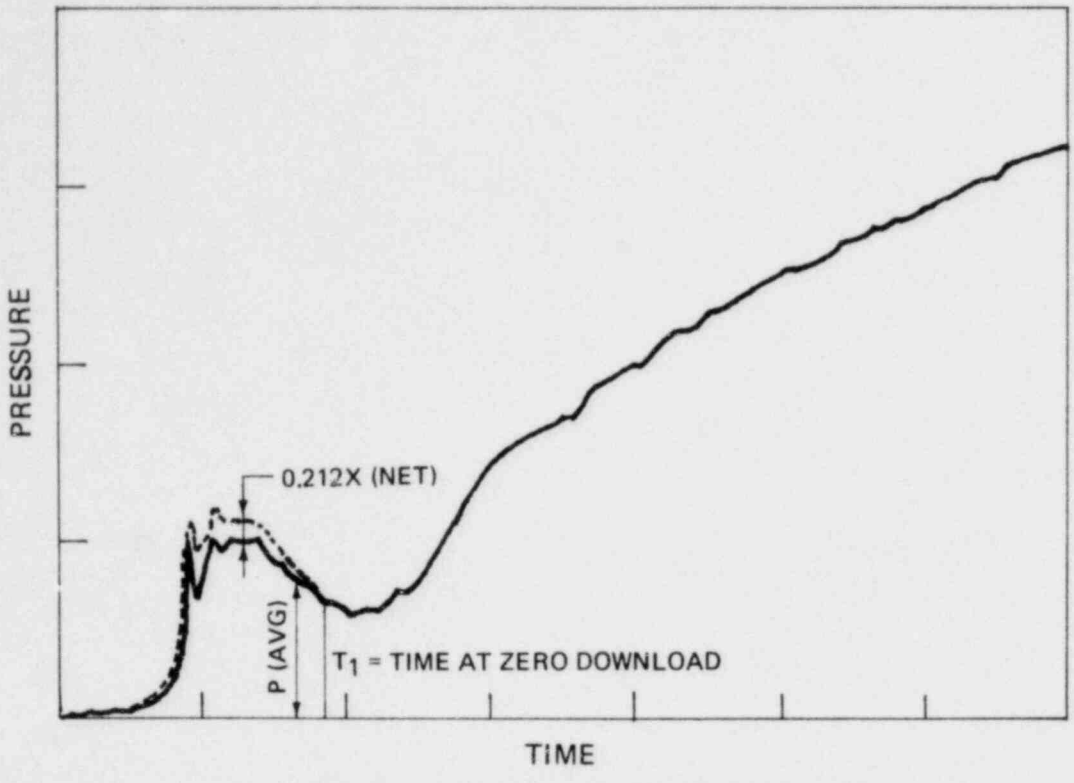

a. ADJUSTED AVERAGE SUBMERGED PRESSURE

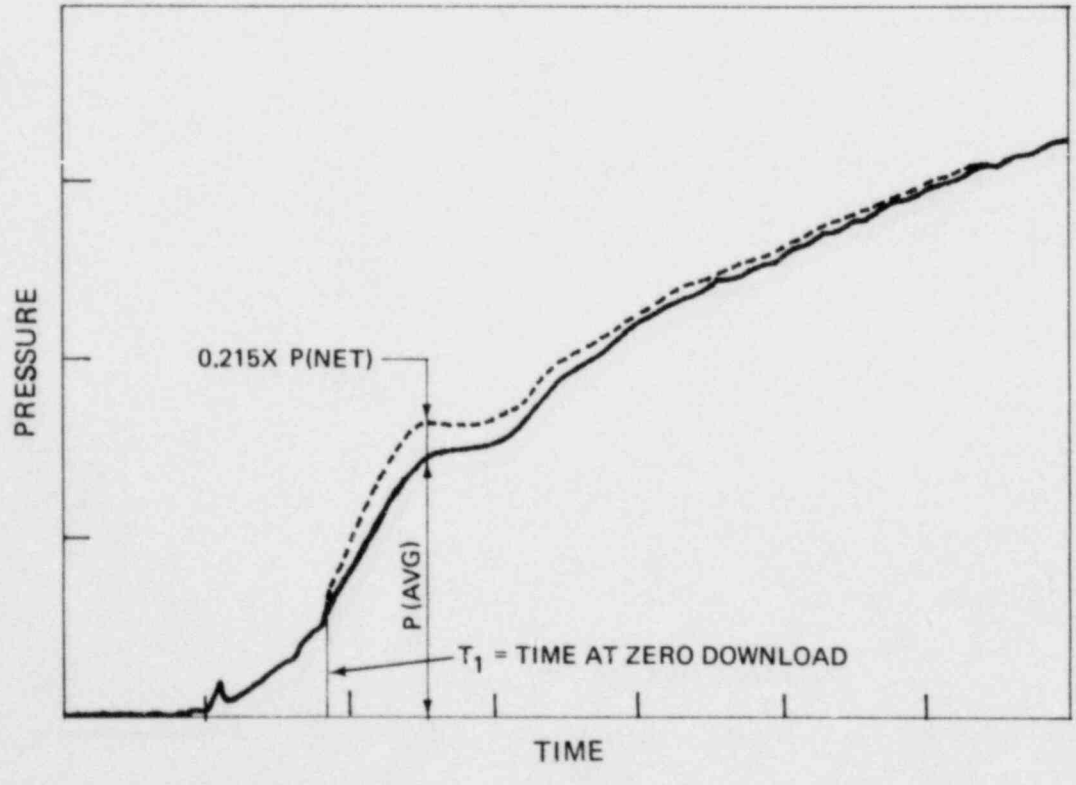

b. ADJUSTED AVERAGE AIR SPACE PRESSURE

FIGURE 6-15 ADJUSTED POOL SWELL PRESSURE TRANSIENTS

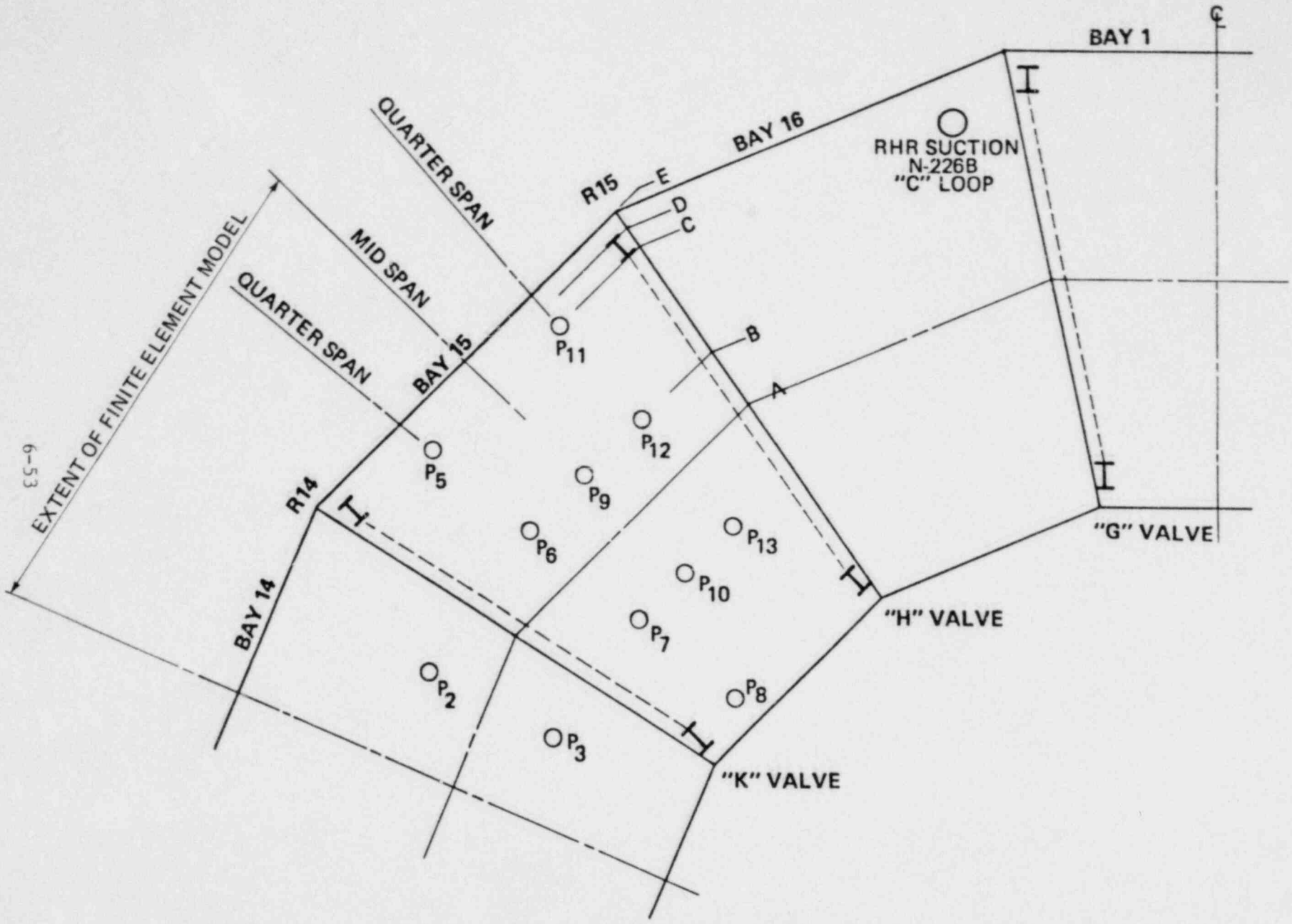

FIGURE 6-16 LOCATIONS OF PRESSURE GAGES

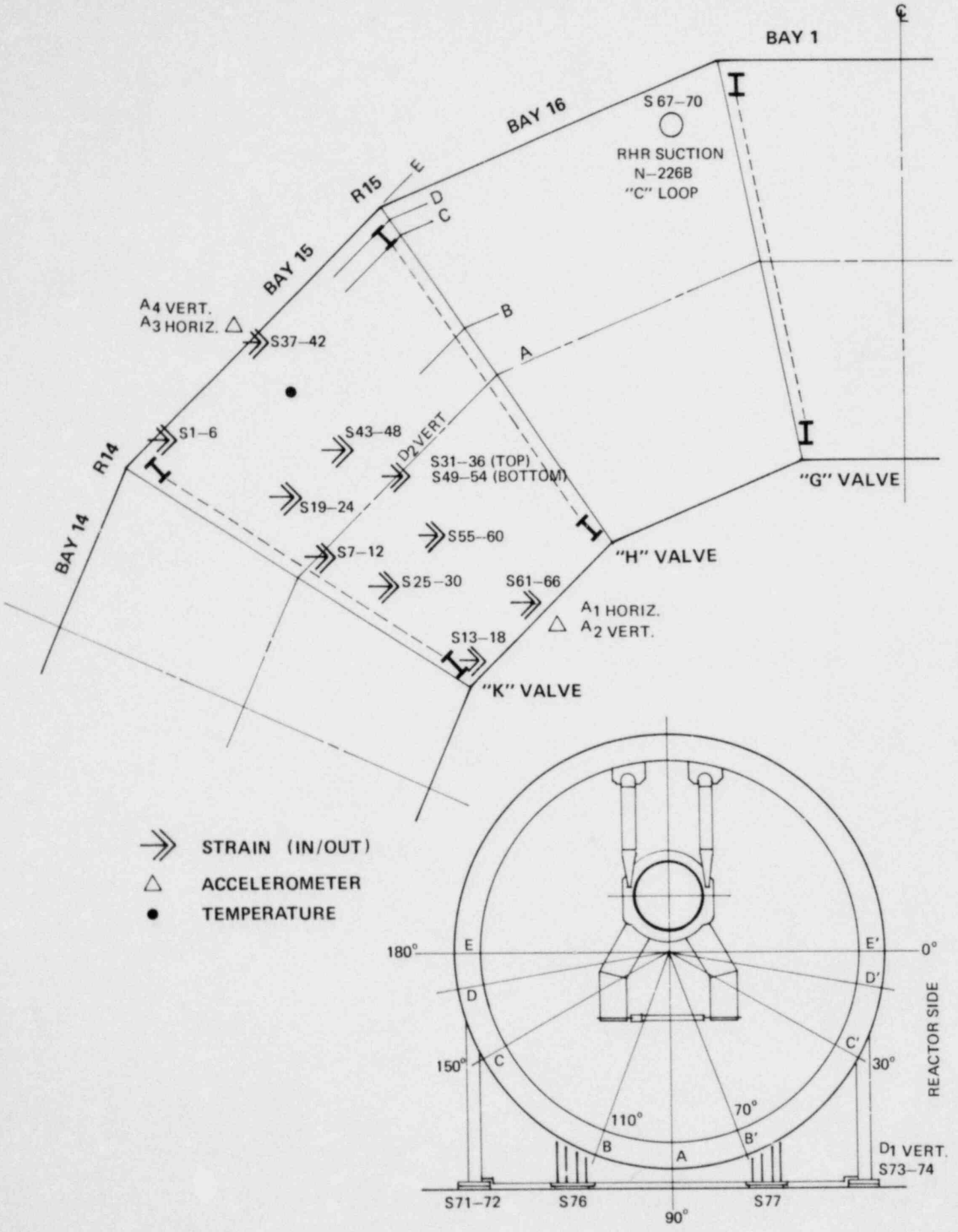

FIGURE 6-17 INSTRUMENTATION LOCATIONS

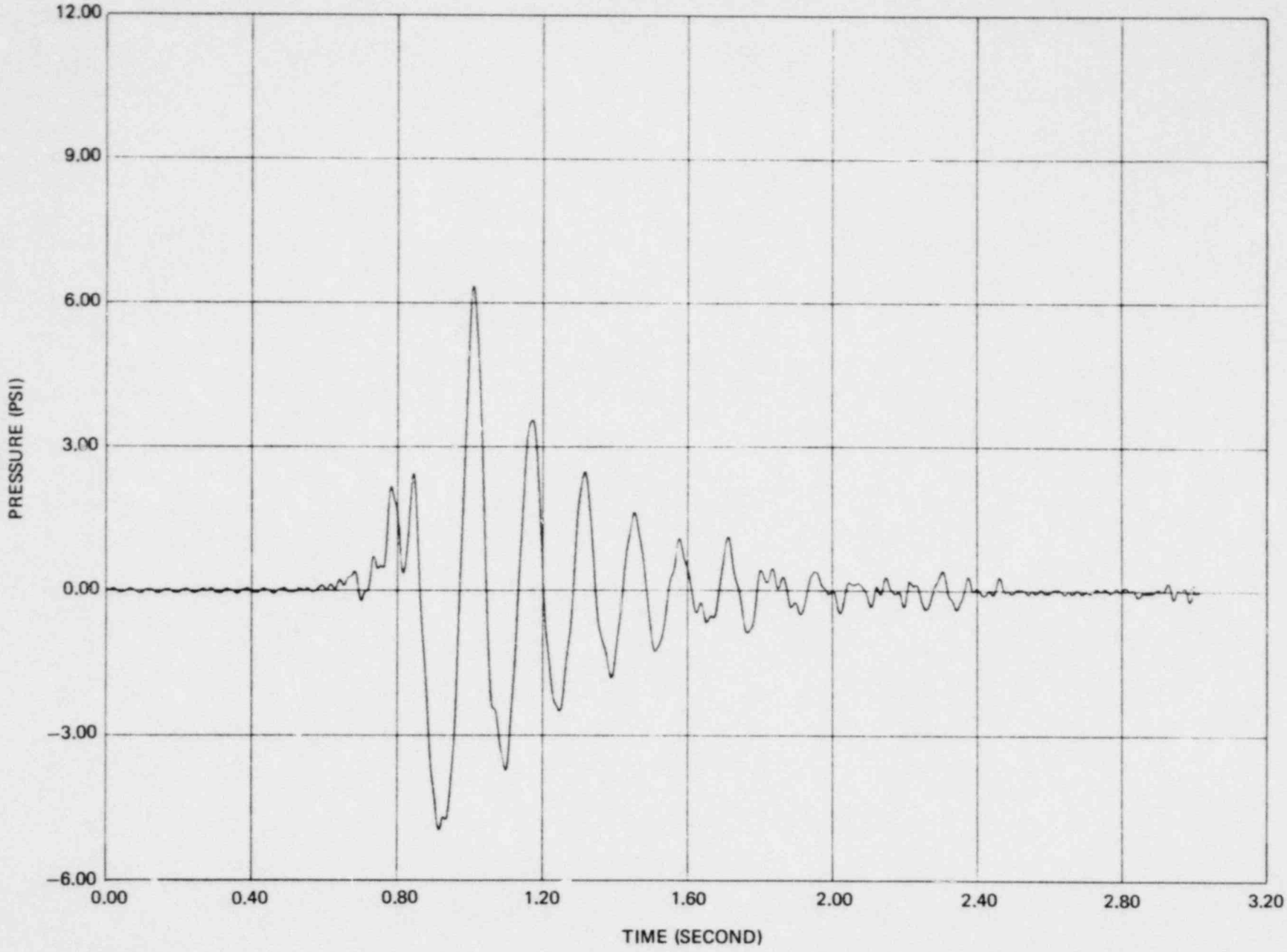

FIGURE 6-18 MEASURED TORUS SHELL PRESSURE TIME HISTORY AT GAGE P6 (TEST 9)

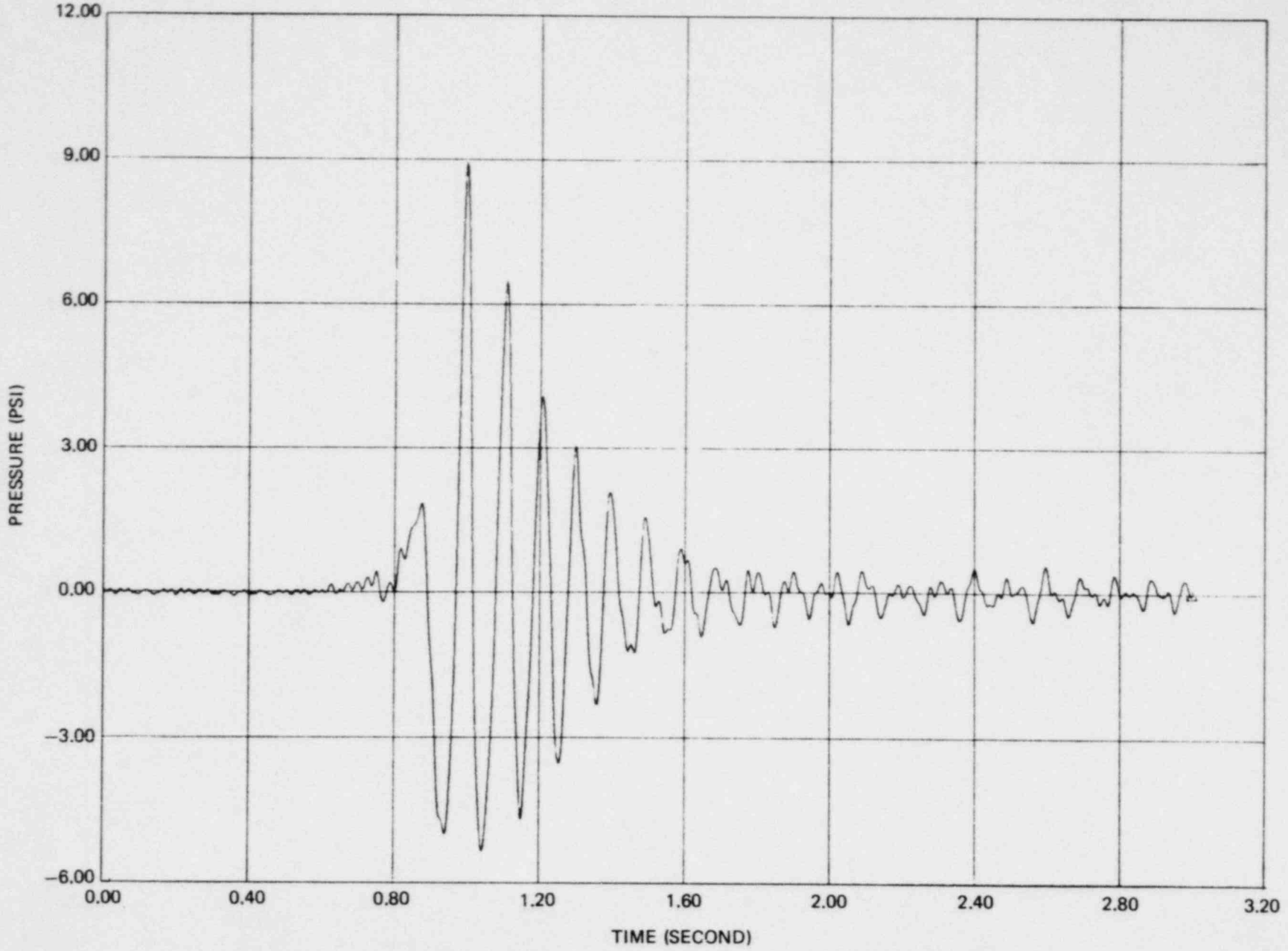

FIGURE 6-19 MEASURED TORUS SHELL PRESSURE TIME HISTORY AT GAGE P6 (TEST 10)

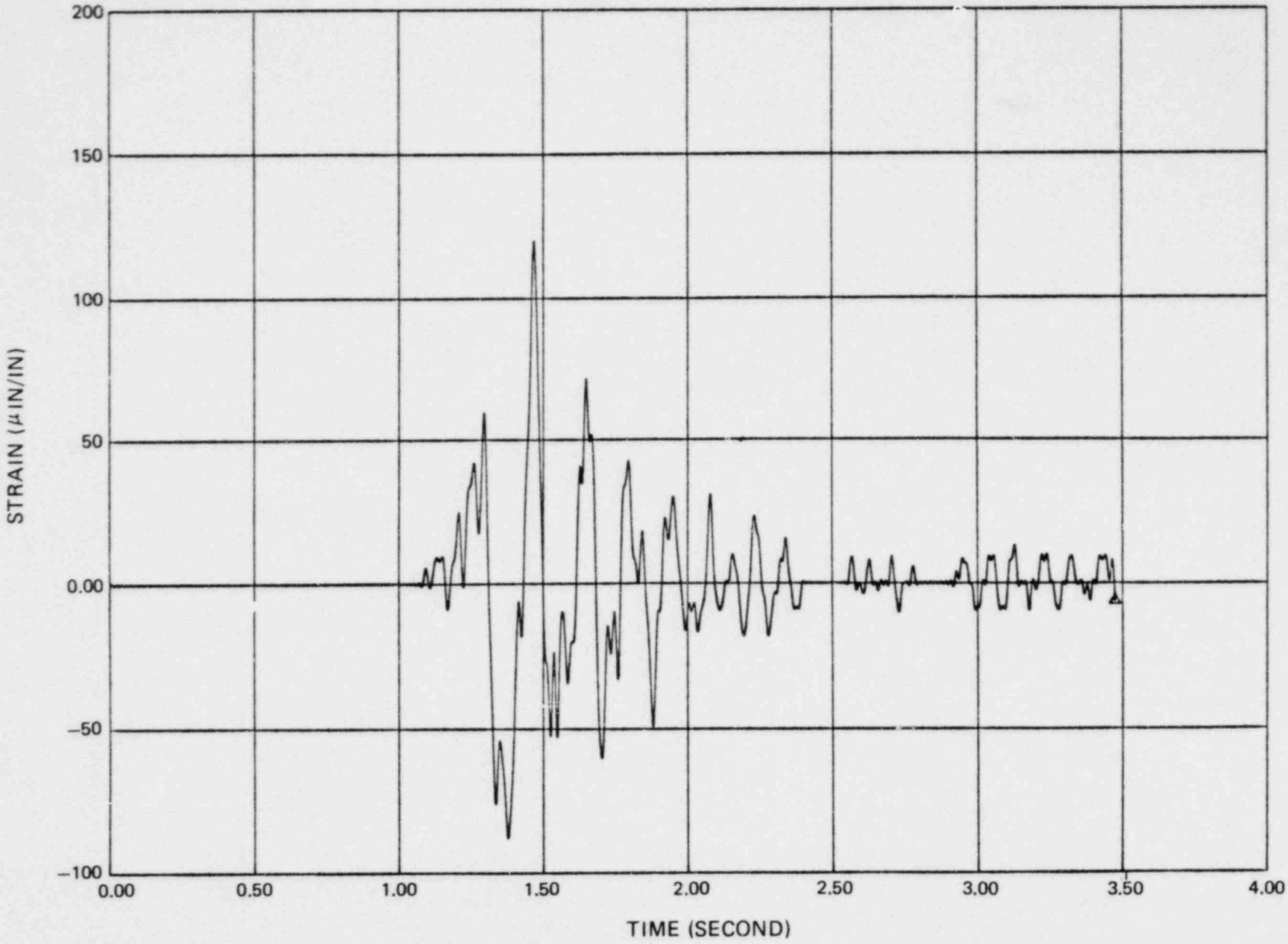

FIGURE 6-20 STRAIN TIME HISTORY AT STRAIN GAGE 54 (MIDBAY BOTTOM), TEST 16

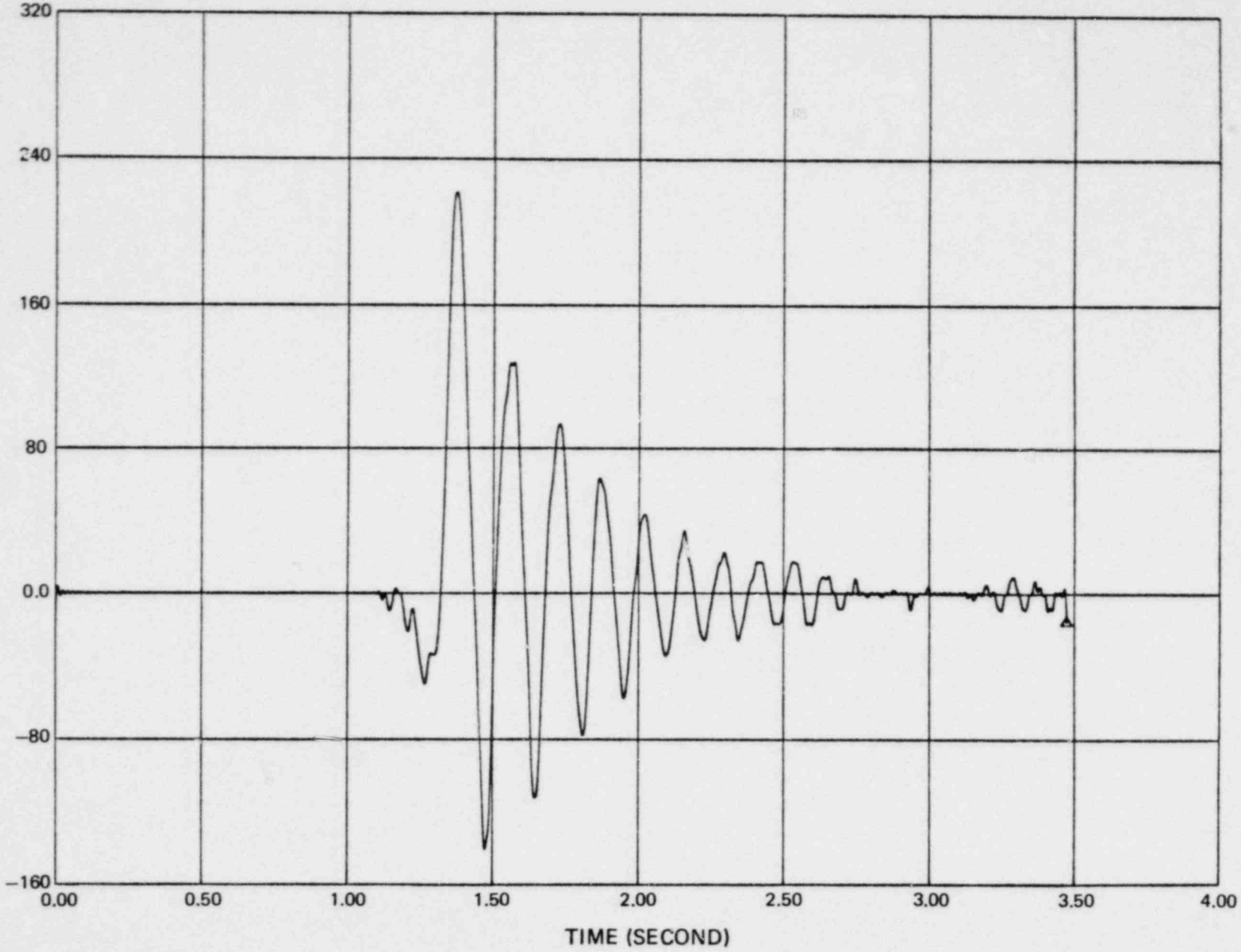

FIGURE 6-21 STRAIN TIME HISTORY AT GAGE 72 (INSIDE FLANGE, OUTSIDE COLUMN), TEST 16

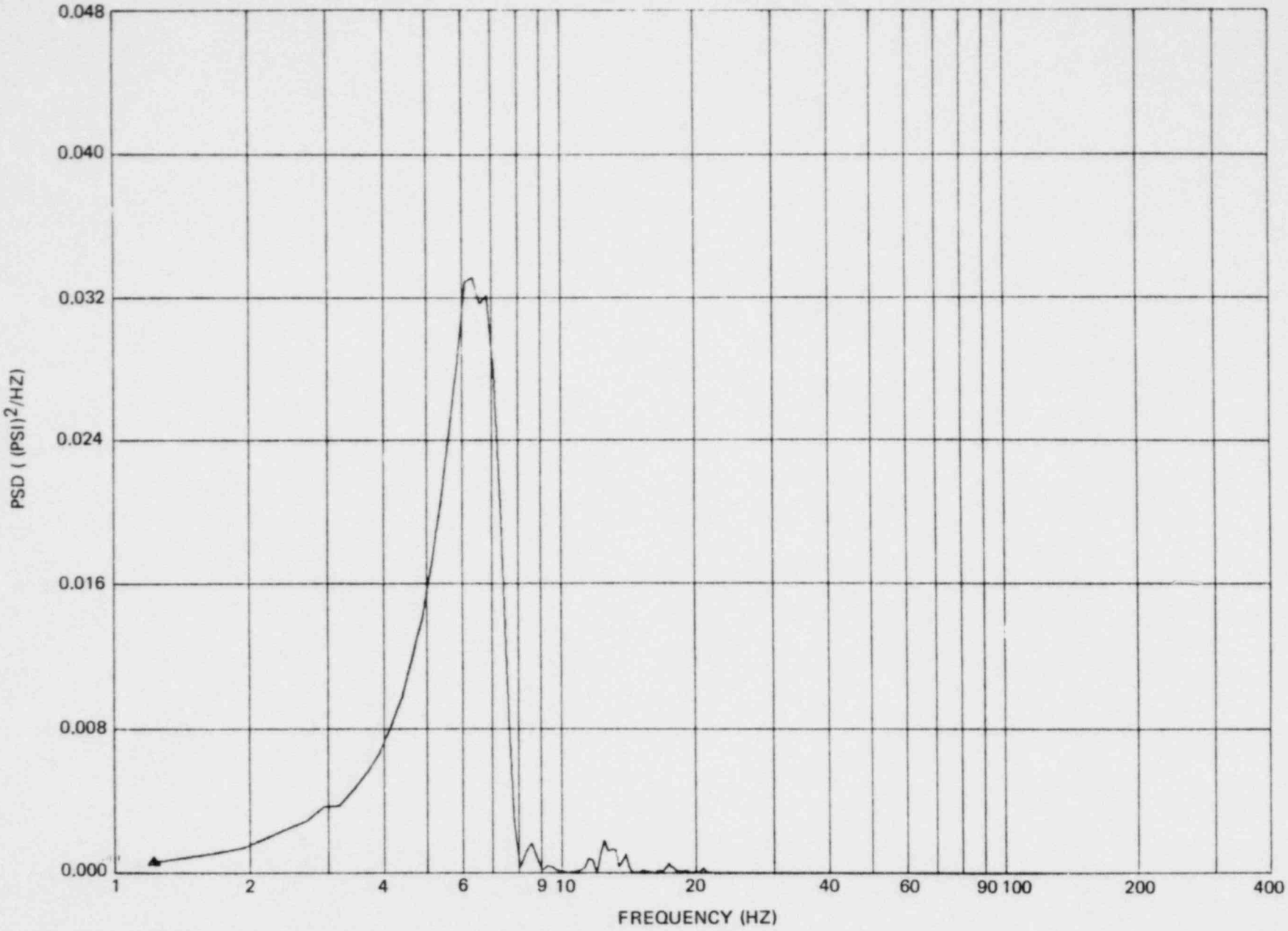

FIGURE 6-22 PSD OF MEASURED TORUS SHELL PRESSURE TIME HISTORY AT GAGE P6 (TEST 9)

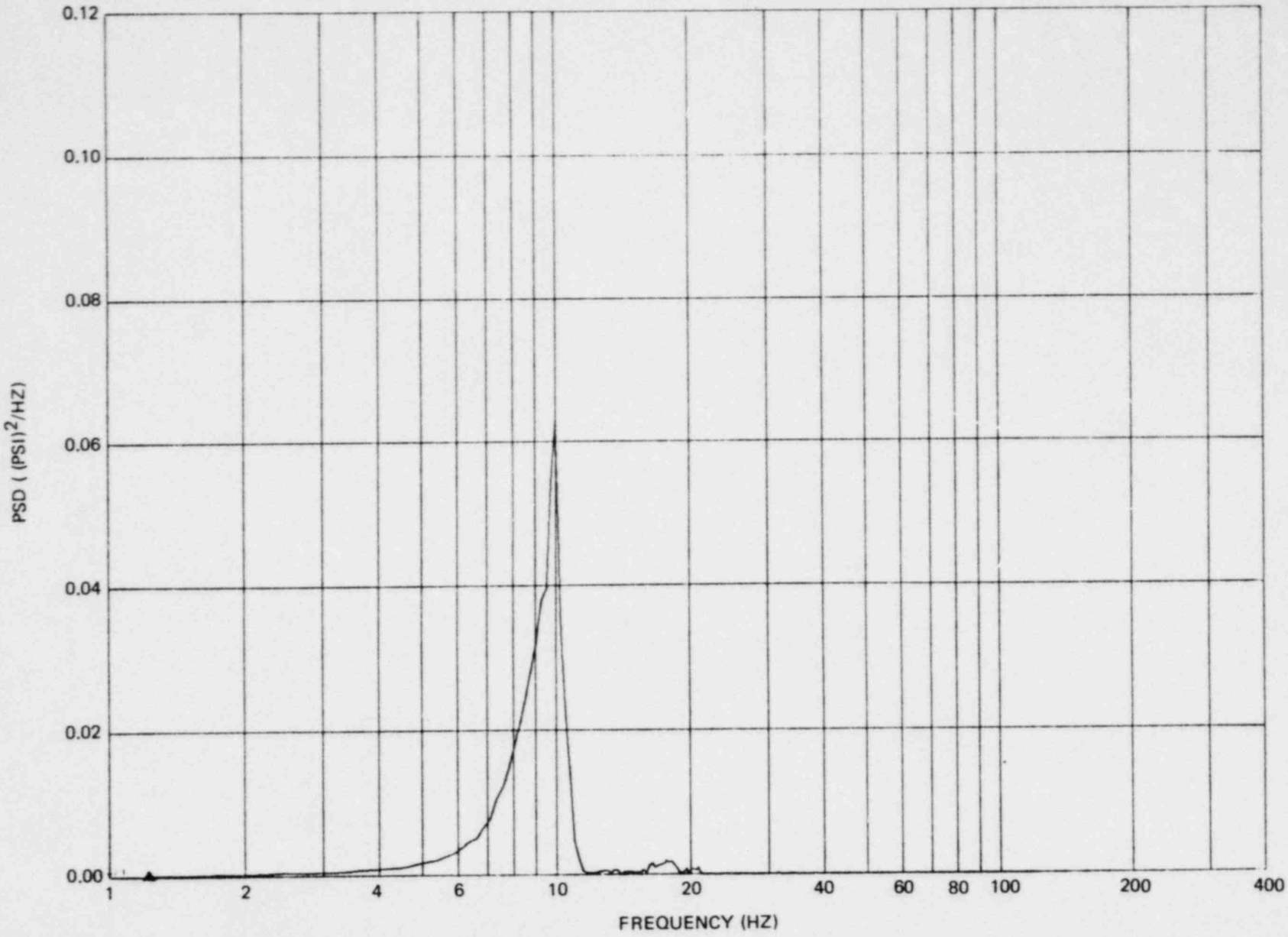

FIGURE 6-23 PSD OF MEASURED TORUS SHELL PRESSURE TIME HISTORY AT GAGE P6 (TEST 10)

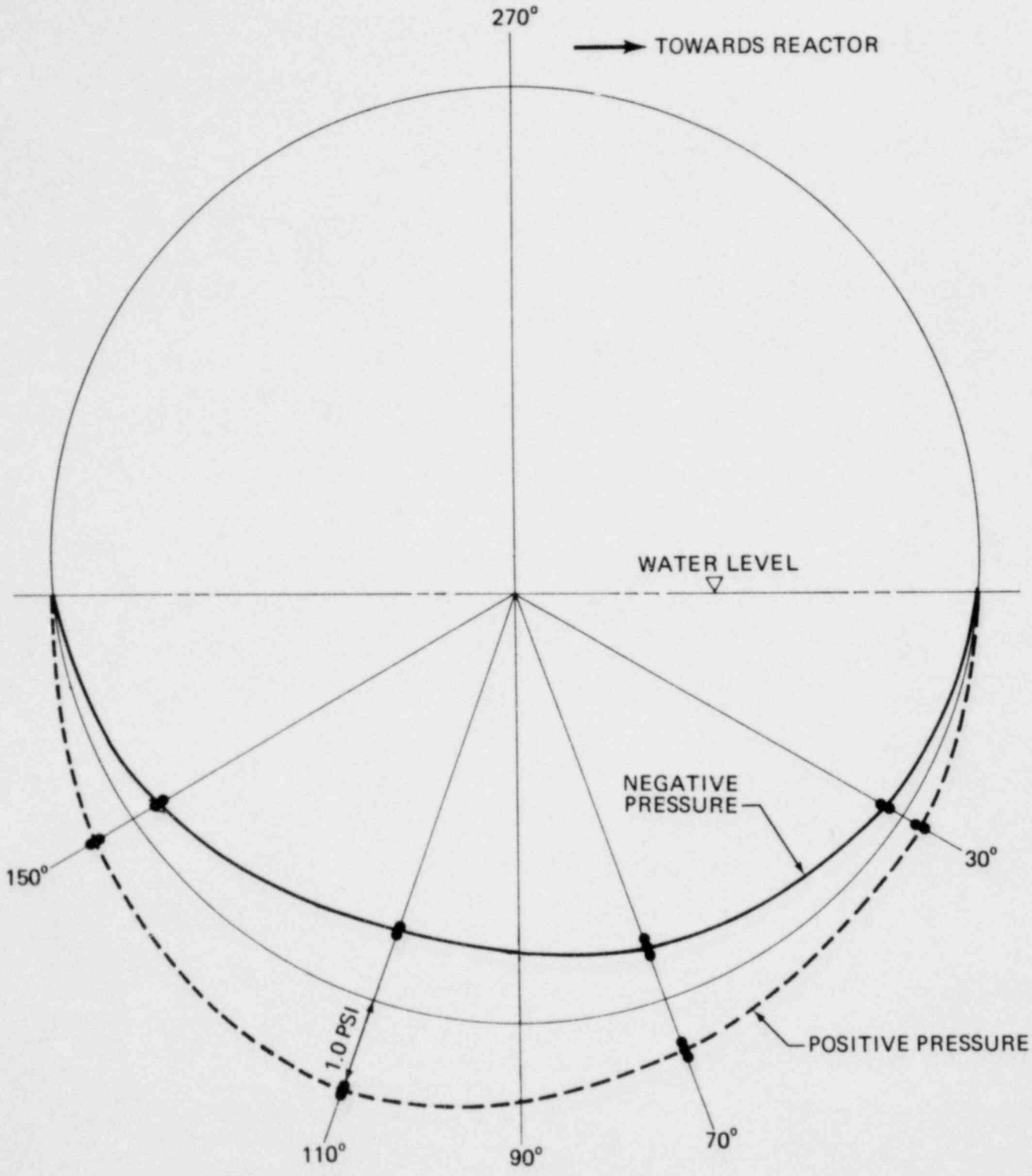

FIGURE 6-24 TYPICAL NORMALIZED PRESSURE DISTRIBUTION AT A CROSS SECTION

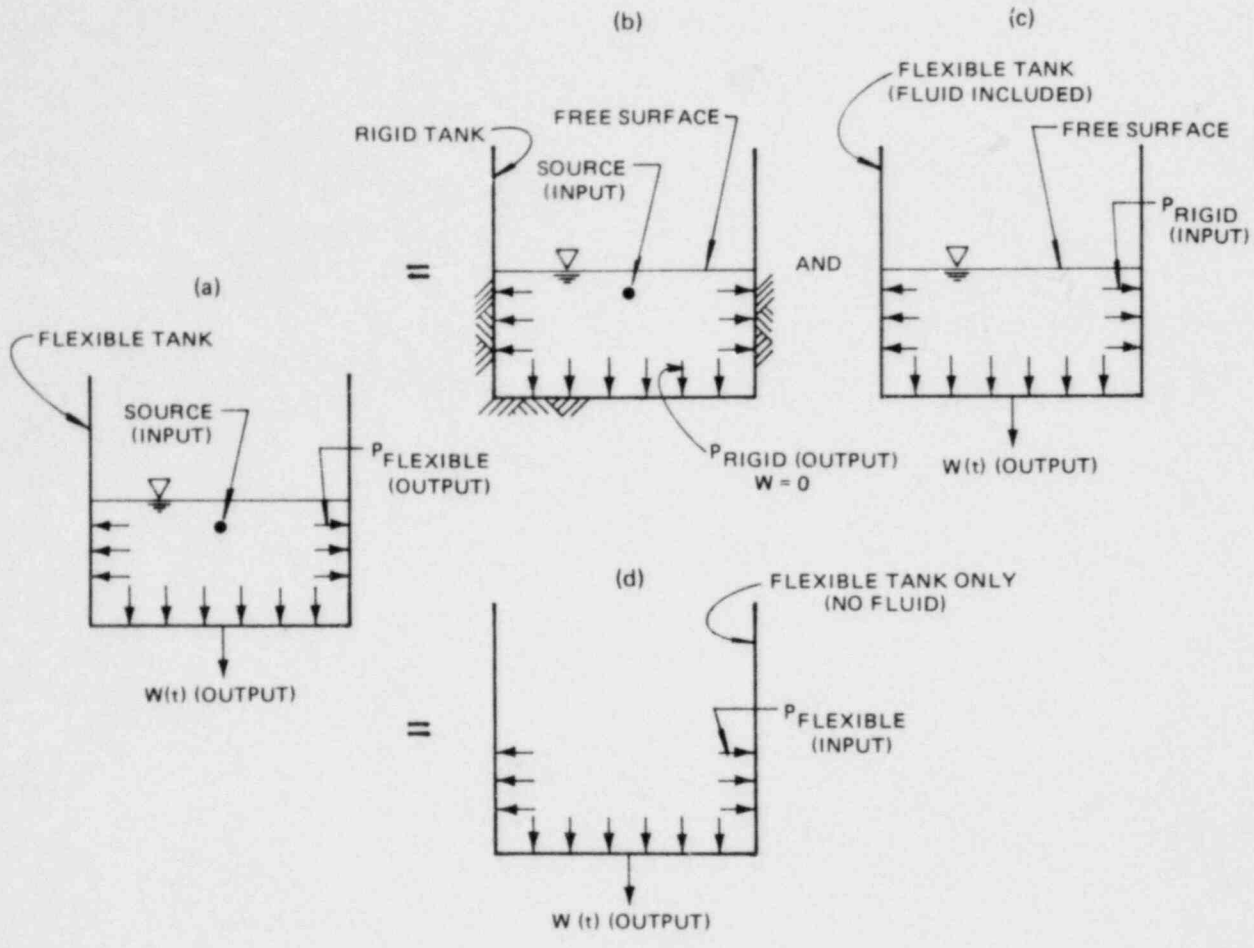

(a) ANALYSIS OF FLEXIBLE TANK WITH FORCING SOURCE — GIVES SAME RESULTS AS (d) ANALYSIS OF FLEXIBLE TANK WITHOUT FLUID WITH FLEXIBLE WALL PRESSURE INPUT AT THE WETTED SURFACE OF THE TANK

(b) ANALYSIS OF RIGID TANK WITH FORCING SOURCE — FOLLOWED BY (c) ANALYSIS OF FLEXIBLE TANK WITH RIGID WALL PRESSURE INPUT AT THE WETTED SURFACE OF THE TANK

FIGURE 6-25 METHODS OF FLUID–STRUCTURE INTERACTION ANALYSIS

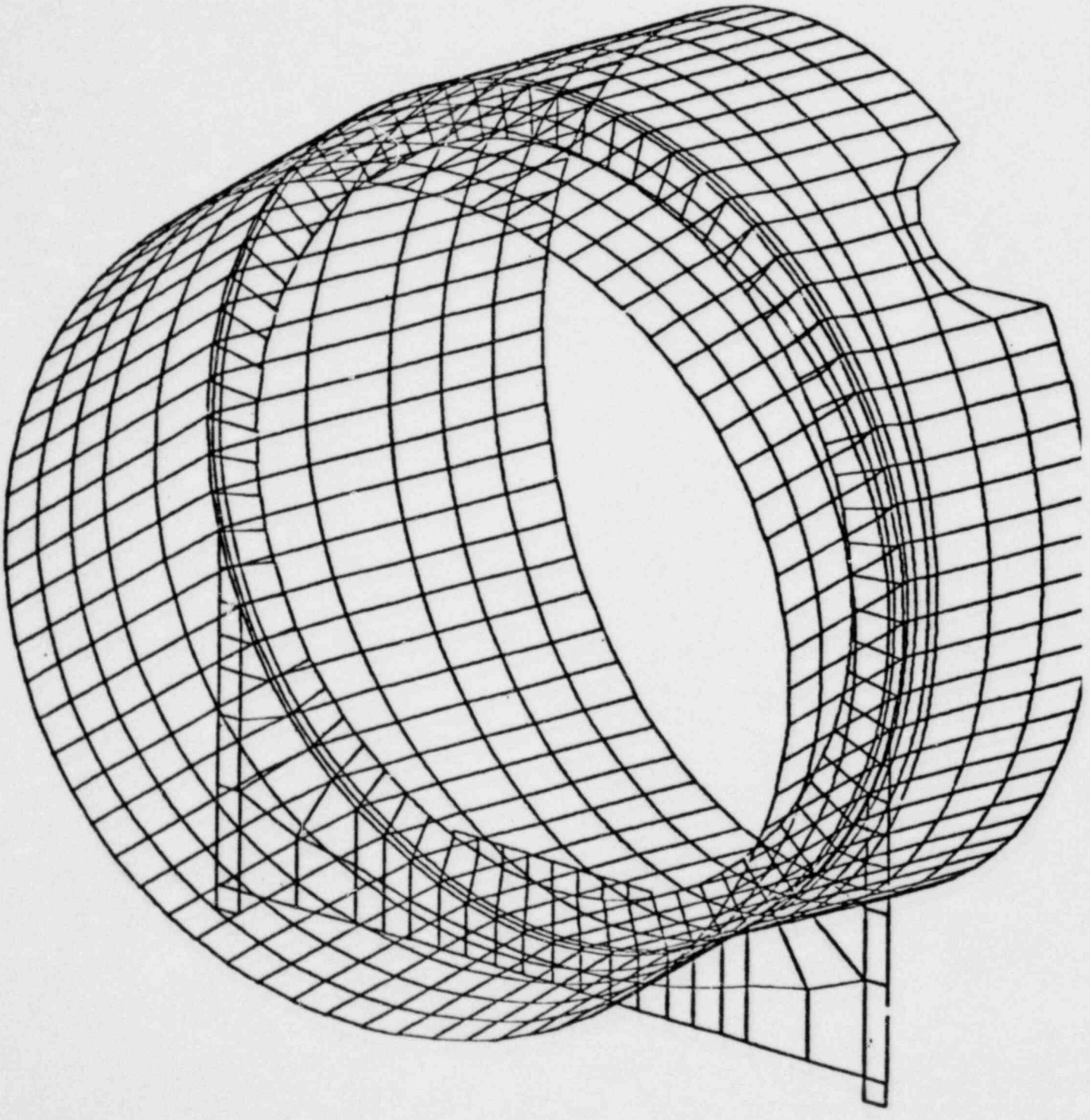

FIGURE 6-26 22.5° SEGMENT MODEL

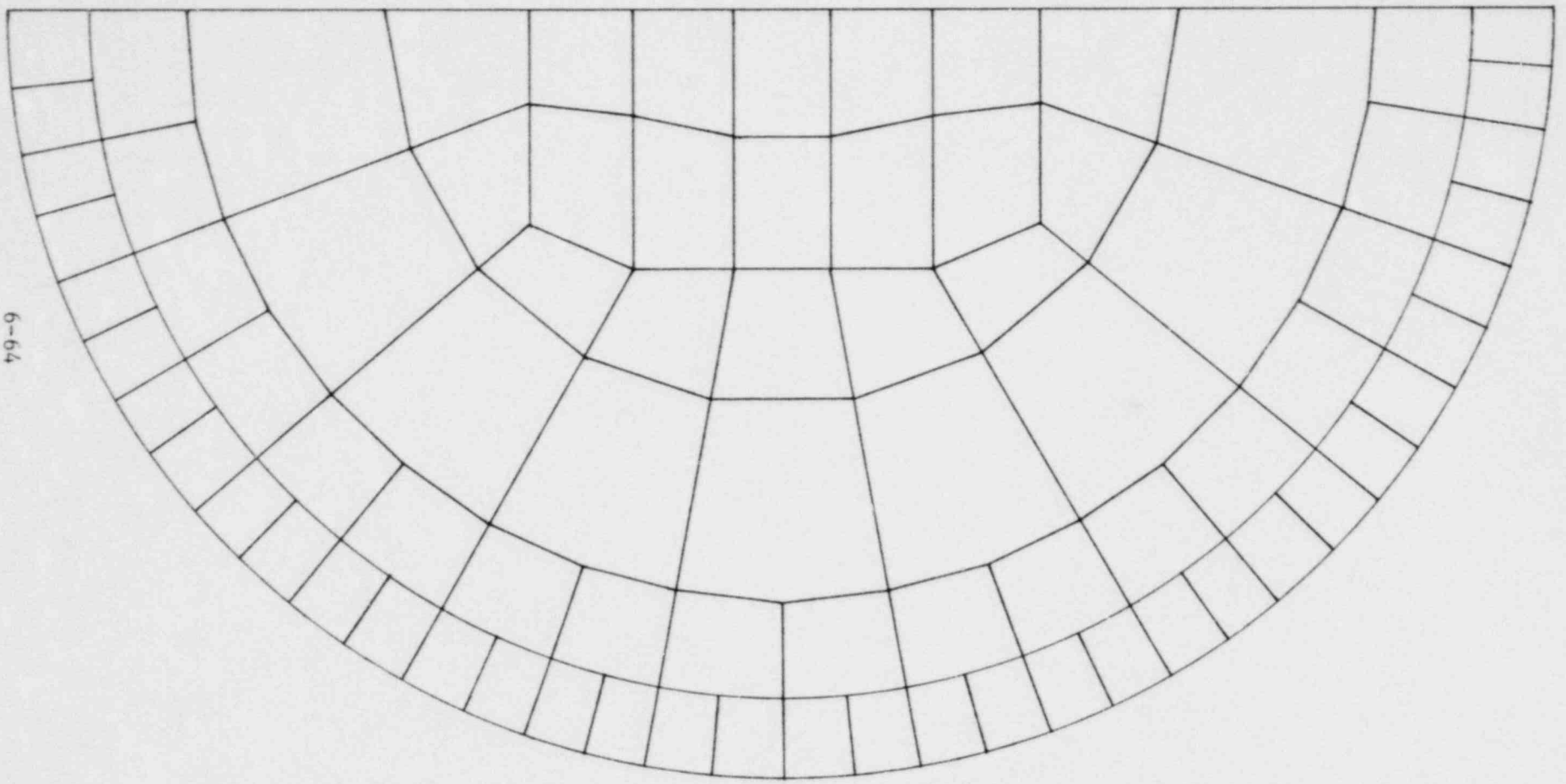

FIGURE 6-27 CROSS SECTION SHOWING TYPICAL GRID FOR FLUID ELEMENTS

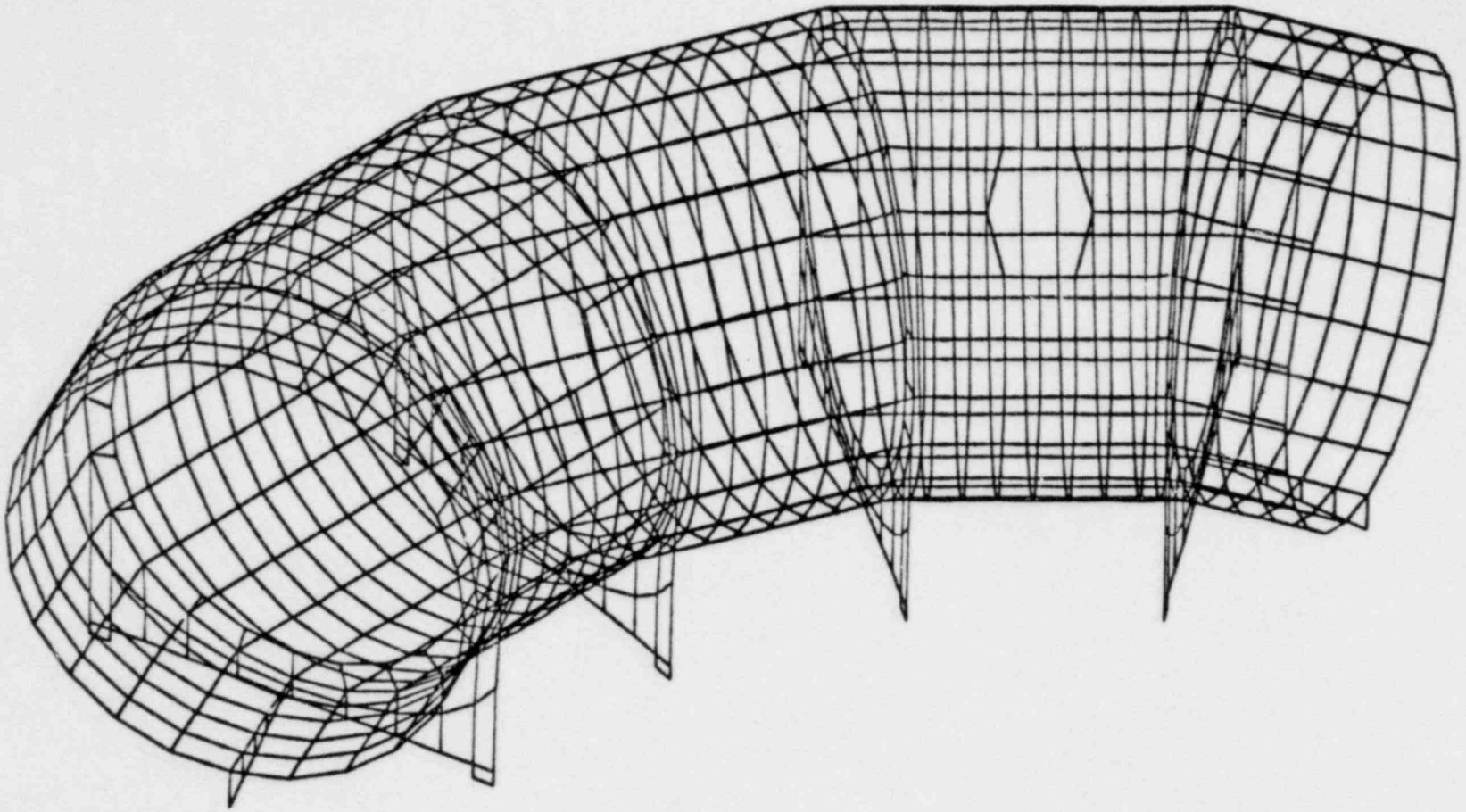

FIGURE 6-28 90° SEGMENT MODEL

NOTE: DDOF at Nozzle Attachment Points not shown.

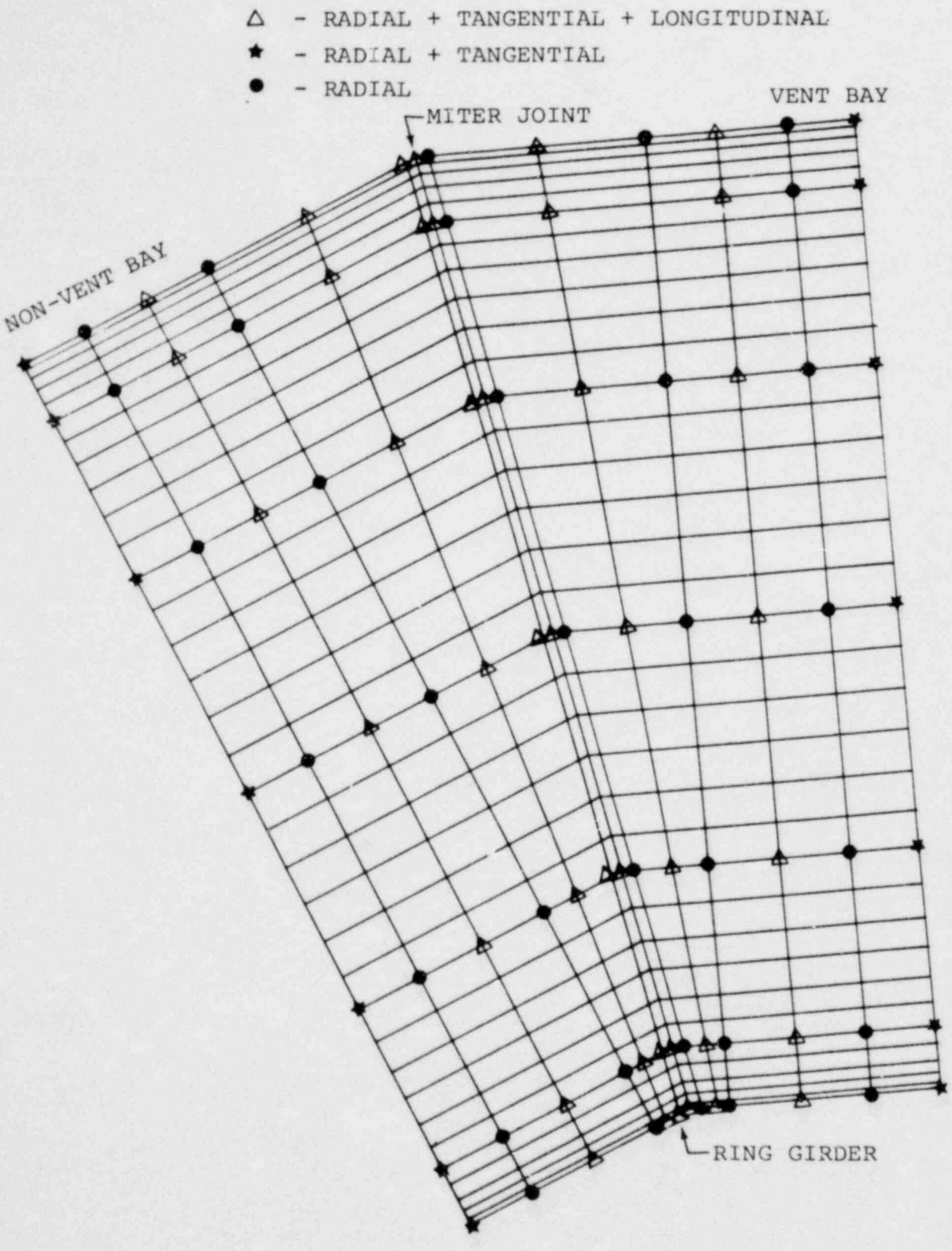

FIGURE 6-29 DYNAMIC DEGREES OF FREEDOM IN BOTTOM HALF

NOTE: DDOF at Nozzle Attachment Points not shown.

△ - RADIAL + TANGENTIAL + LONGITUDINAL
★ - RADIAL + TANGENTIAL
● - RADIAL

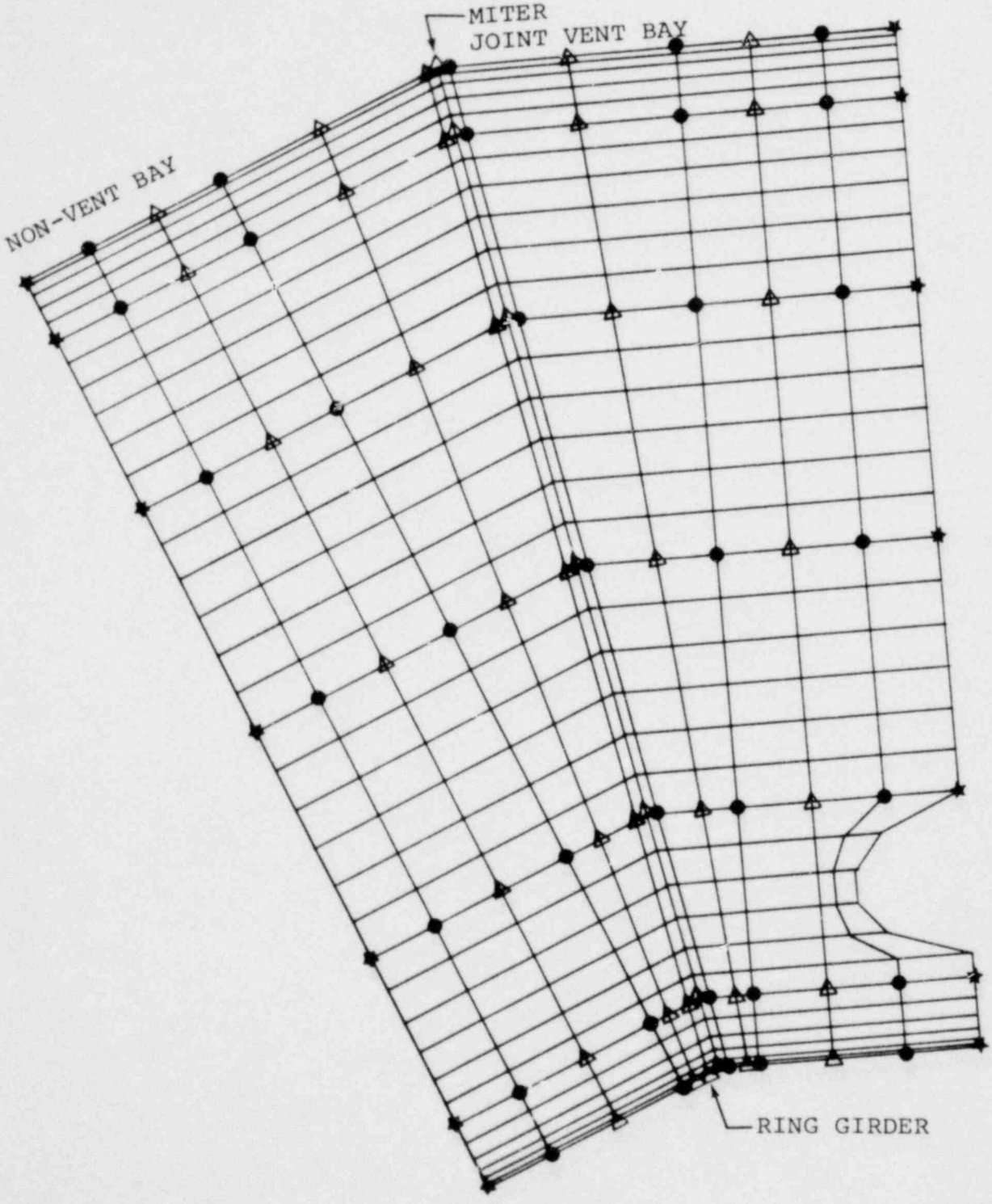

FIGURE 6-30 DYNAMIC DEGREES OF FREEDOM IN TOP HALF

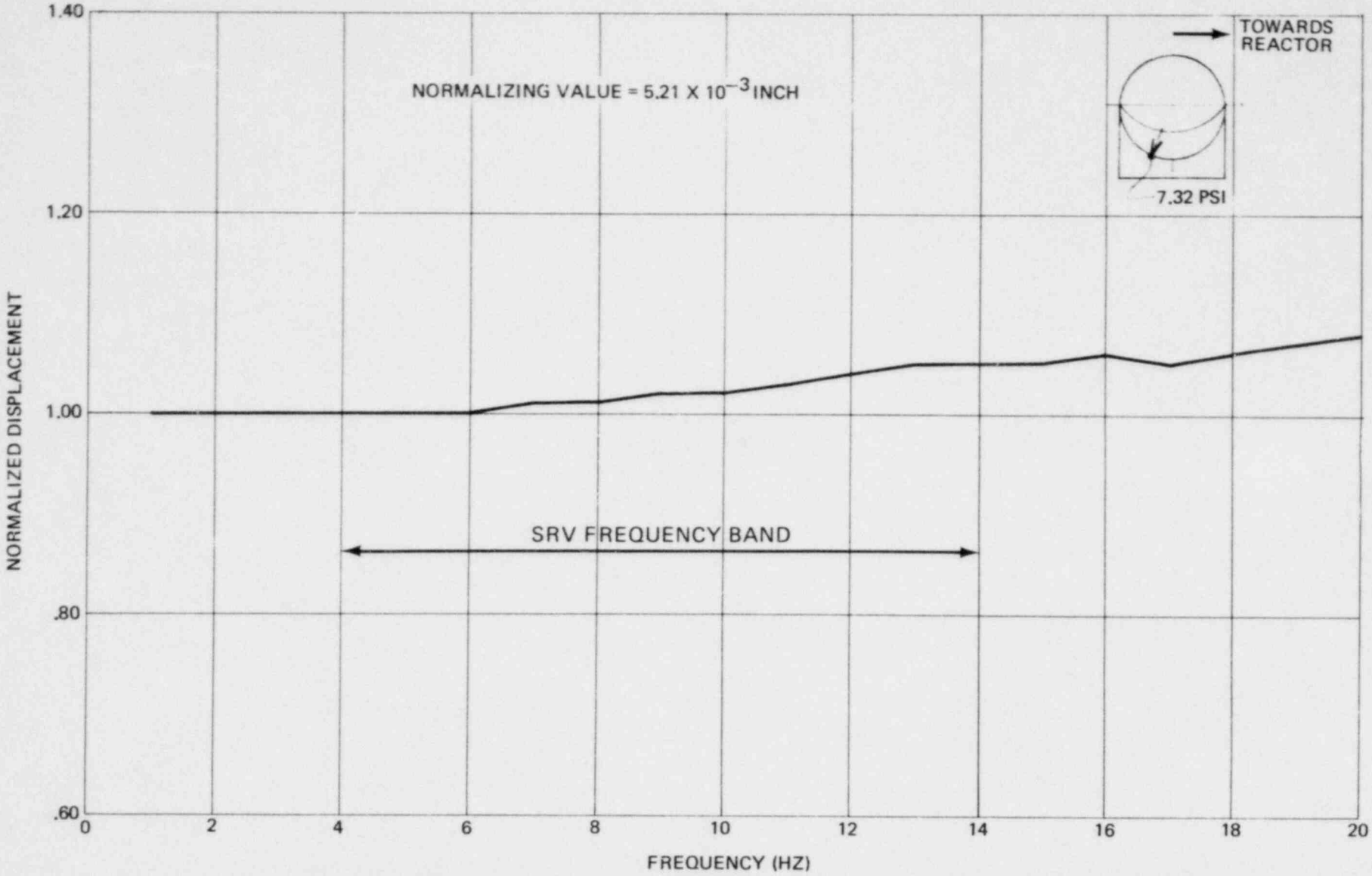

FIGURE 6-31 SHELL DISPLACEMENT AT BOTTOM CENTER AS A FUNCTION OF FREQUENCY

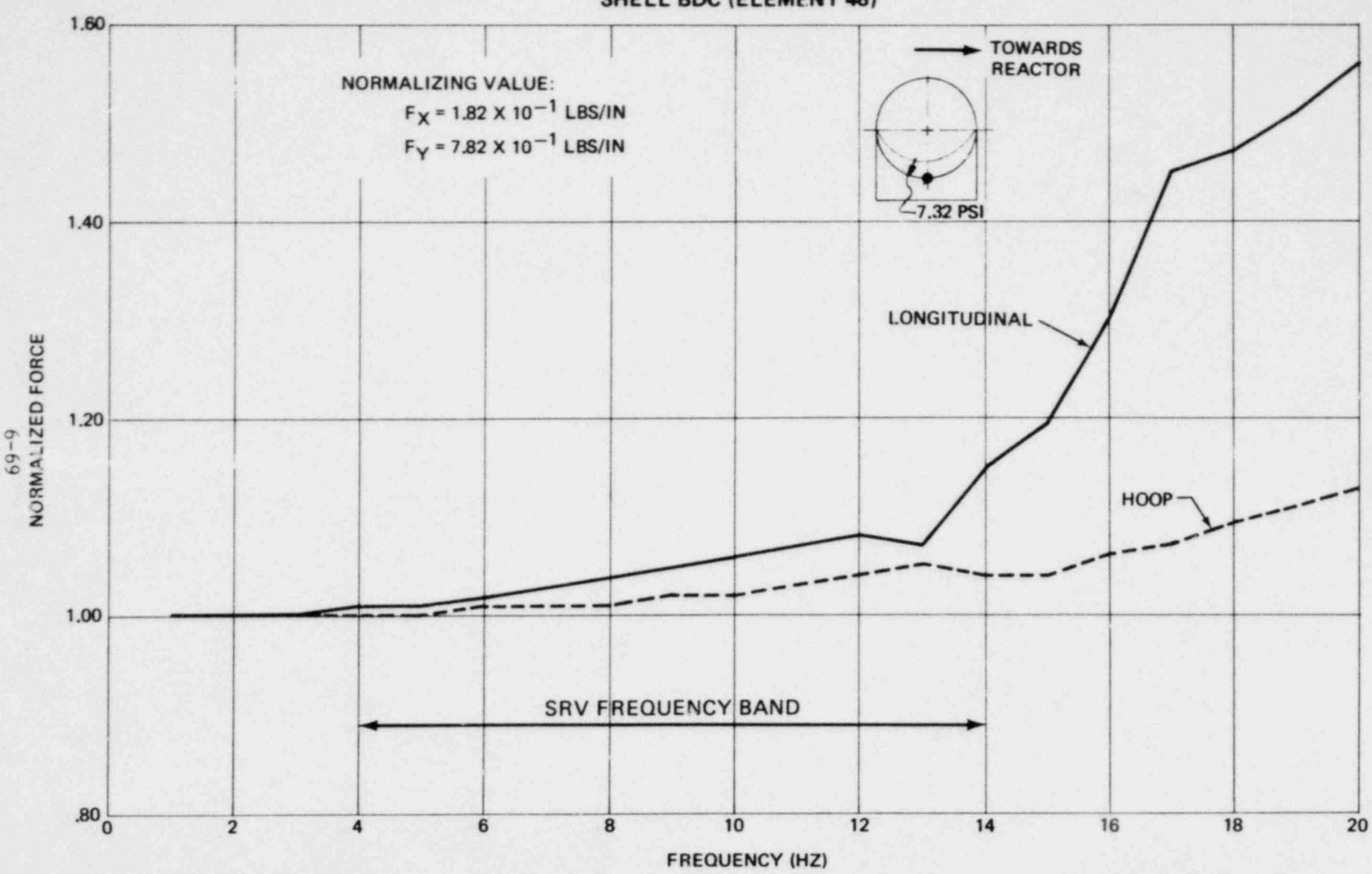

FIGURE 6-32 FORCES IN BOTTOM CENTER SHELL ELEMENTS AS A FUNCTION OF FREQUENCY

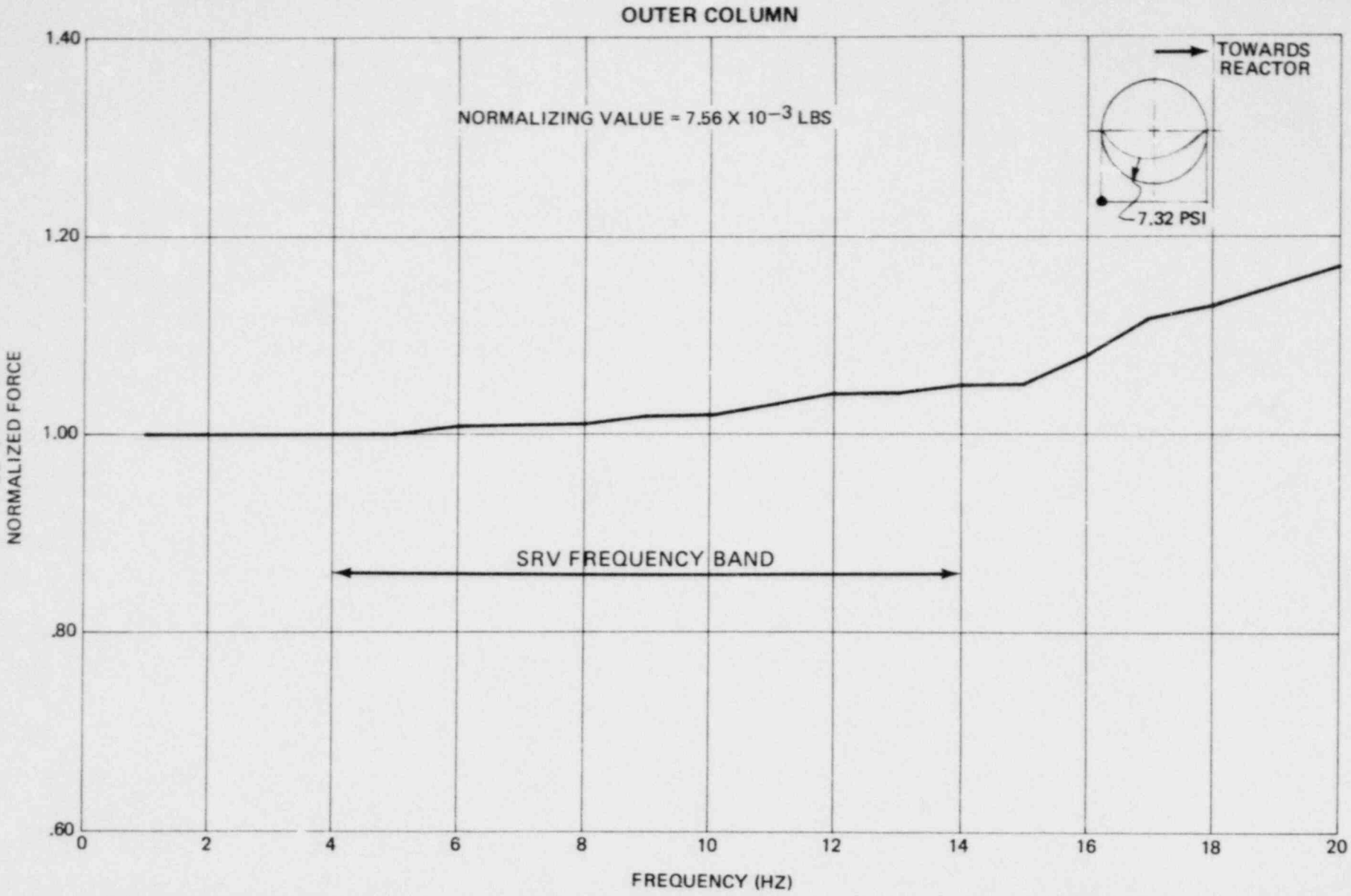

FIGURE 6-33 AXIAL COLUMN LOADS AS A FUNCTION OF FREQUENCY

MODE1, FREQ. = 14.28 HZ

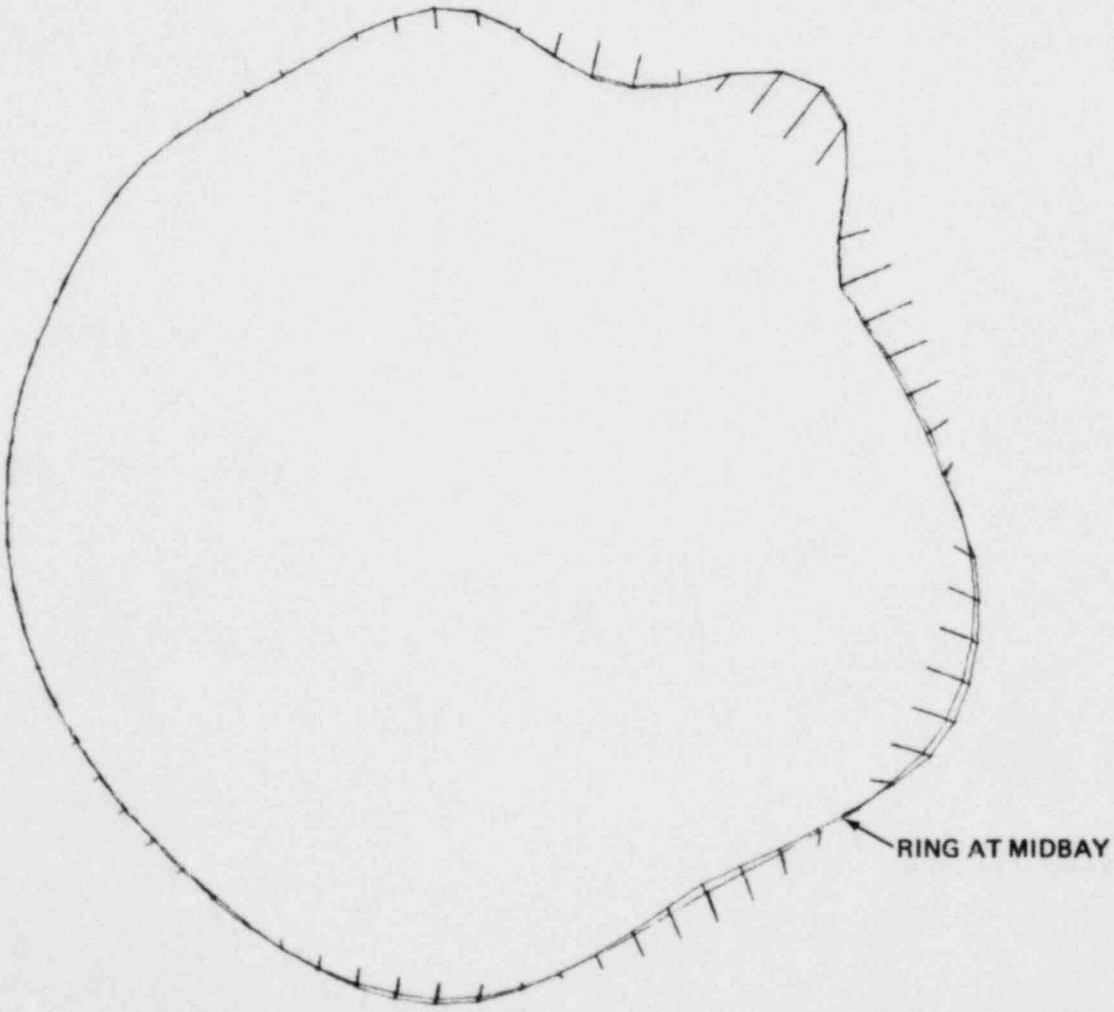

FIGURE 6-34 FIRST SHELL MODE OF COUPLED STRUCTURE

MODE 2, FREQ. = 15.08 HZ

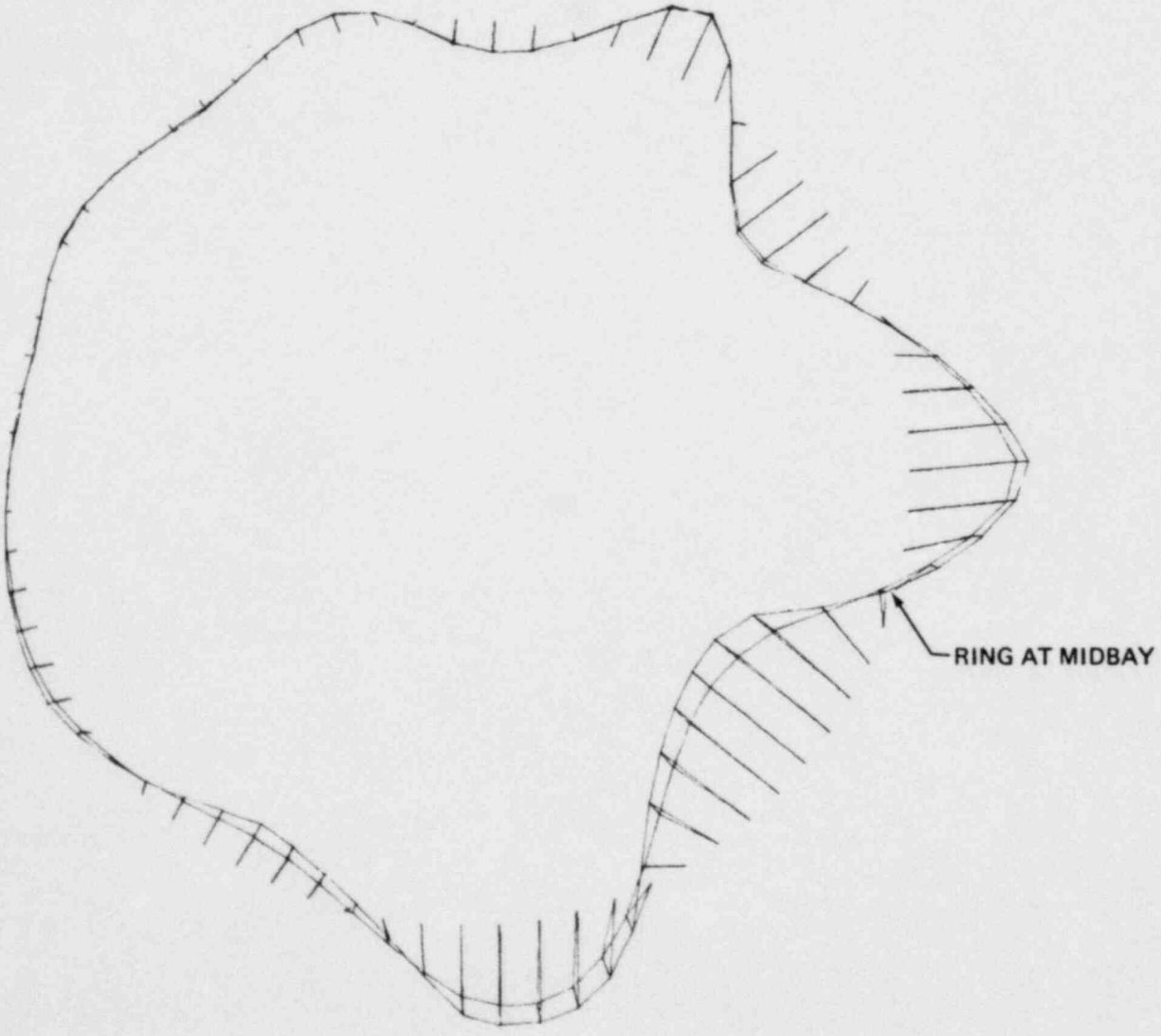

FIGURE 6-35 SECOND SHELL MODE OF COUPLED STRUCTURE

MODE 3, FREQ. = 15.75

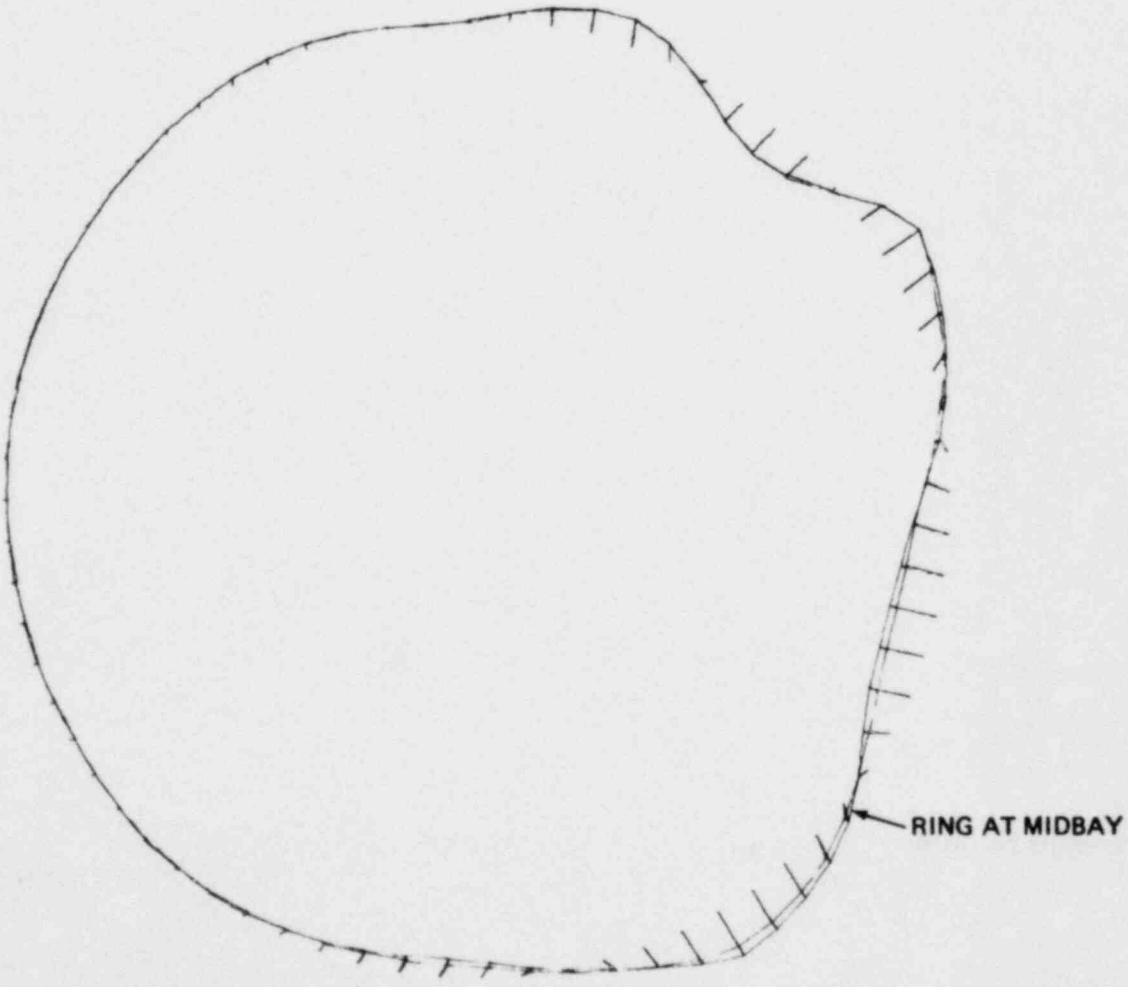

FIGURE 6-36 THIRD SHELL MODE OF COUPLED STRUCTURE

MODE 1, FREQ. = 17.35 HZ

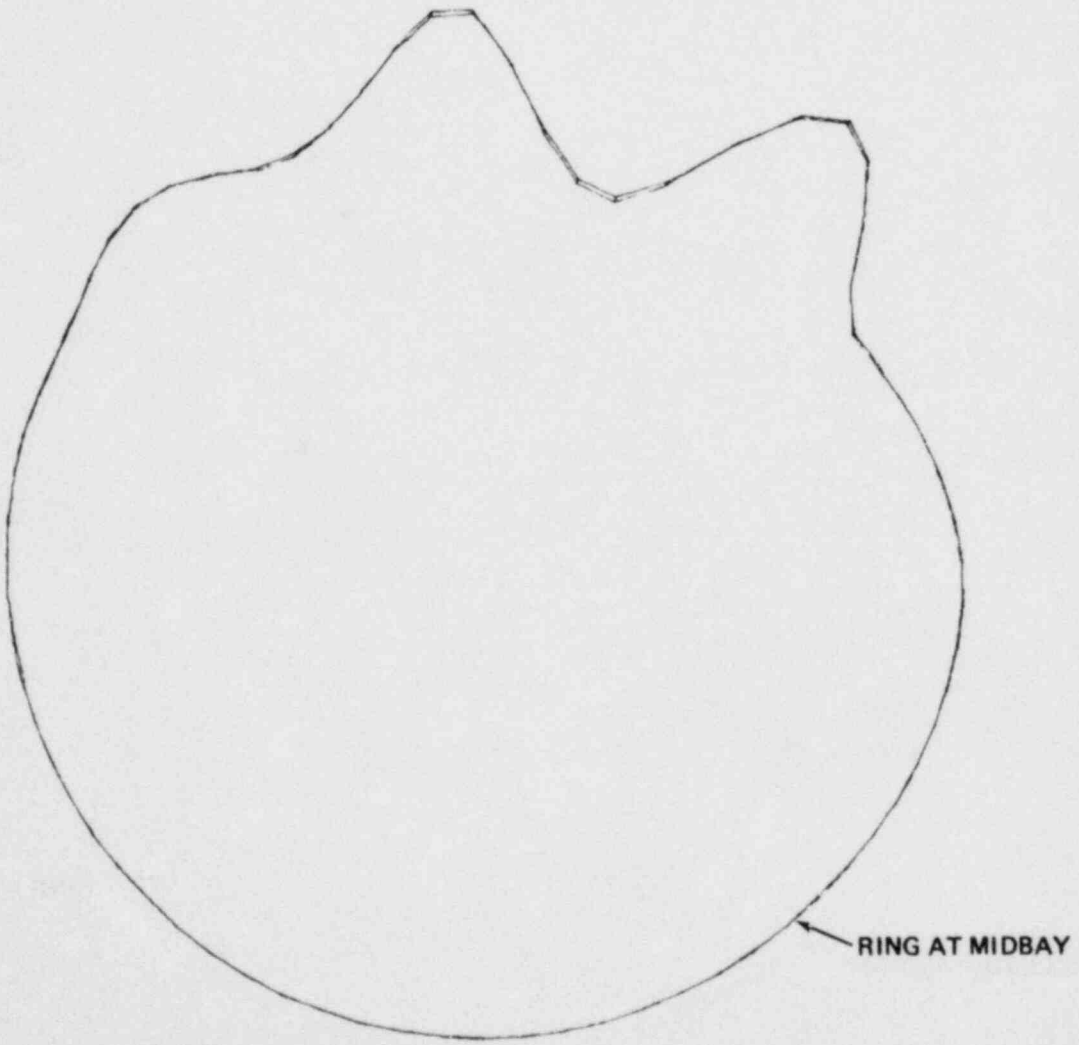

FIGURE 6-37 FIRST SHELL MODE OF DRY STRUCTURE

MODE 2, FREQ. = 17.90 HZ

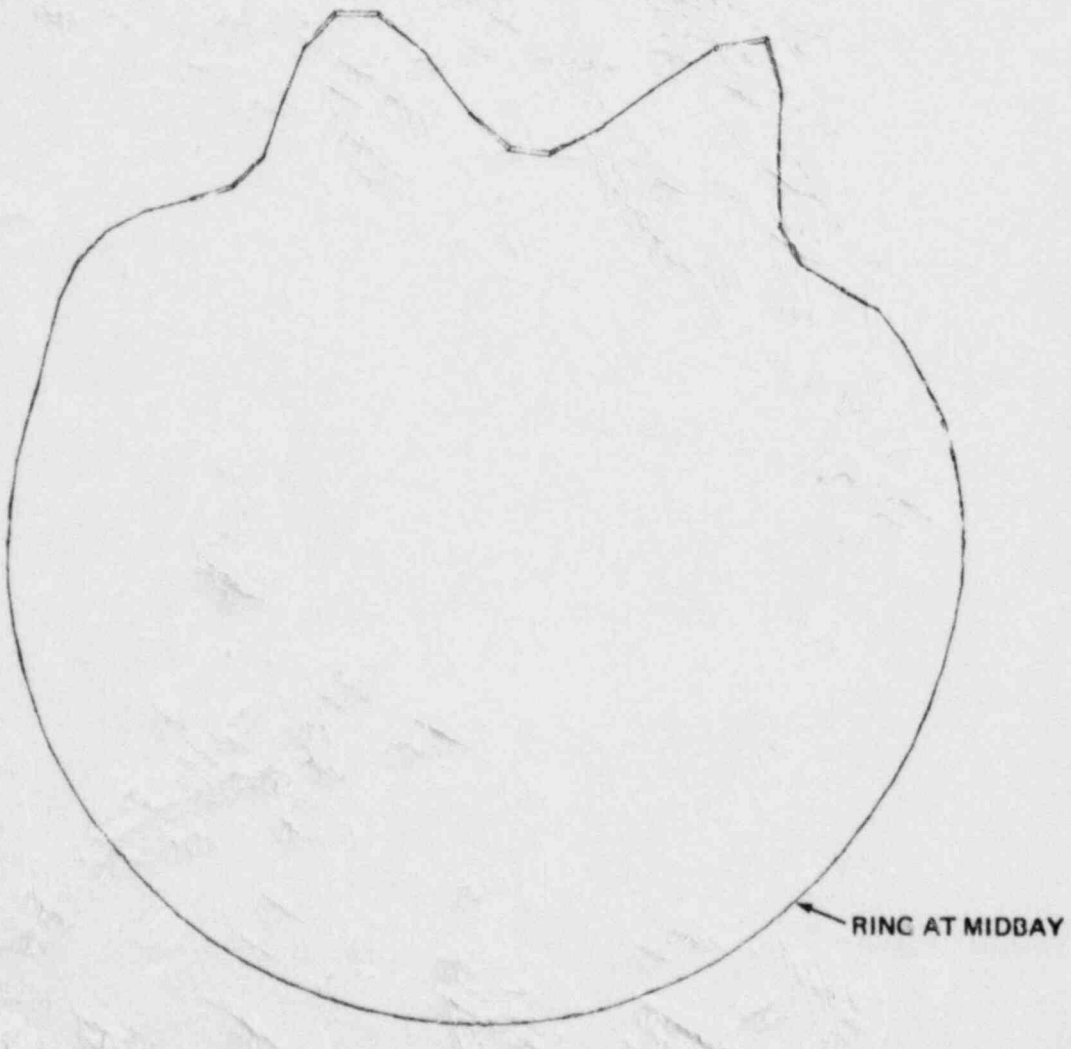

FIGURE 6-38 SECOND SHELL MODE OF DRY STRUCTURE

MODE 3, FREQ. = 22.41 HZ

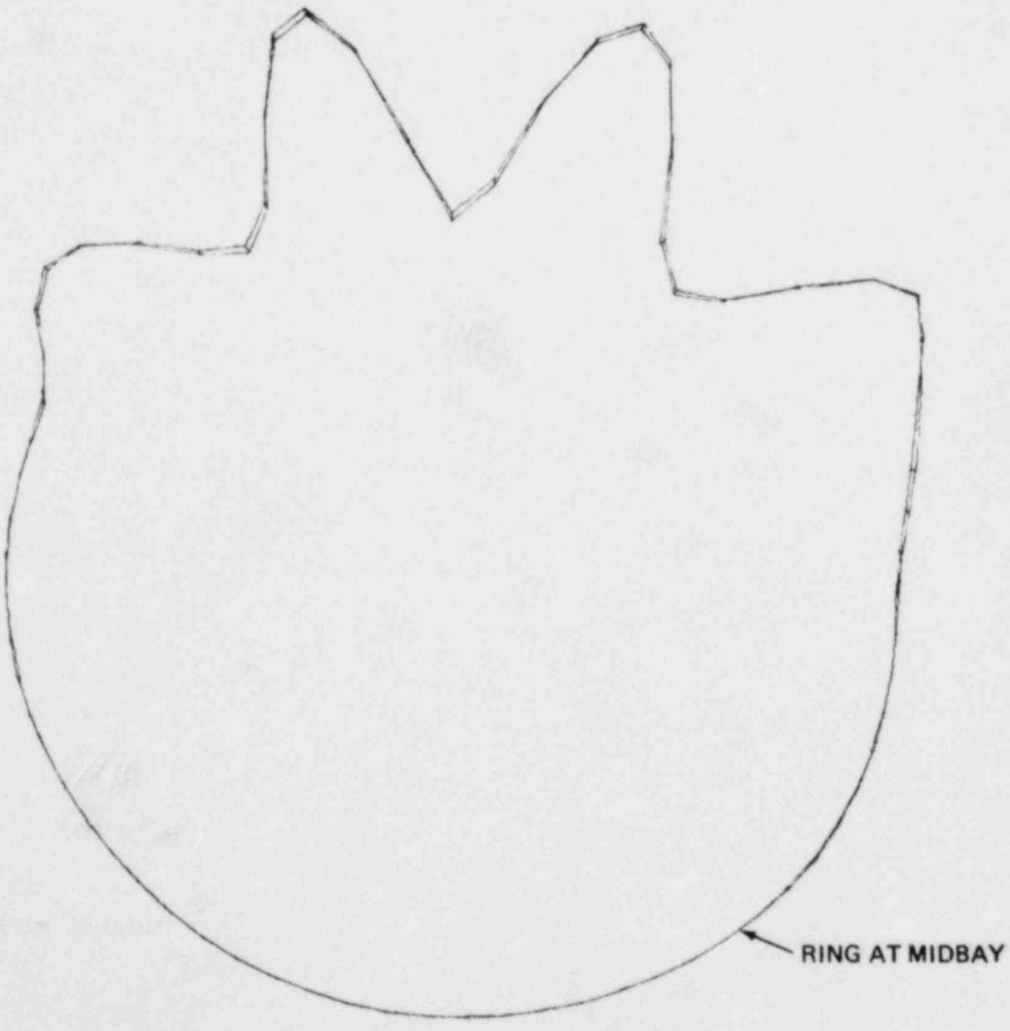

FIGURE 6-39 THIRD SHELL MODE OF DRY STRUCTURE

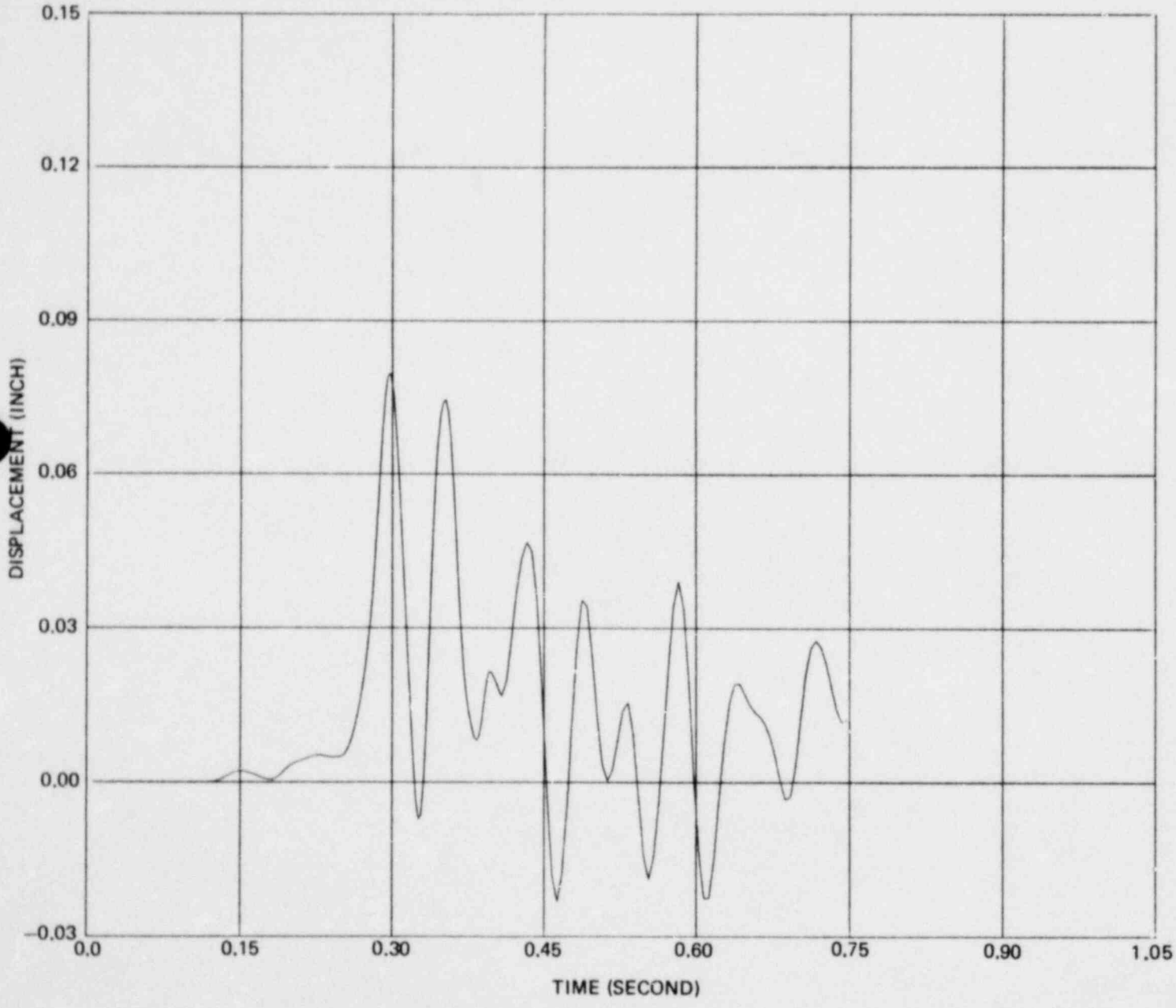

FIGURE 6-40 RADIAL DISPLACEMENT AT MIDBAY BOTTOM CENTER DUE TO POOL SWELL

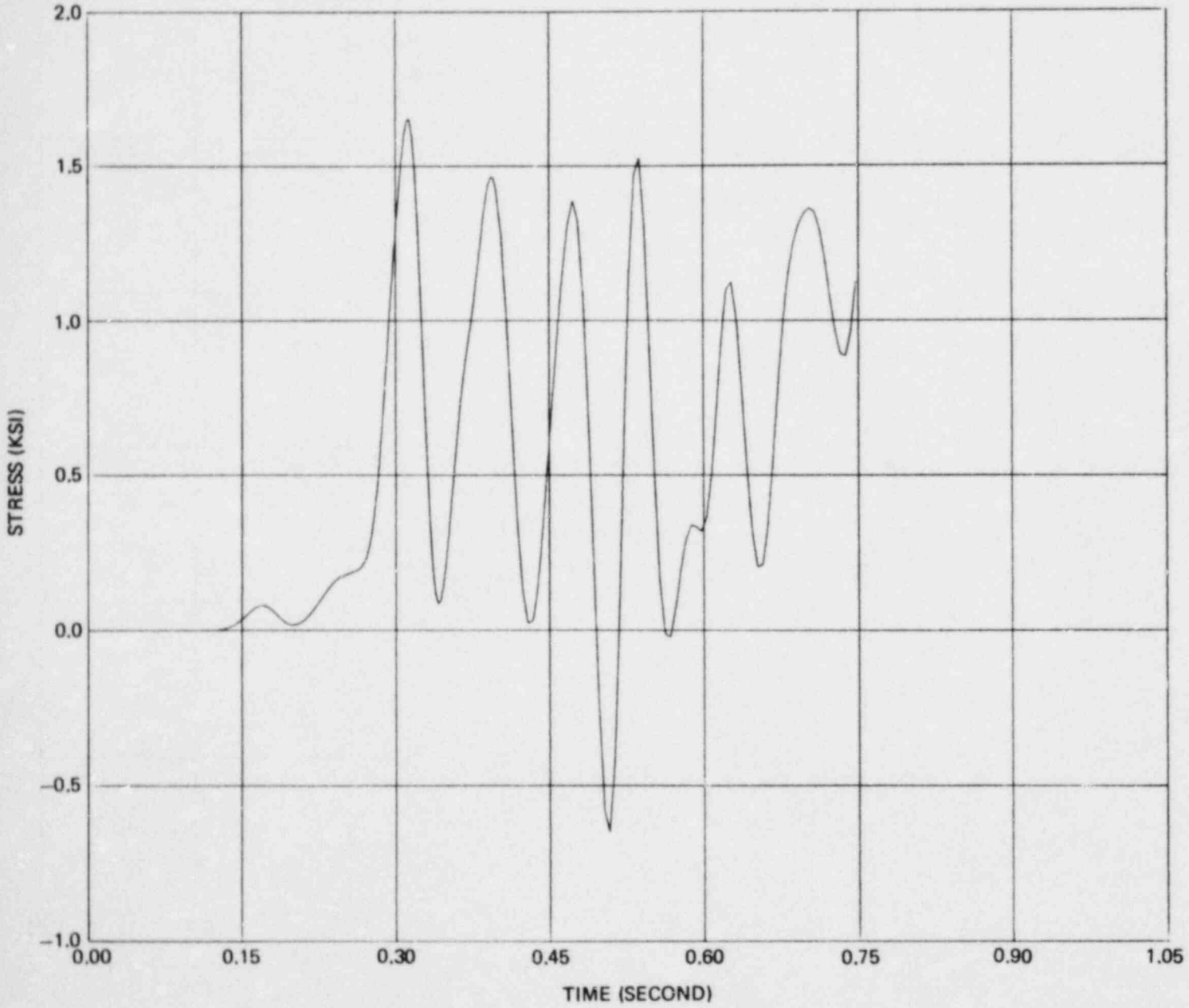

FIGURE 6-41 LONGITUDINAL MEMBRANE STRESS AT MIDBAY BOTTOM CENTER DUE TO POOL SWELL

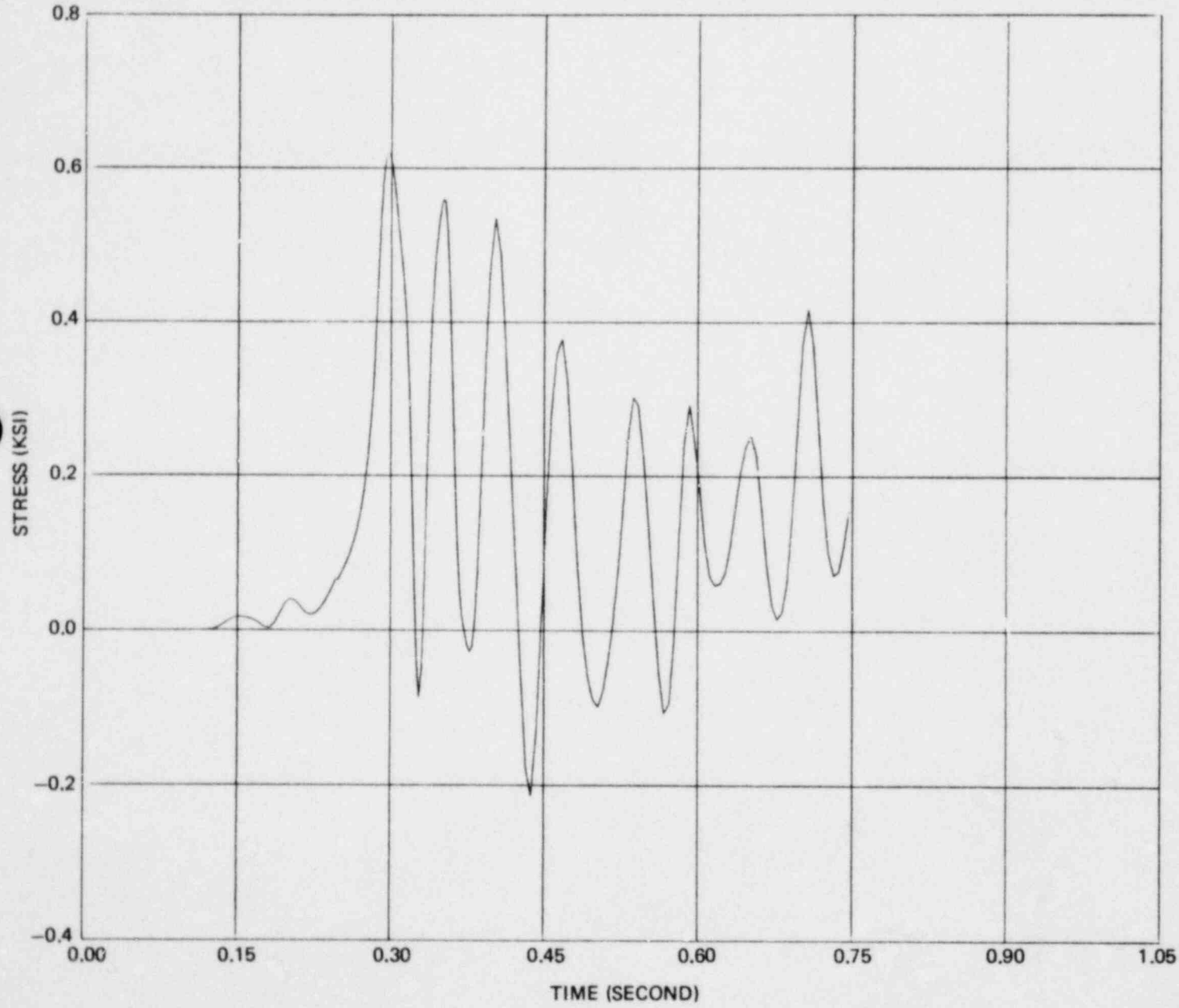

FIGURE 6-42 HOOP MEMBRANE STRESS AT MIDBAY BOTTOM CENTER DUE TO POOL SWELL

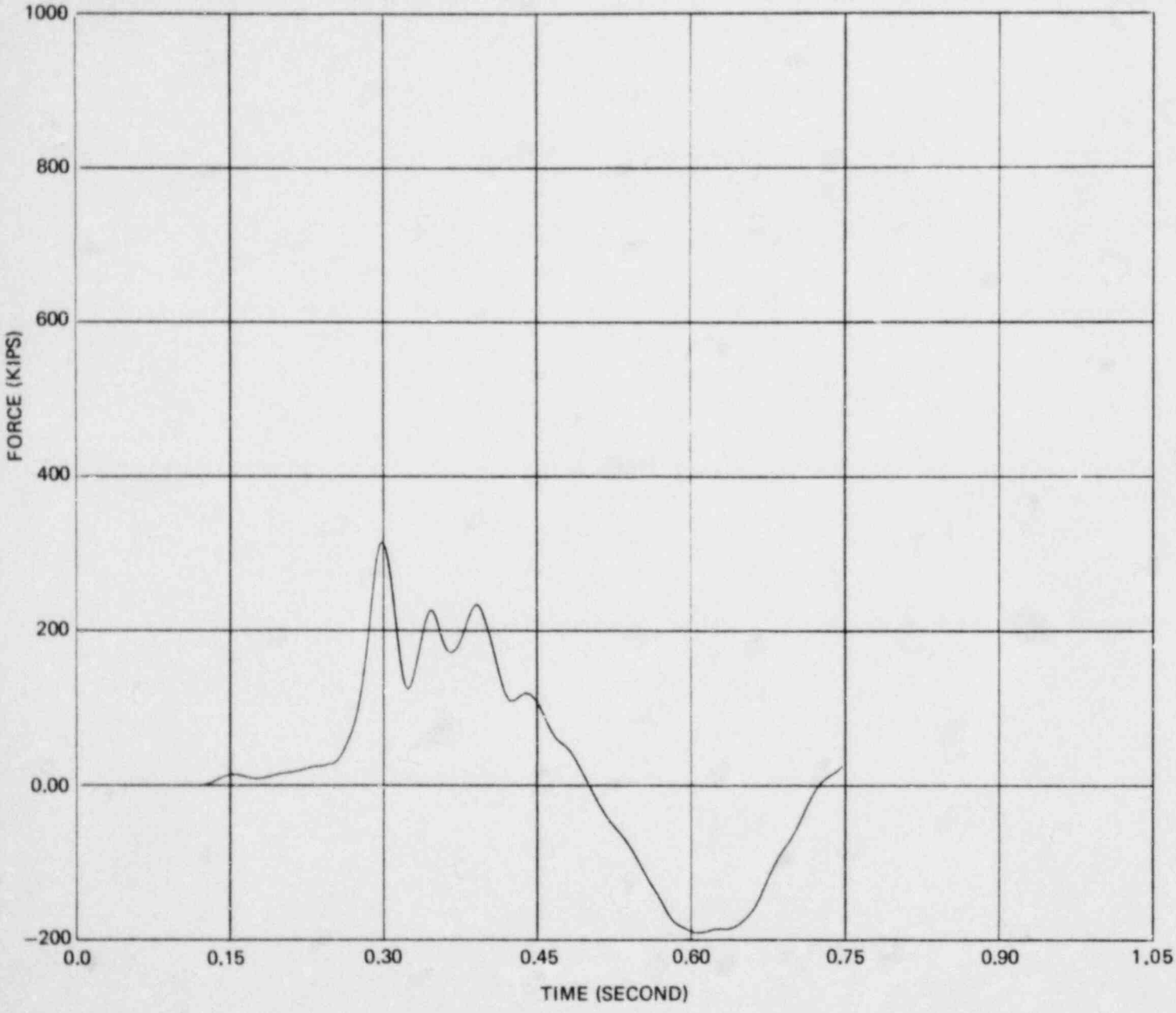

FIGURE 6-43 INSIDE COLUMN REACTION DUE TO POOL SWELL

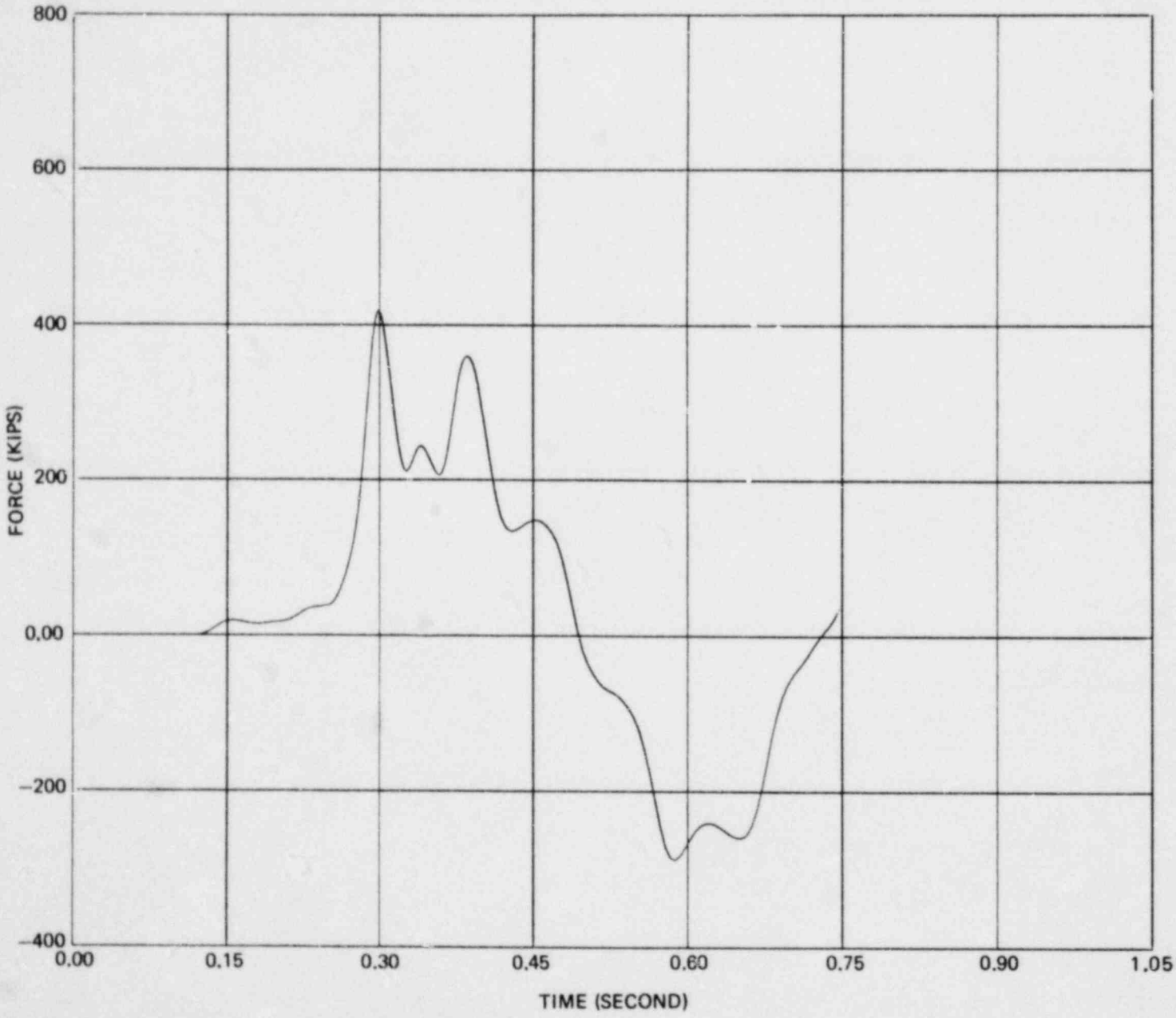

FIGURE 6-44 OUTSIDE COLUMN REACTION DUE TO POOL SWELL

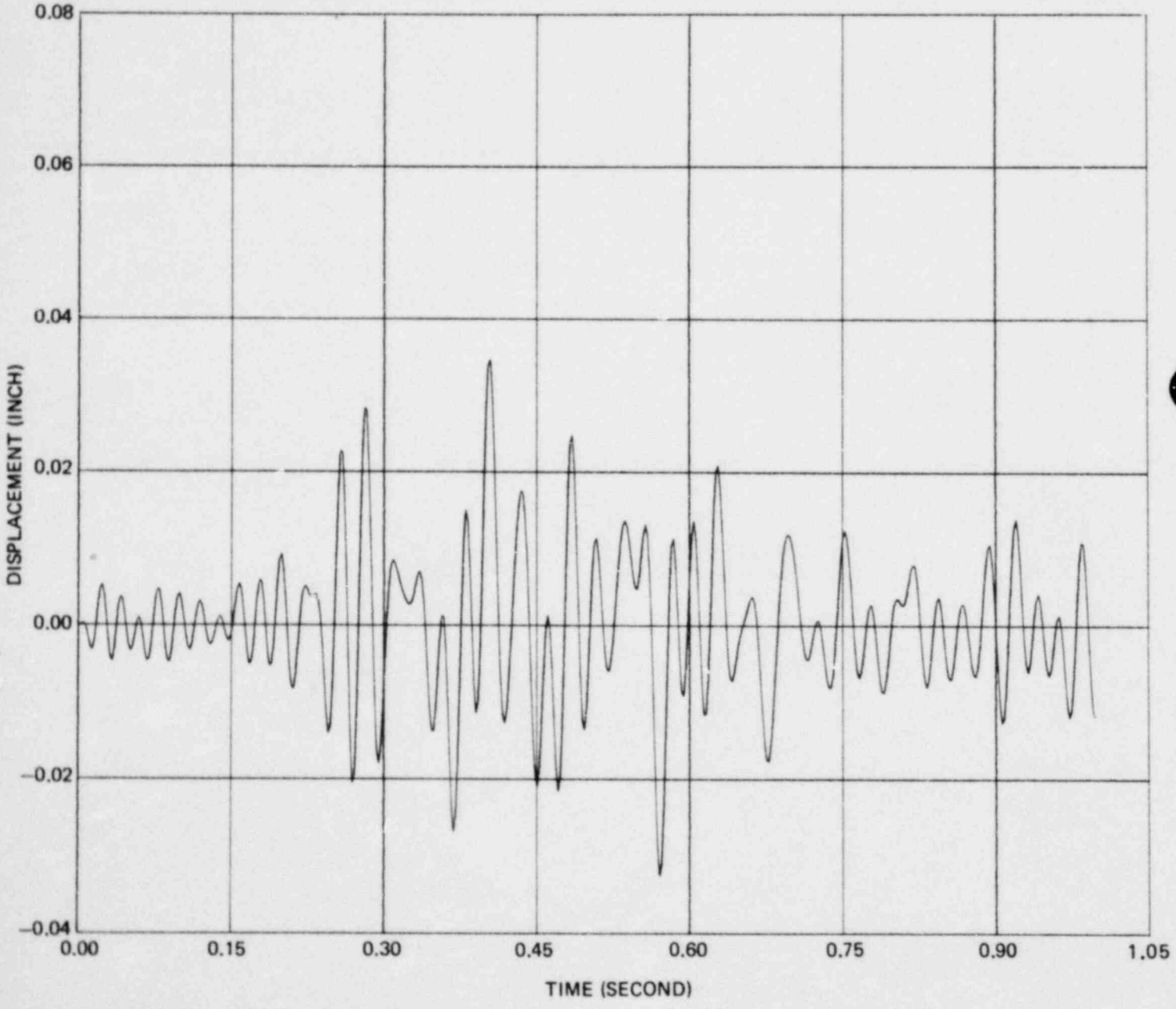

FIGURE 6-45 RADIAL DISPLACEMENT AT MIDBAY BOTTOM CENTER DUE TO SRV DISCHARGE

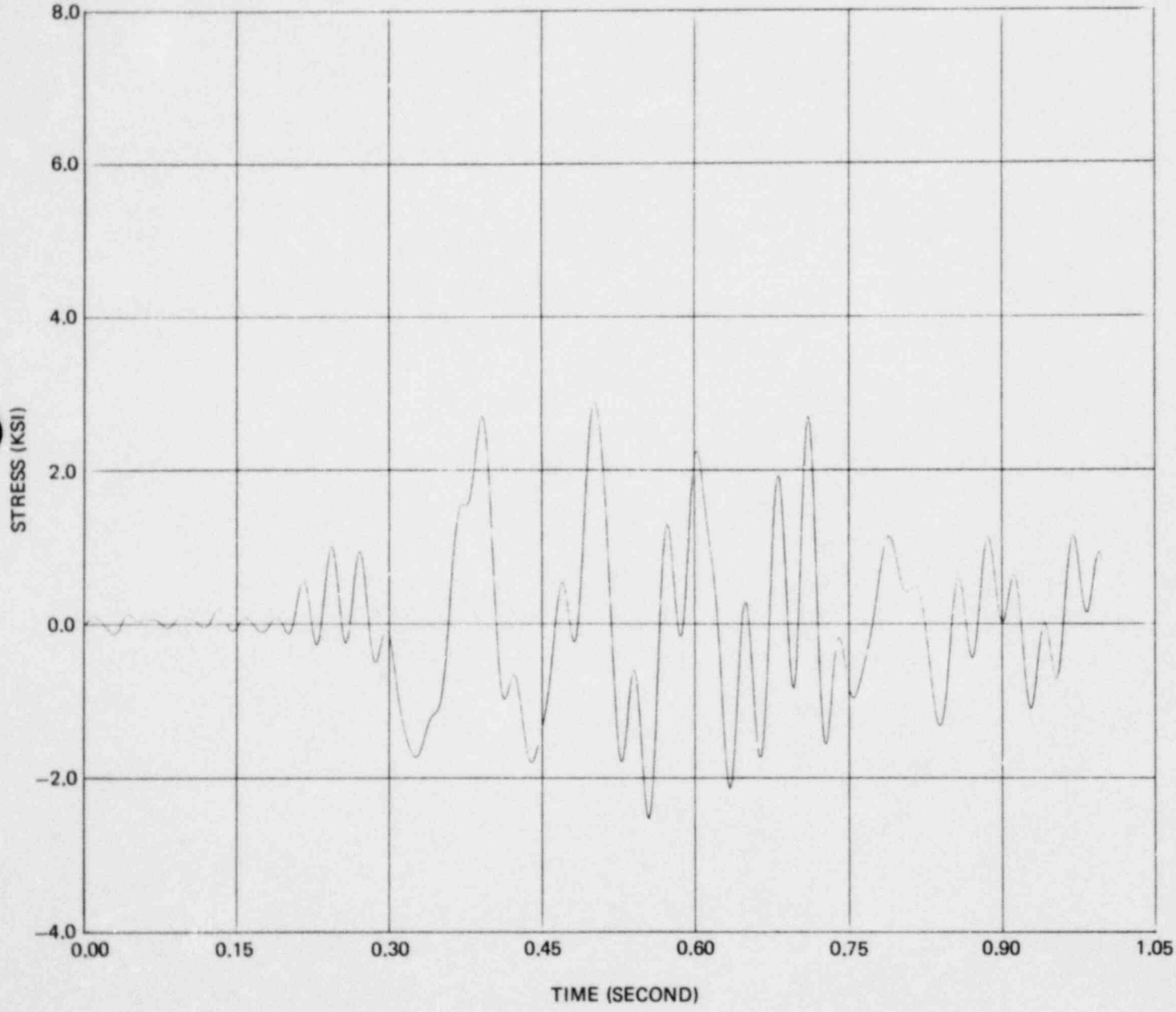

FIGURE 6-46 LONGITUDINAL MEMBRANE STRESS AT MIDBAY BOTTOM CENTER DUE TO SRV DISCHARGE

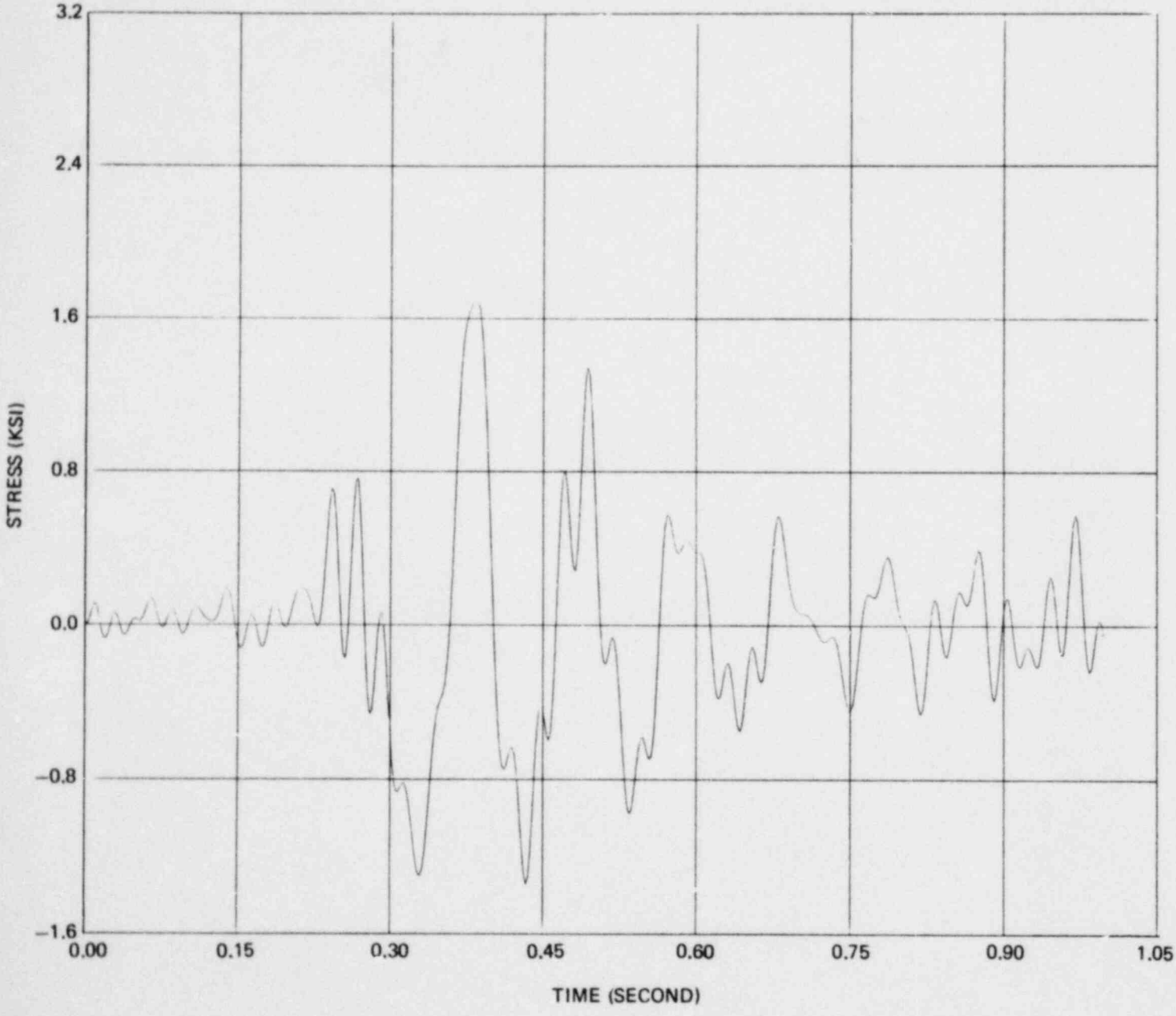

FIGURE 6-47 HOOP MEMBRANE STRESS AT MIDBAY BOTTOM CENTER DUE TO SRV DISCHARGE

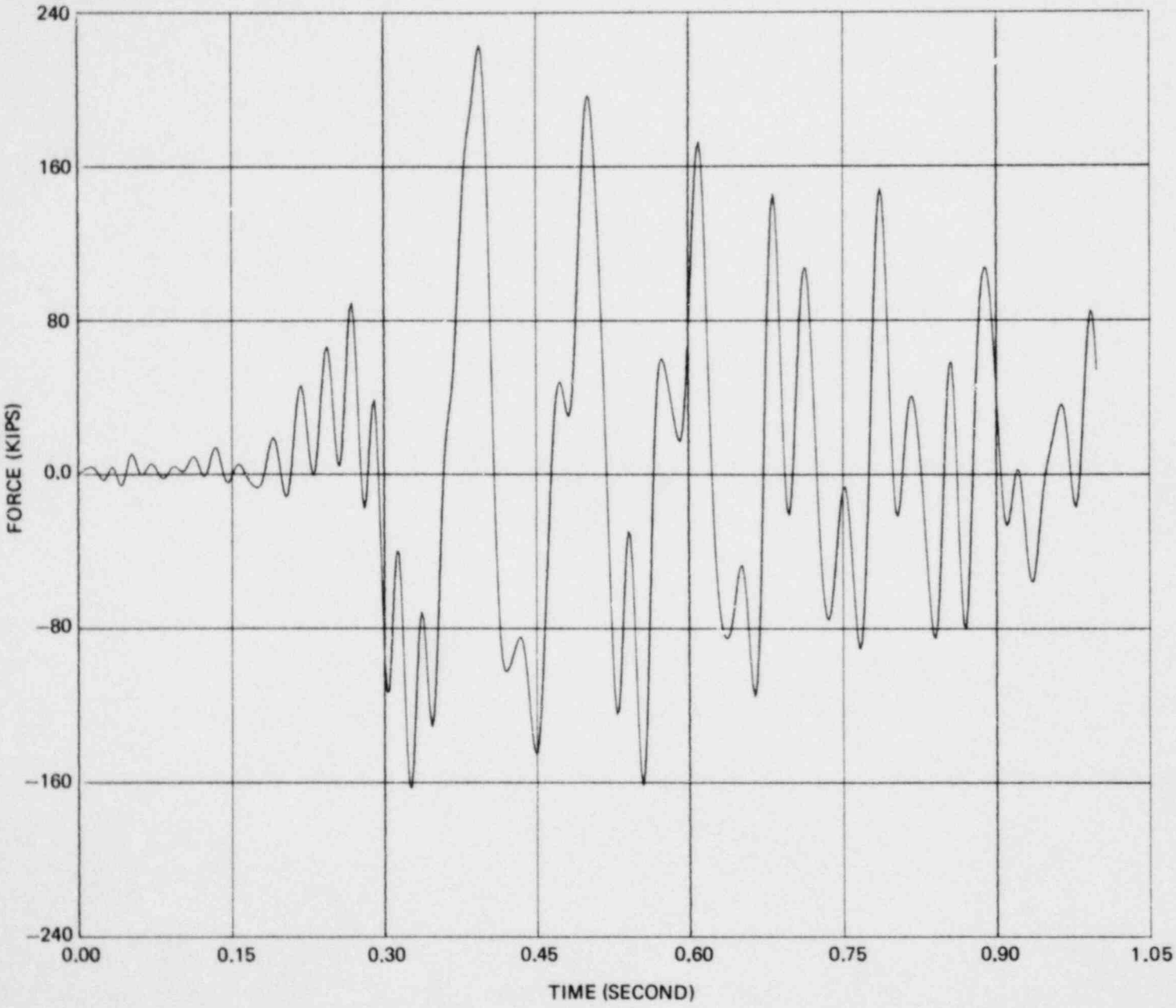

FIGURE 6-48 INSIDE COLUMN REACTION DUE TO SRV DISCHARGE

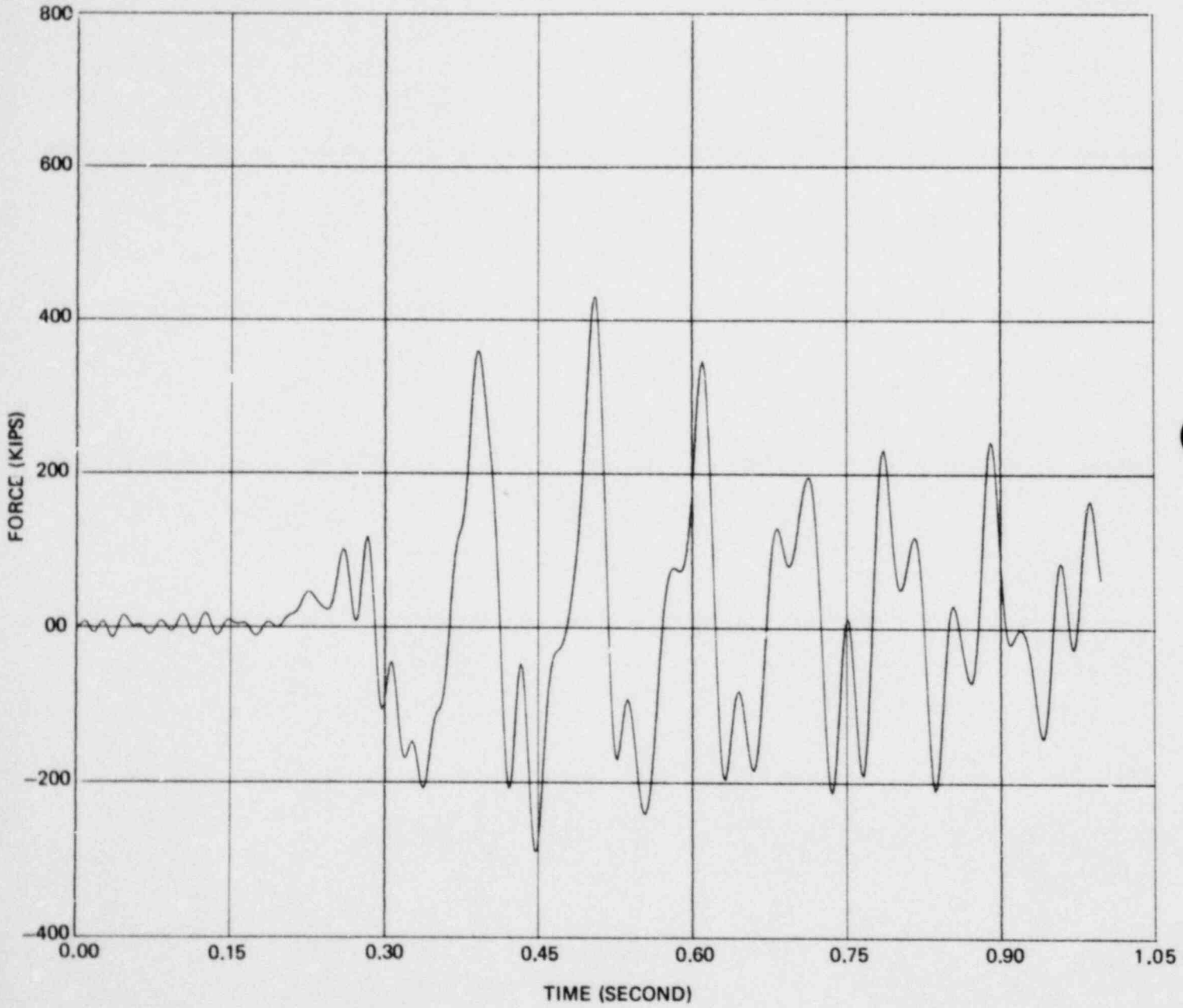

FIGURE 6-49 OUTSIDE COLUMN REACTION DUE TO SRV DISCHARGE

Section 7
STRUCTURAL EVALUATION OF THE VENT SYSTEM

Section 7

STRUCTURAL EVALUATION OF THE VENT SYSTEM

The vent system is a part of the containment boundary. It interconnects the drywell and the torus to provide the necessary flow path for pressure suppression. During the Long Term Program (LTP), several modifications were identified to mitigate the loads and/or increase the load carrying capacity of the structural components. This section describes the modifications performed and summarizes the hydrodynamic loads, analyses performed to calculate the stresses, and structural evaluation.

7.1 DESCRIPTION OF STRUCTURES AND MODIFICATIONS

The configurations of the vent systems for Peach Bottom Units 2 and 3 are identical except for the main vent-vent header intersections. Stresses at the main vent-vent header intersections are small. Therefore the analysis results obtained for Unit 2 were considered representative of Unit 3. Figure 7-1 is the plan of part of the vent system. The cross section of the vent header is shown in Figure 7-2.

The torus is made up of 16 mitered cylindrical segments called bays. Eight main vent lines extend radially outward from the drywell, entering the torus in every second bay. The main vent lines are interconnected by a vent header. A total of 96 downcomers direct flow from the vent header downward into the pool. The distribution of the downcomers is such that a non-vent bay contains twice as many downcomers as a vent bay. Thus, more of the flow will enter the suppression pool in the non-vent bays. Consequently, pool swell impact loads are higher in non-vent bays. The vent header is supported by pipe columns attached to the ring girder above. The vent lines, vent header, and downcomers are fabricated from SA516 Grade 70 material. The columns are fabricated from SA333 Grade 6 material.

Extensive structural modifications to the original vent system were performed to mitigate the effects of hydrodynamic loads. These modifications included the installation of vent header deflectors and strengthening of the vent header and other components. The modifications are described below.

7.1.1 Vent Header Deflectors

In the event of a postulated large break LOCA, the initial clearing of air through the downcomers into the suppression pool would cause the pool to swell upward, impacting the vent header and potentially causing higher stresses in the header. Vent header deflectors were installed in the non-vent bays under the header and above the pool surface. The deflectors protect the vent header by diverting pool swell flow away from the header.

The deflector consists of an 18-inch diameter pipe suspended under the header spanning the non-vent bay. The 8-inch angles are welded to each side of the pipe to give the deflector a wedge profile suitable for flow diversion. Each deflector is supported from the vent header support collars at either end of the bay. The connection of the deflector to the collar is made using stainless steel pins, with a sliding arrangement to allow differential thermal expansion between the vent header and deflector.

7.1.2 Downcomer Tie Modification

Flow through the vent system would result in dynamic thrust and lateral loads on the downcomers. Existing tension-only ties between pairs of downcomers were replaced by 3.5-inch schedule 40 pipe sections. Use of the round pipe section limits drag loads on the tie.

7.1.3 Vent Header Supports

The vent header was originally supported from the bottom of the torus using a pair of pipe columns. These vent header support columns had to be removed to allow for installation of the new quenchers. Now these columns support the vent header from above.

The new vent header columns are similar to the existing columns except that the supports are heavier. The columns have a clevis and pin detail at each end that permits rotation and relative thermal expansion of the vent system with respect to the torus.

7.1.4 Reinforcement of the Vent Header and Downcomer Junction

The downcomers are partially submerged in water. During a LOCA or SRV discharge, the submerged portion of the downcomer would be subjected to hydrodynamic loads. The junctions of the vent header and downcomer were reinforced to reduce the stresses at the structural discontinuity (Figure 7-3).

7.1.5 Reinforcement of the Vent Header in the Vent Bays

To reduce the load on the vent header, deflectors were installed in the non-vent bays only. Although pool swell loads are higher in the non-vent bays, they are significant in the vent bays. Therefore, reinforcement was provided at the vent header in the vent bays as shown in Figure 7-4.

7.1.6 Reinforcement of the Vacuum Breaker Nozzle

The purpose of this reinforcement was to increase the rigid area at the junction of the vacuum breaker to the main vent to such an extent that the stresses beyond the rigid area are within the allowable values. Reinforcements for Units 2 and 3 are shown in Figures 7-5 and 7-6 respectively. The main vent-vent header intersections are different for Peach Bottom Units 2 and 3, as are the reinforcing details at the vacuum breakers. However, the basic reinforcing philosophy is the same. As shown in these figures, the reinforcement is provided by means of circular and radial gusset plates.

7.2 LOADS

The vent system was evaluated for normal loads, LOCA loads, and SRV discharge loads. These are described below.

7.2.1 Normal Loads

Normal loads for the vent system consist of the combination of dead load and thermal effects during operation of the plant.

7.2.2 Seismic Loads

Seismic loads for the evaluation are given in Section 5.

7.2.3 LOCA Loads

LOCA loads are caused by a design break accident (DBA), intermediate break accident (IBA), or small break accident (SBA). They could be caused by pool swell, condensation oscillation, or chugging. The loads are in the form of impact, thrust, drag, pressure, or thermal loads. Peach Bottom Units 2 and 3 operate with no pressure differential between the drywell and wetwell. All the LOCA loads used in the plant unique analysis are given in the LDR and PULD (References 14 and 18) and are summarized below.

7.2.3.1 Vent System Pressurization and Thrust Loads

A DBA causes the most rapid pressurization of the containment system, the largest vent system mass flow rate, and, therefore, the most severe vent system thrust loads. The equivalent static vent system thrust loads along with their location and direction are shown in Figure 7-7.

7.2.3.2 Vent System Impact and Drag Loads

Expulsion of the air through the downcomers beneath the suppression pool surface during a LOCA creates an expanding air bubble. A layer of water at the top of the pool is thrown upward against the vent header and main vents. The pool swell pressure transient at any impact location consists of a short duration impact pulse followed by a drag load.

Vent system impact and drag loads include loads on the vent header, downcomer, and main vent. These loads are based on experimental data

obtained from the QSTF plant unique tests. Pool swell impact and drag loads are given in Reference 18. The loads on the downcomer and the main vent are given in Reference 14.

Figure 7-8 shows a pool swell impact loading sequence. Initial impact occurs not at the bottom dead center but away from it as shown in Figure 7-8. Figure 7-9 shows a typical local impact pressure transient at the bottom center of the vent header.

7.2.3.3 Vent System Thermal Loads

Vent system thermal loads result because of the temperature difference between the drywell and wetwell during a DBA, IBA, or SBA. The thermal loads are given in Reference 18.

7.2.3.4 Vent Header Deflector Loads

Vent header deflectors are provided in non-vent bays to protect the vent header from the pool swell impact and drag loads. The deflector loads were obtained from the QSTF plant unique tests and are given in Reference 18.

7.2.3.5 Condensation Oscillation Loads

The LDR defines the vent system CO loads. The loading is defined in terms of harmonic pressure amplitudes for specific frequency bands. The selection of the frequency depends on the plant unique vent system dominent frequency.

The CO loads are broken up into two parts; namely, internal pressurization and dynamic lateral load. The internal pressurization of the main vent, vent header, and downcomers produces the hoop response of these structures.

The dynamic lateral load has the following two components:

(a) Internal pressure load of equal magnitude in each downcomer pair

(b) Differential pressure load between downcomers in a pair.

The amplitudes and frequency ranges for the DBA and IBA CO loads are given in the LDR.

7.2.3.6 Chugging Loads

Vent system chugging loads consist of two components; namely, vent system pressure loads and downcomer loads. Vent system pressure loads and the methodology for calculating plant unique chugging loads on the tied downcomers are given in the LDR.

7.2.4 Drag Loads Due to SRV Discharge

Oscillating bubbles resulting from an SRV actuation create an unsteady three-dimensional flow field in the suppression pool and induce acceleration and standard drag forces on the submerged portions of the downcomers. T-Quencher bubble drag loads on the downcomers were obtained according to procedures described in the LDR.

7.3 ALLOWABLE STRESSES

The governing load combinations and their corresponding allowable service limits for the vent system, vent header penetration, and vent header deflector are given in Tables 5-3 through 5-6 respectively. The allowable stresses for the various service levels for different vent system components are given below.

7.3.1 Stress Limits for Vent Header, Downcomers, and Main Vent

Levels A and B service limits for stress intensity are:

$$P_m \leq S_m$$

$$P_L \leq 1.5\ S_m$$

$$P_L + P_b \leq 1.5\ S_m$$

$$P_L + P_b + Q \leq 3.0\ S_m$$

where

P_m = membrane stress intensity

P_L = local membrane stress intensity

$P_L + P_b$ = membrane plus bending stress intensity

Q = secondary stress intensity

S_m = membrane stress allowable

= 19.3 ksi for SA 516 Grade 70 material.

Level C service limits for stress intensity are:

$P_m = 1.2\ S_m \leq S_y$

$P_L = 1.8\ S_m \leq 1.5\ S_y$

$P_L + P_b = 1.8\ S_m \leq 1.5\ S_y$

S_y = yield stress

= 38.0 ksi for SA 516 Grade 70 material.

7.3.2 Limits on Column Stresses

The vent support column assemblies are considered as linear component supports. Criteria for linear component supports are given in subsection NF 3000 and Appendix XVII of the ASME Code.

7.3.2.1 Pipe Columns

Tension. The Levels A and B service limits for stress are:

On the net section,

$$F_t = 0.60\ S_y \leq 0.50\ S_u$$

where F_t = allowable tensile stress.

The Level C service limits for stress are:

$$F_t = 0.80\ S_y \leq 0.67\ S_u$$

S_y = yield stress

= 28.3 ksi for 300°F, 8-inch schedule 80 pipe, SA 333 Grade 6

S_u = ultimate stress

= 60.0 ksi for 8-inch schedule 80 pipe, SA 333 Grade 6.

Compression. On the gross section of axially loaded compression members, when Kl/r, the largest effective slenderness ratio of any unbraced segment, is less than C_c, the allowable stress in compression shall be:

$$F_a = \frac{S_y \left[1 - \frac{(Kl/r)^2}{2C_c^2}\right]}{\frac{5}{3} + \frac{3(Kl/r)}{8C_c} - \frac{(kl/r)^3}{8C_c^3}} \quad \text{for Level A}$$

$$F_a = \frac{2}{3} S_y \left[1 - \frac{(Kl/r)^2}{2C_c^2}\right] \quad \text{for Level C}$$

where

$$C_c = \sqrt{\frac{2\pi^2 E}{y}}$$

F_a = allowable compressive stress

K = effective length factor

l = actual unbranced length

r = radius of gyration

E = Young's modulus.

Note that for the vent header support columns, the Kl/r ratio is about 24 whereas the C_c value is about 132.

7.3.2.2 Vent Header Deflector

The Levels A and B service limits for stress are:

$$F_b = 0.60\ S_y$$

where F_b = allowable bending stress.

The Level C service limits for stress are:

$$F_b = 0.80\ S_y\ .$$

The Level D service limits for stress are:

$$F_b = 1.20\ S_y \leq 0.77\ S_u$$

where

S_u = ultimate stress
= 58.0 ksi for SA 36
= 60.0 ksi for SA 333 Grade 6

S_y = yield stress
= 35.0 ksi for SA 333 Grade 6
= 36.0 ksi for SA 36.

7.4 METHODS OF ANALYSIS

A 22.5° segment of the vent system was chosen for the structural analysis so that the symmetry of the vent system and the imposed loading could be fully utilized. This segment consists of one-half of a vent bay and one-half of a non-vent bay. The segment includes a portion of the vent header, half of a main vent pipe cut across its longitudinal axis, and six downcomers. The segment is repeatable; 16 such segments make up the complete vent system. A finite element shell model of the 22.5° segment of the vent system was created. Using this finite element model, appropriate static and dynamic analyses were performed for loads discussed in Section 7.2. The NASTRAN computer program was used for the analyses.

7.4.1 Description of Finite Element Model

The complete finite element shell model is shown in Figures 7-10 through 7-12. Figure 7-10 shows the vent header and main vent nodes and elements. Figure 7-11 shows the nodes and elements for the vacuum breaker nozzle and the vent header-downcomer stiffeners. Figure 7-12 shows the downcomer nodes and elements. Figure 7-13 is a composite computer plot of the entire model. The model is made up of 1770 nodes and 1790 elements and has about 9900 static degrees of freedom.

The vent header, downcomers, and main vent were modeled using isoparametric quadrilateral thin shell (QUAD4) elements. For some portion of the vent cap and for the transitions from smaller to larger elements, isoparametric triangular thin shell (TRIA3) elements were used. The vent header collar and stiffener at the vent header miter joints were modeled using isoparametric quadrilateral thin shell (QUAD4) elements.

The vent header support columns and ties between two downcomers were modeled as truss (ROD) elements, which can resist axial load and torsional moment only.

The bottom half of the vent header was modeled using elements 10° wide. The upper portion of the vent header was modeled using elements 20° wide. At the intersection between the downcomer and vent header, smaller elements were used to capture the local stresses. The main vent was not highly loaded and was therefore modeled using larger elements. In the modeling of the vent header, the reinforcing plate was considered integral to the header shell to which it is attached.

Symmetric boundary conditions were used for the model boundaries at both ends, i.e., midbay in the non-vent region (Ring 1) and at the middle of the vent region. The nodes at the end of the main vent were tied to the center point (node 3150) by rigid elements so the end plane would act as a rigid plate. All degrees of freedom of the node at the center point were fixed except the one that allows for rotation of the main vent about the horizontal axis in the end plane. This simulates a hinged end condition at the main vent-drywell intersection.

The bottoms of the vent header support columns were attached to the vent header collar and the tops of the columns were attached to the ring girder.

Young's modulus E of steel was taken to be 27,900 ksi. Poisson's ratio was assumed to be 0.30.

7.4.2 Structural Analysis

Structural analyses of the vent system were performed using a 22.5° segment finite element model of the vent system. Static and dynamic analyses were performed as appropriate for the loads described in Section 7.2. These analyses are briefly described here. The results of these analyses are discussed in Section 7.7.

7.4.2.1 Static Analysis

A static analysis was performed for the normal loads and other quasi-static loads where no dynamic effects were expected. Various load cases were analyzed. The results from these load cases were combined appropriately to obtain stresses for the prescribed load combinations. Symmetric boundary conditions were used at the planes of symmetry.

7.4.2.2 Dynamic Analysis

A dynamic analysis was performed to determine critical stresses in the vent system caused by pool swell loads, LOCA condensation oscillation loads, and SRV discharge drag loads. Modal transient analyses were performed for pool swell loads and SRV discharge drag loads. A direct frequency response analysis was carried out for condensation oscillation loads.

Mode shapes and frequencies of the vent system structural model were obtained as a first step of the modal transient analysis. The generalized dynamic reduction option available in NASTRAN was used to condense the size of the mass and stiffness matrices. Symmetric boundary conditions were used at the planes of symmetry. Additional mass, representing the mass of water contained in the submerged portion of the downcomers, was added to the structural mass at these locations. Added mass was also considered for the vent header deflector as specified in the LDR. A modified Given's method was used to extract the frequencies and mode shapes.

An additional modal analysis was performed to obtain the lowest vent system frequency to be used for calculating the maximum chugging design load for a downcomer. For this analysis, the hydrodynamic mass, equaling twice the mass of the water contained in the submerged portion of the downcomers, was used. This was necessary because during chugging water is inside the submerged portion of the downcomer. Modal transient analyses were carried out to obtain the structural response for the SRV discharge loads and pool swell loads. Two percent of the critical damping was used. The stresses for critical elements, nodal deflections at important locations, and reaction forces at support points were calculated as functions of time.

A direct frequency response analysis was performed for the DBA and IBA condensation oscillation loads since the prescribed loadings are harmonic. The dominant mode of the vent system is 8.03 Hz; therefore, the harmonic analysis was carried out at 8.0, 16.0, and 24.0 Hz according to DBA and IBA CO load definitions described in Section 7. A damping equal to 2% of critical was used. Eight different load cases were considered to obtain the most critical load case. Four of them are shown in Figure 7-14. The remaining four cases are the mirror image of those shown in the figure.

7.5 CALCULATION OF STRESSES

The computer output results for the static and dynamic analyses are in the form of element hoop, longitudinal, and shear stresses. This information was obtained for selected critical elements. The dynamic time-history results were surveyed to identify maximum values.

The output stresses were post-processed, as described in Section 6, to calculate the stress intensities. The calculated stress intensities were compared with the ASME Code allowable values.

7.6 FATIGUE EVALUATION

The vent system experiences cyclic loads during SRV discharge and LOCA. Fatigue evaluation is therefore necessary because of these cyclic loads. Since the stresses are higher at discontinuities, the fatigue evaluation was considered at any location having a significant discontinuity. The governing location for fatigue evaluation was at the junction of the vent header and the downcomer. The fatigue evaluation was based on the ASME Code rules and guidelines.

LOCA loads for which a fatigue evaluation was necessary were DBA and IBA condensation oscillation loads and DBA, IBA, and SBA chugging loads. In addition, a fatigue evaluation was performed for T-Quencher bubble drag loads.

A fatigue evaluation for chugging loads was carried out according to the LDR methodology. For condensation oscillation and bubble drag loads, stresses at discontinuities were obtained from the dynamic analyses and appropriate stress amplification factors were used to obtain the usage factors during the life of the plant.

7.7 EVALUATION

This section presents and evaluates the results of the analyses described in Section 7.5 for the loads given in Section 7.2. Calculated stresses are compared with the allowable limits established in Section 7.3. The following discussion covers both structural response behavior and the acceptability of the calculated stresses.

7.7.1 Static Analysis Results

The static analysis cases included dead weight, internal pressure, thrust loads, thermal loads, and unit loads applied to the tips of the downcomers. Static analyses were used to check the accuracy of the finite element model as well as to calculate stresses caused by specified or equivalent static loads.

Part of the model checkout involved applying unit vertical loads at the ends of downcomers 1 and 2 and a uniform internal pressure throughout the vent system. Figure 7-15 shows the deformation of the vent header at ring 5 (refer to Figure 7-10). Figure 7-16 shows its radial deformation for a uniform internal pressure. From these figures, symmetrical behavior is evident.

7.7.2 Dynamic Analysis Results

As discussed in Section 7.4.2.2, frequencies and mode shapes were calculated for the 22.5° vent system model with a full water mass attached to the submerged portion of the downcomers. Table 7-1 lists the frequencies of the vent system up to the first 10 modes. Figures 7-17 through 7-19 show the mode shapes for the cross section at ring 3 (see Figure 7-10) of

the vent system model. Figures 7-20 through 7-22 show the mode shapes for the plan view at the downcomer tips. From Figures 7-17 through 7-22, it is clear that the first three modes of the vent system represent the swinging motion of the vent system, with the downcomers swinging in phase in the first mode but out of phase in modes 2 and 3. It is also clear that load case 1 of Figure 7-14 for downcomer CO loading would be the most critical.

Stresses from modal transient and frequency response analyses were obtained at critical locations for comparison with allowable values. Figure 7-23 shows principal stresses at a typical downcomer-vent header intersection for pool swell loading. Figure 7-24 shows vent header support outside column reaction for the same loading.

7.7.3 Stress Evaluation at Key Locations

Stresses at key locations were calculated for different load cases and membrane stress intensities were calculated for the governing load combinations (see Tables 5-2, 5-3, and 5-6). Tables 7-2 and 7-3 compare the calculated stress intensities at key vent system locations with the allowable limits. Table 7-2 shows the comparison for service Level A allowable cases while Table 7-3 shows this comparison for service Level C allowable cases. Table 7-2 shows very high stresses at the downcomer vent header intersection near the centerline of the bay. These high stresses resulting from condensation oscillation loads were anticipated because of the very conservative load definition. The stresses in the main vent near the drywell are very low. The stresses in the main vent-drywell intersection also will be very low compared with the allowable values. Hence, the intersection was not analyzed in detail. Tables 7-4 through 7-6 compare the calculated stresses with the allowable limits for vent system supports for service Levels A, C, and D respectively. The results shown in Tables 7-2 through 7-6 demonstrate that the vent system and the supports including the vent header deflector have adequate safety margins against hydrodynamic loads resulting from LOCA and SRV discharges.

7.7.4 Results of Fatigue Evaluation

As discussed in Section 7.6, a fatigue evaluation for the vent system was carried out for LOCA, CO, chugging, and SRV discharge drag loads. The results of this evaluation show that the maximum usage factor is less than 1.

Table 7-1

VENT SYSTEM FREQUENCIES

Mode	Frequency (Hz)
1	8.03
2	11.02
3	11.07
4	13.31
5	13.64
6	13.87
7	14.16
8	14.47
9	14.87
10	17.09

Table 7-2

STRESS EVALUATION AT KEY LOCATIONS
SERVICE LEVEL A

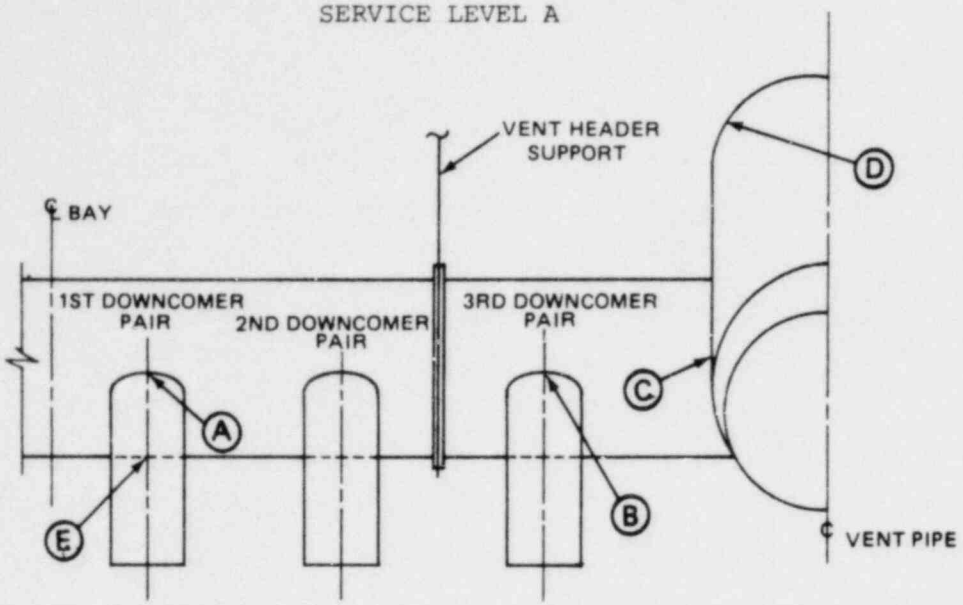

Location	Stress Type	Calculated SI (ksi)	Allowable SI (ksi)	Ratio
Intersection between header and D/C 1 (A)	P_L	28.33	29.00	0.98
	$P_L + P_b + Q$	50.26	58.00	0.87
Intersection between header and D/C 3 (B)	P_L	8.01	29.00	0.28
	$P_L + P_b + Q$	38.30	58.00	0.66
Intersection between header and vent (C)	P_L	10.37	29.00	0.36
	$P_L + P_b + Q$	10.64	58.00	0.18
Main vent (D)	P_M	3.14	19.30	0.16
	$P_L + P_b$	3.34	29.00	0.12
	$P_L + P_b + Q$	3.68	58.00	0.06
Header between D/C 1 and D/C 2 (E)	P_M	10.08	19.30	0.52
	$P_L + P_b$	13.76	29.00	0.47
	$P_L + P_b + Q$	23.20	58.00	0.40

Table 7-3

STRESS EVALUATION AT KEY LOCATIONS
SERVICE LEVEL C

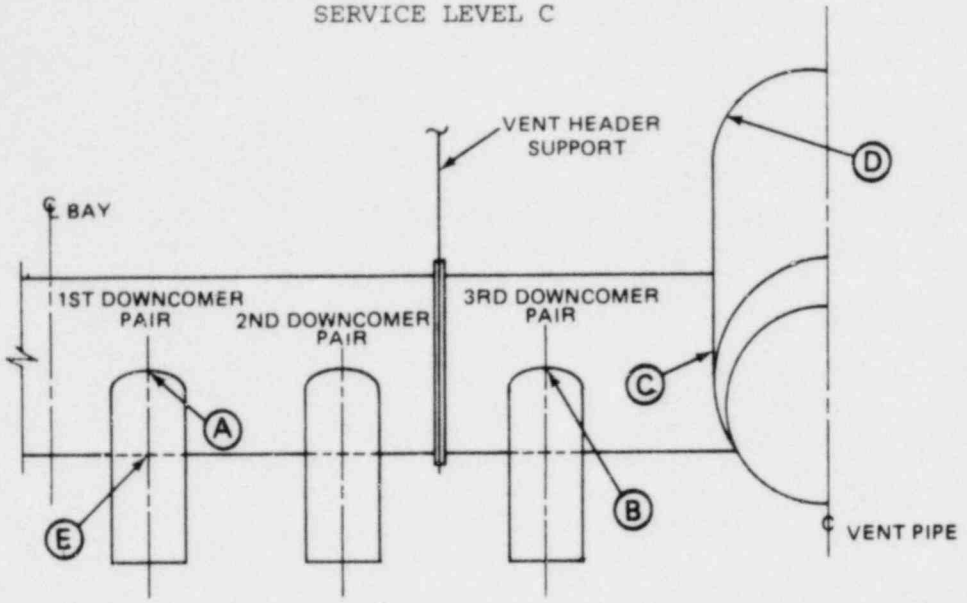

Location	Stress Type	Calculated SI (ksi)	Allowable SI (ksi)	Ratio
Intersection between header and D/C 1 (A)	P_L	36.65	57.00	0.64
	$P_L + P_b + Q$	-	-	-
Intersection between header and D/C 3 (B)	P_L	9.34	57.00	0.16
	$P_L + P_b + Q$	-	-	-
Intersection between header and vent (C)	P_L	9.14	57.00	0.16
	$P_L + P_b + Q$	-	-	-
Main vent (D)	P_M	4.48	38.00	0.12
	$P_L + P_b$	3.59	57.00	0.06
Header between D/C 1 and D/C 2 (E)	P_M	11.42	38.00	0.30
	$P_L + P_b$	15.34	57.00	0.27

Table 7-4

STRESS EVALUATION FOR SUPPORTS AND DEFLECTOR
SERVICE LEVEL A

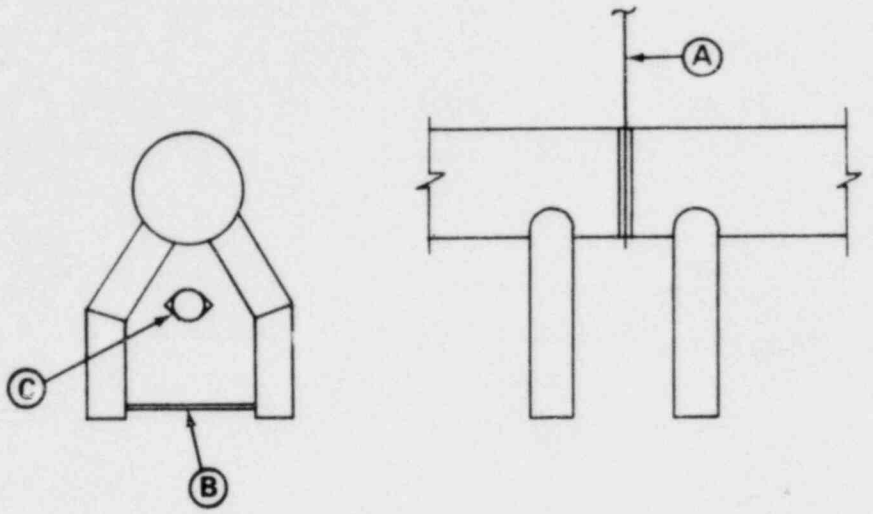

Location	Calculated Stress (ksi)	Allowable Stress (ksi)	Ratio
Vent header support tension (A)	4.20	18.60	0.23
Vent header support compression (A)	7.80	17.60	0.44
Downcomer tie-bar compression (B)	2.60	15.70	0.17
Downcomer tie-bar (B)	7.40	18.60	0.40
Vent header deflector (C)	1.10	18.60	0.06

Table 7-5

STRESS EVALUATION FOR SUPPORTS AND DEFLECTOR
SERVICE LEVEL C

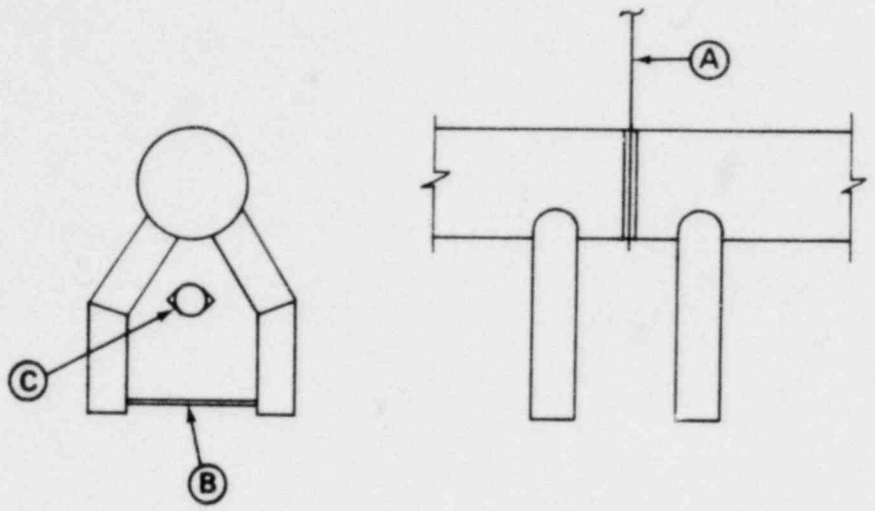

Location	Calculated Stress (ksi)	Allowable Stress (ksi)	Ratio
Vent header support tension (A)	-	-	-
Vent header support compression (A)	8.00	20.30	0.39
Downcomer tie-bar compression (B)	2.60	19.00	0.14
Downcomer tie-bar (B)	7.40	24.80	0.30
Vent header deflector (C)	1.60	24.80	0.06

Table 7-6

STRESS EVALUATION FOR SUPPORTS AND DEFLECTOR
(SERVICE LEVEL D)

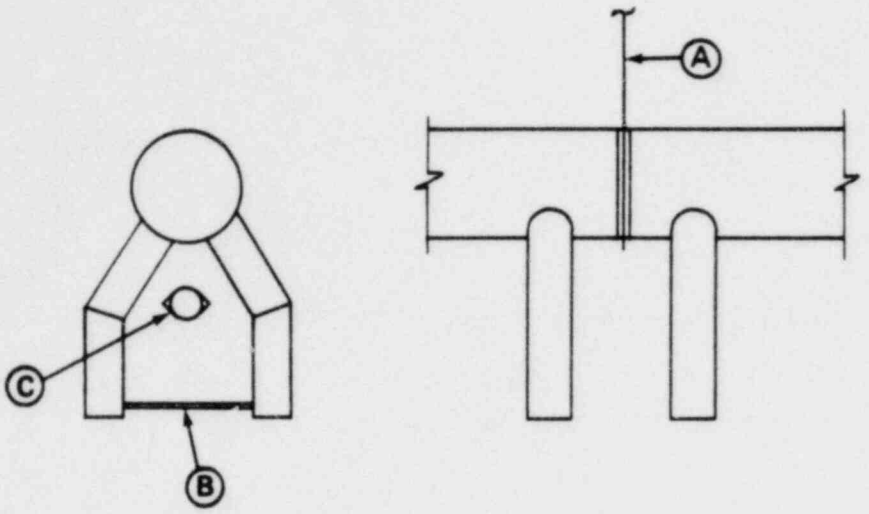

Location	Calculated Stress (ksi)	Allowable Stress (ksi)	Ratio
Vent header support tension (A)	-	-	-
Vent header support compression (A)	-	-	-
Downcomer tie-bar (B)	-	-	-
Vent header deflector (C)	14.80	37.20	0.40

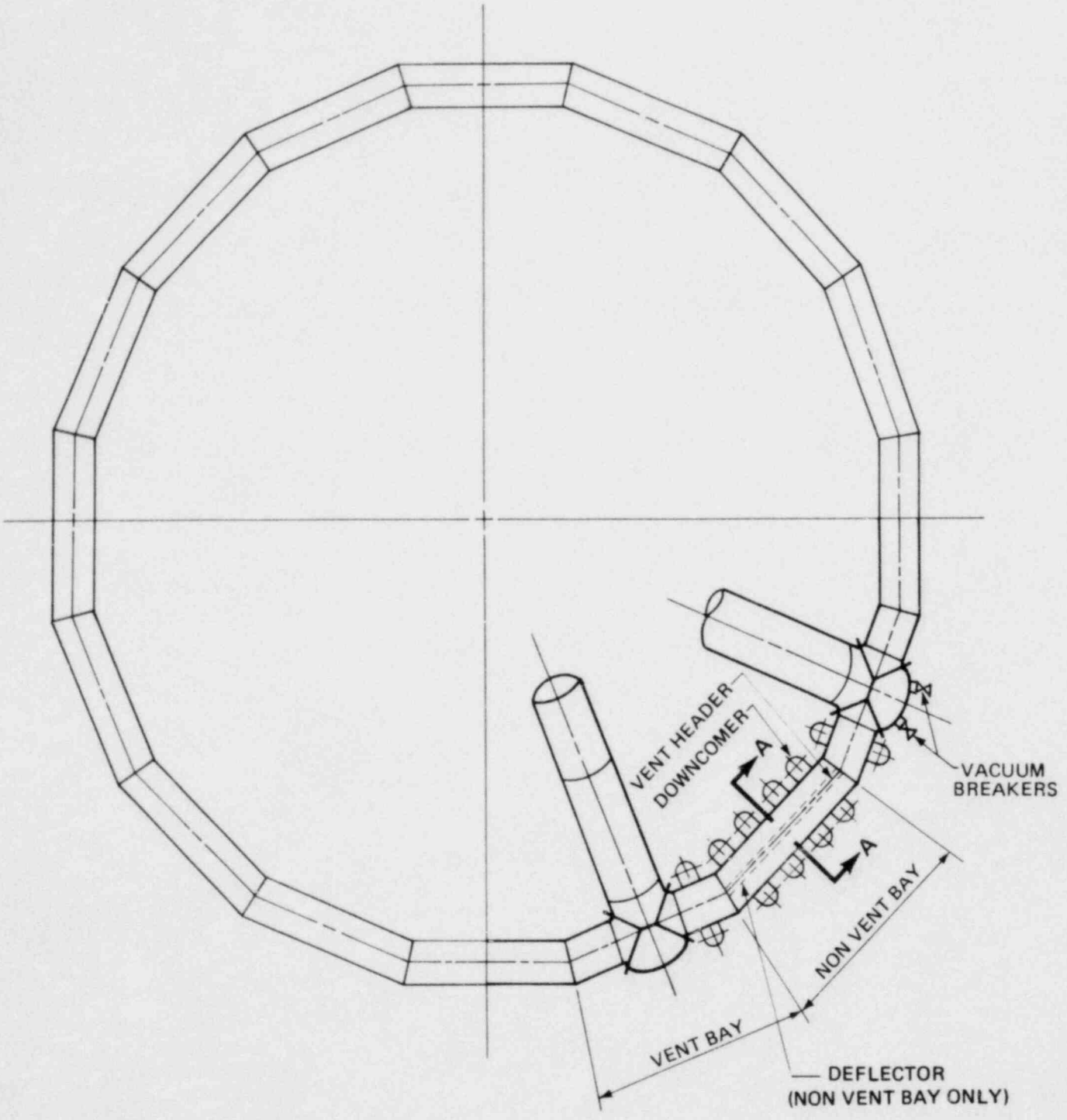

FIGURE 7-1 PLAN OF VENT SYSTEM (UNIT 2)

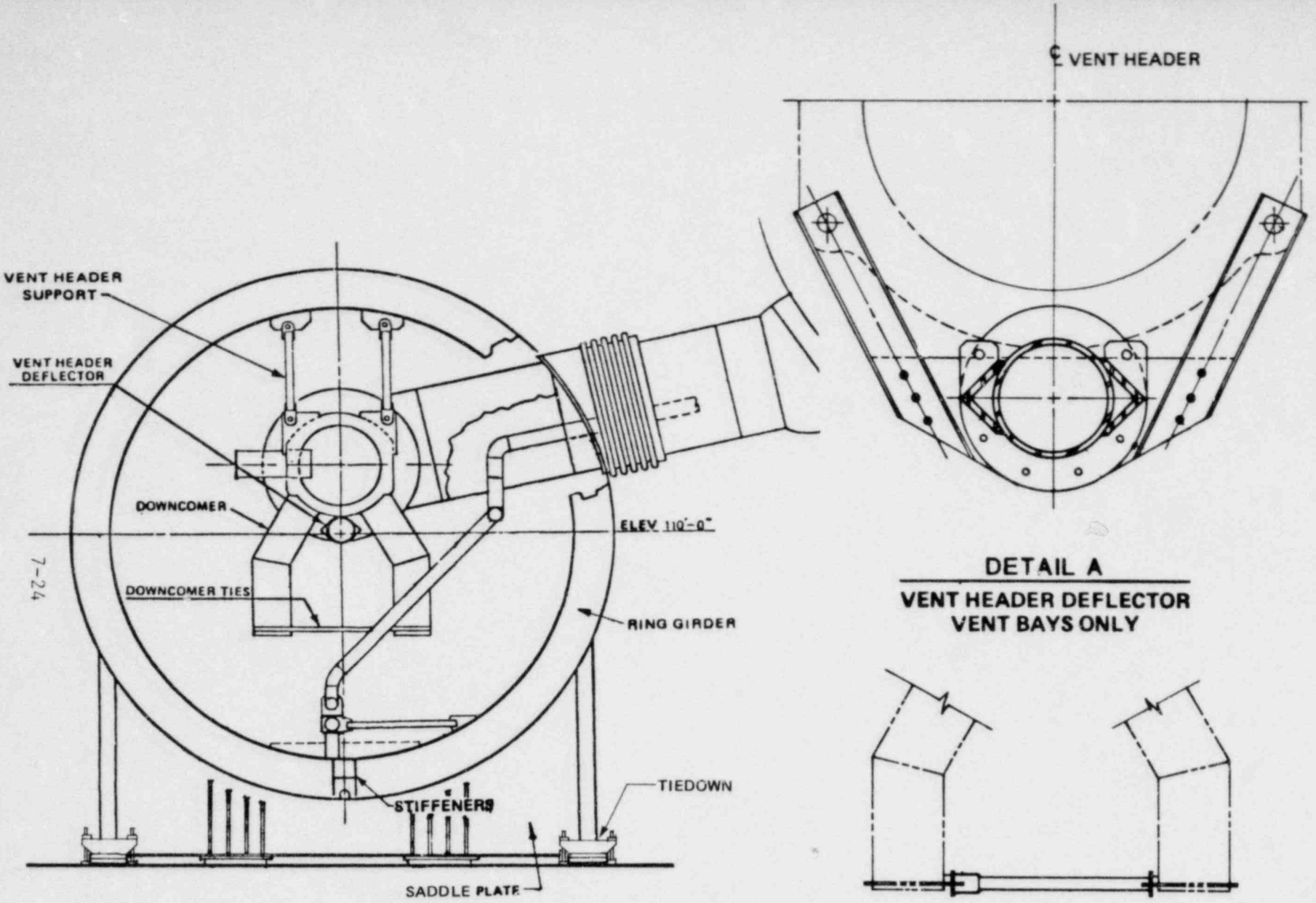

FIGURE 7-2

VENT HEADER DEFLECTORS, DOWNCOMER TIES AND VENT HEADER SUPPORTS

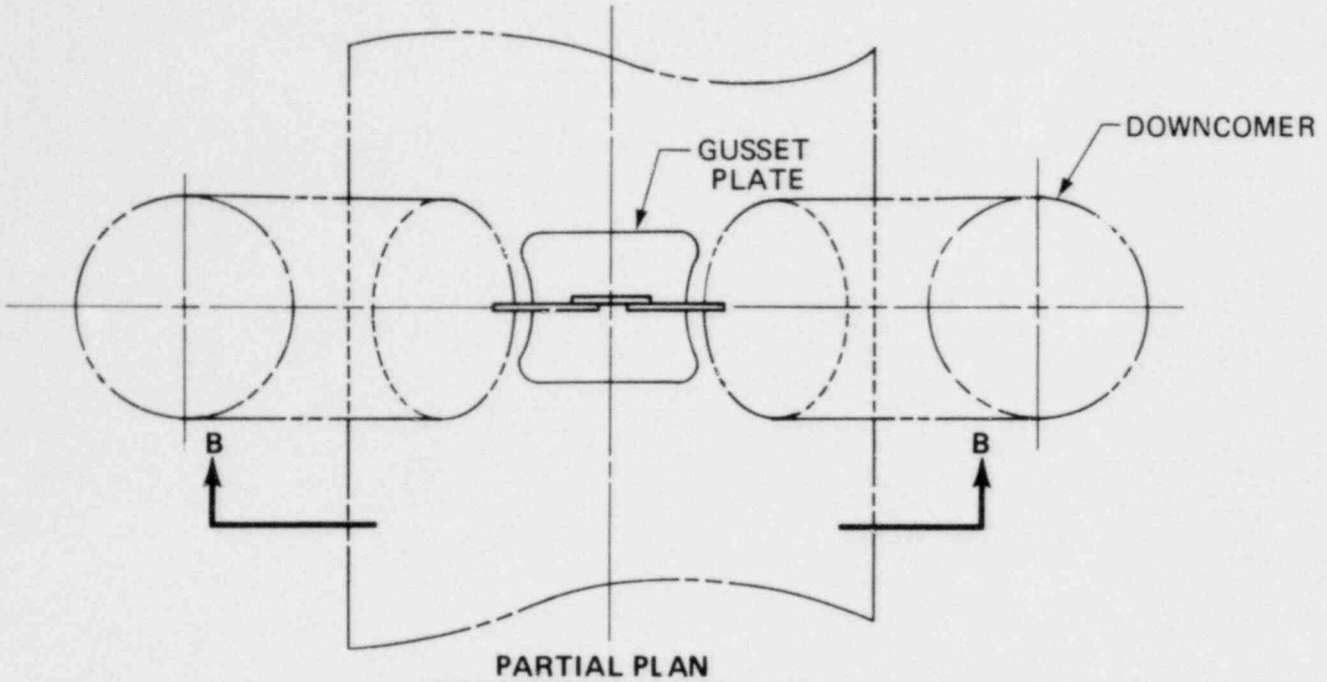

PARTIAL PLAN

BOTTOM OF VENT HEADER
(NON VENT BAY)

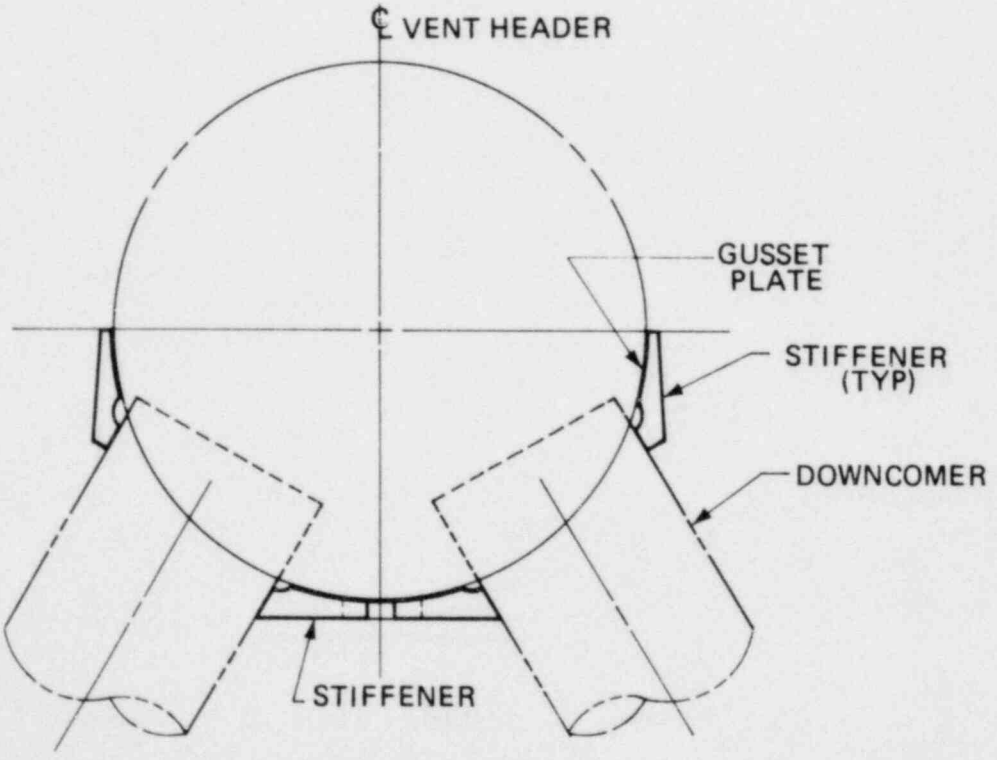

SECTION B–B

FIGURE 7-3 REINFORCEMENT OF VENT HEADER AND DOWNCOMER

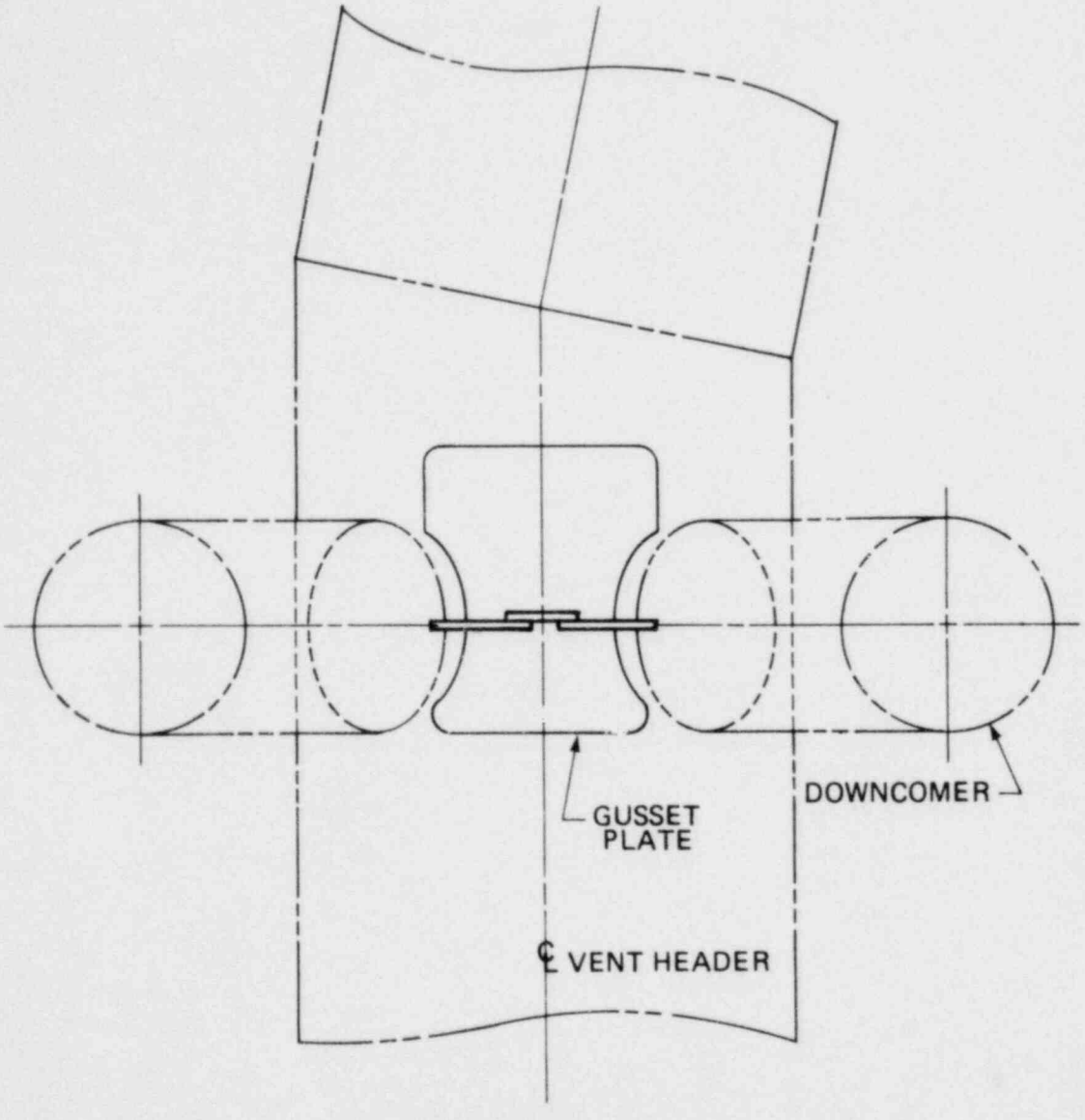

VIEW FROM BOTTOM

FIGURE 7-4 REINFORCEMENT OF VENT HEADER (VENT BAY)

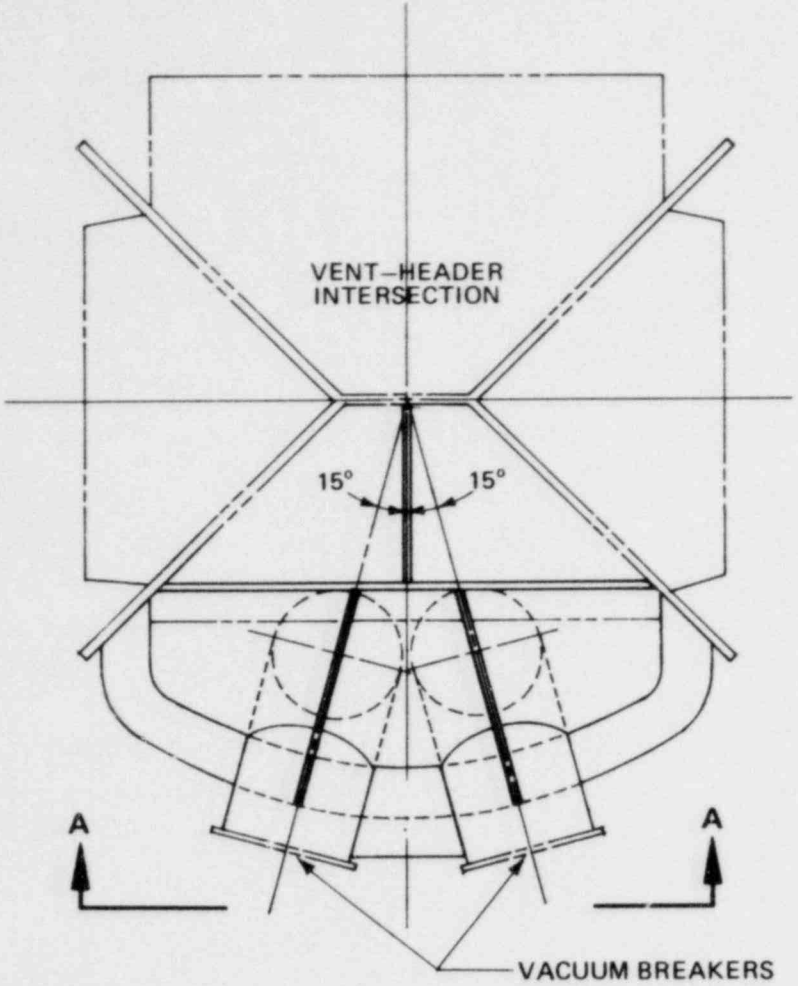

PLAN

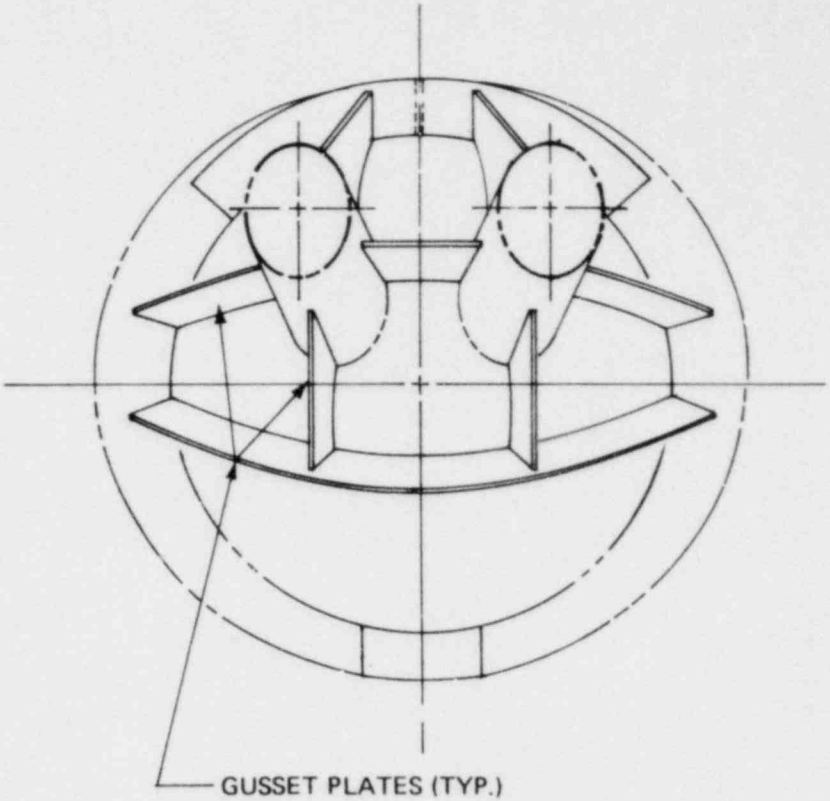

VIEW A–A

FIGURE 7-5 VACUUM BREAKER REINFORCEMENT (UNIT 2)

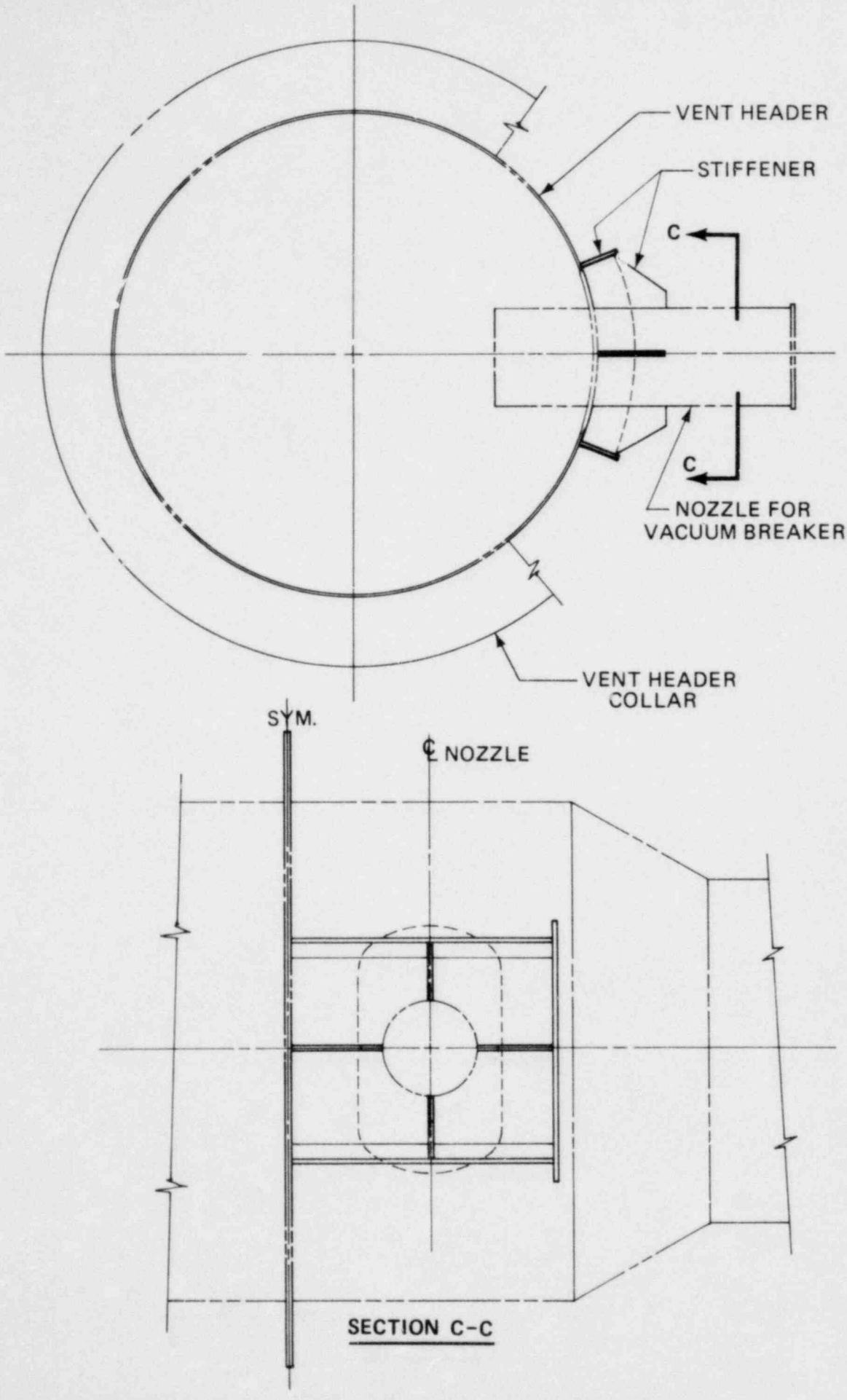

FIGURE 7-6 VACUUM BREAKER REINFORCEMENT (UNIT 3)

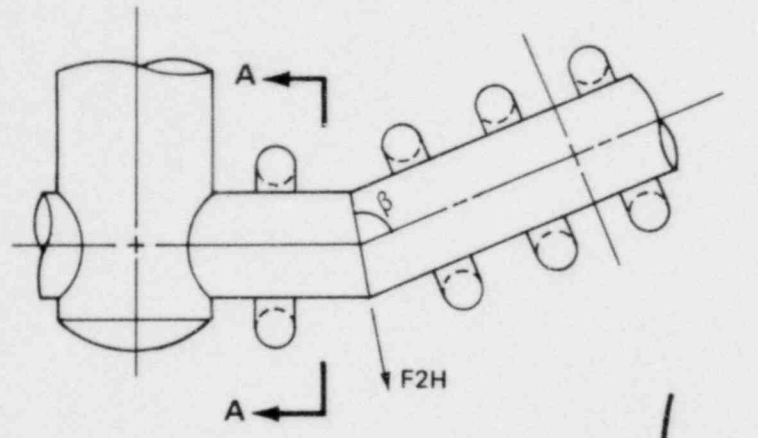

PLAN

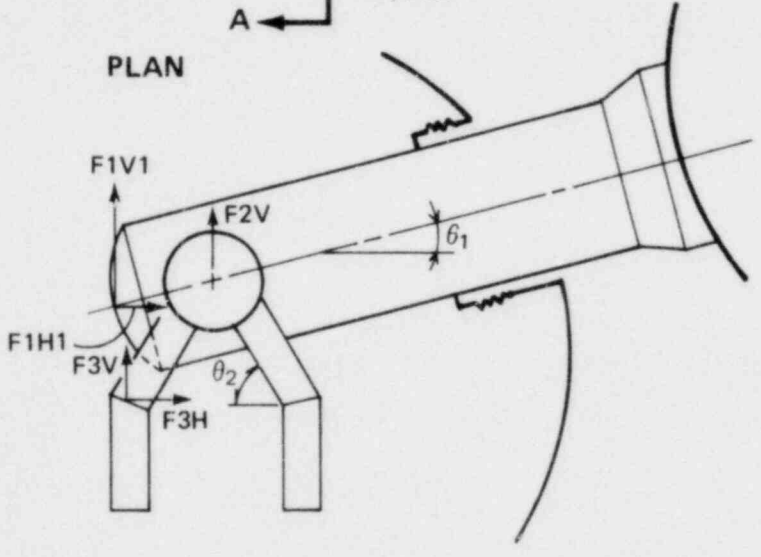

SECTION A–A

F1V1 = VERTICAL FORCE ON MAIN VENT END CAP = 60.0 K

F1H1 = HORIZONTAL FORCE ON MAIN VENT CAP = –145.0 K

F2V = VERTICAL FORCE ON VENT HEADER (PER MITRE BEND) = –56.0 K

F2H = HORIZONTAL FORCE ON VENT HEADER (PER MITRE BEND) = 22.0 K

F3V = VERTICAL FORCE ON DOWNCOMER MITRE BEND = 1.0 K

F3H = HORIZONTAL FORCE ON DOWNCOMER MITRE BEND = –3.7 K

FORCES ARE SHOWN IN THEIR ASSUMED POSITIVE DIRECTION

FIGURE 7-7 VENT SYSTEM THRUST LOADS

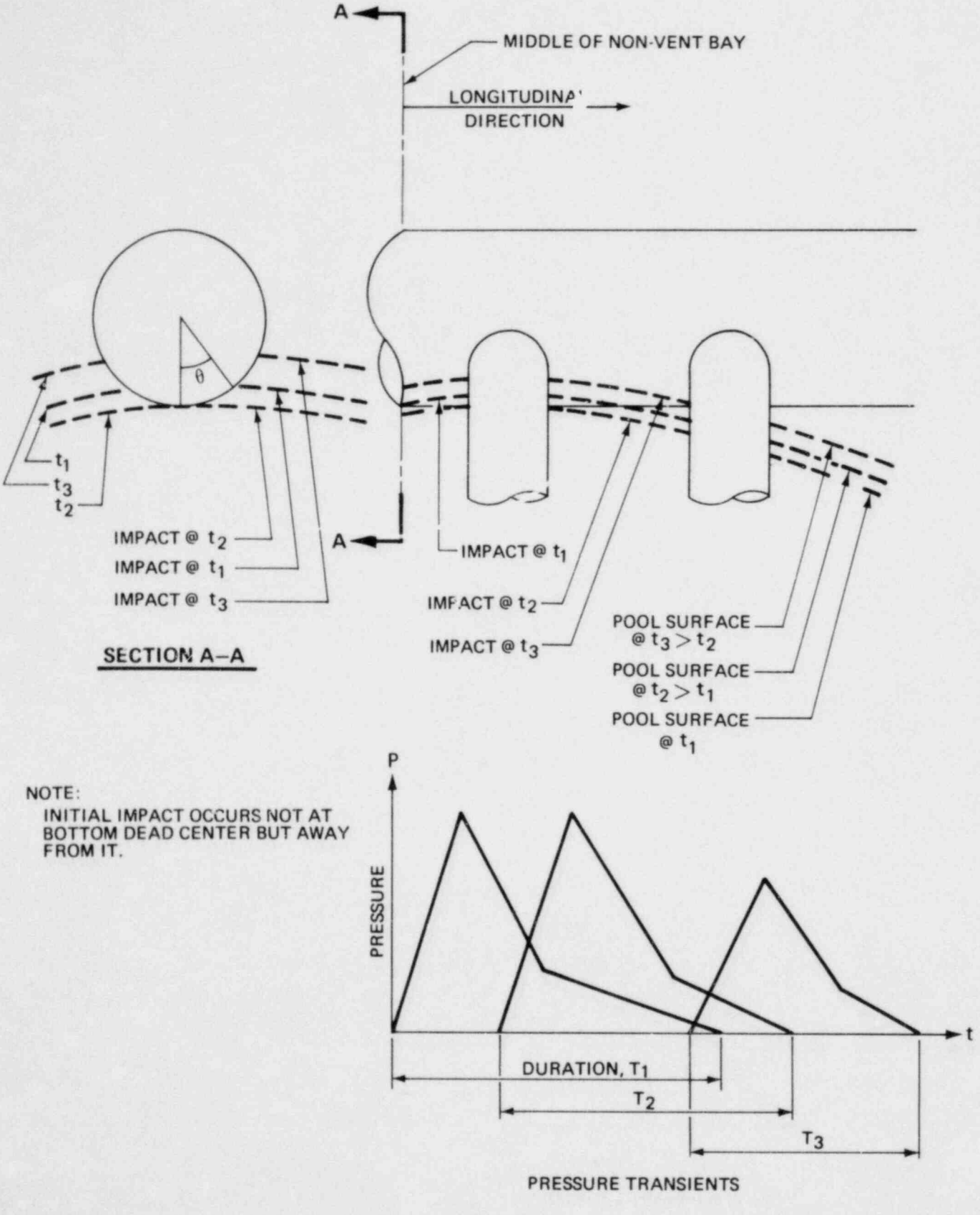

FIGURE 7-8 POOL SWELL IMPACT LOADING SEQUENCE

NOTE : TIME 0.0 CORRESPONDS TO THE TIME OF INITIAL IMPACT ON THE HEADER.

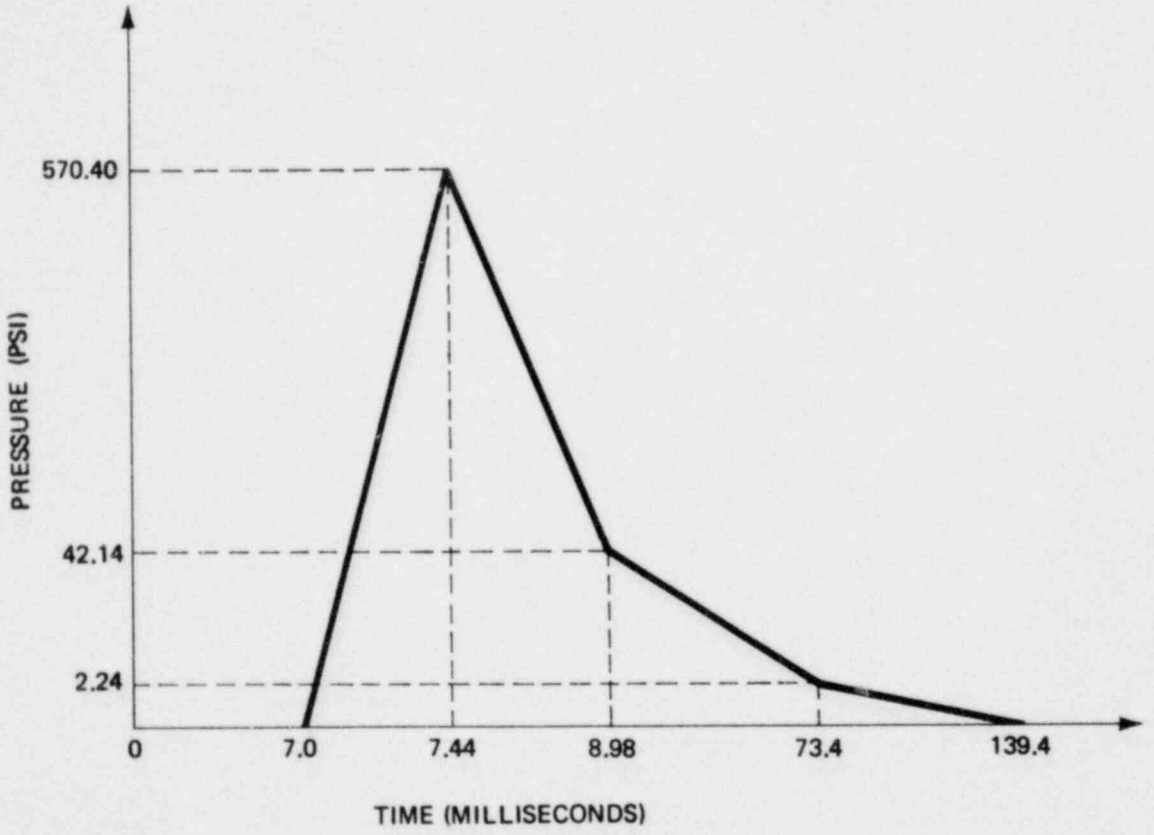

P(t) AT BOTTOM CENTER OF NON-VENT BAY

FIGURE 7-9 TYPICAL LOCAL PRESSURE TRANSIENT

SCALING RULES

GEOMETRY OF VENT HEADER SYSTEM (22.5° MODEL)

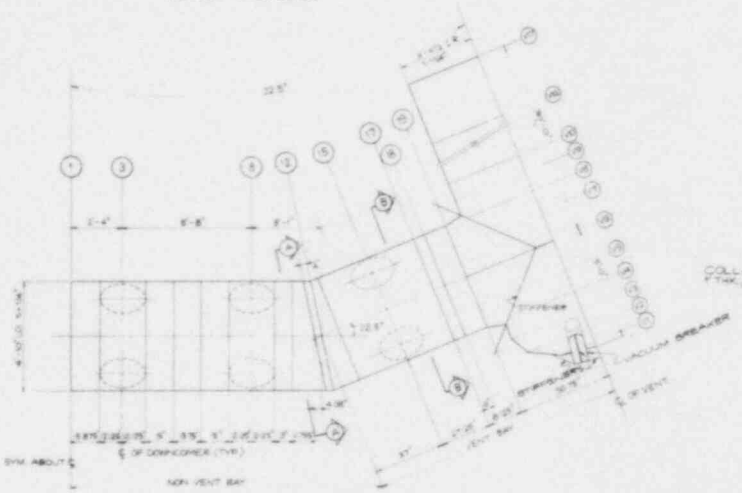

PLAN

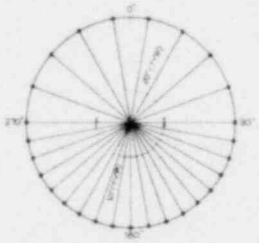

TYPICAL RING ON HEADER
27 NODES PER RING

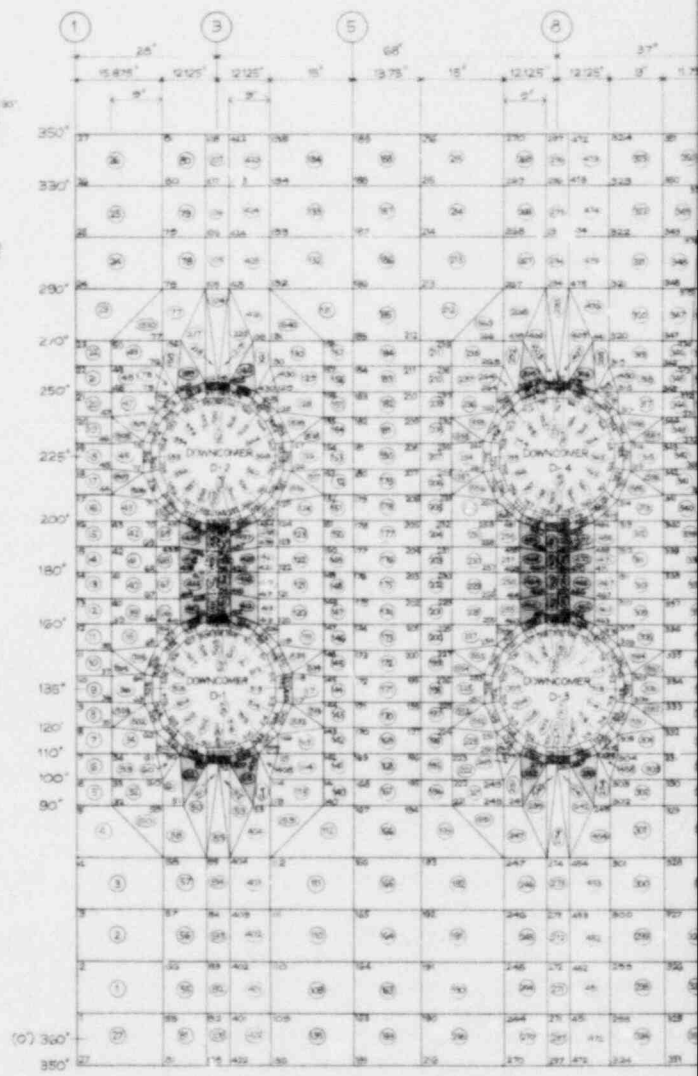

NOTE:
SHADED AREAS = STIFFENED PLATE, 1" THICK
UNSHADED AREAS = 1/4" THICK

FINITE ELEMENT

8 | 7 | 6

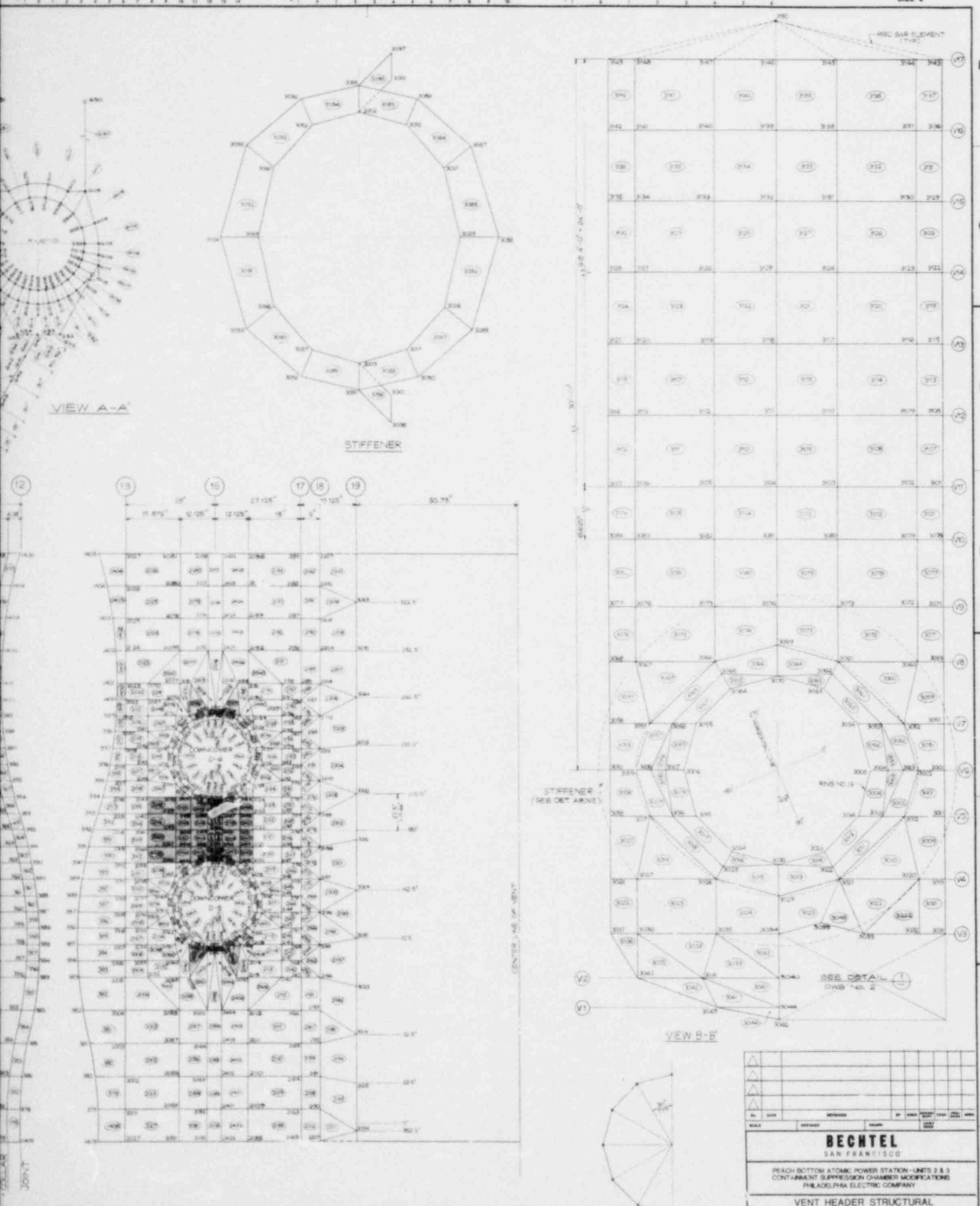

FIGURE 7-10
MODEL OF MAIN VENT AND VENT HEADER

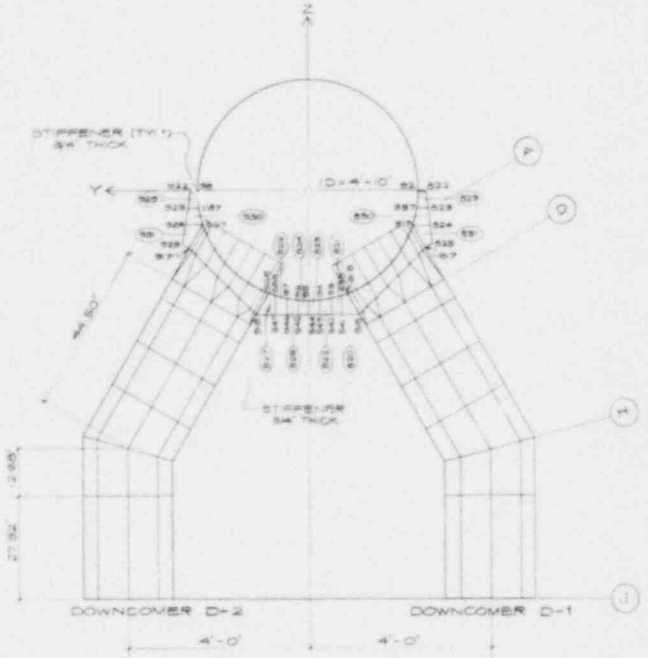

SECTION @ RING 3

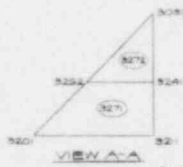

VIEW A-A

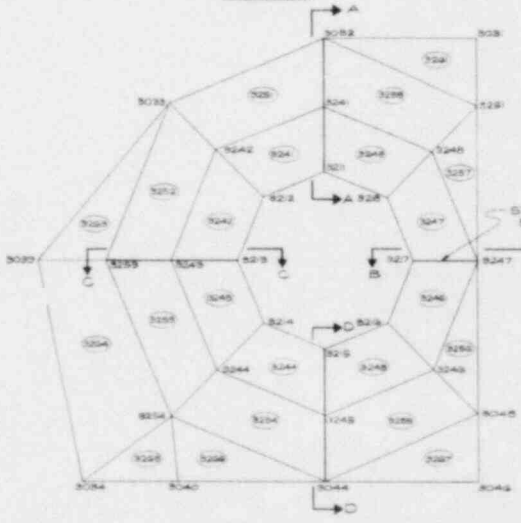

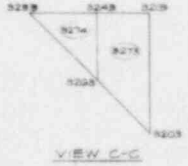

VIEW C-C

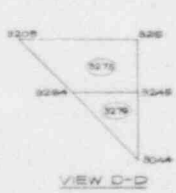

VIEW D-D

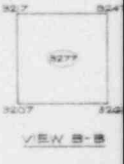

VIEW B-B

DETAIL 1

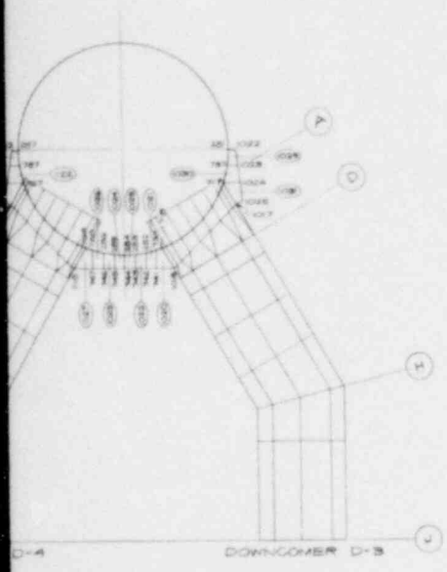

SECTION @ RING 8

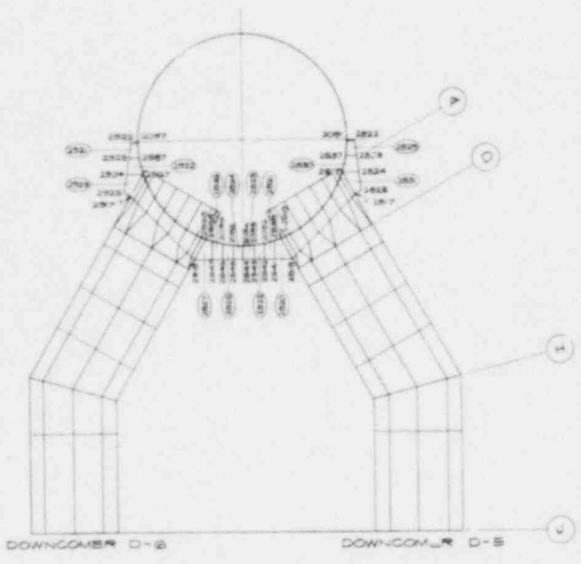

SECTION @ RING 15

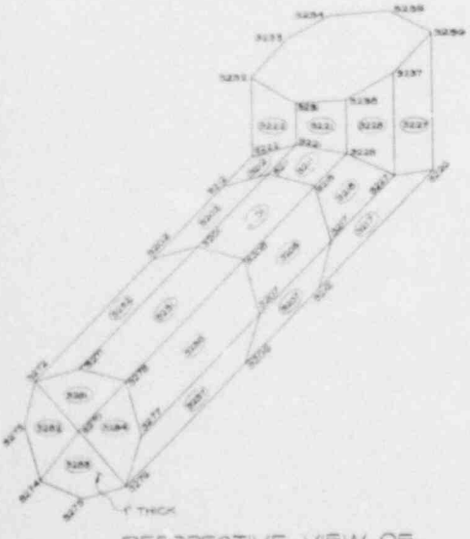

PERSPECTIVE VIEW OF VACUUM BREAKER

DEVELOPMENT OF VACUUM BREAKER

FIGURE 7-11
ADDITIONAL VENT SYSTEM DETAILS

BECHTEL
SAN FRANCISCO

PEACH BOTTOM ATOMIC POWER STATION - UNITS 2 & 3
CONTAINMENT SUPPRESSION CHAMBER MODIFICATIONS
PHILADELPHIA ELECTRIC COMPANY

JOB No. 11187-015 | DRAWING No. 2 | REV.

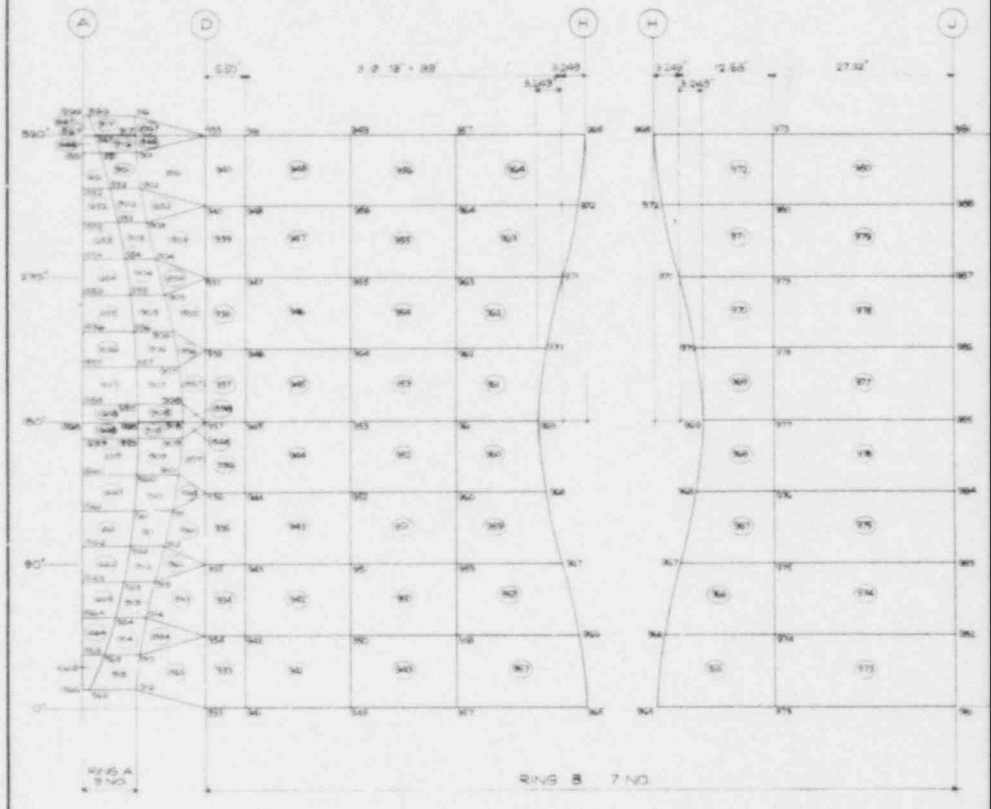

DOWNCOMER D2

(FOR DOWNCOMER D8, ADD 2000 IN NODE NUMBERS AND ELEMENT NUMBERS OF D2)

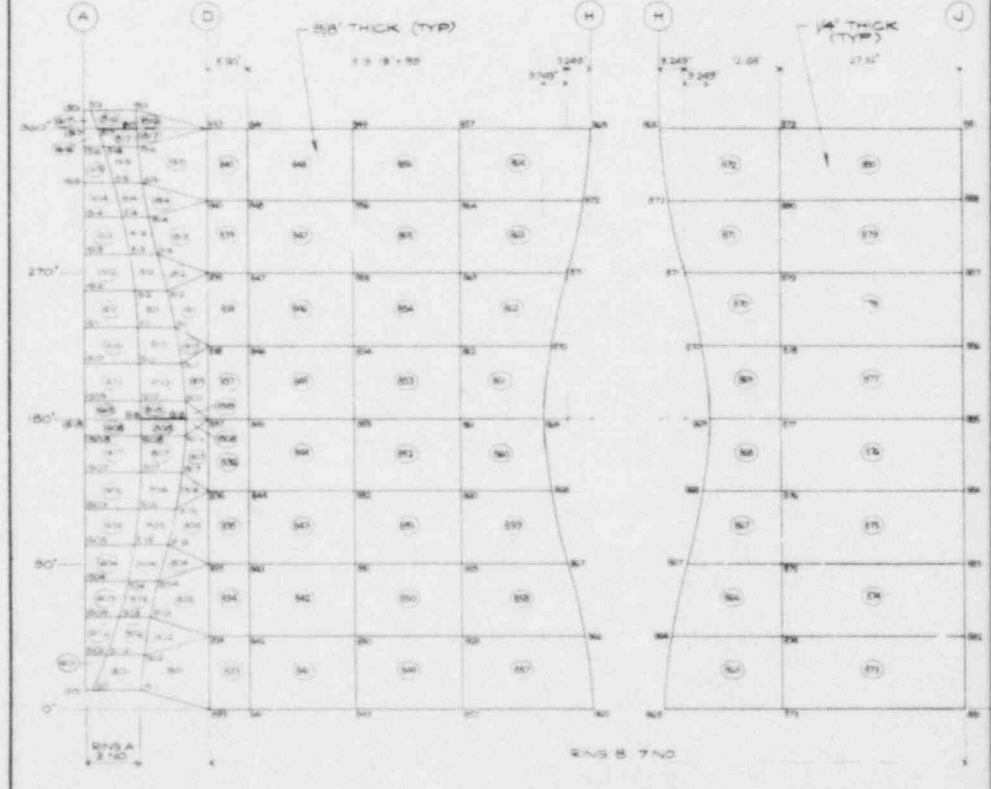

DOWNCOMER D1

(FOR DOWNCOMER D5, ADD 2000 IN NODE NUMBERS AND ELEMENT NUMBERS OF D1)

FINITE ELEME

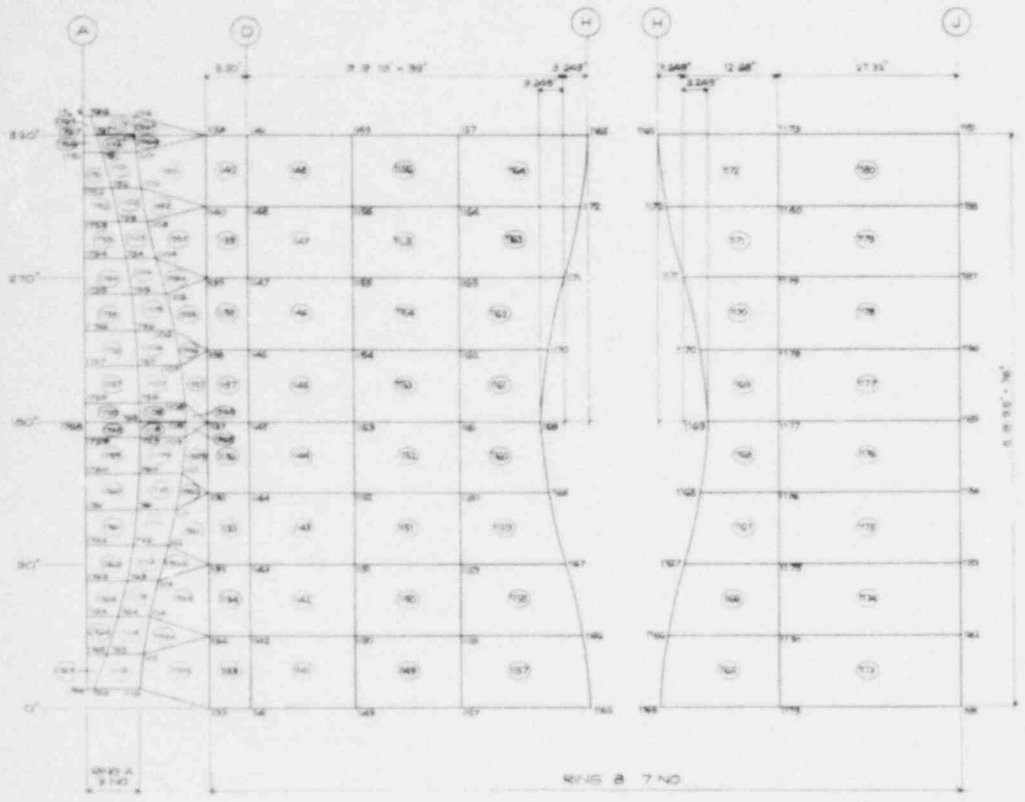

DOWNCOMER D4

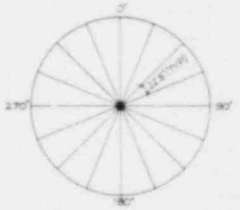

TYPICAL RING A
10 NODES

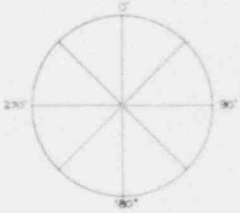

TYPICAL RING B
8 NODES

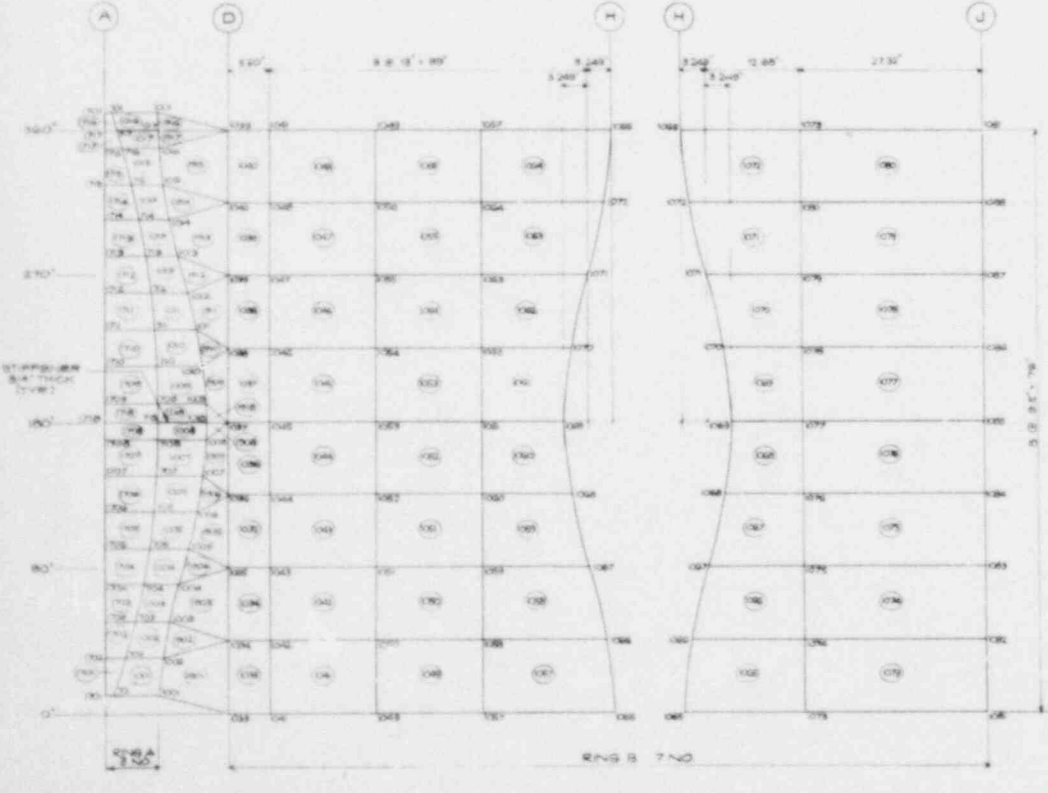

DOWNCOMER D3

FIGURE 7-12
IT MODEL OF DOWNCOMERS

BECHTEL
SAN FRANCISCO

PEACH BOTTOM ATOMIC POWER STATION UNITS 2 & 3
CONTAINMENT SUPPRESSION CHAMBER MODIFICATIONS
PHILADELPHIA ELECTRIC COMPANY

VENT HEADER STRUCTURAL
ASSESSMENT
(VENT BAY)

JOB NO.	DRAWING NO.	REV
11187-015	3	

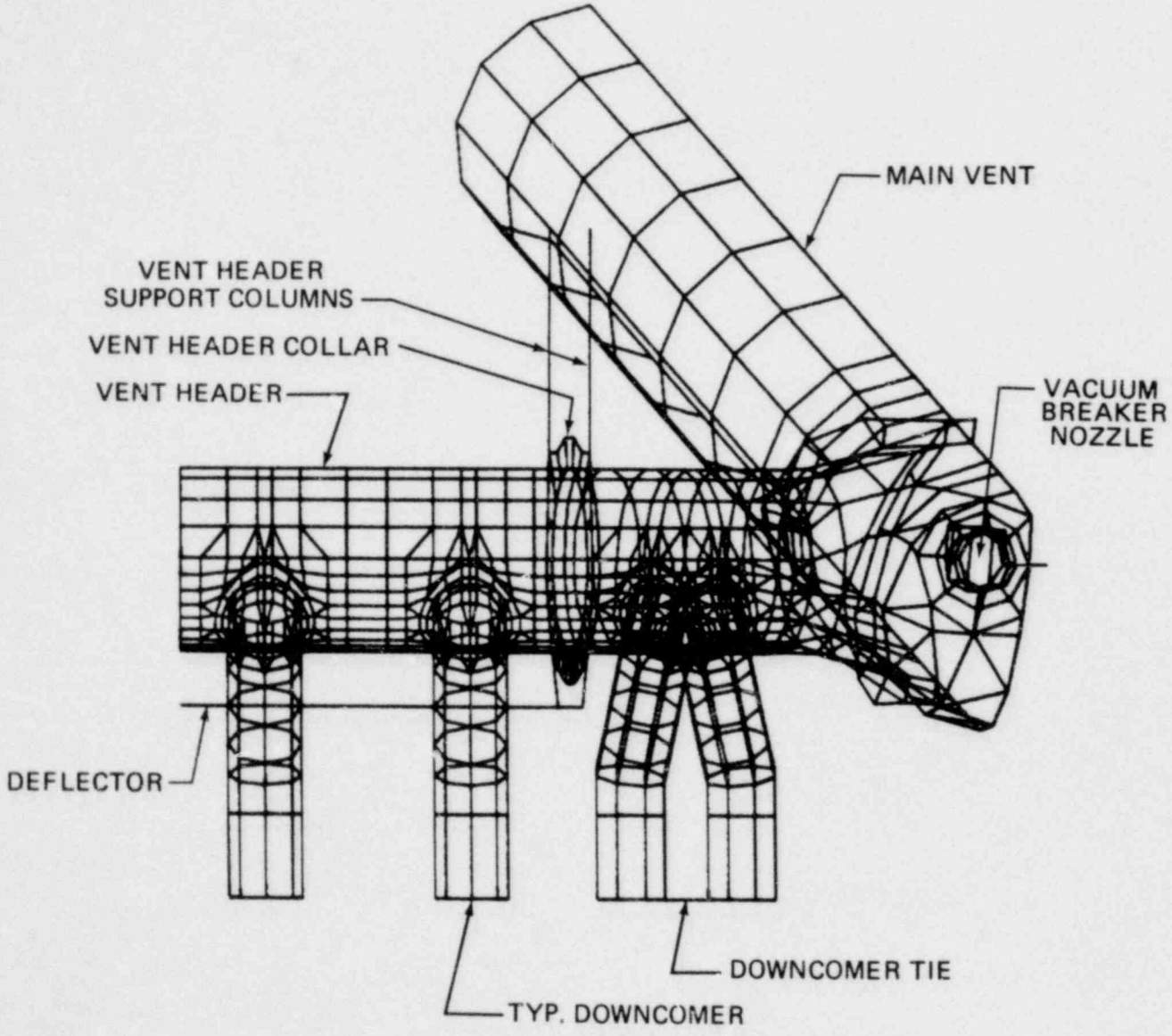

FIGURE 7-13 COMPUTER PLOT OF VENT SYSTEM 22.5° FINITE ELEMENT MODEL

● D/C FOR INITIAL DIFFERENTIAL PRESSURE LOAD
ALL D/Cs HAVE INTERNAL PRESSURE LOAD

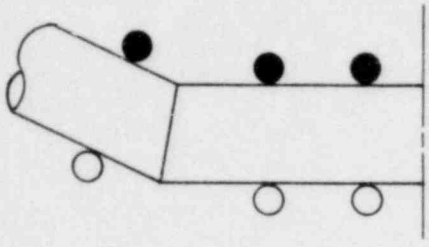

CASE 1

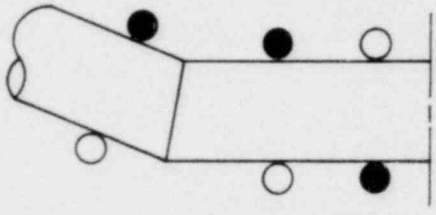

CASE 2

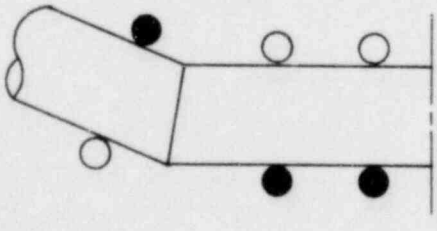

CASE 3

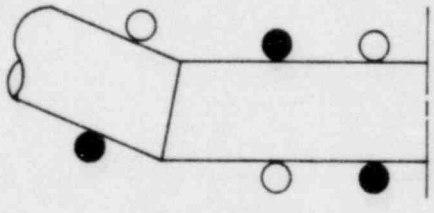

CASE 4

FIGURE 7-14 DOWNCOMER CO LOAD APPLICATION

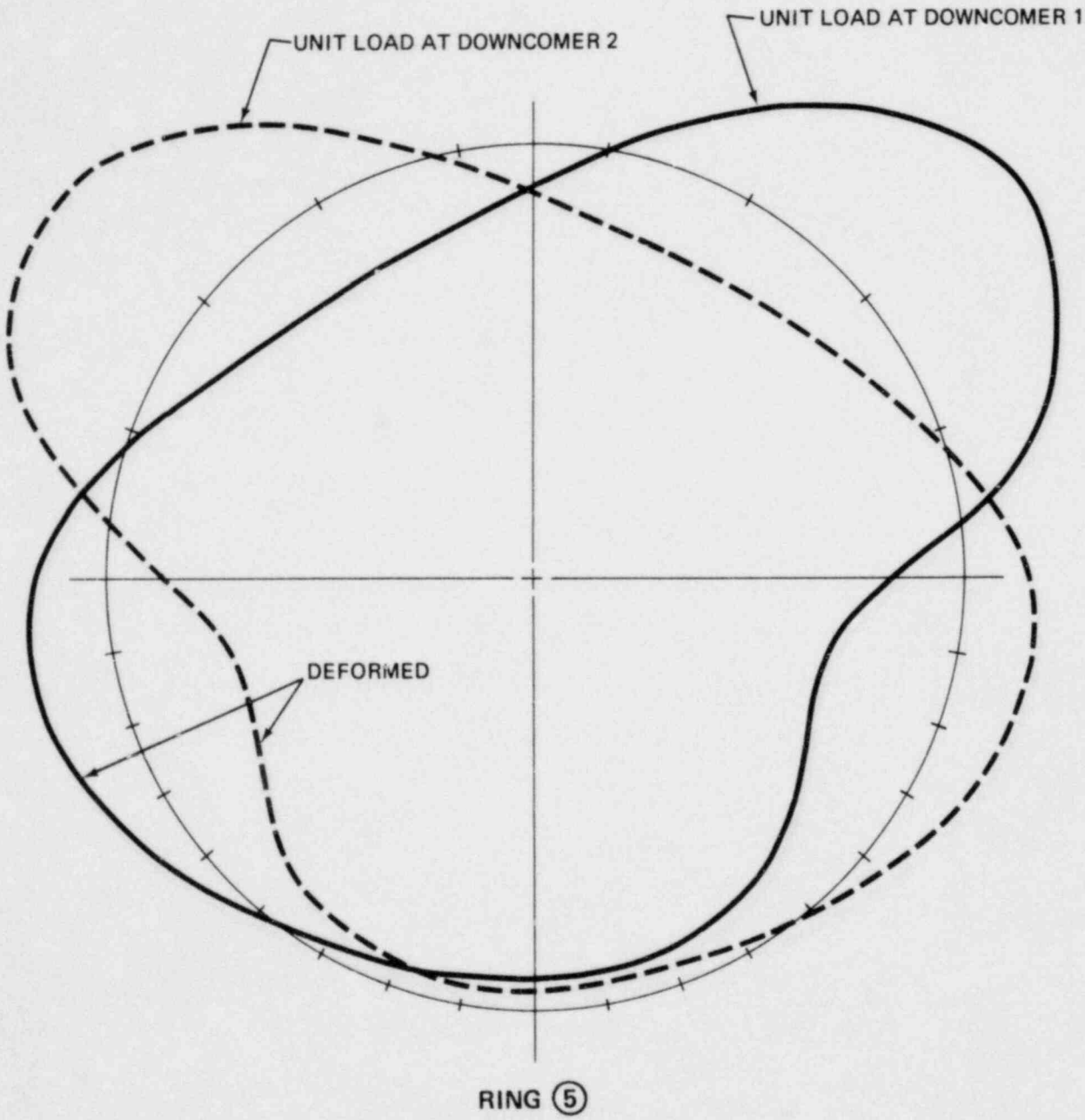

FIGURE 7-15 DEFORMATION DUE TO UNIT VERTICAL LOADS

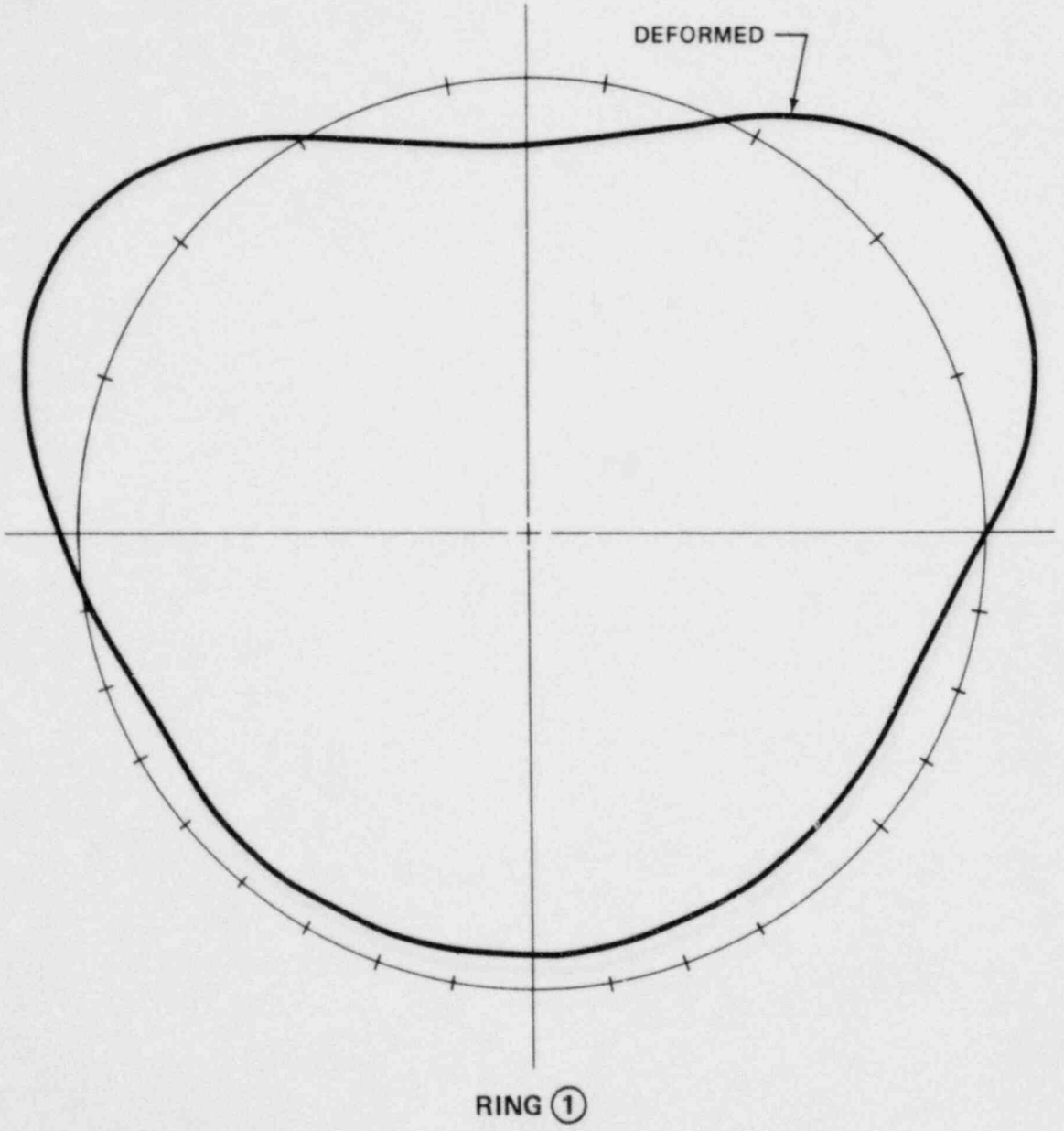

FIGURE 7-16 RADIAL DISPLACEMENT DUE TO UNIFORM INTERNAL PRESSURE

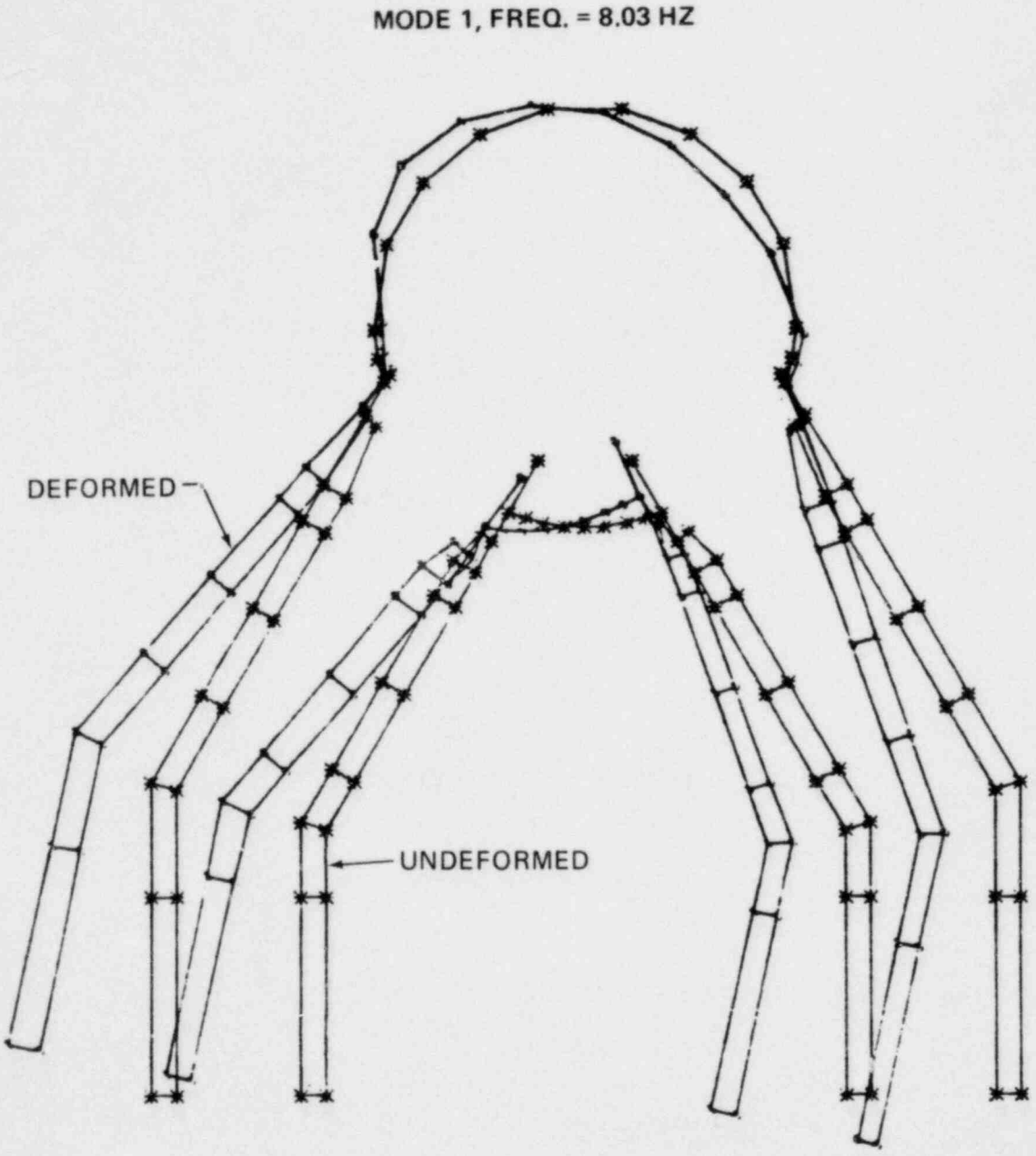

FIGURE 7-17 FIRST MODE SHAPE FOR CROSS SECTION THRU RING 3

MODE 2, FREQ. = 11.02 HZ

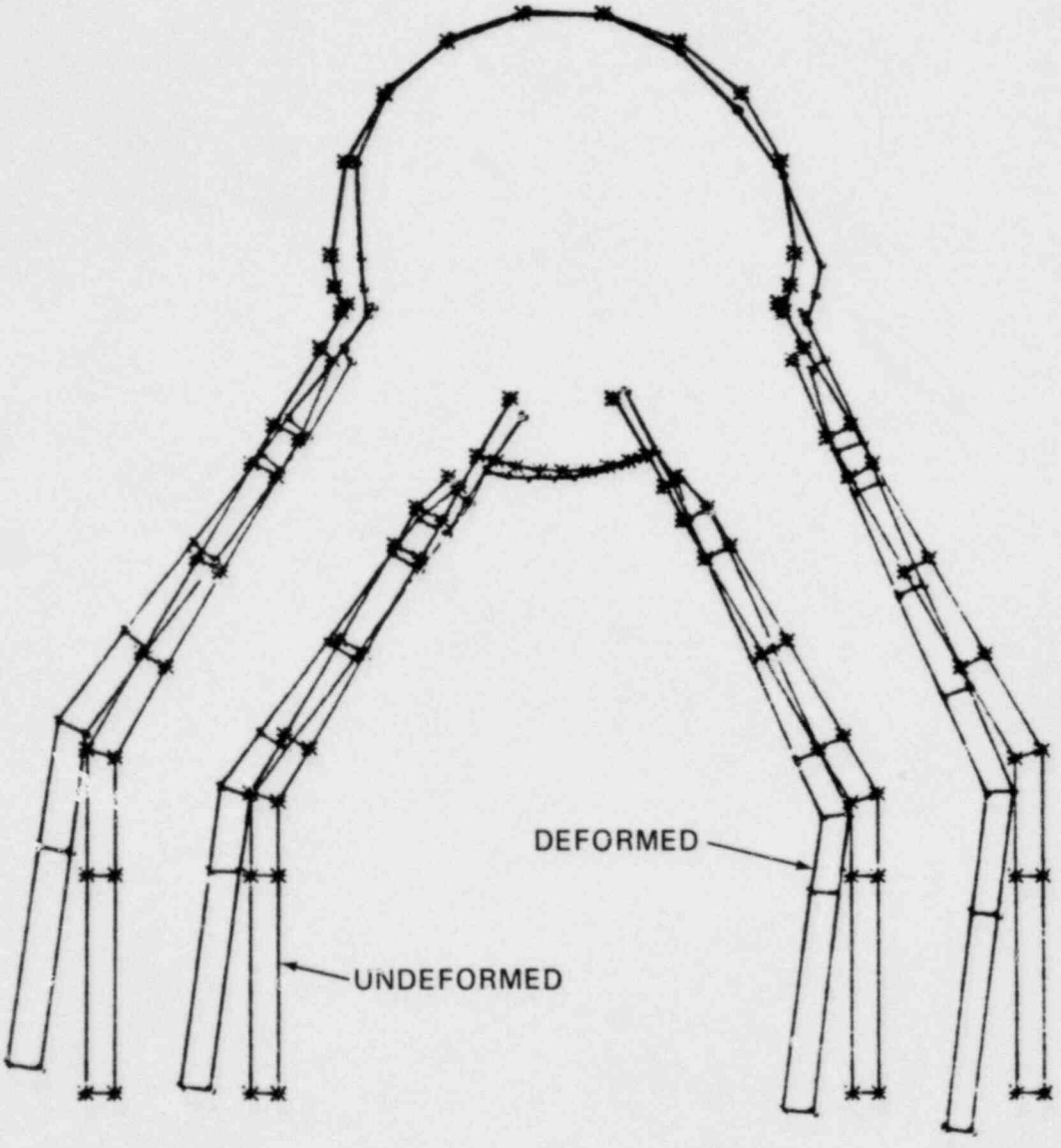

NOTE: TIE BAR AND VENT HEADER
DEFLECTOR NOT SHOWN.

FIGURE 7-18 SECOND MODE SHAPE FOR CROSS SECTION THRU RING 3

MODE 3, FREQ. = 11.07 HZ

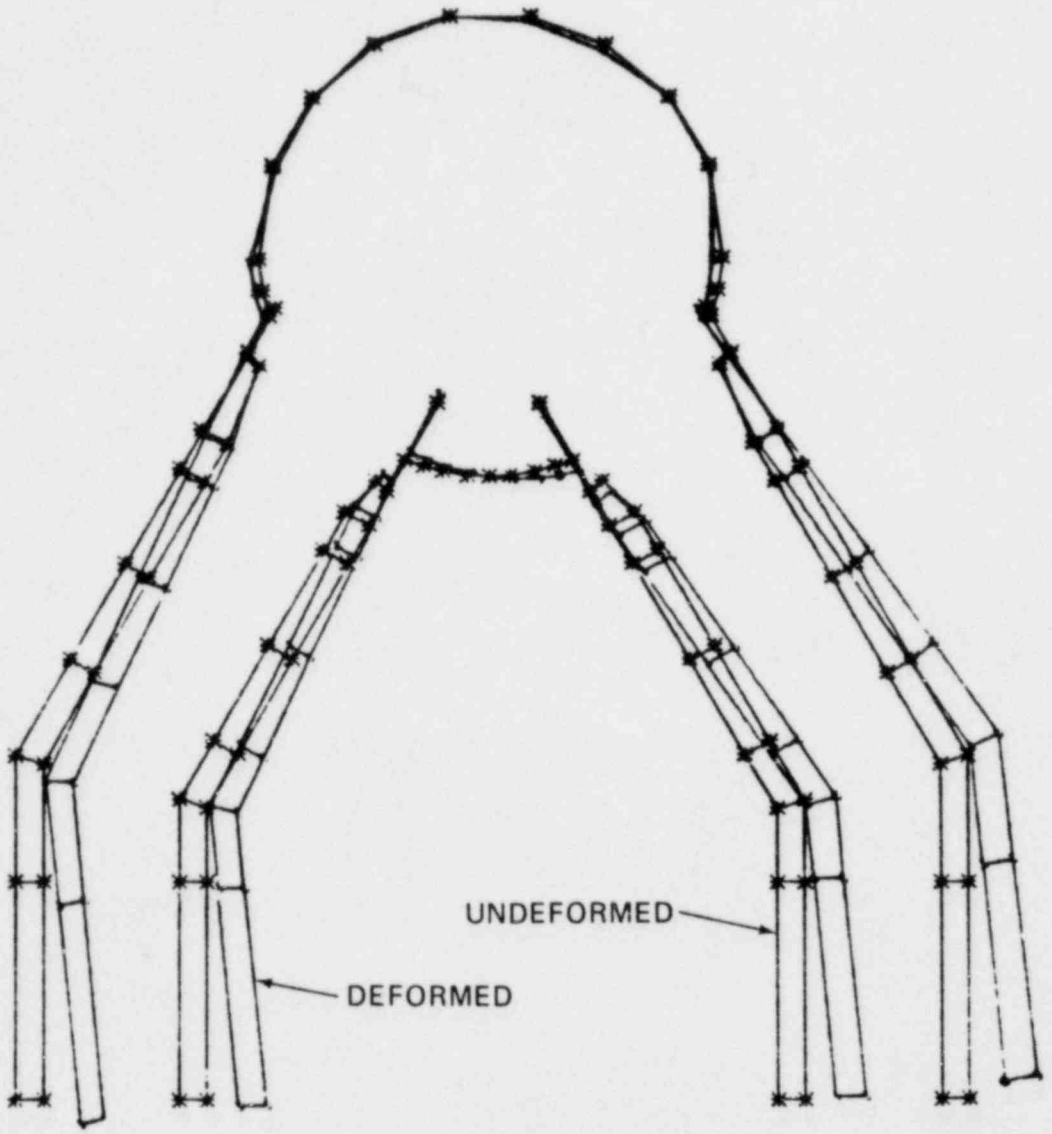

NOTE: TIE BAR AND VENT HEADER
DEFLECTOR NOT SHOWN

FIGURE 7-19 THIRD MODE SHAPE FOR CROSS SECTION THRU RING 3

MODE 1, FREQ. = 8.03 HZ

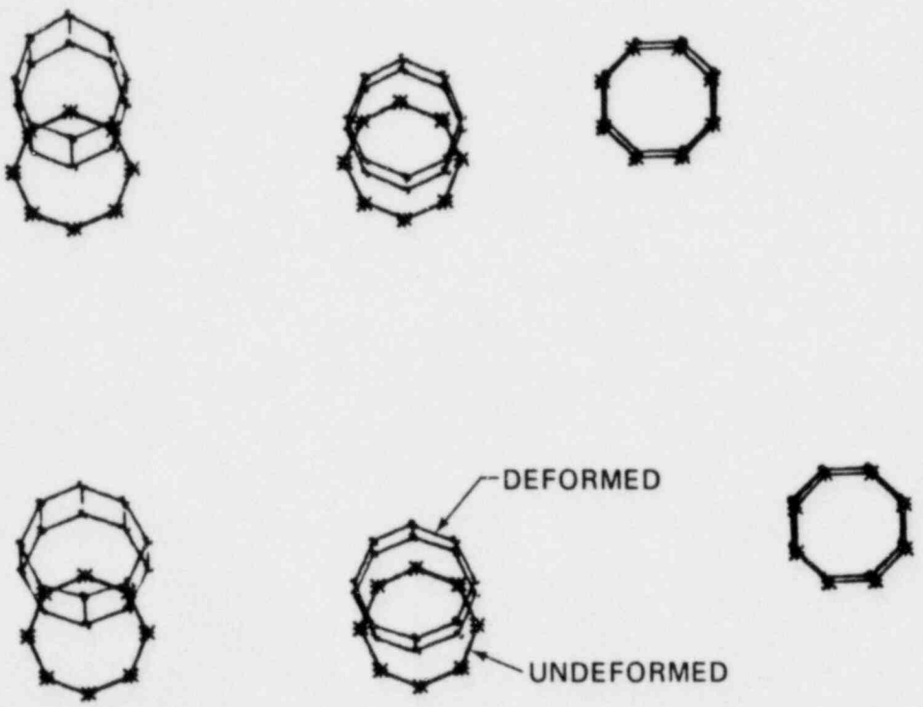

NOTE: TIE BAR NOT SHOWN

FIGURE 7-20 FIRST MODE SHAPE FOR THE PLAN VIEW AT DOWNCOMER TIPS

MODE 2, FREQ. = 11.02 HZ

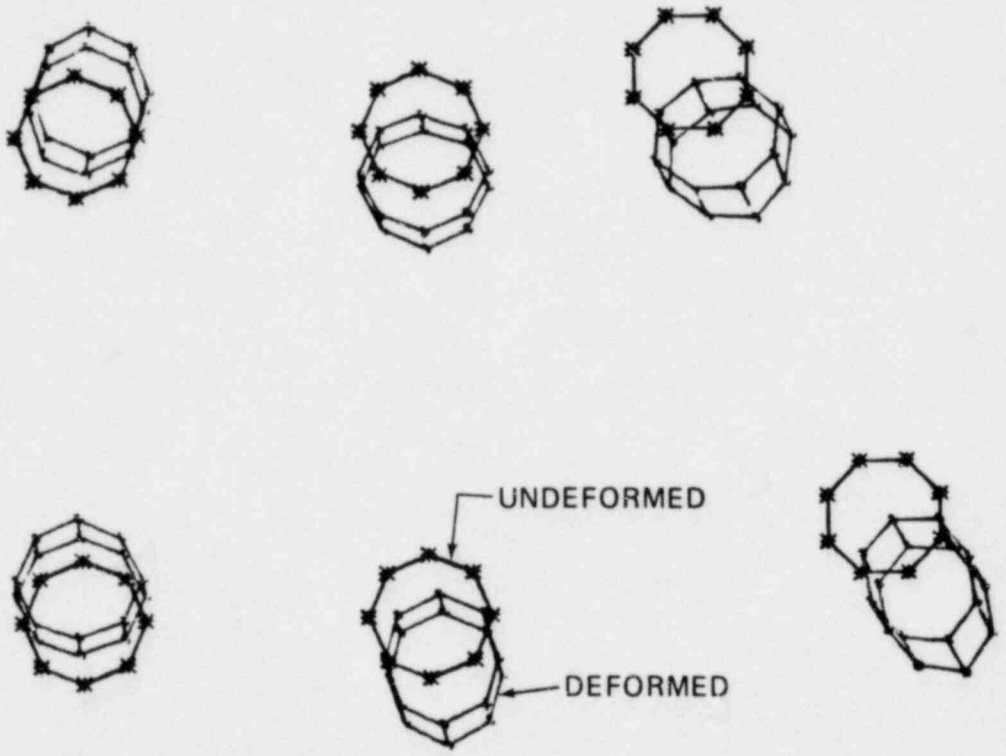

NOTE: TIE BAR NOT SHOWN.

FIGURE 7-21 SECOND MODE SHAPE FOR THE PLAN VIEW AT DOWNCOMER TIPS

MODE 3, FREQ. = 11.07 HZ

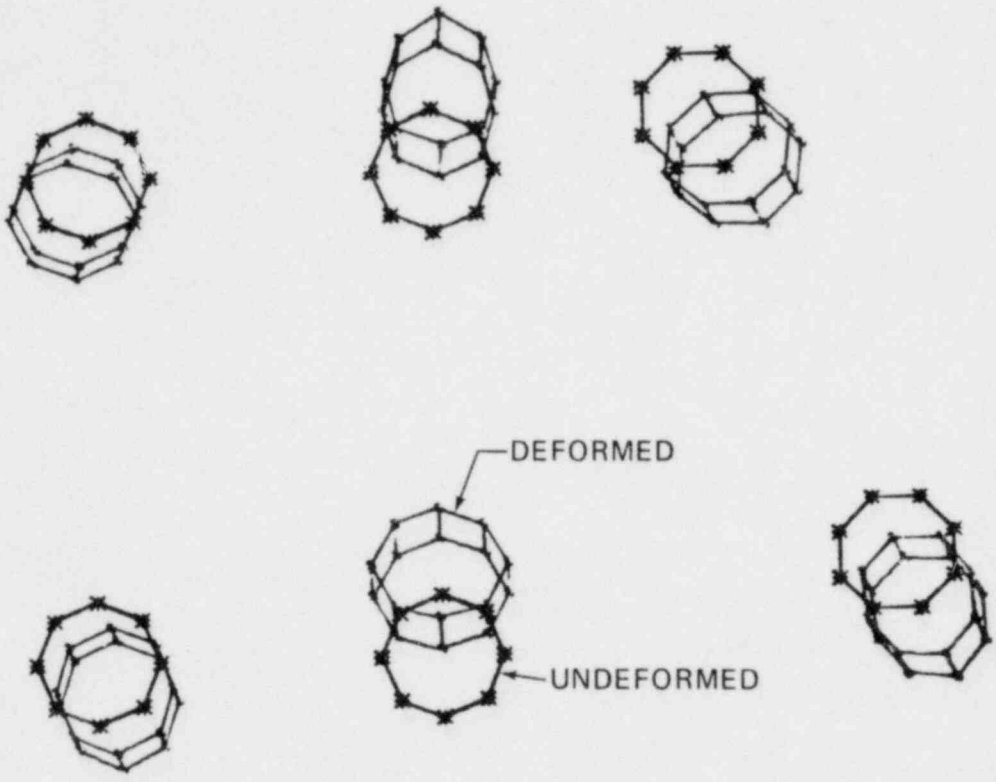

NOTE: TIE BAR NOT SHOWN.

FIGURE 7-22 THIRD MODE SHAPE FOR THE PLAN VIEW AT DOWNCOMER TIPS

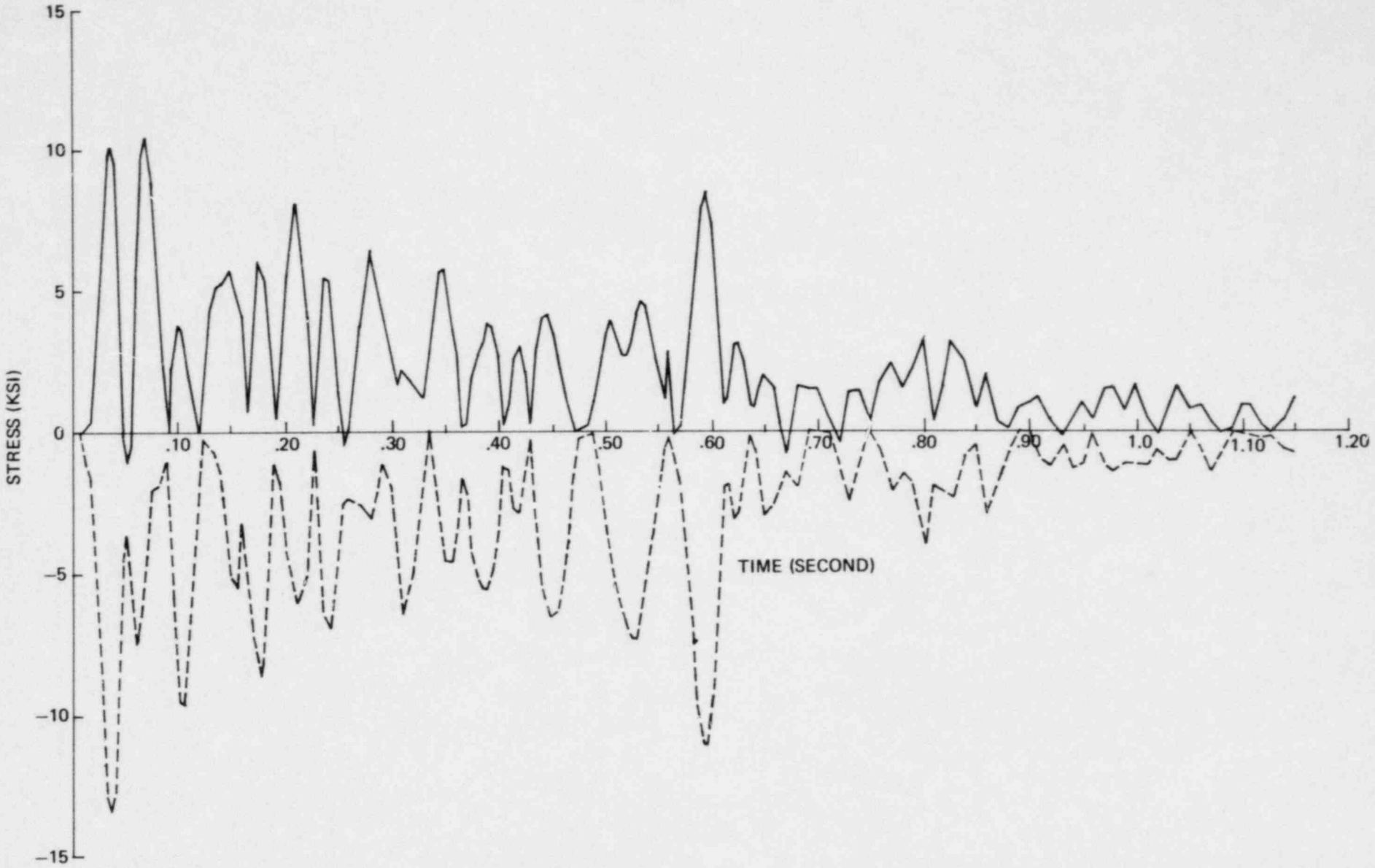

FIGURE 7-23 PRINCIPAL STRESSES AT DOWNCOMER /VENT HEADER INTERSECTION FOR POOL SWELL

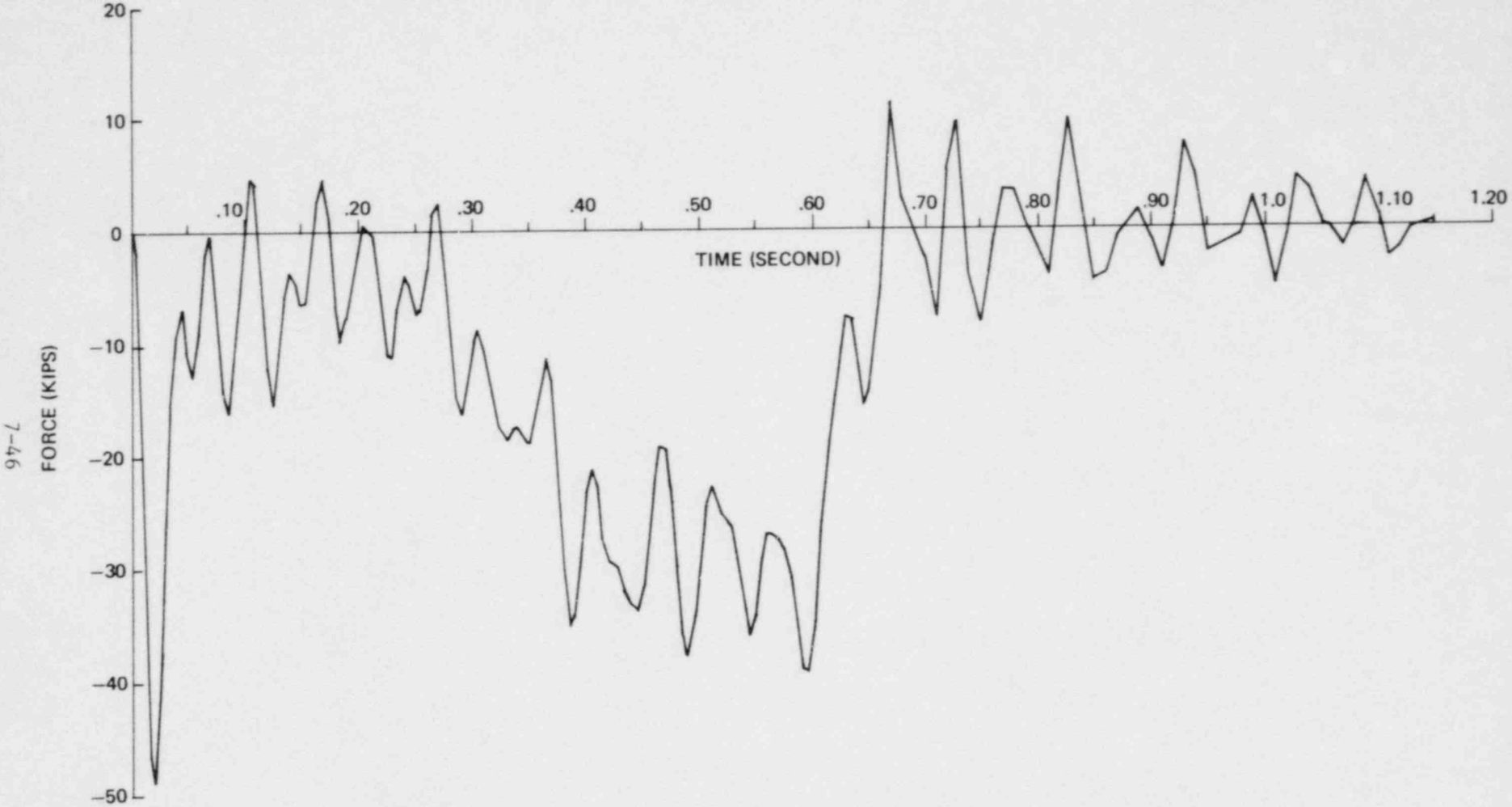

FIGURE 7-24 VENT HEADER SUPPORT OUTSIDE COLUMN REACTION FOR POOL SWELL LOADING

Section 8
STRUCTURAL EVALUATION OF TORUS INTERNAL STRUCTURES

Section 8

STRUCTURAL EVALUATION OF TORUS INTERNAL STRUCTURES

The torus internal structures considered for the structural evaluation include piping systems internal to the torus, T-Quenchers and their supports, and nonsafety related elements such as monorails and catwalks. A few of these structures are submerged below the normal pool water level. During the LTP, several modifications were developed to mitigate the loads and/or increase the load carrying capacity of the structural components. This chapter summarizes the modifications performed, the loads applied to the internal structures, the analyses performed to calculate the stresses, and the structural evaluation.

8.1 DESCRIPTION OF STRUCTURES AND MODIFICATIONS

All internal structures considered for the evaluation and their modifications are briefly described here.

8.1.1 T-Quencher and Supports

Eleven main steam relief valve discharge lines are in each unit of the Peach Bottom Atomic Power Station. The original discharge mechanism for the SRV line was through an open ramshead discharge device. However, for the purpose of load mitigation and steam condensation, these ramshead devices were replaced by T-Quenchers. Figure 6-6 shows the plan of the torus with the SRV discharge line quenchers.

A quencher is installed on each of the 11 discharge lines inside the torus and is centered at a ring girder near the vertical centerline of the torus. Quenchers are Class 3 piping components.

It was necessary to support the quencher arms, which would experience thrust and hydrodynamic drag loads. Each of the arms is supported by a system of guides and support beams connected to the ring girder.

Figures 6-7 and 6-8 show all the quencher support details. The loads from each quencher are transferred to a quencher support beam, located directly below the quencher, by means of three guide plate supports at each quencher arm. From the center of the support beam, a vertical and lateral stub extend to the ring girder. A vertical stub column is located under each quencher arm and is supported by bottom support beams spanning the area between adjacent ring girders. The quencher support system is made up almost entirely of 14-inch schedule 120 pipe. The SRV discharge quencher supports are Class 3 component supports.

8.1.2 Catwalk Platform and Supports

A catwalk service platform running circumferentially around the inside of the torus is located above the normal pool water level on the outboard side of the torus (Figure 8-1). The catwalk decking consists of an open type steel grating supported by a framework of channel and wide flange sections. The top of the grating is at elevation 111'-6". Although the catwalk is not a safety related item, the original platform was modified to ensure that it did not damage or interfere with the operation of safety related components during a postulated LOCA.

The original platform was supported on columns (angle sections) submerged in the suppression pool. These columns were found to be inadequate for the hydrodynamic loads and therefore were replaced with pipe columns connected to the ring girder at the top of the torus. The platform itself was reinforced with new channel supports and welded gratings to prevent failure under pool swell loading. Two longitudinal channel sections support the grating on each side span between the W8x31 sections at each end. These modifications are shown in Figure 8-2.

8.1.3 Monorail and Supports

In the interior of the torus, a monorail system used for maintenance operations is located on the upper half of the shell above the catwalk (Figure 8-1). During a postulated LOCA, the monorail beam would experience froth loading because the pool would impact on the vent system.

Although the monorail is a nonsafety related item, it must not impair the proper functioning of safety related systems. To meet this requirement, the original supports consisting of 7/8-inch diameter hanger rods were replaced by 4-inch schedule 40 pipe struts attached to the torus shell as shown in Figure 8-3. Two additional supports, consisting of 7/8-inch diameter hanger rods, are located approximately 11 feet from the center supports in alternate segments (Figure 8-1). At each ring girder location, the beam is further supported by a 3/4-inch plate welded to both the beam and ring girder. The monorail is located at elevation 121'-6.5" at a radial distance of 63'-2.5" from the reactor centerline.

8.1.4 Spray Header and Supports

The spray header consists of a 4-inch schedule 40 pipe installed circumferentially around the torus centerline at elevation 122'-0" (Figure 8-1). The piping penetrates the torus shell vertically near the top center. The header is supported at 16 locations by hangers consisting of a 2-inch x 3/8-inch strap and a 3/4-inch plate (Figure 8-3) attached to the ring girder flange. Spray nozzles are located at the mid-span of each torus bay. The spray header is Class 3 piping and its supports are Class 3 component supports.

8.1.5 RHR Torus Cooling and Pump Test Lines and Supports

Each of the Peach Bottom units has two RHR torus cooling and pump test lines, designated as N210A and N210B. Each line is made of 18-inch schedule 80 pipe. For both Peach Bottom units, line N210A is located at segment 5 and line N210B at segment 13 (Figures 2-5 through 2-7). Each line penetrates the torus radially at elevation 121'-0" and extends vertically downward into the pool as shown in Figure 2-7, Section D. The discharge end is at elevation 105'-0". A 90° elbow is provided at the discharge end of the line. The N210 lines are Class 3 piping.

Each N210 line is supported by two struts, in the horizontal plane just above the elbow, made of 4-inch diameter double extra strength pipe. The line is supported just above the elbow at the discharge end. One support

is anchored to the torus shell. The second is anchored either to the ring girder (for support in segment 5) or to an existing W14 beam (for support in segment 13). N210 supports are Class 3 component supports. Figure 8-4 shows details of typical internal pipe supports.

8.1.6 HPCI Turbine Exhaust Line and Support

The HPCI turbine exhaust (N214) line is located in segment 5 of Unit 2 and segment 13 of Unit 3 (Figures 2-5 and 2-6). The N214 line is 24 inches in diameter and 0.844 inch thick. It penetrates the torus shell horizontally at elevation 112'-0", extends vertically downward into the pool to its discharge end at elevation 105'-0", and connects to a 90° short radius elbow. Connected to the elbow is a 2 feet-8 inch horizontal pipe with end caps, both of which are perforated with 1-inch diameter holes. The N214 line is Class 3 piping.

At the end cap, the line is supported by two 1.5-inch diameter rods with turnbuckles, as shown in Figure 8-5. The rods are anchored to a horizontal W14x68 beam spanning the area between two adjacent ring girders. At elevation 106'-6", the N214 line is partially boxed in by ST sections that are welded to the horizontal W14x68 beam. The W14x68 beam is braced with 6-inch diameter schedule 80 pipes attached to the W14 beam and the torus ring girder. The N214 support system is a Class 3 component support.

8.1.7 RCIC Turbine Exhaust Line and Support

The RCIC turbine exhaust (N212) line is located in segment 6 of Unit 2 and segment 12 of Unit 3 (Figures 2-5 and 2-6). Each N212 line penetrates the torus horizontally at elevation 112'-0" and extends vertically downward into the pool (Figure 2-7, Section C). Its discharge end is at elevation 105'-0". A 45° elbow is provided at the discharge end of the line. The N212 line, which is made of 12-inch diameter schedule 80 pipe, is Class 3 piping.

Just above the 45° elbow, the N212 line is enclosed by a box-like section made of ST sections welded to a W14x30 beam spanning the area between ring

girders. The W14x30 beam is reinforced with two 15 inch x 1 inch plates. The N212 support system is a Class 3 component support. Figure 8-6 shows the details of the modifications to the RCIC turbine exhaust pipe support.

8.1.8 Vacuum Breaker Drain Lines and Supports

Each Peach Bottom unit has six pairs of vacuum breakers. A pair of vacuum breakers is located in segments 2, 4, 6, 10, 12, and 16 (Figure 2-4). A 1-inch schedule 80 pipe serves as the drain pipe. The drain pipe starts from the bottom of the vacuum breaker at about elevation 114'-0" and extends vertically downward to the discharge end at elevation 106'-0".

At elevation 109'-0", a support to the vacuum drain pipe was added. The support consists of a pipe strap welded to a 1-inch thick vertical plate (42" x 3") which in turn is welded to the catwalk support channel (Figure 8-7) approximately at elevation 110'-5". Vacuum breaker drain line supports are Class 3 component supports.

8.1.9 Thermowells

Thermowells were installed in 13 of the 16 torus bays of each Peach Bottom unit to monitor the torus pool temperature. Figure 8-8 shows the torus plan with the location of the thermowell assemblies. At least one quencher arm will discharge steam in a bay where a thermowell assembly is located.

Figure 8-9 shows the section and detail of a typical thermowell assembly. The thermowells, approximately 10 inches long, were inserted in holes drilled in the shell below the normal pool water level. A weld couplet acts as a closure for the opening. Sensors are connected to the thermowell to provide pool temperature data to the plant operator.

8.1.10 Main Vent Drain Lines and Supports

Each of Peach Bottom Units 2 and 3 have eight main vents. At each intersection between the main vent and the vent header, a drain line is located. Each drain line is 1 inch in diameter and about 5 feet-7 inches

long. The drain line runs from the bottom of the main vent vertically downward into the pool. The discharge exit is at elevation 105'-0". Vent line drains are Class 3 piping.

Lateral supports are provided to each vent line drain by means of (2 x 2 x ¼) angles that are inclined 45° from vertical in both the longitudinal and transverse directions. The two ends of each angle are welded to the plates which are in turn welded to the main vent drain and vent header respectively. The main vent drain supports are Class 3 component supports. These supports did not require modification.

8.1.11 ECCS Suction Nozzles

The ECCS suction nozzles are located at penetrations N225, N226A through D, N227, and N228A through D (Figure 2-7, Section B). The nozzles penetrate radially the lower half of the torus shell at a 30° angle with the vertical. The nozzles consist of a flanged connection at the interior of the torus with stainless steel strainers bolted to the flange. These strainers are of a conical shape with a diameter of 24 inches at the bottom and 15.25 inches at the top. The largest diameter strainer is at N226, so this nozzle was conservatively chosen for the load calculations. No modification was required for the nozzles.

8.1.12 Instrument Air Line Piping

The instrument air line piping consists of a 1-inch schedule 40 pipe penetrating the torus shell at an angle of 45° with the vertical. This piping is located in segment 7 of Unit 2 and segment 11 of Unit 3 (Figures 2-5 and 2-6). The pipe passes through a series of elbows, a small hand-operated valve, and a check valve before extending vertically downward to the catwalk platform (Figure 8-10). The line then branches into a header that runs circumferentially around the underside of the platform. The vertical portion of the line is supported by two struts made of 3-inch schedule 40 pipe welded to the torus shell. The portion below the catwalk is supported by a pipe strap welded to a 1/2-inch thick plate attached to the platform channel at a spacing of approximately 5 feet. The air line is

classified as nonessential piping. Only the portion of the line between the torus penetration and the valves is Q-listed.

8.1.13 HPCI Minimum Recirculation Line

The HPCI minimum recirculation (N216) line is made of 4-inch schedule 80 pipe. It is located in segment 5 of Unit 2 and segment 13 of Unit 3 (Figures 2-5 and 2-6). The line penetrates the torus shell horizontally at elevation 112'-0" and extends vertically downward into the pool to its discharge end at elevation 105'-0" as shown in Figure 2-7, Section C. The N216 line is Class 3 piping. This line did not require modification.

8.1.14 RCIC Vacuum Pump Discharge Line

The RCIC vacuum pump discharge (N221) line is made of 2-inch schedule 80 pipe. It is located in segment 6 of Unit 2 and segment 12 of Unit 3 (Figures 2-5 and 2-6). It penetrates the torus shell horizontally at elevation 112'-0" and extends vertically downward into the pool to its discharge end at elevation 108'-0" as shown in Figure 2-7, Section D. The N221 line is Class 3 piping and did not require modification.

8.1.15 Condensate Line from HPCI Turbine Drain Pot

The condensate line from the HPCI turbine drain pot (N223) is located in segment 5 of Unit 2 and segment 13 of Unit 3 (Figures 2-5 and 2-6). It is made of 2-inch schedule 80 pipe. It penetrates the torus shell horizontally at elevation 112'-0" and extends vertically downward into the pool. Its discharge end is at elevation 108'-0". The N223 line is Class 3 piping and did not require modification.

8.1.16 Core Spray Test and Flush Lines

The core spray test and flush (N224 and N234A and B) lines are located in segment 5 of Unit 2 and segments 5 and 13 of Unit 3 (Figures 2-5 and 2-6). These lines are made of 10-inch schedule 80 pipe. They penetrate the torus shell radially at a 45° angle with the vertical (Figure 2-7, Section D) and

extend vertically downward into the pool. The torus shell penetrations are at approximately elevation 121'-0" and the discharge ends are at elevation 105'-0". These lines are Class 3 piping.

8.1.17 Core Spray Minimum Flow Lines

The core spray minimum flow (N229) line is located in segment 7 of Unit 2 (Figure 2-5). The N229 line is made of 6-inch schedule 80 pipe. For Unit 3, two core spray minimum flow lines, designated as N236A and N236B, are located in segments 7 and 11 (Figure 2-6) respectively. The N236 lines are made of 4-inch schedule 80 pipe. In both units, they penetrate the torus shell horizontally at elevation 112'-0" and extend vertically downward into the pool. Their discharge end is at elevation 105'-0". These lines are Class 3 piping and did not require modification.

8.1.18 RCIC Pump Recirculation Line

The RCIC pump recirculation (N230) line inside the torus is located in segment 6 of Unit 2 and segment 12 of Unit 3 (Figures 2-5 and 2-6). The N230 line is made of 4-inch schedule 80 pipe. It penetrates the torus shell horizontally at elevation 112'-0" and extends vertically downward into the pool. Its discharge end is at elevation 105'-0". The vertical portion is 13.5 feet from the torus centerline, as shown in Figure 2-7, Section C. The N230 line is Class 3 piping and did not require modification.

8.1.19 HPCI and RCIC Test and Flush Lines

For Unit 2, the HPCI and RCIC test and flush (N233) line is located in segment 9 (Figure 2-5). The N233 line is made of 10-inch schedule 80 pipe. For Unit 3, the HPCI and RCIC test and flush (N235) line is located in segment 9 (Figure 2-6). The N235 line is made of 4-inch schedule 80 pipe. HPCI and RCIC test and flush lines in both units penetrate the torus shell radially at a 45° angle with the vertical and extend vertically downward

into the pool. The torus shell penetrations are at elevation 121'-0" and the discharge ends are at elevation 105'-0". These lines are Class 3 piping and did not require modification.

8.1.20 Electrical Canisters

Several electrical canisters are located at penetrations N220 and N231A and B. At N220, the piping penetrates the shell radially at a 45° angle with the vertical and runs into a metal junction box with dimensions of 17 inches x 17 inches x 22 inches. A 4.5-inch diameter conduit extends vertically downward into another junction box supported from the catwalk platform. This box is then connected to the box on penetration N231A by a 4.5-inch diameter conduit running horizontally at the platform elevation. At N231A and B, the piping penetrates the shell radially at a 60° angle with the vertical and runs to a junction box with dimensions of 20 inches x 20 inches x 22 inches. A conduit connects N231A to N220 as noted above. No additional conduit exists on N231B. The electrical canisters and associated conduit inside the torus are nonsafety related structures. The canisters are tied to the catwalk supports as shown in Figure 8-11. No modification to electrical junction boxes was required.

8.2 LOADS

The torus internal structures have been evaluated for all required loads including normal, seismic, LOCA related, and SRV discharge loads. These are described below.

8.2.1 Normal Loads

Normal loads for the internal structures consist of the combination of dead loads and thermal effects during plant operation.

8.2.2 Seismic Loads

Seismic loads considered are given in Section 5.1.

8.2.3 LOCA Loads

These loads could be caused by pool swell, condensation oscillation, or chugging. Pool swell loads could be further categorized into pool swell impact, pool swell drag, pool fallback, froth impingement loads, LOCA water jet, and LOCA bubble drag loads. Submerged internal structures also experience drag loads because of condensation oscillation and chugging. These loads are briefly discussed here.

8.2.3.1 Pool Swell Impact and Drag Loads

During the pool swell transient, the rising pool will impact structures above the initial pool surface and below the maximum pool swell height. As the pool surface rises, it impacts structures located within its range of travel. Consequently, loads are generated because of both impact and drag forces. These loads for the appropriate internal structures were calculated according to procedures and guidelines given in the LDR (Reference 11).

8.2.3.2 Froth Impingement Loads

Froth is an air-water mixture that rises above the pool surface during pool swell and may impinge on structures within the torus air space. Afterward, the froth will fall back, creating froth fallback loads. Froth impingement loads have been calculated according to LDR criteria.

8.2.3.3 Pool Fallback Loads

Following the pool swell transient, as the pool water falls back to its original level it generates fallback loads. After the pool surface has reached its maximum height because of pool swell, it falls back under the influence of gravity, creating drag loads on structures inside the torus shell that are between the maximum bulk pool swell height and the downcomer exit level. These loads have been calculated according to LDR guidelines.

8.2.3.4 LOCA Water Jet Loads

As the drywell pressurizes during a postulated LOCA, the water column standing in the submerged portion of each downcomer is accelerated downward into the suppression pool. As the mass of water enters the pool, it forms a jet that could potentially load structures intercepted by the discharge. Pool acceleration and velocity induced by the advancing jet front also induce drag loads. The calculation of these loads was based on LDR methodology.

8.2.3.5 LOCA Drag Loads

During the initial phase of a DBA, pressurized drywell air is purged into the suppression pool through the submerged downcomers. After vent clearing, a single bubble is formed around each downcomer. For a DBA, the duration of the LOCA bubble is typically 0.2 second from its initial formation until it breaks through the pool surface. It is during the bubble growth period that unsteady fluid motion is created within the suppression pool, exposing all the submerged structures to transient hydrodynamic loads. Calculation of these drag loads was based on LDR methodology.

8.2.3.6 Drag Loads Due to Condensation Oscillations and Chugging

During a postulated LOCA, steam condensation begins after the vent is cleared of water and the drywell air has been carried over into the suppression chamber. The condensation oscillations induce bulk water motion and therefore create drag loads on structures submerged in the pool. Steam chugging at the downcomers induces similar drag forces on the submerged structures. These loads were calculated based on LDR methodology.

8.2.4 SRV Discharge Loads

SRV discharge loads on the submerged structures consist of T-Quencher water jet loads and T-Quencher bubble induced drag loads.

8.2.4.1 T-Quencher Water Jet Loads

When an SRV is actuated, water initially contained in the submerged portion of the SRV discharge line is forced out of the T-Quencher arm through the arm holes, forming orifice jets. Some distance downstream, the orifice jets merge to form column jets. Further downstream, the column jets merge to form the quencher arm jets. As soon as the water flow through the arm holes ceases, the quencher arm jet velocity decreases rapidly and the jet penetrates a limited distance in the pool. These T-Quencher water jets create drag loads on the nearby submerged structures that are within the jet path. Jet load calculations were performed based on LDR methodology.

8.2.4.2 T-Quencher Bubble Drag Loads

Oscillating bubbles resulting from an SRV actuation create an unsteady three-dimensional flow field and therefore induce an acceleration with standard drag forces on the submerged structures in the suppression pool. Drag loads were calculated according to the LDR guidelines.

8.3 ALLOWABLE STRESSES

The internal structures are classified either as nonsafety related components or as Class 3 piping with linear component supports. For the stress evaluation of internal structures, the governing design loading combinations and the corresponding service levels are given in Table 5-5, which was derived from Table 5-1 of Reference 14. Similar governing load combinations for Class 3 essential piping systems inside the torus and the linear component supports are given in Table 5-7, which was derived from Table 5-2 of Reference 14. The allowable stress values for each structural component are briefly discussed below.

8.3.1 Class 3 Piping Systems

The requirements that must be satisfied for Class 3 piping components are given in article ND 3600 of the ASME Code (Reference 13) along with allowable service limits. These requirements fall into two major

categories; namely, pressure design, ND 3600, and the consideration of design conditions, ND 3652. Satisfaction of pressure design requirements is based on the specified pressure and pipe section properties while satisfaction of design conditions requires calculation of internal moments caused by the design loads and substituting these moments in code equations to check the resultant stresses with the allowable limits. The allowable limits for different service levels are:

Service Level A = 1.0 S_h
Service Level B = 1.2 S_h
Service Level C = 1.8 S_h
Service Level D = 2.4 S_h

where S_h is the basic material allowable stress at the design temperature and equals 13.7 ksi for piping material SA333, Grade 1, and 14.4 ksi for SA333, Grade 6.

8.3.2 Nonsafety Related Components

Internal structures such as the catwalk platform and monorail were designed using the stress values given in Appendix XVII of the ASME Code and are similar to those used for linear component supports. The criteria for the linear component supports are based on article NF 3000 and Appendix XVII of the ASME Code. The allowable limits for service limit Levels C and D are 1.33 and 1.88 times the service Level A allowable limit.

For the Level A service limit, the allowable stresses are given below.

For pipe columns under tension and bending on the net section, the allowable stress in tension is:

$$F_t = 0.60\ S_y$$

but not more than 0.5 times the minimum tensile strength of the steel.

The allowable stress in bending is:

$$F_b = 0.66\ S_y$$

where S_y is the specified minimum yield strength.

For pipe columns under compression and bending when the pipe column is subjected to both compression and bending simultaneously, the stresses shall satisfy the following interaction equation:

$$\frac{f_a}{F_a} + \frac{f_b}{(1 - \frac{f_a}{F'_e})F_b} \leq 1.0$$

where

f_a = calculated compressive stress

F_a = allowable compressive stress

f_b = calculated bending stress

F_b = allowable bending stress

$$F'_e = \frac{12\pi^2 E}{23(K\frac{l}{r})^2}$$

K = effective length factor

l = actual unbraced length

r = radius of gyration

E = Young's modulus.

For SA 333, Grade 6, the allowable yield stress is equal to 35.0 ksi and for SA 36 it is equal to 36.0 ksi. Their respective tensile strengths are 60.0 ksi and 58.0 ksi.

8.4 STRUCTURAL EVALUATION

A structural stress analysis was performed for the torus internal structures. All the applicable loads described in Section 8.2 were considered in the evaluation. The most critical stress values were obtained by using the governing load combinations discussed in Section 8.3. The analysis of the internal structures was accomplished through the use of hand calculations and simple computer modeling. Appropriate dynamic load factors were used for the equivalent static analysis to take into consideration the dynamic nature of the loads. The method of analysis and the results of the stress evaluation are discussed briefly in this section.

8.4.1 Method of Analysis

Hydrodynamic loads were evaluated at critical points along the length of each member of the internal structure under consideration. The actual time-history forcing function was calculated using the appropriate computer code and the guidelines prescribed in the LDR. The actual time-histories were then idealized to permit the calculation of dynamic load factors. The time-histories for the LOCA bubble and pool swell were idealized by simple impulse forms. The time-histories for condensation oscillation and T-Quencher discharge were idealized as harmonic functions. Dynamic load factors were determined using standard charts based on the idealized load transients and the calculated frequencies of the structures. A damping of 2% was used in calculating the loads. Equivalent static loads were calculated, equal to the transient peak load multiplied by the dynamic load factor. In addition, where appropriate, additional load factors were included for the inteference effects. These factors were calculated according to LDR guidelines. In general, there were three load components for the structural element under evaluation. These equivalent static loads were used in the subsequent stress analysis of the structures. The stresses obtained from the analyses for the various structural components were compared with the ASME allowable stresses. The results of the stress evaluation are described below.

8.4.2 Results of Stress Evaluation

During the design of the torus modifications, scoping calculations were performed to select member sections and to size connections and other details. This section describes the results of the final stress evaluation based on the analyses performed for the as-built configuration of the internal structures.

8.4.2.1 T-Quencher and T-Quencher Supports

Computer program STRUDL was used in the stress evaluation of the T-Quencher and its supports. The lowest frequency of the quencher and quencher support was 13.0 Hz and 33.1 Hz respectively. Both the T-Quencher and supports were analyzed for appropriate hydrodynamic loads and a stress evaluation was performed for the governing load combinations. The results of the stress evaluation, shown in Tables 8-1 through 8-3, indicate that the stresses are within the allowable limits.

8.4.2.2 Catwalk Platform and Supports

The catwalk platform and its supporting system were evaluated using hand calculations and simple beam models. The grating was checked to ensure that applied loads were less than the manufacturer's recommended allowable load. The pool swell loads on the catwalk and supporting system were conservatively applied over the entire length as a uniform load having an amplitude equal to the peak calculated load. The results of the stress evaluation for the catwalk platform and supports are shown in Tables 8-4 and 8-5. The results indicate the structural adequacy of the catwalk platform and supports. The effect of catwalk support reactions on the torus shell was included in the torus shell stress evaluation.

8.4.2.3 Monorail and Supports

The monorail and its supporting system were evaluated using simple beam models and hand calculations. This system experiences froth impingement loads. In a manner identical to the catwalk, the peak froth impingement

loads were conservatively applied as uniform loads to the monorail beam. Tables 8-4 and 8-5 show the results of the stress evaluation for the governing load combinations. The results show that the stresses are within the allowable limits. Finally, the effect of the monorail support reactions on the torus shell was considered in the torus stress evaluation.

8.4.2.4 Spray Header and Supports

The spray header piping and its supports were analyzed using simple hand calculations. The froth impingement load is the only hydrodynamic load experienced by this line and occurs only on a small portion between the torus penetration and the vent header. The froth pressure on this portion produces a small vertical load resulting in negligible pipe stresses. A simple modification to the existing hangers was made to prevent upward movement of this piping. The stresses in the support system were found to be well within the allowable limits.

8.4.2.5 RHR Torus Cooling and Pump Test Lines and Supports

The RHR line and supports were analyzed using a simple beam model and hand calculations. These structures essentially behave as rigid structures. Stresses in the pipe supports were determined by conservatively applying a uniform load over the entire submerged portion, with a concentrated load at the pipe end because of the thrust from the additional elbow. Results of the stress evaluation, shown in Tables 8-1 through 8-3, indicate that this piping system is adequate to withstand the imposed hydrodynamic loads. Reaction loads resulting from the support system were considered while performing the torus shell evaluation.

8.4.2.6 HPCI Turbine Exhaust Line and Support

The HPCI turbine exhaust line and its support system were analyzed using the STRUDL computer program. The pipe and its supporting system consist of a horizontal beam and two struts modeled as interconnected beams. The fundamental frequency of the piping system was found to be 7.9 Hz while

that of the support system was 27.0 Hz. The results of the stress evaluation, shown in Tables 8-1 through 8-3, indicate that the piping system and the supports are adequate.

8.4.2.7 RCIC Turbine Exhaust Line and Support

A three-dimensional analytical model of the RCIC turbine exhaust line and its support system was developed. The computer program STRUDL was used for the analysis. The lowest frequency of the piping was 9.2 Hz and for the support was 8.5 Hz. Stresses in the pipe and support beam were checked to ensure they were within the allowable stress limits. Tables 8-1 through 8-3 show the results of the stress evaluation for the governing load combinations for this piping system.

8.4.2.8 Vacuum Breaker Drain Line and Supports

The vacuum breaker drain line was rerouted with new supports added as a result of the catwalk platform modifications. The modified configuration was analyzed using a simple beam model and hand calculations. Although the drag loads vary along the length of the submerged portion of the member, a uniform load was conservatively assumed. The stress evaluation results show that the stresses in the vacuum breaker drain line and supports are well below the allowable limits. These results are shown in Tables 8-1 through 8-3.

8.4.2.9 Thermowells

Thermowells were evaluated for hydrodynamic and other appropriate loads using simple hand calculations. The results of the stress evaluation for the governing load combinations indicate that the stresses are well within the allowable limits.

8.4.2.10 Main Vent Drain Lines and Supports

The main vent drain lines and their supporting systems were analyzed using a three-dimensional model and the NASTRAN computer program. The results of

the stress evaluation are shown in Tables 8-1 through 8-3. These results indicate that the main vent drain lines and their supports are structurally adequate to withstand hydrodynamic loads.

8.4.2.11 ECCS Suction Nozzles

The stress evaluation for ECCS suction nozzles was done using simple hand calculations. All applicable hydrodynamic loads were included in the evaluation. The resulting stresses for the governing load combinations were found to be extremely small.

8.4.2.12 Instrument Air Line Piping

The instrument air line piping is divided into the essential piping (the portion above the catwalk) and the nonessential piping (the portion below the catwalk). For the essential portion of the line, the NASTRAN computer program was used for the stress evaluation. For the nonessential portion of the line, the analysis was performed using simple beam models and hand calculations. The essential portion of the line experiences froth impingement loads while the nonessential portion experiences pool swell loads. For the sake of conservatism, the peak calculated loads were applied uniformly for both segments of the pipe. The resulting stresses were found to be within allowable limits. Tables 8-1 through 8-3 show the results of the stress evaluation.

8.4.2.13 HPCI Minimum Recirculation Line and Others

The HPCI minimum recirculation line was analyzed using simple hand calculations. The fundamental frequency of the system was calculated to be 13.0 Hz. The results of the stress evaluation are given in Tables 8-1 through 8-3, which indicate that the stresses are within allowable limits.

The HPCI minimum recirculation line is a piping system without any supports and for which no structural modifications were necessary. The stress evaluation results for this piping system are typical of the results obtained for similar piping systems (without any supports) described in

Section 8.1. Therefore, the results of the stress evaluation for the remaining lines such as the RCIC vacuum pump discharge line, condensate line from the HPCI turbine drain pot, cold spray test and flush line, cold spray minimum flow lines, RCIC pump recirculation line, and HPCI and RCIC test and flush lines are not discussed here.

8.4.2.14 Electrical Canisters

The electrical canisters and associated piping were evaluated using simple hand calculations. The froth impingement load is the only hydrodynamic load experienced by these structures. Stresses for the governing load combinations are well within allowable limits.

Table 8-1

SUMMARY OF STRESS EVALUATION FOR
INTERNAL PIPING SYSTEMS

SERVICE LEVEL B

Piping System	Stress Type	Calculated Stress (ksi)	Allowable Stress (ksi)	Ratio
T-Quencher	Eq 9 (1)	14.33	17.28	0.84
T-Quencher Support	Flexure	17.01	23.10	0.74
Main Vent Drain Line				
a. Piping	Eq 9 (1)	5.65	16.44	0.34
b. Support	Flexure	9.89	17.56	0.56
Vacuum Breaker Drain Line	Eq 9 (1)	2.36	16.44	0.14
RHR Torus Cooling and Test Pump Line				
a. Piping	Eq 9 (1)	10.90	16.44	0.66
b. Support	Axial + Flexure (2)	-	1.00	0.56
HPCI Minimum Recirculation Line	Eq 9 (1)	15.82	16.44	0.96
RCIC Turbine Exhaust Line				
a. Piping	Eq 9 (1)	8.90	16.44	0.54
b. Support	Flexure	16.80	21.60	0.77
HPCI Turbine Exhaust Line				
a. Piping	Eq 9 (1)	15.20	21.00	0.72
b. Support	Flexure	3.90	21.60	0.18

Notes: (1) Eq 9 refers to Equation 9 of ND 3652 of ASME Code (Reference 13)

(2) Interaction equation for combined axial + flexure

Table 8-2

SUMMARY OF STRESS EVALUATION FOR
INTERNAL PIPING SYSTEMS

SERVICE LEVEL $B_{(3)}$

Piping System	Stress Type	Calculated Stress (ksi)	Allowable Stress (ksi)	Ratio
T-Quencher	Eq 9 (1)	17.90	25.92	0.69
T-Quencher Support	Flexure	17.85	30.72	0.58
Main Vent Drain Line				
a. Piping	Eq 9 (1)	11.24	24.66	0.46
b. Support	Axial + Flexure (2)	-	1.00	0.92
Vacuum Breaker Drain Line	Eq 9 (1)	5.28	24.66	0.21
RHR Torus Cooling and Test Pump Line				
a. Piping	Eq 9 (1)	10.90	31.50	0.35
b. Support	Axial + Flexure (2)	-	1.00	0.57
HPCI Minimum Recirculation Line	Eq 9 (1)	15.82	24.70	0.64
RCIC Turbine Exhaust Line				
a. Piping	Eq 9 (1)	17.20	24.70	0.70
b. Support	Flexure	18.40	28.80	0.64
HPCI Turbine Exhaust Line				
a. Piping	Eq 9 (1)	15.20	31.50	0.48
b. Support	Flexure	23.40	28.80	0.81

Notes: (1) Eq 9 refers to Equation 9 of ND 3652 of ASME Code (Reference 13)

(2) Interaction equation for combined axial + flexure

(3) For explanation of service level $B_{(3)}$, see Table 5-7

Table 8-3

SUMMARY OF STRESS EVALUATION FOR
INTERNAL PIPING SYSTEMS

SERVICE LEVEL $B_{(4)}$

Piping System	Stress Type	Calculated Stress (ksi)	Allowable Stress (ksi)	Ratio
T-Quencher	Eq 9 (1)	32.01	34.56	0.93
T-Quencher Support	Flexure	20.25	46.20	0.44
Main Vent Drain Line				
a. Piping	Eq 9 (1)	11.24	32.88	0.34
b. Support	Flexure	-	1.00	0.62
Vacuum Breaker Drain Line	Eq 9 (1)	5.28	32.88	0.16
RHR Torus Cooling and Test Pump Line				
a. Piping	Eq 9 (1)	10.90	42.00	0.26
b. Support	Axial + Flexure (2)	-	1.00	0.48
HPCI Minimum Recirculation Line	Eq 9 (1)	27.30	32.90	0.83
RCIC Turbine Exhaust Line				
a. Piping	Eq 9 (1)	18.30	32.90	0.56
b. Support	Flexure	35.40	40.60	0.87
HPCI Turbine Exhaust Line				
a. Piping	Eq 9 (1)	15.20	42.00	0.36
b. Support	Flexure	23.40	40.60	0.58

Notes: (1) Eq 9 refers to Equation 9 of ND 3652 of ASME Code (Reference 13)

(2) Interaction equation for combined axial + flexure

(3) For explanation of service level $B_{(4)}$, see Table 5-7

Table 8-4

SUMMARY OF STRESS EVALUATION FOR
INTERNAL STRUCTURES (OTHER THAN PIPING SYSTEMS)

SERVICE LEVEL A

Structure	Stress Type	Calculated Stress (ksi)	Allowable Stress (ksi)	Ratio
Catwalk Platform	Bending	9.01	18.00	0.50
Catwalk Support	Bending	12.00	21.40	0.56
Monorail	Bending	17.40	23.80	0.73
Monorail Support	Axial	6.30	22.50	0.28

Table 8-5

SUMMARY OF STRESS EVALUATION FOR
INTERNAL STRUCTURES (OTHER THAN PIPING SYSTEMS)

SERVICE LEVEL D

Structure	Stress Type	Calculated Stress (ksi)	Allowable Stress (ksi)	Ratio
Catwalk Platform	Bending	16.30	33.96	0.48
Catwalk Support	Bending	30.44	40.58	0.75
Monorail	Bending	17.40	44.62	0.39
Monorail Support	Axial	6.30	45.00	0.14

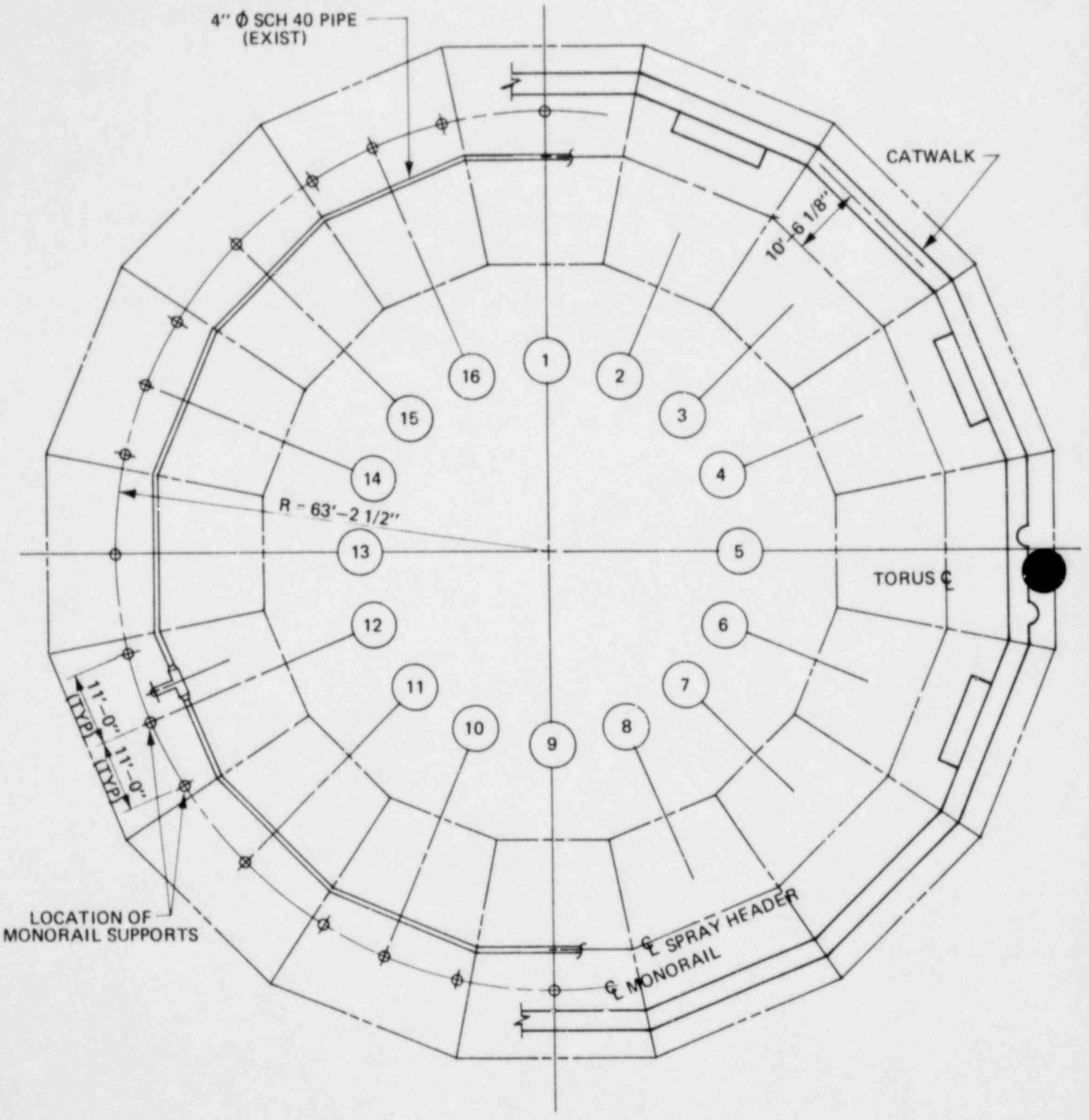

FIGURE 8-1 PLAN OF CATWALK, MONORAIL AND SPRAY HEADER

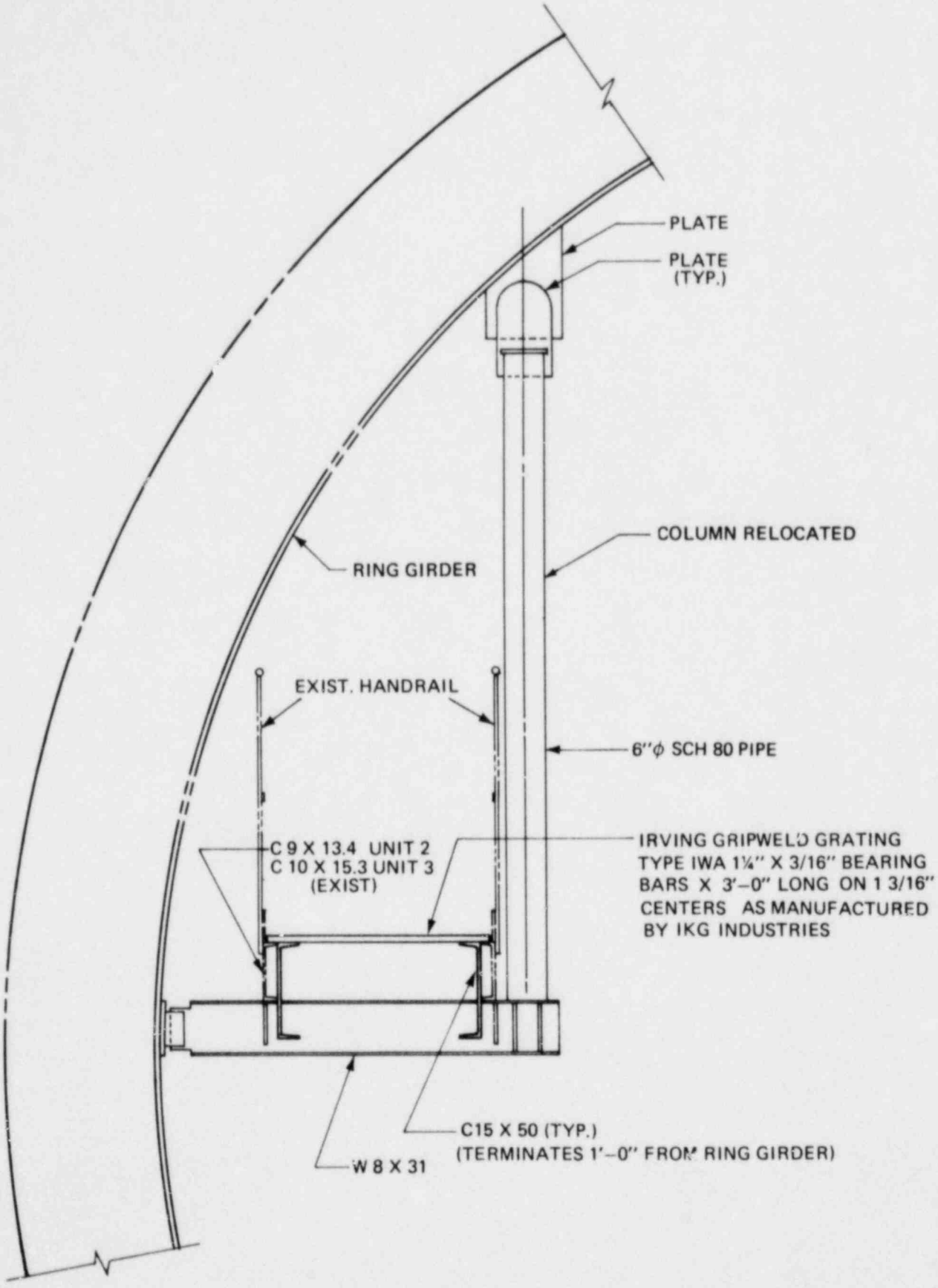

FIGURE 8-2 CATWALK MODIFICATIONS

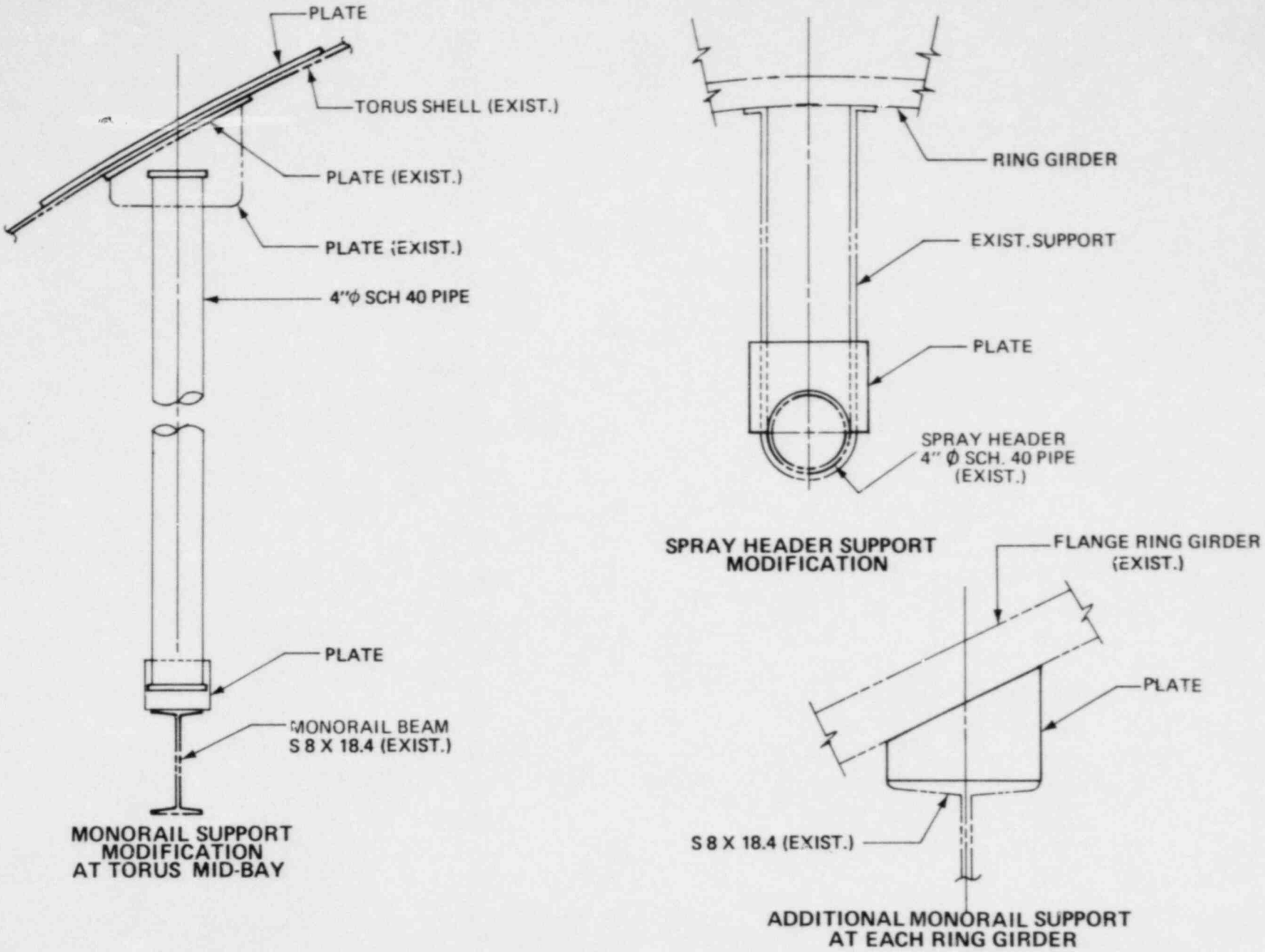

FIGURE 8-3 MONORAIL AND SPRAY HEADER SUPPORT MODIFICATIONS

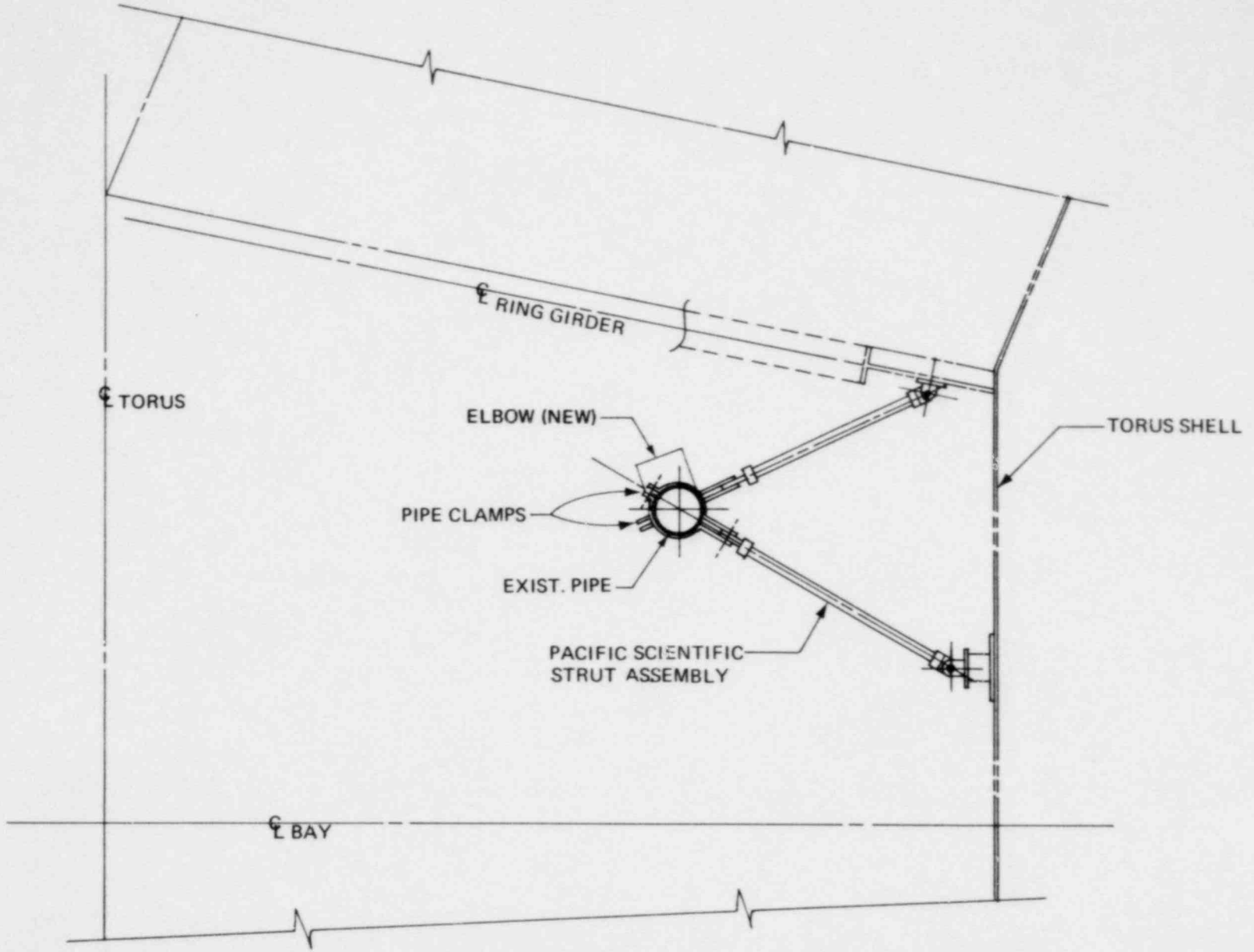

FIGURE 8-4 RHR ELBOW AND SUPPORT

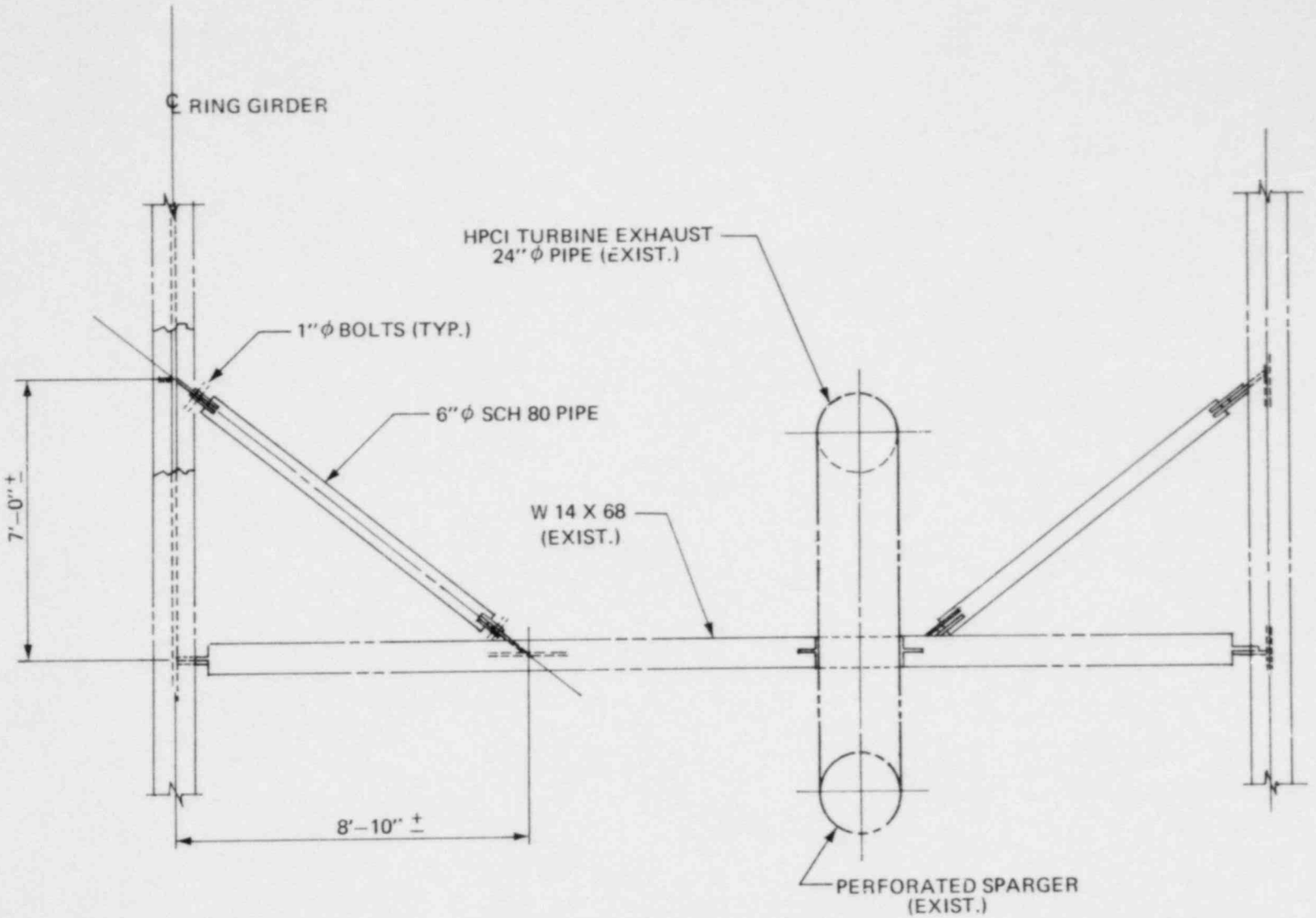

FIGURE 8-5 MODIFICATIONS TO HPCI TURBINE EXHAUST PIPE SUPPORT

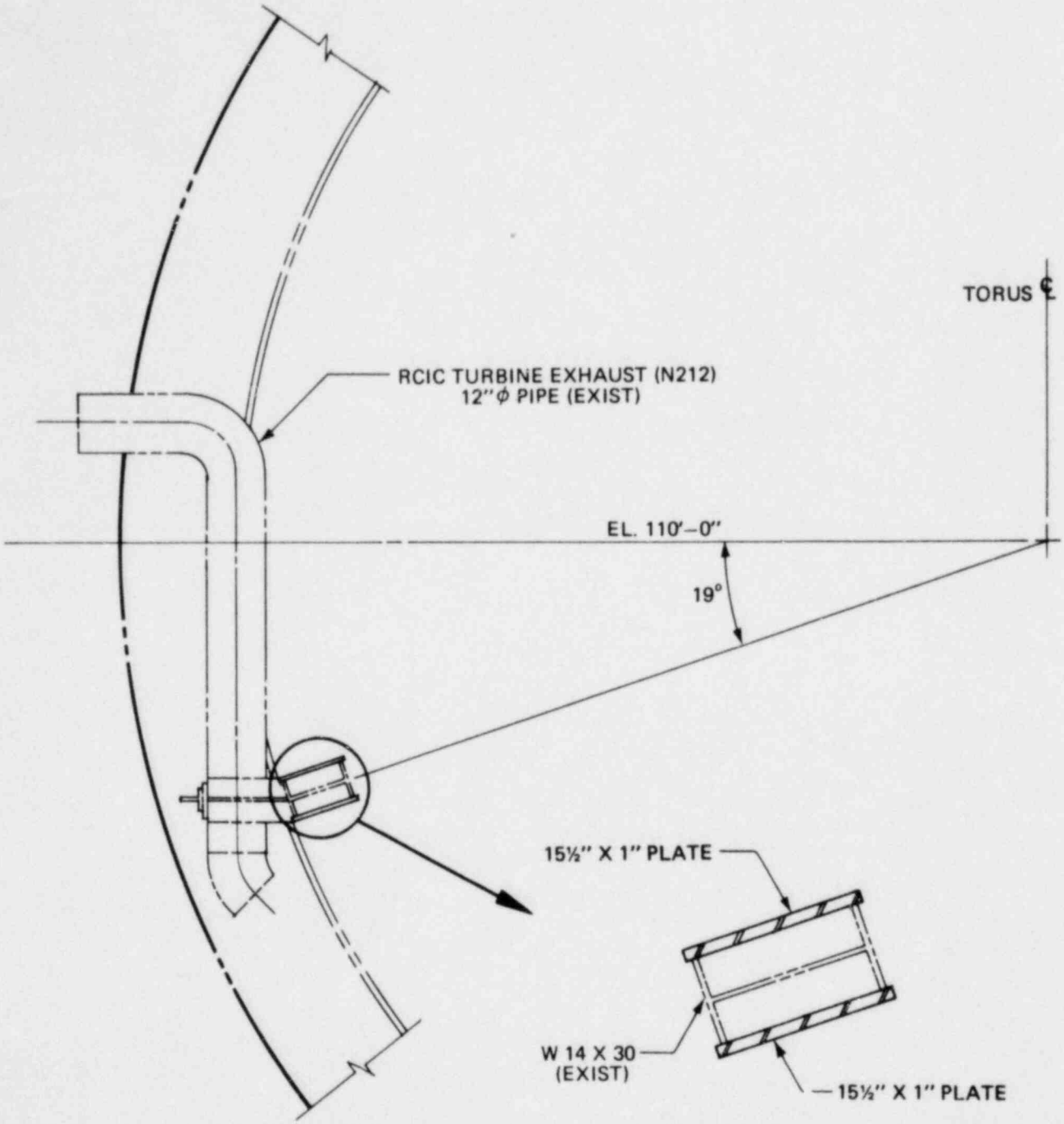

FIGURE 8-6 MODIFICATIONS TO RCIC TURBINE EXHAUST PIPE SUPPORT

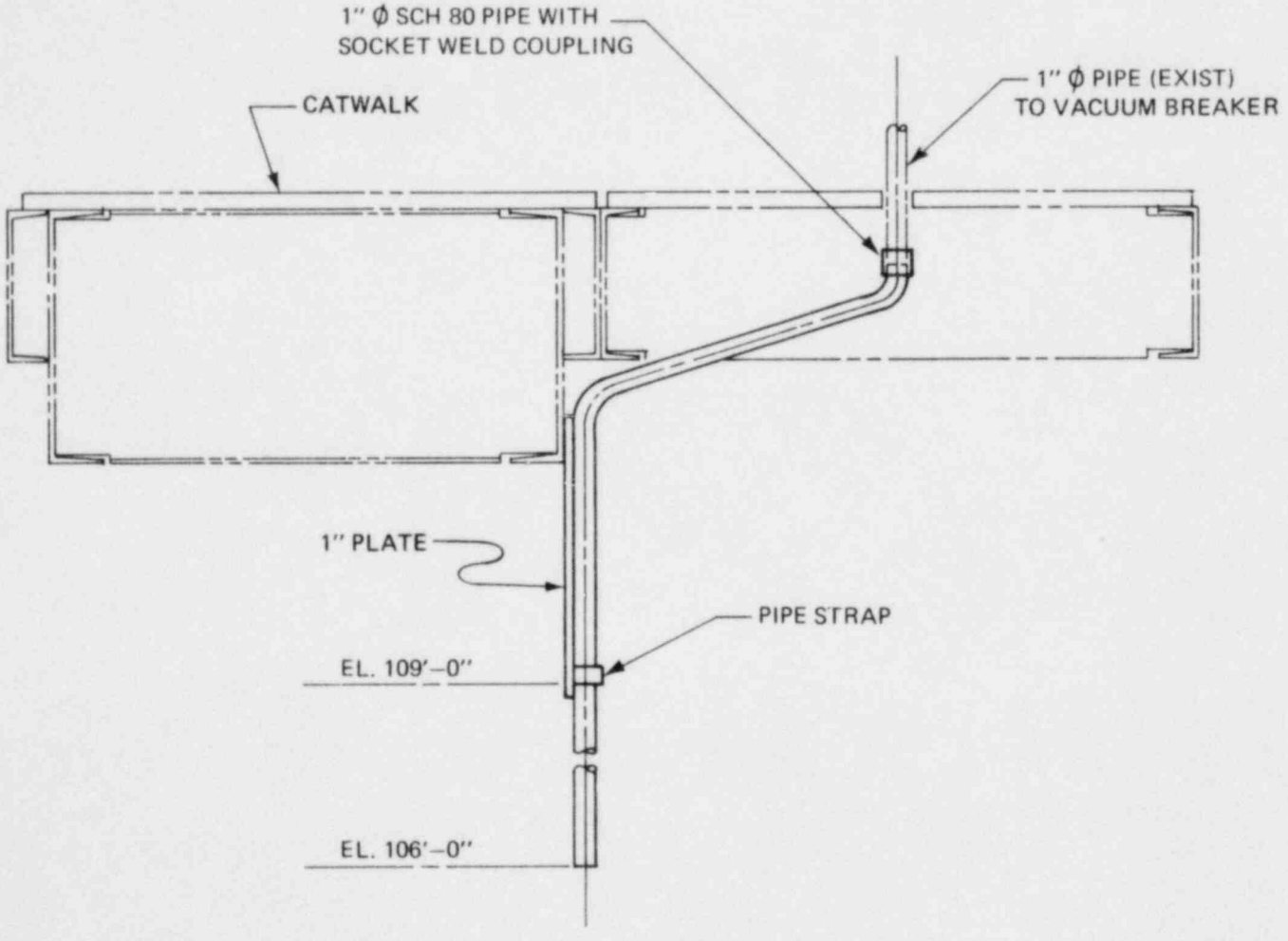

FIGURE 8-7 VACUUM BREAKER DRAIN LINE SUPPORTS

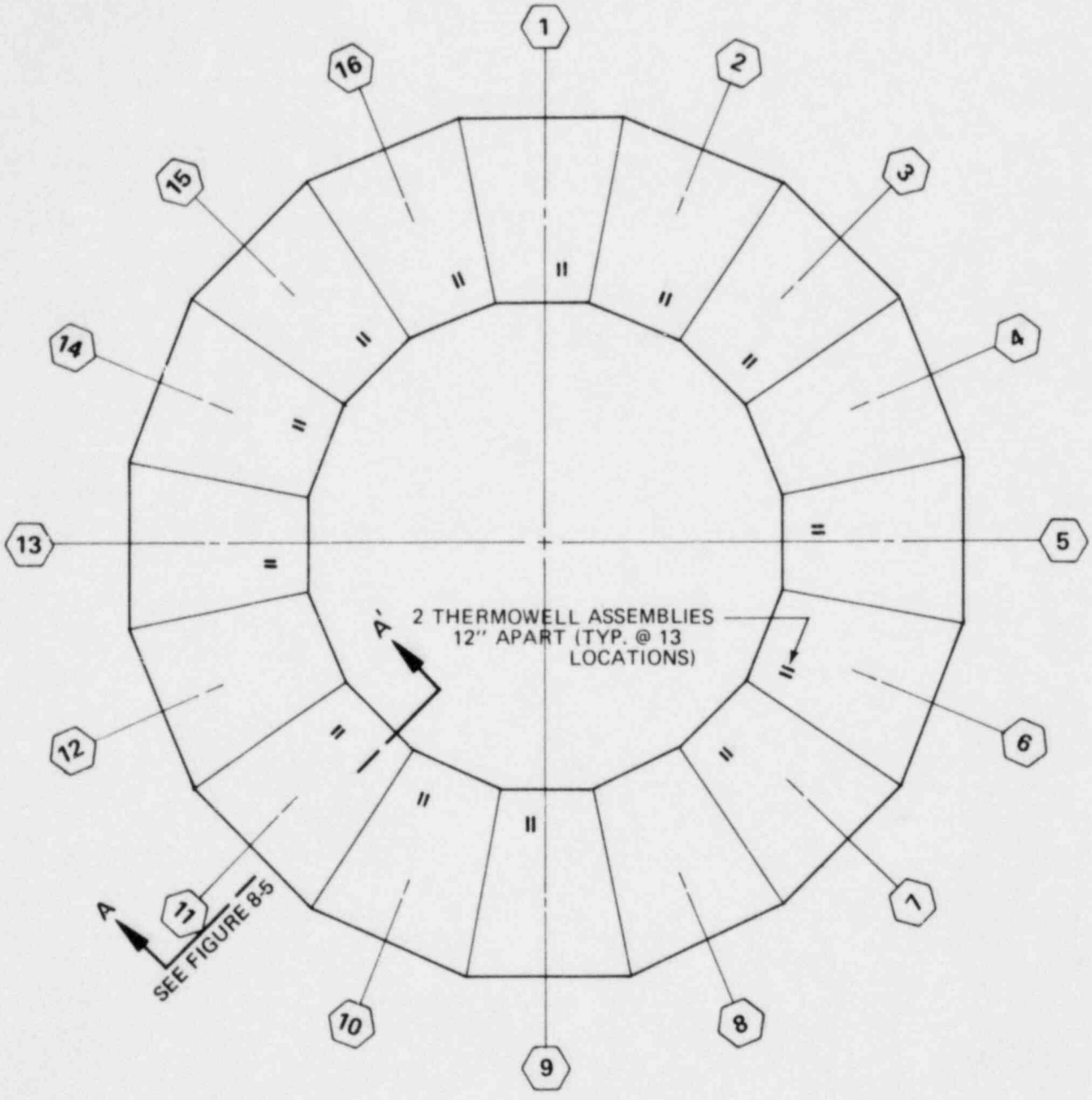

FIGURE 8-8 TORUS PLAN SHOWING LOCATION OF THERMOWELL ASSEMBLY

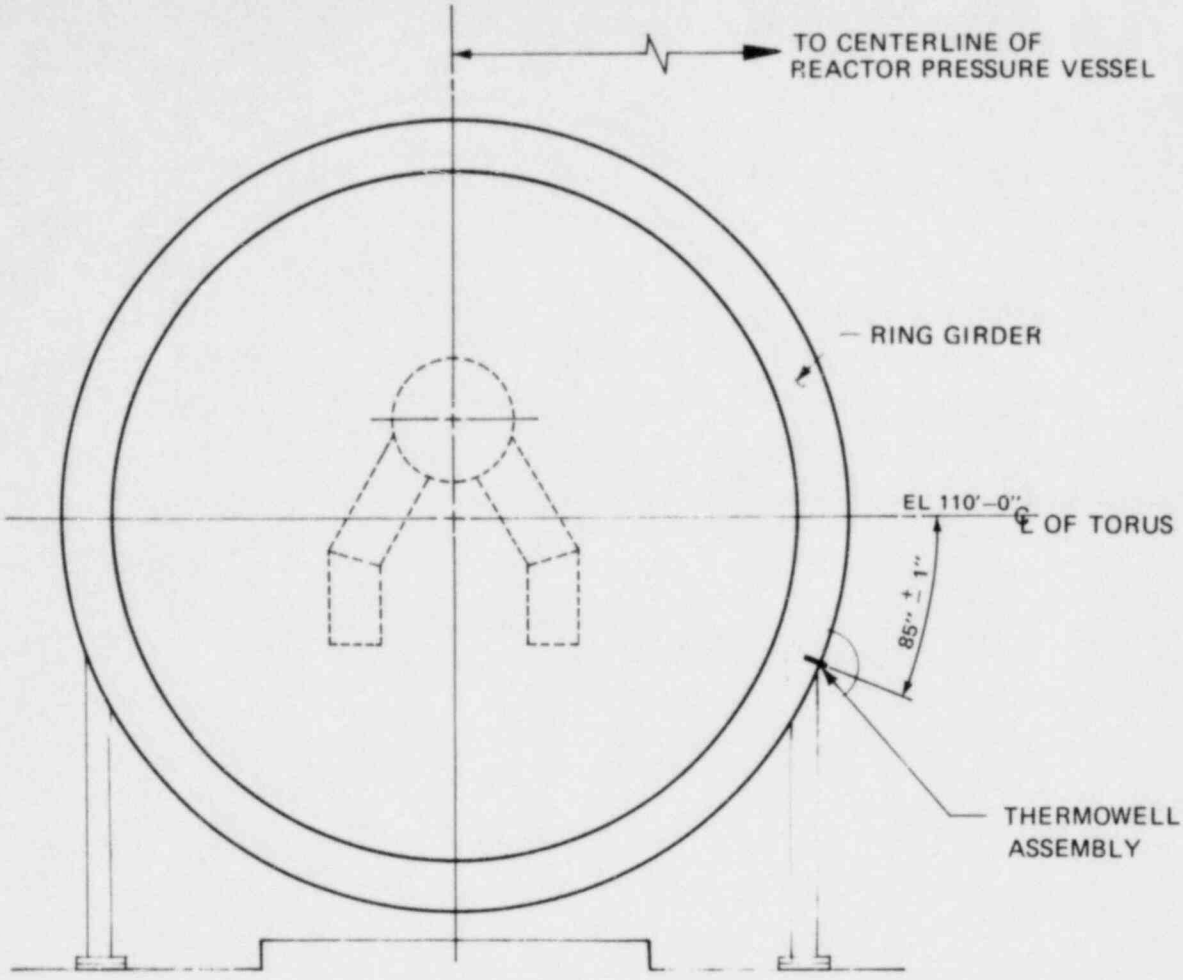

SECTION A–A'

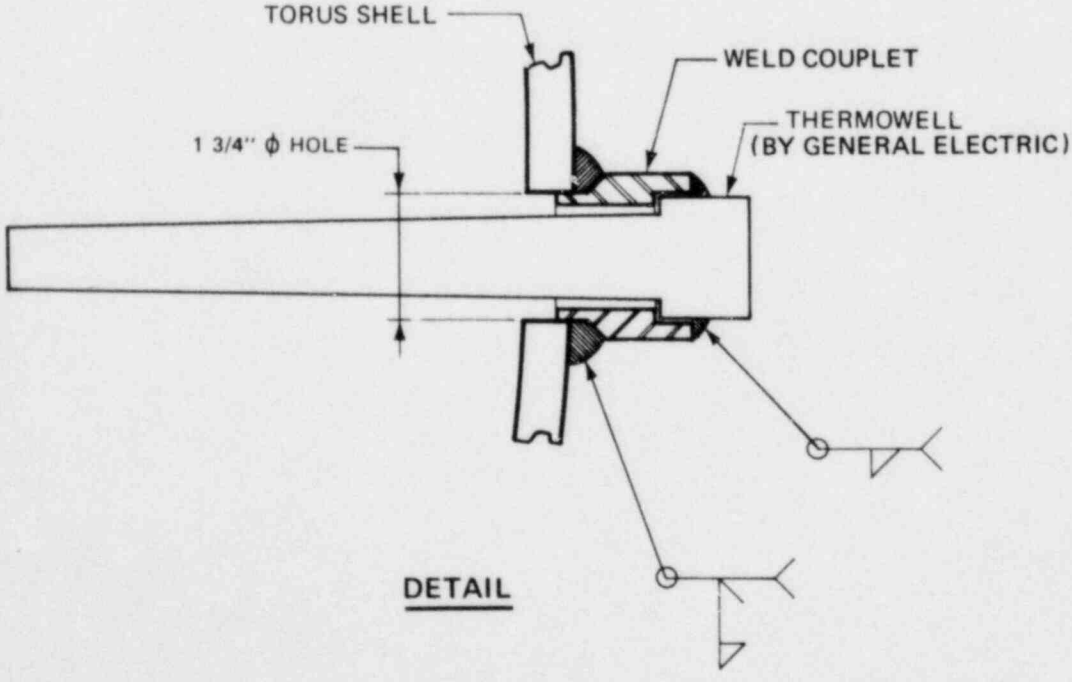

DETAIL

FIGURE 8-9 SECTION AND DETAIL FOR THERMOWELL ASSEMBLY

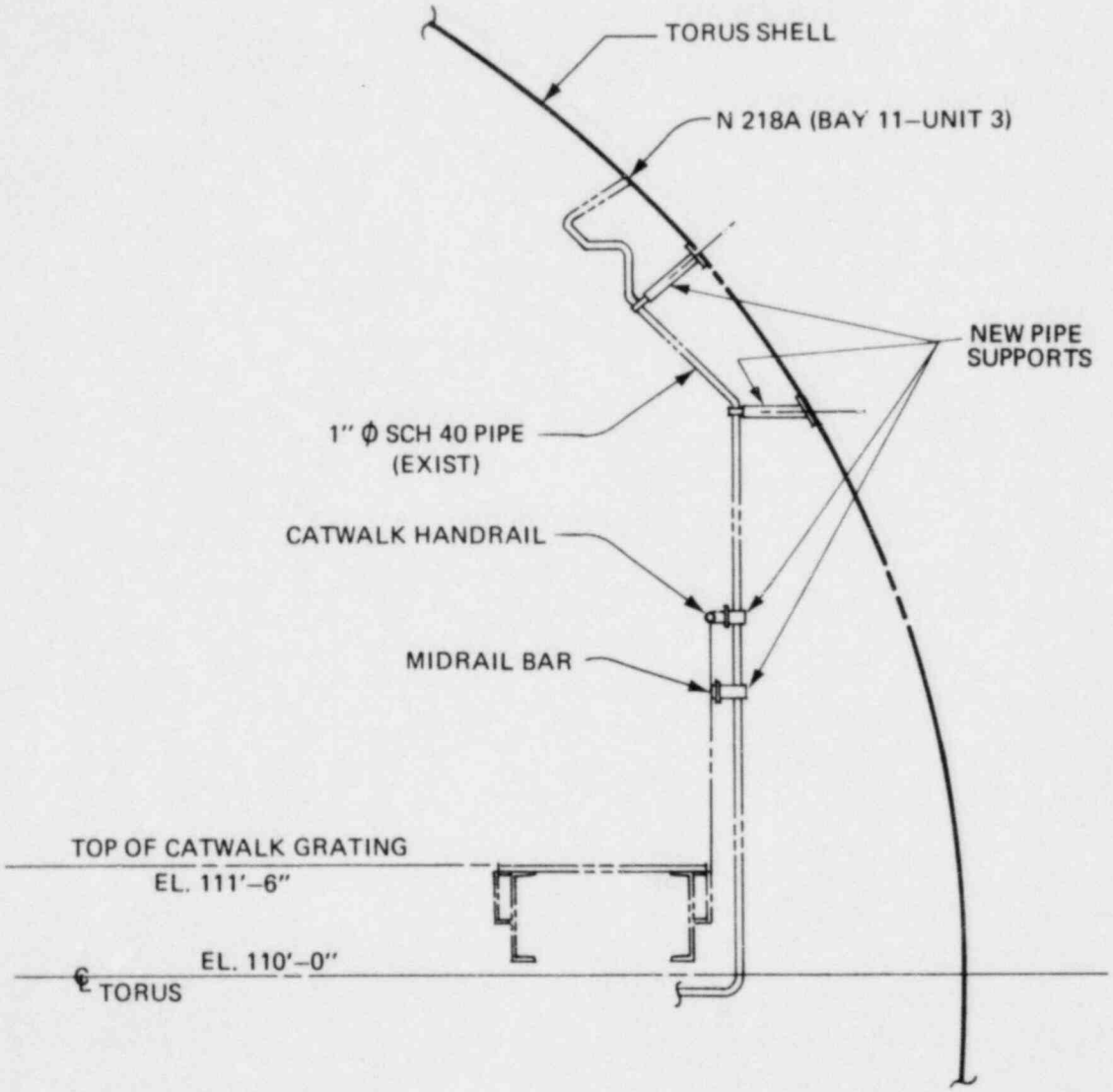

FIGURE 8-10 MODIFICATIONS TO INSTRUMENT AIR LINE

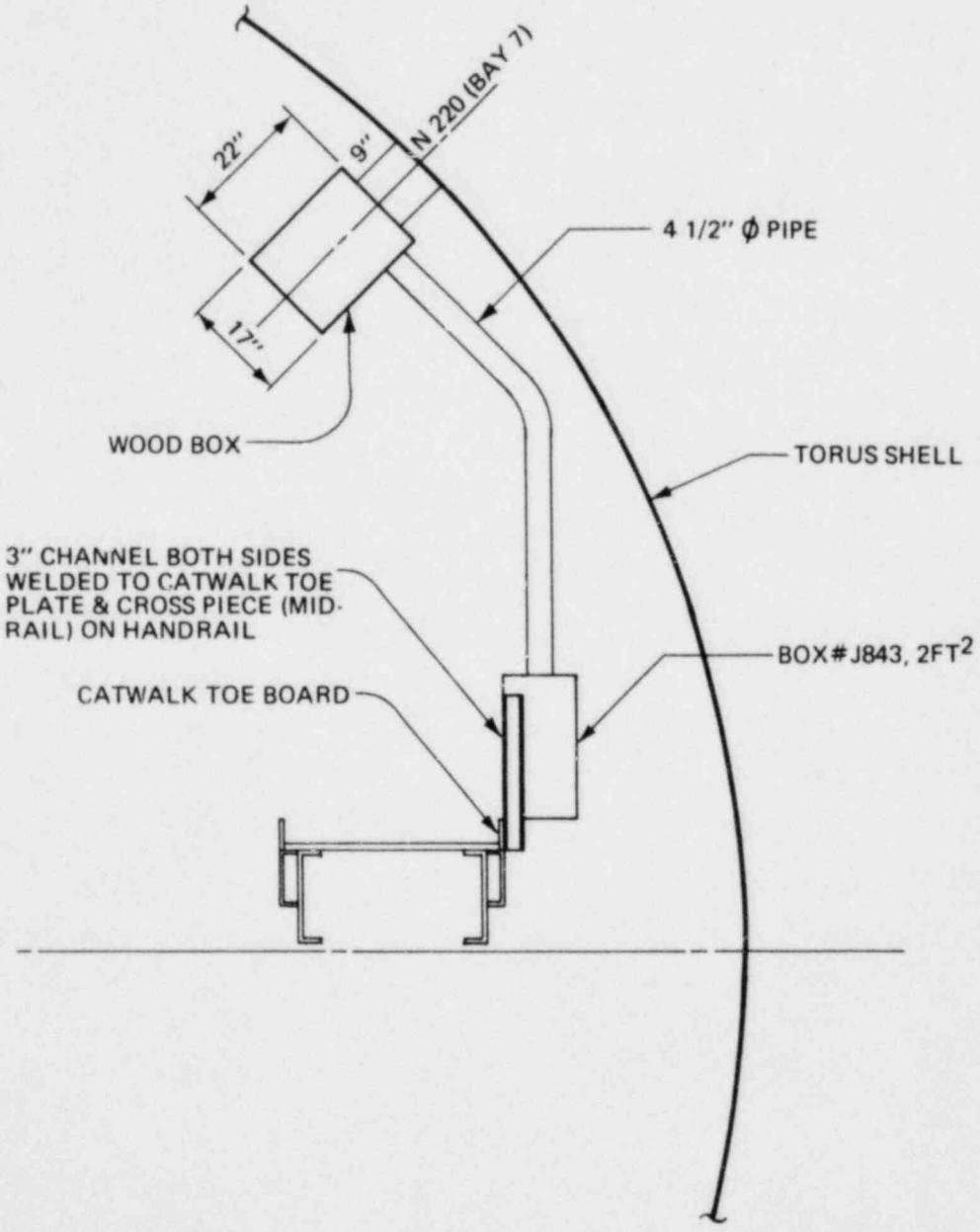

FIGURE 8-11 ARRANGEMENT OF ELECTRICAL CANISTER

Section 9
SUMMARY AND CONCLUSIONS

Section 9

SUMMARY AND CONCLUSIONS

A plant unique analysis has been performed for each Peach Bottom torus and its internal structures. The analysis has taken into account all the modifications performed to mitigate the hydrodynamic loads and/or strengthen the structural members to resist loads. Loading in the analysis includes LOCA loads as defined in the Mark I Load Definition Report, SRV discharge loads based on in-plant tests, and normal loads as specified in the Peach Bottom Atomic Power Station FSAR. The structural analysis techniques and the structural acceptance criteria were as specified in the Mark I Plant Unique Analysis Application Guide.

The stresses in the torus shell, shell stiffeners, ring girder, columns, saddles, anchors, and all connecting welds meet ASME Code allowable stresses. Saddle supports and the shell stiffeners reduce the stresses considerably.

The stresses in the main vents, vent header, and vent support columns meet ASME Code allowable values. Other components that connect the columns to the ring girder and the vent header have been relocated and strengthened to meet ASME Code allowable values.

Other internal structures such as return lines and supports also meet ASME Code allowable values.

Based on the results of this plant unique analysis, it is concluded that the modified Peach Bottom Units 2 and 3 tori meet all ASME Code allowable stress limits and therefore meet the original intended margin of safety.

REFERENCES

REFERENCES

1. General Electric Company, Mark I Containment Evaluation Short-Term Program - Final Report, Volume I, Program Description and Summary of Conclusions, NEDC-20989-P, September 1975.

2. General Electric Company, Mark I Containment Evaluation Short-Term Program - Final Report, Volume II, LOCA Related Hydrodynamic Loads, NEDC-20989-P, September 1975.

3. General Electric Company, Mark I Containment Evaluation Short-Term Program - Final Report, Volume III, Load Application and Screening of Structural Elements, NEDC-20989-P, September 1975.

4. Bechtel Power Corporation, Mark I Containment Evaluation Short-Term Program - Final Report, Volume IV, Structural Evaluation, NEDC-20989-P, September 1975.

5. Teledyne Materials Research, Mark I Containment Evaluation Short-Term Program - Final Report, Volume V, Independent Assessment of the Mark I Short-Term Program, NEDC-20989-P, September 1975.

6. Bechtel Power Corporation, Mark I Containment Evaluation Short-Term Program - Final Report, Addendum 1 to Volume IV, Structural Evaluation, NEDC-20989-P, November 1975.

7. General Electric Company, Mark I Containment Evaluation Short-Term Program - Final Report, Addendum 2, NEDC-20989-P, June 1976.

8. General Electric Company, Mark I Containment Evaluation Short-Term Program - Final Report, Addendum 3, NEDC-20989-P, August 1976.

9. Bechtel Power Corporation, Analysis of Torus Support System for the Peach Bottom Atomic Power Station, Units 2 and 3, Rev. 1, October 1976; and Addendum 1, Rev. 1, August 1977.

10. U.S. Nuclear Regulatory Commission, Safety Evaluation Report, Mark I Containment Long Term Program, NUREG-0661, July 1980.

11. General Electric Company, Mark I Containment Program - Load Definition Report, Rev. 2, NEDO-21888, November 1981.

12. Peach Bottom Atomic Power Station, Units 2 and 3, Final Safety Analysis Report.

13. American Society of Mechanical Engineers, Boiler and Pressure Vessel Code, Nuclear Power Plant Components, Div I, Section III, 1980 Edition.

14. General Electric Company, Mark I Containment Program - Structural Acceptance Criteria, Plant Unique Analysis Application Guide, Rev. 1 NEDO-24583-1, October 1979.

15. AISC, Inc., Manual of Steel Construction, 8th Edition, 1980.

16. Nuclear Technology, Inc, Mark I Containment Program - Cumulative Distribution Functions for Typical Dynamic Responses of a Mark I Torus and Attached Piping Systems, NEDE-24632, December 1980.

17. U.S. Nuclear Regulatory Commission, Regulatory Guide 1.61.

18. General Electric Company, Mark I Containment Program - Plant Unique Load Definition - Peach Bottom Atomic Power Station, Units 2 and 3, Rev. 1, NEDO-24577, January 1981.

19. Philadelphia Electric Company, Peach Bottom Atomic Power Station Unit Number 2, Test Report, Response of Suppression Chamber to Main Steam Relief Valve Discharge, Rev. 1, March 1978.

20. American Society of Mechanical Engineers, Boiler and Pressure Vessel Code, Code Cases, Nuclear Components, 1980 Edition.

21. Williams Form Engineering Corp, Williams Prestressed Rock Bolt Manual, Bulletin RB7677, 1976.

22. A.A. Sonin, Rationale for a Linear Perturbation Method to Deal With the Flow Field Perturbations in Complex Fluid-Structure Interaction Problems, Massachusetts Institute of Technology, March 1979.

23. Everstine, G.C., "A NASTRAN Implementation of the Doubly Asymmetric Approximation for Underwater Shock Response," NASTRAN: User's Experience, October 1976, pp. 2-7-225.

24. Documentation for NASTRAN Computer Program:

    (a) The MacNeal-Schwendler Corporation, MSC/NASTRAN User's Manual, Volumes I and II, 1980.

    (b) The MacNeal-Schwendler Corporation, MSC/NASTRAN Application Manual, Volumes I and II, CDC 7600 Edition, September 1979.

25. Expansion Joint Manufacturers Association, Inc, Standard of Expansion Joints, 5th Edition, 1980.